IADC

PRACTICAL
WELLBORE HYDRAULICS
AND HOLE CLEANING

Unlock faster, more efficient, and trouble-free drilling operations

MARK S. RAMSEY, P. E.

GP

PRACTICAL WELLBORE HYDRAULICS AND HOLE CLEANING

Practical Wellbore Hydraulics and Hole Cleaning

Unlock Faster, More Efficient, and Trouble-Free Drilling Operations

MARK S. RAMSEY, P. E.
Texas Drilling Associates

For Information on all Gulf Professional Publishing publications
visit our website at https://www.elsevier.com/books-and-journals

Working together
to grow libraries in
developing countries

www.elsevier.com • www.bookaid.org

FOREWORD

Practical Wellbore Hydraulics and Hole Cleaning is an excellent learning and applications book for the experienced engineer and the new comer to drilling engineering technology applications for today's drill well challenges. The format in which the book is written allows the reader to first understand the physics behind the challenges and then how the right technology is applied to drill the best well possible.

The flow for the book walks the reader through the process involved in making hole, cleaning the hole, and producing a quality wellbore which will allow completing and producing the desired production intervals in the most efficient way possible. To do this, the author draws on many technical applications proven in both laboratory and modeling work and in the field over many years by industry experts. These technologies and procedures address how to drill and clean the hole, how to manage power to drill at an optimum rate, how to drill a gauge hole, how to optimize bit life, and how to drill and complete the most cost-efficient wellbore.

The author does an excellent job of explaining the variables that the engineer has to work these problems and uses practical field examples to show how they are applied. This book will be one that any career drilling engineer will always want as part of their library.

Juan A. Garcia, P. E.
(Retired) Worldwide Drilling Manager, ExxonMobil

FOREWORD

Both novices and experienced professionals in the oil and gas industry will derive much benefit from *Practical Wellbore Hydraulics and Hole Cleaning*. This book provides state-of-the-art practical guidelines on how to design and get the most from drilling fluid and hardware to optimize drilling operations, while explaining in easy-to-understand terms the underlying physics and mechanics.

I have known Mark Ramsey since we crossed paths in the early 1990s at Amoco Production Co, when I was working in the Drilling Fluids & Solids Control Group and he was consulting for that company in various capacities within the drilling organization. I was impressed with the breadth of Mark's drilling expertise and his friendly, down-to-earth approach to solving drilling problems. He brought these consummate skills to the forefront with his very popular courses on improving drilling performance, which he continues to teach. For all his contributions, Mark has been recognized by his alma mater, Texas Tech University, as a Distinguished Engineer, and he currently serves as the President of the University's Academy of Mechanical Engineers.

The original working subtitle of this book, "Using Drilling Mud, Pumps, and Bit Nozzles for Better Drilling Performance," provides a window to the approach Mark uses for optimization of drilling operations. Enhancing and optimizing drilling performance is indeed the ultimate objective of this book, and the means to that end is optimization of hydraulics throughout the well. Bit hydraulics and removal of cuttings under the drill bit are addressed first, followed by transporting cuttings up the wellbore. Next come critical chapters on maximizing drilling efficiency and rate, and calculating pressure drops across all components in the drilling column. Two chapters follow that are dedicated to drilling fluids: rheology and the effects of downhole pressure and temperature on rheology and hydraulics. A brief survey of pumps and some helpful appendices completes the work.

Every chapter includes detailed explanations of the processes at work and provides ample references to both lab tests and field operations. Mathematical modeling ties all this together; students in particular will find useful that some of the equations are derived to reveal the fundamental physico-mechanics behind the theory. Most importantly, in each

chapter, Mark provides examples of calculations that are based on actual studies.

In summary, this is a book that belongs to every drilling engineer's library. It will undoubtedly become a standard in the field of drilling hydraulics and be used as both textbook and handbook for improving hydraulics and drilling performance.

Fred Growcock, PhD
(Retired) Global Fluids Specialist Occidental Oil & Gas Corp

FOREWORD

This is a peer-reviewed book about rig hydraulics, covering theory and practical application, written by an award-winning, professional engineer with extensive rig experience. The author has a great reputation as a teacher, and this talent shines through the writing in the book which explains a very complex subject in an easily understood manner.

Drilling fluid has many important functions while drilling wells. Three important ones are to prevent blowouts, to remove cuttings from the bottom of the hole, and to transport those cuttings to the surface. Cuttings removal and transport require an understanding of drilling fluid rheology and hydraulics which are completely explained in this book.

Improving hydraulics frequently is interpreted to mean "pump faster." The reason that this is incorrect is very clearly explained in this book. Pumping as fast as possible means that most of the surface pressure generated by the mud pumps will be consumed in the drill string, and very little pressure will be left for the bit nozzles. This book discusses how to select the proper flow rate to maximize the hydraulic impact or the hydraulic power of the fluid flowing though the bit nozzles.

Satisfactory cuttings removal from the bottom of the wellbore requires the drilling fluid strike the bottom of the hole with the most force possible or use the most hydraulic power possible. No matter which criteria are used, the pressure loss in the circulating system must be known. Within the well, the flow may be laminar in parts of the well and turbulent in the other part. The calculation of pressure loss in laminar flow requires one set of equations, and the calculation of pressure loss in turbulent flow requires another set of equations. Not only does the pressure loss in the system depend upon how much of the flow is laminar or turbulent but it also depends upon the temperature of the fluid and in nonaqueous drilling fluid (NADF) the temperature and the pressure. These variables change with the exact ingredients in the drilling fluid.

Most computer programs use approximations of these equations because the effects of these variables are unknown downhole. The best estimations can be made with the theory as presented in this book. The problem with the best theoretical solution is the inability to determine the flow profile or the viscosities of the fluid in the wellbore. While the well is being drilled, a simple set of surface measurements will permit an

accurate determination of the correct nozzle sizes and flow rate to give the maximum hydraulic force or hydraulic power. These surface measurements permit accurate calculation of the pressure loss in the well for all of the components of the drill string and all sections of the annulus.

The transport of the cuttings up the annulus is also described using the method which has been accepted in API RP13C. This calculation has been field tested for many years and works well in wells up to the angle of repose of cuttings in the wellbore—usually between 35 and 42 degrees. In high angle wells, the transport is much more complicated and is very well explained in this book.

The book even discusses a process which has shown some hope of allowing horizontal holes to be cleaned: pumping a viscoelastic drilling fluid. If an excess amount of XC polymer is added to a water-based drilling fluid, an elastic modulus can be created and has been shown to transport cuttings in horizontal holes. One serious stumbling block remains, however. No one markets a product to create the elastic modulus in NADF. Most of the long-reach, horizontal holes are being drilled with PDC (Polycrystalline Diamond Compact) bits and NADF.

This book bridges the gap between theory and application. It presents techniques refined and tempered with operations experience that enable the well designer to account for the inadequacies of the theoretical approaches described above. These techniques for both optimum hydraulics and hole cleaning are practical, proven, and well presented in the text.

The industry would be well served to have a copy of this book in all offices of drilling engineers, tool pushers, well site supervisors (company men), and service company engineers worldwide.

Leon H. Robinson, PhD
(Retired) Research Advisor, Exxon Production Research Company

DISCLAIMER

This book was prepared under the auspices of the IADC Technical Publications Committee but has not been reviewed or endorsed by the IADC Board of Directors. While the committee strives to include the most accurate and correct information, IADC cannot and does not warranty the material contained herein. The mission of the IADC Technical Publications Committee is to publish a comprehensive, practical, and readily understandable series of peer-reviewed books on the petroleum drilling industry in order to educate and guide industry personnel at all levels.

If I have seen further it is by standing on the shoulders of Giants.
—*the Sir Isaac Newton letter to Robert Hooke, February 5, 1676*

ACKNOWLEDGMENTS

I wish to thank a number of influential people who had impact on both my career and this book. Though many helped over the years, some deserve special recognition.

First, *Leon H. Robinson, PhD* was my mentor as a young engineer when I was breaking out at Exxon Production Research Company in Houston in the early and mid-1980s. His keen insights into wellbore physics and knowledge of what had been tried and tested is encyclopedic. He gave all of the young engineers in that group needed head starts, and his influence has served as a lifelong source of inspiration. Dr. Robinson, a World War II veteran who helped liberate France and Europe, was a pioneer of many tools and techniques for improving drilling performance. He never forgot that it remains the men on the rigs that must ultimately make it happen.

Juan Garcia, a former direct supervisor at Exxon who later became the Worldwide Drilling Manager of ExxonMobil, and *Fred Growcock, PhD*, a former colleague from Amoco, who perhaps more than any other committee members, painstakingly reviewed the manuscripts and offered significant improvements, as well as encouragements throughout.

Significant other reviewers of the manuscripts included, *Ron Sweatman*, *Max Wang*, *Les Skinner*, *Mark Morgan*, *Nace Peard*, *Bob Line*, and *ASME Fellow Tom Sifferman, PhD*.

Members of the IADC Technical Publications Committee donated uncounted hours of volunteer time in the hope that knowledge and experiences accumulated over their lifetimes and careers (somewhat inseparable for most of us) may be captured and transferred to others in our great industry. They remain hard at work at their Mission: Create a comprehensive, practical, and readily understandable series of peer-reviewed publications on well construction and integrity in the oil and gas industry to educate and guide personnel at all levels.

Other highly influential drilling specialists offered insights, opinions, advice, and other help over the years on hole cleaning, hydraulics, drilling fluid, and rheology issues. These include notably *Max Annis, Stan Christman, Miles Peroyea, Fred Dupriest, and Robert "Bob" Garrett*.

In numerous drilling courses that I have taught on six continents over almost four decades, students who asked interesting questions have been invaluable in honing the way concepts are presented.

Fran Kennedy and Mike Killalea helped in the early days of the project. The publisher, Elsevier, and in particular my editors Katie Hammon and Jo Collett, have been part of this project nearly since inception and have been of great assistance in the final publishing details.

My wife Pauline and my children, Michelle, Josh, and David, encouraged me and sacrificed during both my career and the writing and editing of the book.

Last, but most importantly, I am grateful to my Lord and Savior Jesus Christ, who made the world we marvel at to be consistent and predictable, not chaotic or random, so that we can observe, study, and understand it. He gives each of us gifts, challenges, and opportunities for our service to mankind and to honor Him. Jeremiah 32:17.

Introduction

Contents

In today's competitive oil and gas–drilling environment, all available skills should be utilized by rigsite and office personnel to maximize efficiencies in constructing the wellbore. A thorough understanding of wellbore hydraulics and its close associate, hole cleaning, are two of those critical skills. An engineer's job is, in part, to predict the future. Operations personnel make that future happen. Wellbore hydraulics and hole cleaning enable both to control that future with respect to drilling a well.

1.1 WELLBORE HYDRAULICS

As the title of this book suggests, there are two broad overarching and connected technologies covered. The first, and perhaps the most misunderstood, is that of wellbore and bit hydraulics. Understanding and properly utilizing the various levers of adjustment around wellbore hydraulics can literally make the difference in drilling ahead or not, but more commonly it is a matter of how efficiently the drilling is progressing. Significantly, the ability to drill longer laterals can also be a function of proper wellbore hydraulics. Last, but always of great importance to drillers, tool pushers, and drilling engineers alike, rate of penetration can be greatly enhanced through the proper use of wellbore hydraulics.

While not the only critical component of a well-designed and executed drilling project, the optimum selection of flow rates, pipe sizes (where this is an option), and nozzle sizes can truly make-or-break the economics of a well.

1.2 HOLE CLEANING

An older operations superintendent in this author's early engineering days advised that "it is not how much hole you make, it is how much hole you keep!" He wisely recognized that there were ways to improve rate of penetration short term that could lead to longer term problems or even complete loss of a well. A key component of "keeping" the hole is to have a consistent and reliable approach to removing cuttings from both under the bit and from the wellbore itself—transporting them out of the hole at the surface.

There is an enormous variety, some might say endless variety of well designs today. Directionally, these designs range from more-or-less vertical to fully horizontal (or higher angle). Plan views (or birds-eye top-down views) of wells range from a straight line to a curved line to a full 180 degree or more "hook."

Due in part to this variety, there are numerous difficulties in both transporting cuttings from the wellbore to the surface where they can be removed from the mud system.

1.3 ORGANIZATION OF THE BOOK

Wellbore hydraulics and hole cleaning are the title topics of this book, and the following two chapters address them.

Within those chapters, the solution to the problem is presented in several ways. Typically, a quick and usable solution is given for those situations when extensive analysis is neither warranted nor practical due to limited time constraints. When you come upon an accident victim needing assistance, stop the bleeding first.

After the quick-but-usable solution is presented, more detailed discussions and more elegant technical approaches are examined. Where time is

available or well criticality requires it—for example, when drilling through an extremely narrow pore-pressure/frac-pressure window—the more detailed approach may be preferred.

In this manner, the book may be effectively used as a quick reference tool to solve immediate and pressing problems and yet also serves the inquisitive to bore deeper into the issues.

1.4 RATE OF PENETRATION

The chapter after those two ties the wellbore hydraulics, bit hydraulics, and hole cleaning together in the interest of drilling faster, near and dear to all drillers' hearts.

After these cardinal chapters, the remaining chapters in the book address tightly related subjects in sufficient details with suitable equations to permit modeling of pressure losses.

The overall approach is that some pressure losses are required by the drilling operation and cannot nor should not be minimized. Mud motor losses come to mind as these (and the associated torque and rpm they impart to the bit) can be extremely important to drilling rate. However, if the rig pumping capability is sufficient, any extra pressure that is available should be spent across the bit nozzles, rather than being wasted as friction loss in pumping drilling fluid through the drill string and up the annulus.

1.5 PRESSURE LOSSES

To the uninitiated, pressure losses seem simple to calculate, especially if the reader has a background or coursework in calculating pressure losses in Newtonian liquids flowing through pipes. However, for the case of a drill well, the liquid is not Newtonian, the flow regime is never fully laminar nor fully turbulent (the two cases simplest to model), and the flow is in a nonuniform series of conduits, some of which change sizes along their length and others are moving!

The result is that it is extraordinarily difficult to accurately model pressure losses accurately downhole. Hence, an entire chapter is devoted to these pressure loss issues in a manner not found in any extant text.

1.6 RHEOLOGY

"*Panta rhei*"—everything flows. The study of rheology is next. In order to deal with pressure losses and modeling, an understanding of rheology is important, so a chapter on this subject is next. Everything that flows exhibits some resistance to flow. That resistance, in the case of drilling fluids or muds, takes the form typically as a "shear-thinning" liquid. In such liquids, the viscosity is fairly high when the fluid is shearing (particle or streamline to particle or streamline) slowly. Conversely, the viscosity actually decreases as the shearing (or shear rate) is increased, much in the same way that ketchup from a plastic bottle is higher viscosity while in the bottle than while going through the cone-shaped nozzle as the bottle is squeezed.

1.7 DOWNHOLE PROPERTIES

Next to last in this first edition is a chapter discussion on the variability of fluid properties as the fluid is transported down the drill pipe, through the nozzles, and back up the annulus in a wellbore. Increased pressure increases density and viscosity. Increased temperature decreases density and viscosity. Pressure and temperature can affect the effect of chemicals in the mud on their properties. Low shear rate values may be affected in a different manner than high shear rate ones. Chemical additives to accomplish other functions, such as protect the formation from damage, may interact with the rheology differently downhole than on the surface.

1.8 PUMPS

Last, a brief discussion on rig pumping equipment is provided. These include both kinetic (or centrifugal) pumps and positive displacement types generally used to store energy (as pressure as the mud compresses) for use downhole.

1.9 OPERATORS, DRILLING CONTRACTORS, AND SERVICE COMPANY PARTNERS

In an industry where many of the players may have differing economic interests in various parts of drilling a well, wellbore hydraulics and hole cleaning can benefit all of the companies. A good understanding of how energy is used in a wellbore—usually measured as pressure losses—can greatly improve the drilling performance for the operator who is paying for the operation. For the drilling contractor and service companies involved, that efficiency plays out as significantly improved life of capital-intensive equipment.

It is the author's desire that this book's readers reap economic benefits far in excess of the monetary cost and time to read and understand it on the very first well it is used on. Though equipment and measuring techniques improve with time, its concepts are timeless and can be used on all wells thereafter.

Enjoy your read.

Bit Hydraulics

Contents

One of the most powerful tools in a driller or drilling engineer's toolbox involves the optimum use of hydraulic energy in the wellbore.

Hydraulics is one of the most misunderstood yet potentially the most valuable tools in a drillers arsenal. There are many, many misconceptions about the best way to run hydraulics. Similarly, there are legitimate differences of opinion as to how to best optimize the use of hydraulic energy. We will discuss the most important issues and techniques.

Any suite of technology tools for the efficient and successful drilling of any difficult wellbore should include an understanding of hydraulics, which will be taken here to broadly include the following:

- designing bit nozzle/flow rate conditions,
- cleaning the hole, and
- managing downhole pressures such as the equivalent circulating density (ECD).

Two other critically important issues that are not just misunderstood but also often understood *wrongly* are addressed in the separate chapter on pressure calculations. The first is surge-and-swab pressure and the last is the problem of hole "washout."

Even for a water-based mud these are challenging, but for a nonaqueous drilling fluid (NADF), they can become more so, owing primarily to a relative lack of experience with individual base fluids (compared to the experience industry has amassed with water-based muds) and a lower degree of predictability downhole when compared to water-based fluids.

This chapter will review basic principles involved, present some field-proven methods of calibrating computer models for these, and highlight issues related to hydraulics and hole cleaning as they relate to both water-based and NADFs.[1]

In a nutshell, if the hydraulic power and pressures are not being used to accomplish the above items, then in terms of efficiencies, it is being wasted. All other consumers of energy, such as the pressure drops through the drill pipe and the bottom hole assembly (BHA), are mostly parasitic in nature and do not help drill the well better. (The exceptions relate to powering downhole BHA components, which do obviously convey benefit to the overall operation but are parasitic with respect to optimizing bit nozzle sizes and flow rates.) They are necessary evils, but we want to minimize those parasitic losses in order to have more power or pressure to use beneficially.

Referring to Fig. 2.1[2], mud is energized (pressurized) by the rig mud pump, travels through hard piping to the top of the standpipe, then flows through the rotary hose and then through either a swivel/kelly (shown), or a top drive (not shown), then to the drill pipe, drill collars, through the bit, and up the return annuli (drill collar by hole ID, drill collar by casing ID, drill pipe by hole ID, drill pipe by casing, etc.) before exiting at atmospheric pressure to the flow line—"return line" in above diagram. At that point, all energy from the pump is expended.

---

[1] For greater in-depth treatment on the topic of wellbore hydraulics, please refer to the full book this chapter is from, *Practical Wellbore Hydraulics and Hole Cleaning* by Mark S. Ramsey, P.E. (2019).

[2] The University of Texas at Austin Petroleum Extension Service, A Primer of Oilwell Drilling, seventh ed., The University of Texas at Austin Petroleum Extension Service, 2008, p. 129, figure 149.
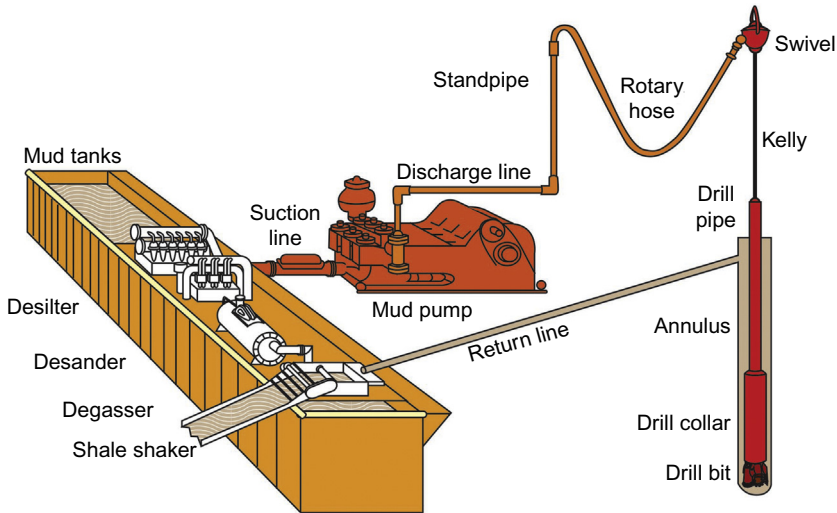
Figure 2.1 Typical rig circulation system. *Courtesy: University of Texas Petroleum Extension Service (PETEX)[2].*

2.1 INTRODUCTION AND IMPORTANCE OF BIT HYDRAULICS OPTIMIZATION

The proper design of bit hydraulics is one of the potentially most beneficial aspects of drilling wellbore hydraulics. When properly utilized, it can result in

- improved rate of penetration (ROP), due to improved removal of newly formed cuttings from beneath the bit, eliminating the need to "drill the hole twice" before new cuttings are removed;
- decreased ECD, due to optimization typically resulting in lower flow rates compared to nonoptimized conditions;
- reduce the risk of stuck pipe from cuttings accumulating on the low side of the hole;
- decreased wear and tear on pressure generating machinery, due to a more efficient use of available hydraulic energy, and hence less wasted energy or pressure; and
- reduced diesel or other fuel usage and hence less associated pollution and greenhouse gas emissions.

Optimized bit hydraulics is one of the rare technologies that offer a true "win" for both the drilling contractor *and* the operator.

To the *operator*, optimized bit hydraulics presents the opportunity to drill faster and hence incur less cost in drilling a particular wellbore or series of wells. This translates into an *improved drilling efficiency* in an economic sense.

To the *drilling contractor*, optimized bit hydraulics presents the opportunity to drill more efficiently in a purely technical sense, thus *extending equipment maintenance and ultimate life*, thus adding to the profit bottom line of a particular rig or the drilling contractor, corporately.

Briefly, the task facing the wellbore hydraulic designer is to optimize the combination of flow rate and pressure drop across (or through) the bit nozzles. He or she cannot do this in a vacuum and must also accomplish this optimization while honoring the limits of other design constraints, typically caused by drilling rig equipment, drill string components, third-party hardware limits or requirements, and occasionally the formation itself.

2.1.1 Illustration of the problem

A simple analogy of the problem of bit hydraulics optimization follows. This illustration remains very relevant and instructive today.

In your mind's eye, imagine you are about to clean off a concrete driveway that has sand and clay on it, perhaps left from washing a truck dirty from a week-end of off-road fun. To do so, you choose to use an ordinary garden hose. You go to the hose bib valve located at the house and turn it on all the way counterclockwise but discover you have no brass nozzle to efficiently restrict, accelerate, or direct the water flow. Naturally, you improvise and partially cover the open end of the garden hose with your thumb, restricting the flow but increasing the jet velocity of the water stream.

The question of bit hydraulics is akin to determining how you place your thumb over the flow. In the two extremes, you might either not restrict the flow significantly with your thumb or you could restrict the flow almost completely, such that only a thin pencil–lead–diameter beam of water emerges. In the former case, maximum water flow would be realized, but with little associated velocity (or pressure drop across your thumb). In the latter, velocity would be high (as would the associated pressure drop across your thumb), but little volume would accompany that velocity.

Neither extreme case would efficiently clean the driveway.

The open–ended garden hose would obviously not clean the concrete efficiently. The reason is simply not enough velocity (or pressure drop . . .

essentially interchangeable in the bit hydraulics world).[3] There will be insufficient force of impact by the water to loosen the clay or dirt particles that are stuck to the concrete.

Less obviously, the pencil-lead-beam would not clean *the whole driveway* efficiently either. It would clean exceptionally well in the tiny high-impact area where it struck the concrete, but of course there would be a highly insufficient volume of flow washing the dislodged material away in an efficient or timely manner.

In both extremes, the driveway would be cleaned either very poorly or slowly, or perhaps both.

The solution of course is to adjust your thumb placement to the *best combination of both velocity and volume flow rate*. The same is true of the bit nozzle design problem, except that we have to do it with assumptions, equations, measurements, and knowledge rather than a simple feedback mechanism (visually seeing the effectiveness of your thumb placement and adjusting it accordingly).

Our brains are designed to have a tremendous ability to recognize patterns. More specifically, we readily recognize cause-and-effect relationships. This ability results in our being hardwired to provide real-time and "automatic feedback" as we accomplish various tasks, usually with the result of improving our efficiency at the task. This is especially true if improvements (i.e., adjusting your thumb for the best results) result in our finishing a task at hand faster or easier.

Even a small child could adjust his or her thumb, without even vaguely understanding the science of hydraulics or other technical issues and principles underlying that adjustment.

The task for the wellbore designer is nearly identical, except that the bit nozzles are not adjustable nor do we realize any instantaneous (or real-time) feedback. Hence, mathematical considerations, prior knowledge, measurements, and judgments—rather than hand-eye feedback and coordination—must guide our selection of jet nozzles for the bit before it goes into the hole. Optimally, those mathematics should be executed immediately before the bit is screwed onto the BHA, not days, weeks, or months in advance, in order to fully utilize what data we do have from the wellbore under construction.

---

[3] Velocity and pressure drop across the bit nozzles are proportional to each other, either linearly or exponentially, as can be seen in this chapter's appendix.

2.1.2 Organization of the chapter

In terms of using available hydraulic energy most efficiently, this is clearly the most important chapter of the book. As such, it is hoped that it will be useful for all levels of situations and need for accuracies. As a result, this chapter is presented in order of increasing complexity depending on the degree of accuracy needed by the well-site toolpusher or engineer, or the design or operations engineering team.

Different than most chapters in this book or others, please note that this chapter has been divided into several sections of progressing complexity (and resulting accuracy). For the toolpusher or driller or drilling engineer without much time to arrive at the near-perfect answer, a "Drillers' Hydraulics Method" is presented that will give more than adequate results in most cases.

For those desiring a more exacting solution, the "Engineers' Hydraulics Method" is given. This gives the designer the ability to tailor the wellbore hydraulics to subtleties of the drilling fluid system, rig equipment, and wellbore geometries in a highly calibrated yet still straightforward manner. For deep or otherwise hydraulically limited wells, the latter method is recommended. Once the Engineers' Hydraulics Method is fully understood and programmed into a suitable calculator or spreadsheet or fit-for-purpose software package, it is quite reasonable to perform, time wise.

Note of course that there is no connection between the bit hydraulics "Driller's Hydraulics Method" or "Engineers' Hydraulics Method" and the well control kick circulation techniques (or other drilling topic techniques) of similar nicknames.

Once hydraulics have been optimized for wells in a particular field, then for similar wells and for similar well plans [especially as related to drilling fluid density (or "mud weight"), flow rates, and drill string including measurement while drilling (MWD), and other third-party downhole consumers of drilling fluid-transmitted power (as pressure)], then the hydraulics do not necessarily require reevaluation on each subsequent well. If the physical parameters relating to pressure drops remain similar (lengths, diameters, mud viscosities, mud weights, flow rates, etc.), then the fluid mechanics (or "physics") of the systems will yield similar optimization results.

After the drillers' hydraulics method and the engineers' hydraulic method have been presented, various more unusual cases are addressed, and a brief history of the development of bit hydraulics technology is given.

2.2 DRILLING FLUID CHALLENGES RELATING TO WELLBORE HYDRAULICS

Drilling fluid (or "mud") must accomplish or assist with many things at the bottom of a borehole as relates to drilling the well. Some of those include the following:

- The drilling fluid must remove the cuttings from the bottom of the hole. Cuttings that are not removed are ground finer by the next cutter. Regrinding results in new smaller cuttings and prevents their removal as well as absorbs mechanical energy from the bit that should be applied to breaking fresh new rock.
- The drilling fluid must clean the drill bit itself. Formation cuttings tend to adhere to or wedge between and around the cutting structures. "Sticky" formations such as soft or "gumbo" clays and other shales can also stick to other areas of the bit, stabilizers, and the BHA.
- The drilling fluid must transport the cuttings to the surface with as little regrinding and degradation (mechanical and/or chemical) as possible.
- Oftentimes the fluid must also power downhole equipment such as drilling fluid motors, MWD, and logging while drilling (LWD) tools. This requirement is especially common offshore, where nearly all wells are now drilled with one or more downhole powered-by-the-drilling fluid components in the BHA.
- Related to the above functions for MWD and LWD tools, the fluid must be suitable for transmitting compressional waves used by data transmission systems. Usually this implies a low solids content and very low gaseous content (entrained air, formation gas, etc.).

Optimum use of bit hydraulic energy enables each of these to be accomplished either adequately or if drilling so deep or with insufficient pump power and pressure to do this inadequately, to make the very best use of all available power and energy, even under nonoptimized conditions.

2.3 TERMS

There are several key concepts related to optimum bit hydraulics that will be discussed. There are also several competing techniques for

optimized hydraulic design. These concepts and techniques are listed below and are discussed later in this chapter.

P_{CIRC}	The circulation system pressure losses (or wasted energy), which includes essentially, everything except the bit
Founder point	The point where increased bit loading no longer produces a proportional increase in drilling ROP. Some texts, articles, and papers use the term "flounder point," which for our purposes is interchangeable
Hydraulic power	Hydraulic power measurement is given by the basic relationship: power $= \rho QV$
Hydraulic horsepower	Hydraulic horsepower, where pressure drops are known or are being calculated (which implicitly includes density effects) is given by: $\text{HHP} = \dfrac{P \times Q}{1714}$ in US Oilfield units
	Note that sometimes hydraulic power is *maximized* and at other times hydraulic HSI is monitored to ensure some *minimum* amount is present
Hydraulic impact or Jet impact force (JIF)	Hydraulic force measurement given by the following: $\text{JIF} = \rho QV^2$
Jet velocity	Velocity of the fluid as it exits the bit nozzle
Flow rate	Volumetric flow of the drilling fluid

ROP, rate of penetration; *JIF*, jet impact force; *HIS*, horsepower per square inch.

These are discussed separately below and afterward used for selection of optimum nozzle sizes and associated flow rates. For readers who are already reasonably familiar with these terms, you may wish to skip ahead to which deals with how to optimize each one.

2.3.1 P_{CIRC}—circulation system pressure losses

Circulating-system pressure losses, P_{CIRC}, represent the pressure losses in all of the circulating system except for the bit [surface connections, rotary hose, swivel, top drive (or kelly), drill pipe—inside and outside, and drill collars—inside and outside]. They are the wasted energy losses, at least with regard to drilling rate improvements. For the purposes of bit hydraulics optimization, parasitic pressure losses such as those required to power downhole drilling tools— mud motors, turbines, MWD tools, LWD tools, pressure while drilling (PWD) tools, etc. —will be considered as part of the overall wasted energy, even though there is obvious benefit derived from these tools. The energy used on such tools is not available to improve bit efficiency.

2.3.2 Founder point

When a tricone bit loading is increased at constant RPM by increasing the weight on bit (WOB), the drilling rate will increase in a more or less proportional and linear fashion to the bit weight over a short interval.[4] Increasing bit weight by 10% would increase ROP by approximately 10%, increasing bit weight by 20% would result in 20% faster ROP, etc.

Note that many other factors are certainly involved. As a result, countless drilling rate equations have been published incorporating a variety of parameters. Note that for milled toothed and carbide toothed bits, it has been reported that rather than linear, the ROP response may be exponential[5]. In general, for the exponential squared response, tricone bit ROP can be generalized with

$$\text{ROP} \propto \left(\frac{\text{WOB}}{D}\right)^2 \tag{2.1}$$

where ROP is the rate of penetration, WOB is the weight on bit, and D is the bit diameter.

However, at some point (dependent on a number of factors, not just hydraulics), the increase in bit weight will cease to provide a commensurate increase in drilling rate. After this condition is reached, the drilling rate may

• continue to increase, but not as much relative to the bit weight increase;
• remain approximately the same with increasing bit weight;
• reverse the trend in extreme cases and may actually decrease with increasing bit weight as shown in Fig. 2.2[6].

The point where the linear relationship between WOB and ROP breaks down is called the "founder point" (or "flounder point" in some texts and industry papers) and is considered by many to be the maximum recommended place to run the bit weight. If this founder point is due to limited or incorrectly designed hydraulics, it can be raised higher, and hence ROP may be increased and overall drilling efficiencies improved.

---

[4] Some researchers have reported that prior to the founder point being reached, the increase in penetration rate as WOB is increased is actually an exponential function (e.g., $\text{ROP} \propto \text{WOB}^x$) where the exponent would be between 1 and 1.8.

[5] L. Robinson, Ph.D., Private Correspondence and Numerous Discussions, Oct 5, 2013.

[6] F.E. Dupriest, W.L. Koederitz, Maximizing drill rates with real-time surveillance of mechanical specific energy, in: IADC/SPE Paper No. 92194 Presented at SPE/IADC Drilling Conference, Amsterdam, The Netherlands, 23−25 February, 2005.
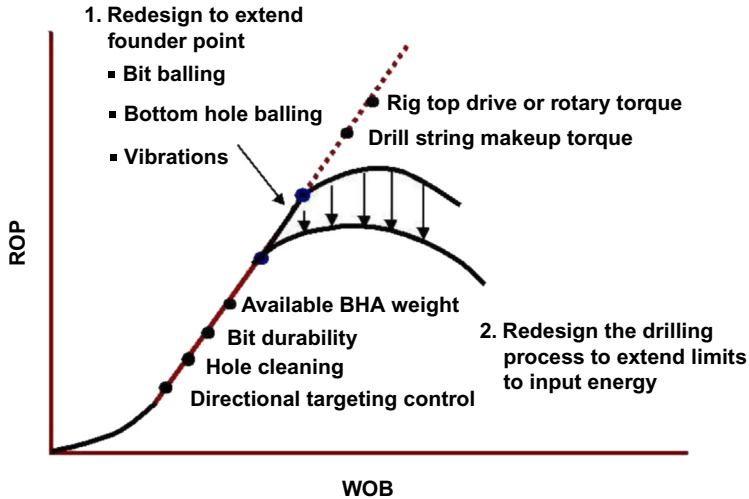
Figure 2.2 Founder point. *Courtesy: F.E. Dupriest, W.L. Koederitz, Maximizing drill rates with real-time surveillance of mechanical specific energy, in: IADC/SPE Paper No. 92194 Presented at SPE/IADC Drilling Conference, Amsterdam, The Netherlands, 23–25 February, 2005.*

If the founder point is caused by other factors, it may not respond to improved hydraulics.

Importantly, after any design or operational change is made to hydraulics, procedures, drilling fluids, or a formation change is suspected, the founder point should be reevaluated by field personnel.

Similarly, even if drilling proceeds relatively unchanged, as the well is deepened and new formations are encountered, the founder point may again need reinvestigation by the driller.

Drilling below the founder point is wasteful in that it does not optimally use the rig equipment and bit to drill as fast or as efficiently as possible. Drilling beyond the founder point can, depending on the formation type and bit type, result in accelerated and unnecessary bit wear and even bit balling, a potentially catastrophic result for polycrystalline diamond compact (PDC) bits.

2.3.3 Hydraulic horsepower

In general, hydraulic horsepower (HHP) is simply pressure (*P*) times volumetric flow rate (*Q*). In US Oilfield units of pounds per square inch (psi) and gallons per minute (GPM), hydraulic horsepower (HHP) may be calculated as

$$HHP = \frac{P \times Q}{1714} \qquad (2.2)$$

where HHP is the hydraulic horsepower in units of horsepower (hp), P is the pressure (psi), and Q is the volumetric flow rate (GPM).

The concept of hydraulic horsepower has utility both in sizing equipment and estimating operating requirements, as well as being one of the two major techniques used for optimizing pressure drop across bit nozzles.

By way of example, if a rig-pumping system was producing 1500 GPM flow rate at 4500 psi, then the *output* hydraulic horsepower would be simply:

$$HHP = \frac{4500 \times 1500}{1714}$$

$$HHP = 3938 \text{ hp}$$

Note that this is NOT the rated input horsepower to drive the pump itself (or crankshaft input), which due to inefficiencies discussed later, will be higher than the actual hydraulic fluid output power as would be expected.

In kilowatts, hydraulic power would be

$$HkW = \frac{P \times Q}{2298} \qquad (2.3)$$

For the same example problem of pressure and flow rate, this becomes

$$HkW = \frac{4500 \times 1500}{2298}$$

$$HkW = 2938 kW$$

Please note that in both calculations, the hydraulic power (HP or kW) is based on the actual output from the pump, or perhaps the actual pressure drop across a valve, through a pipe, or across nozzles or a downhole tool.

2.3.4 Pump efficiency considerations

Pump efficiencies are certainly important to any well site or office personnel trying to run energy-efficient operations. There are numerous inefficiencies inherent in converting energy to usable fluid power, some of which are entirely pump design issues (and hence not readily changeable once the pump purchase is made). Other efficiency–related items include the flow rate and pressure range a pump is run in and the physical properties of the fluid the pump is being used to energize. For example, if the

mud has entrained air, common in poorly run water-based mud systems, the compression of the air in going from the suction tank (atmospheric pressure) to the pump high pressure discharge (typically several thousand psi) can be quite significant and affects the pump efficiency accordingly.

A fuller discussion of pumps and pump efficiencies is contained in Chapter 8, Pumps, devoted to pumps.

2.3.5 Hydraulic force (jet impact force)

In general, the force created by the nozzle jets is simply the fluid density multiplied by the volumetric flow rate times velocity.

$$\mathrm{JIF}_{\mathrm{JETS}} \propto \rho Q V_N \tag{2.4}$$

Or in US Oilfield units,

$$\mathrm{JIF}_{\mathrm{JETS}} = \frac{\mathrm{MW} \times Q \times V_N}{1930.2} \tag{2.5}$$

where $\mathrm{JIF}_{\mathrm{JETS}}$ is the impact force (pounds force); ρ or MW is the drilling fluid density (lb/gal, ppg); Q is the flow rate through the nozzles (GPM); V_N is the velocity through the nozzles (feet per second).

The concept of jet impact force (JIF) has utility primarily in being the second of two major techniques used for optimizing pressure drop across bit nozzles.

The velocity through the nozzles has been previously shown to be[7]

$$V_N = C_D \times \sqrt{\frac{\Delta P_{\mathrm{BIT}}}{8.074 \times 10^{-4} \times \rho}} \tag{2.6}$$

where C_D is the nozzle coefficient, dimensionless.

And other variables are as defined immediately above.

Combining the general impact force equation and the one for velocity yields

$$\mathrm{JIF}_{\mathrm{JETS}} \propto \rho \times Q \times C_D \times \sqrt{\frac{\Delta P_{\mathrm{BIT}}}{8.074 \times 10^{-4} \times \rho}} \tag{2.7}$$

Or in US Oilfield units as before:

---

[7] Burgoyne, et al. Applied Drilling Engineering, SPE Textbook Series Volume 2, 10th printing, 2005, p. 129.

$$\text{JIF}_{\text{JETS}} = \frac{\rho \times Q \times C_D}{1930.2} \times \sqrt{\frac{\Delta P_{\text{BIT}}}{8.074 \times 10^{-4} \times \rho}} \tag{2.8}$$

Simplifying to

$$\text{JIF}_{\text{JETS}} = \frac{Q \times C_D}{1930.2} \times \sqrt{\frac{\rho \times \Delta P_{\text{BIT}}}{8.074 \times 10^{-4}}} \tag{2.9}$$

$$\text{JIF}_{\text{JETS}} = \frac{Q \times C_D}{54.846} \times \sqrt{\rho \times \Delta P_{\text{BIT}}} \tag{2.10}$$

By way of example, if the same rig-pumping system used above {535.4 GPM flow rate, 12.3 ppg density drilling fluid, five #16 nozzles [16/32nds of an inch diameter each, resulting in a total nozzle flow area (TNFA) for the five nozzles of 0.9817 square inches[8] total nozzle flow area]}, and taking C_D to be 0.98, then JIF would be simply

$$\text{JIF}_{\text{JETS}} = \frac{535.4 \times 0.98}{1930.2} \times \sqrt{\frac{12.3 \times 286.4}{8.074 \times 10^{-4}}} \tag{2.11}$$

$$\text{JIF}_{\text{JETS}} = \frac{535.4 \times 0.98}{54.846} \times \sqrt{12.3 \times 286.4} \tag{2.12}$$

$$\text{JIF}_{\text{JETS}} = 568 \text{lbf}$$

Note that if the more accurate overall nozzle discharge coefficient C_D of 1.03 is used instead of the more conventionally used 0.98, the value for the JIF_{JETS} computes to 597 lbf. The discovery of and preferred use of the 1.03 value is discussed later.

2.3.6 Jet velocity

Jet velocity is *not* commonly used as an optimizing parameter, though some well designers do like to keep some minimum velocity across the bit nozzles. Due to pressure recovery, discussed below, the calculated jet velocities are only accurate at the throat or exit of the nozzle. If one wishes to maximize jet velocity for some reason, the simplest way is to use the minimum acceptable flow rate as an input into the bit pressure drop equation (rearranged to solve for total nozzle flow area), and the

---

[8] Total nozzle flow area, TNFA (or simply TFA) may be calculated (in square inches) with: $\text{TNFA} = \left(\text{nozzle size}^2/1303.8\right) \times$ number of nozzles, where the nozzle size is in 1/32nds of an inch diameter and all nozzles are the same nominal size.

result will give maximum pressure drop across the nozzle and the corresponding maximum jet velocity.

2.3.7 Flow rate

Flow rate simply refers to the volumetric flow per unit of time that the pumps are pumping into the wellbore. The customary unit is GPM, but of course there are many other units in use worldwide. Note that for most calculations, conversations, and reports, rig site personnel will refer to the flow rates, while the critical parameter for many calculations (jet velocity, annular velocity, hole cleaning, etc.) is actually the flow velocity. The velocity of course simply becomes the volumetric flow rate divided by the cross-sectional area the fluid is crossing, in consistent or converted units.

2.4 CIRCULATING-SYSTEM PRESSURE LOSSES (I.E., "WASTED ENERGY")

These combined parasitic losses (P_{CIRC}) almost always obey a "power law" relationship between flow rate and pressure. In its simplest form

$$P \propto Q^u \tag{2.13}$$

where P is the friction pressure through the circulation system (psi); Q is the flow rate (GPM); and is the exponent for the power law relationship (dimensionless).[9]

To review, this means that if flow rate doubles, the associated pressure increases by at least the same doubling (if the exponent were equal to 1.0), but if the exponent is greater than unity, the pressure more than doubles. Fluid mechanics considerations, discussed later in Section 2.4.1, limit the exponent to a range of 1.0–2.0. The higher and higher flow rates generate considerably higher and higher pressures. This is depicted graphically in the following figure. The lowermost line might represent the pressure drops shallow in the hole. The next line is a bit deeper. The third line from the bottom is still deeper, perhaps with an increase in mud

[9] The term "u" is chosen for this exponent due to it is being "unique" and "unknown" until calibrated. Different well conditions geometry, pumping rates, and drilling fluid itself all influence this unknown–until-calibrated value.—Leon Robinson, PhD, private correspondence. *Note*: Some texts will use the Greek symbol μ in place of u.

Parasitic hydraulic losses
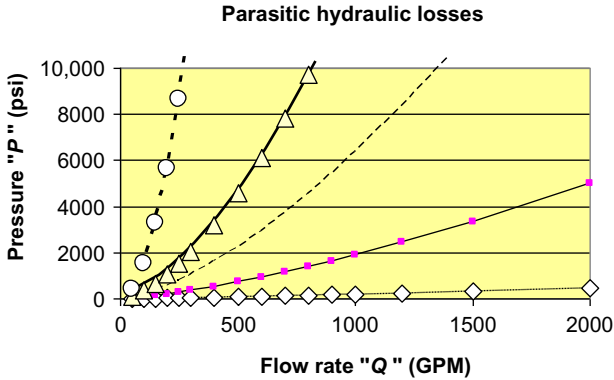
Figure 2.3 Parasitic losses on Cartesian coordinates.

Parasitic hydraulic losses
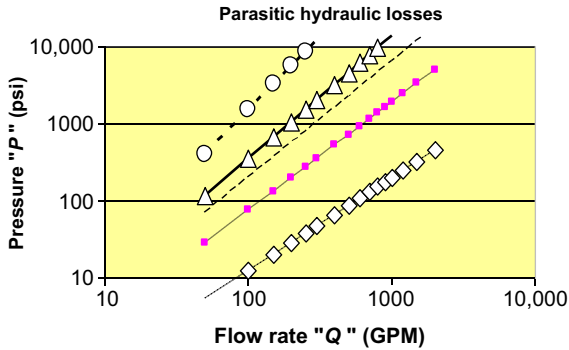
Figure 2.4 Identical data as in Fig. 2.3, plotted on Logarithmic axes.

weight. The top two continue this trend toward higher and higher wasted hydraulic energy, just to circulate the well, before any useful work is obtained at the bit or in lifting cuttings to the surface.

As drill pipe is added to the drill string, these pressure losses increase, creating a family of curves as shown in Fig. 2.3. For calculation purposes, it is not very convenient to use Cartesian plots as in Fig. 2.3. Hence, engineers, scientists, and mathematicians use a convenience for handling this sort of data, which plots the exact same data on axes that are not linear (or "Cartesian"), but rather are logarithmic. By doing this, exponential data then plots in straight lines, as shown in Fig. 2.4. Note this is the identical data—only the scales on the plot are different.

These two plots, the regular Cartesian plot and the Logarithmic one, are of the exact same flow rate (Q) and pressure (P) data but are plotted against different scales.
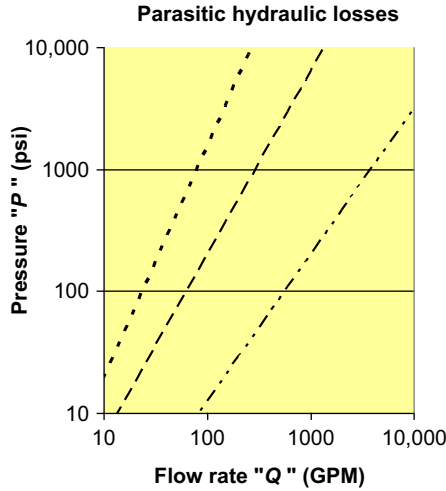
Figure 2.5 Same data sans data point markers (for exercise).

Since the data is now in a straight line, we can make convenient use of it. We can measure the linearly measured slope of the line of pressure versus flow rate data. This slope is, in fact, the exponent on flow rate in the power law model of Eq. (2.13). This will come in useful in a future calculation, permitting exacting predictions of circulating pressures and extraordinarily accurate optimizing of bit hydraulic parameters.

The graph is shown in Fig. 2.5 (which is again the exact same data, but in this case has the individual data points removed and only the straight lines remain.) As an execise, the reader might measure the slope of the three straight lines shown in Fig. 2.5.

The slope of these lines, indicative of the state of the flow, depends upon the drilling fluid properties as well as abrupt change of flow patterns in the circulating system. Hydraulic slide rules and most computer programs generally default or assume a slope (u) of these lines (which again is used here as the exponent in the power law model), generically:

$$P \propto Q^u \tag{2.14}$$

Typical hardwired values for u in these models and programs range from 1.76 to 1.86 or so. This slope can more accurately be measured at the rig site during drilling and will later be a key parameter in accurately calculating optimized hydraulics.

2.4.1 Physical meaning of the exponent in the power law model: laminar, turbulent, and transitional flow

In terms of fluid mechanics, "physics" if you will, the slope of the line can be anywhere between 1.0 and 2.0, inclusive. If the value was 1.0, the flow would be said to be fully *laminar*, which might be thought of as being similar to honey flowing out of a jar. If the value was 2.0, the flow would be considered to be fully *turbulent*. (Laminar and turbulent flow are discussed at greater length in Rheology chapter 6 as the flow characteristics have important implications regarding hole cleaning, the subject of that chapter.) The reason we must measure the flow slope (or exponent u in the power law relationship) is that for virtually all parts of a wellbore (excluding the bit nozzle flow), the flow is neither fully laminar nor fully turbulent—it is somewhere in-between (called *transitional*), and we cannot predict accurately where it is, even with contemporaneous surface rheology measurements. Predicting this flow exponent 2 weeks or 2 months prior to spudding the well with both accuracy and repeatability is even less likely, and given today's state-of-the-art, extremely difficult.

2.4.2 Understanding the pressure-flow rate operating window and parasitic losses

To best understand the big picture of hydraulics, consider Fig. 2.6 depicting the operating window in a flow rate—pressure space log—log plot.
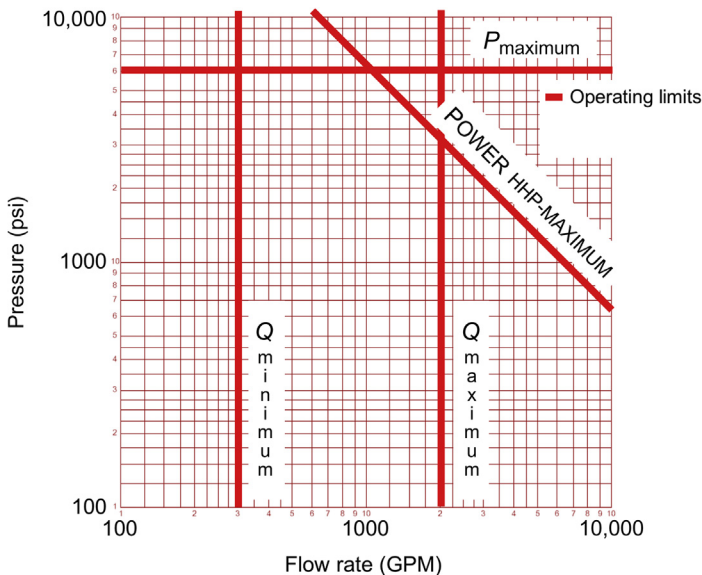

Figure 2.6 Log—log plot of drilling hydraulics operating window. *Courtesy: Texas Drilling Associates.*

To properly understand the beneficial use of hydraulic energy, it is instructive to understand the creation of and the use of energy in the pumping system. While some of the use of energy is productive, other uses are not and become, in essence, wasteful. Unfortunately, we cannot completely eliminate the wasted energy, so we must endeavor to reduce it as best as is possible.

Circulating-system pressure losses, P_{CIRC}, represent the pressure losses in all of the circulating system except for the bit (surface connections, rotary hose, kelly, drill pipe—inside and outside, and drill collars—inside and outside).

A thorough understanding of the series of figures below will solidify the fundamental problem most wells face today with too much "wasted" energy (or pressure losses) and too little productive energy used in the form of bit nozzle pressure losses.

In Fig. 2.6, a typical operating space for the rig-pumping system is shown. In this depiction, the maximum flow rate is 10,000 GPM and the maximum pressure is 10,000 psi. However, the constraints imposed by the well and by each individual rig's equipment will significantly reduce the operating range, both in terms of available maximum pressures and maximum flow rates.

The top horizontal red line, shown at 6000 psi in the figure, represents a typical maximum available standpipe pressure. Actual rig pressure ratings are used, which commonly range from 2000 psi for a small older rig to 10,000 psi for a new drillship. This maximum standpipe pressure may be thought of as the weakest link in the proverbial chain of pressure-handling equipment. If all of the components are rated at 10,000 psi, except the rotary hose that is rated at 5000 psi, then the maximum standpipe pressure would only be 5000 psi.

For most rigs, especially newer ones, this weak link will be determined by the pump liners being utilized, or more correctly, the pressure relief or "pop-off" valve settings on the pumps (that protect those liners from overpressure). Since the liners may be changed, the maximum standpipe pressure line may change over the course of drilling a well.

In addition to pump liners and associated pop-off or pressure protection equipment ratings and settings, there are other potential weak points in rig circulating systems, typically more commonly found in older rigs where wear and tear of equipment is more of an issue. One limiting factor could be the rating (or derating) of the physical piping system on the surface. It could have been rated at, for example, 5000 psi originally, but then due to corrosion and inspections it may be derated to 4500 psi or less.

Flexible piping segments, such as a kelly (or rotary) hose, could also be the weakest link in the pressure chain, as could valves, swivels, or any other component.

Interestingly, this maximum standpipe limit is not limited only by the hardware but may also be limited by operating procedures or even the legally binding agreement or contract between the operator (such as Anadarko, Chevron, CNOOC, ExxonMobil, Petrobras, Shell, etc.) and the drilling contractor (such as Transocean, Diamond, Parker, Rowan, Brasdril, etc.). It is becoming more common for drilling contractors to procedurally limit the maximum pressure they are willing to subject their company-owned-and-maintained pumping equipment to 90% or 95% of the original equipment manufacturer rating in an attempt to ensure longer lifetimes of the consumable and capital equipment components.

The leftmost vertical red line, labeled $Q_{MINIMUM}$, represents the minimum *operating* flow rate that we are willing to pump. This is not to be confused with the well control—related slow circulation rate (SCR, sometimes called slow pump rate or SPR), which could be substantially lower than the $Q_{MINIMUM}$ line.

This minimum flow rate line is similar in concept to the maximum standpipe pressure line in which the wellbore hydraulics designer takes the *highest* of all possible flow rate minimums to use as that *minimum* flow rate. The highest required minimum flow rates at this writing are typically caused by limitations on MWD, LWD, or other BHA-located equipment that requires pressure and/or flow to operate, or by limitations on what is believed to be needed to ensure good hole cleaning.

The rightmost vertical line, labeled $Q_{MAXIMUM}$, is the *smallest* of all possible limits on flow rate. These are typically also downhole tool related but can also be a limit on the maximum speed the pump is designed to run (or as before with pressure limits, an agreed contractual restriction on that speed).

Some personnel may wish to limit the upper flow rate due to concerns about washing out the hole. This author strongly disagrees with that assessment for most (but not all) drilling situations. For further discussion on this, please see the section in the Pressure Losses chapter on hole washouts.

The angled red limit line at the upper right of the figure (which always has a slope of -1 or -45 degrees) is the limit on available delivered hydraulic horsepower for the interval of the hole that is being designed. This limit is the smallest limit of various equipment (or

operating rules or legal contracts). Examples of typical limits are limits on the prime movers (for smaller rigs, typically found in land operations), the electric motors driving the pumps, or the rated input horsepower of the pump crankshaft *derated by the mechanical and volumetric efficiency* as described in Section 2.3.4 and later in the Pumps chapter 8.

Recall that hydraulic horsepower is calculated (in customary US Oilfield units) from the equation

$$HHP = \frac{P \times Q}{1714} \tag{2.15}$$

This relationship results in the hydraulic power line having a slope of -1 or down 45 degrees in a log–log plot of flow rate and pressure. The location of this line can vary up to the intersection of the maximum pressure limit line and the maximum flow rate limit line but cannot exceed this intersection. This becomes essentially a hybrid hydraulics "triple limit" point, where the simultaneous limits of maximum flow rate and maximum pressure can be used to compute the maximum hydraulic power available:

$$HHP_{MAXIMUM} = \frac{P_{MAXIMUM} \times Q_{MAXIMUM}}{1714} \tag{2.16}$$

The next step in our journey of understanding wellbore hydraulics as related to bit nozzle selection is to consider the different parts of the wellbore that consume the pressure stored in the drilling fluid. Generically, they consist of four classic divisions:

- surface equipment;
- drill string (inside, including both drill pipe and the BHA);
- bit pressure drop; and
- annulus [including all different geometry annuli as the outside diameter (OD) of the drill string changes and the hole diameter (or inside casing diameter or riser inside diameter (ID)] changes.

The next figure builds on the prior one but includes an upwardly sloped line from roughly the lower left to the upper right. This upwardly sloped line represents all of the above pressure losses, *except the bit pressure drop*. For bit nozzle selection and understanding hydraulics, we will refer to this upwardly sloped line as the circulating-system pressure losses, P_{CIRC}.

More memorably perhaps, we will refer to this as the "wasted energy" or "wasted pressure" line, since pressure losses spent flowing through the surface equipment, the drill string, and back up the annulus do not

contribute appreciably to drilling rate and may actually slow the ROP. That being said, there are valid uses of the pressure in these areas, primarily

- To simply move the drilling fluid from the surface to the bit and back to the surface again.
- To power downhole "jewelry" such as mud motors, MWD, and LWD equipment. All such equipment losses (or valid uses of hydraulic energy as you may prefer) are included in the upwardly sloping P_{CIRC} line.

The slope of the green line (P_{CIRC}) in Fig. 2.7 must lie between 1.0 and 2.0.

That slope value is used in equations below, designated with the symbol u.

Since flow through an increased length of pipe increases the pressure drop through the pipe, the P_{CIRC} line moves up the page vertically as the well is deepened. Similarly, as the drilling fluid density or rheologies increase, the P_{CIRC} line also moves up the page. Hence, the line represents the P_{CIRC} or wasted pressure at a particular point in the wellbore. Over time and changes in the wellbore, the line's vertical position
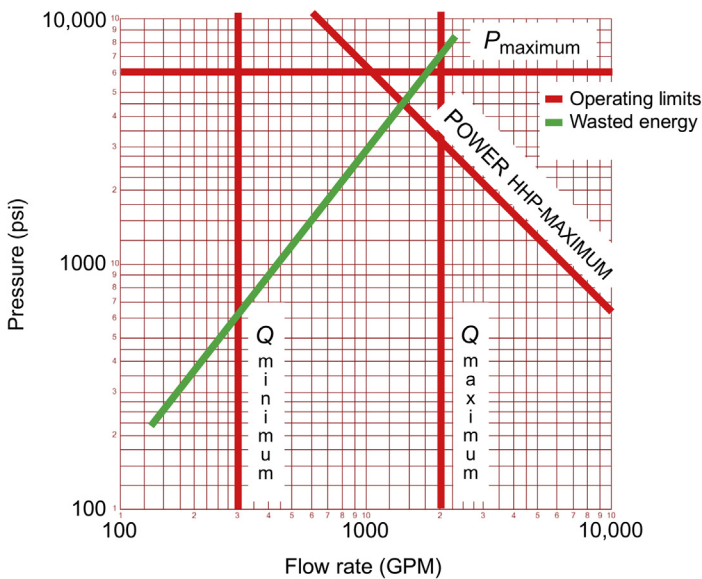

Figure 2.7 P_{CIRC} (or wasted energy) on the log−log operating window. *Courtesy: Texas Drilling Associates.*

changes, and its slope may change slightly, though always remaining in the range between 1.0 and 2.0.

It is important to reiterate that the positive-sloped line represents the physics of the fluid mechanics. Its vertical position and slope at a given point (or time) in the wellbore cannot be easily or quickly changed, if at all. If a driller pumps faster, the pressure required to pump, without a bit even screwed onto the bottom of the drill string (which is, in essence, what this P_{CIRC} line represents), is going to go up accordingly.

The only available pressure that can be used across the bit nozzles is the difference between the upper horizontal P_{MAXIMUM} line (or perhaps the -1 sloped Power$_{\text{MAXIMUM}}$ line at the upper right if not at the triple limit point), and this wasted energy or P_{CIRC} line. Inspection of the graph quickly shows that as flow rate is increased more and more, correspondingly less and less pressure drop is available to dedicate to the bit nozzles and hence bottom hole cleaning. In the extreme, when the P_{CIRC} line *reaches* the -1 sloped Power$_{\text{MAXIMUM}}$ line or upper horizontal P_{MAXIMUM} *limit line, zero pressure is available to expend across the bit and the driller increasing the speed control setting for the pump will have no effect.* As the pressure drop across the bit reduces toward zero, drilling rate can plummet in the case of tricone bits, and torque can escalate in the case of PDC bits. In both bit types, efficiency is sacrificed and bit life will likely suffer accordingly.

2.5 OPTIMUM NOZZLE AND FLOW RATE SELECTION

To actually select the nozzles themselves, there are several relatively straightforward ways to do so, depending on the accuracy desired. In all cases, however, one should strive to optimize hydraulics AND drilling rate together. In most cases, this can be accomplished by first optimizing hydraulics and then experimentally determining the founder point so drilling rate can be optimized.

First, there are two primary bit pressure loss optimization techniques, one based on optimizing hydraulic horsepower (HHP) at the bit and the second based on optimizing hydraulic JIF at the bit $\left(\text{JIF}_{P_{\text{MAX}}}\right)$. Each has powerful arguments and champions in the industry. Derivations and a fuller discussion of each are treated later, but the two methods result in a slightly different optimum pressure drop. Since all of the pressure losses in the system are either categorized as being across the bit or the circulating

system, one can optimize based on either part. For our practical calcula-tion purposes, the optimum pressure drop across the bit, $\Delta P_{\text{BIT OPT}}$, and the *complementary* optimum circulation system losses, $\Delta P_{\text{CIRC OPT}}$, for the two cases are given in Table 2.1.

Note that the optimum equations in the above table are for the case where the limiting factor is maximum standpipe pressure. If the limiting factor was maximum available power, the equations would be modified slightly to reflect that the maximum available pressure would no longer be the absolute maximum standpipe pressure, P_{MAX}, but would decline with increasing flow rate. Though not often used in practice, this $\text{JIF}_{\text{HHPLIMIT}}$ is also shown in the optimization equation table. The full derivation of these equations is contained in this chapter's appendix.

Depending on the value of the slope of P_{CIRC} (the exponent in the power law equation), this results in a slightly different percentage of pressure drop that should be reserved for the bit nozzles, as shown in Table 2.2.

Inspection of the optimum bit pressure drop equations or the table shows that the method based on HHP (rightmost column) will result in a higher bit pressure drop than the one based on JIF. An accurate method for determining the correct value of *u* for any particular wellbore and time is given later in this chapter.

Further note that at typical values of *u* found in modern wellbores (e.g., 1.8), the corresponding bit pressure drop would be 47.4% for the case of JIF optimization and 64.3% in the case of HHP optimization.

For example, if the standpipe pressure was limited to 6000 psi, the JIF case would put 47.4% or 2844 psi across the bit nozzles. For the HHP case, the 64.3% translates to 3858 psi across the nozzles. This latter value, while theoretically accurate if optimizing with HHP, is unlikely to be practical or achievable in the field, as the minimum flow rate limit would typically be higher than what would result from this optimization criteria alone.

For more discussion on nonoptimum conditions, please see Section 2.16.

Note that for the drillers' hydraulic method, it is assumed that the lim-iting case for the hydraulics operating space is the maximum standpipe pressure. This assumption is typically suitable for intermediate and deep hole sections where hydraulics optimization is most important.

The simplest method to optimize hydraulics consists of a choice (being largely a function of the bit type), followed by straightforward mathematics. As discussed below, due to pressure recovery effects, a *tricone bit* typically benefits more from increased pressure drop across the bit (or velocity through the bit nozzles). A *PDC bit*, having nozzles closer to the rock and being more sensitive to thermally accelerated cutter wear, typically benefits

Table 2.1 Optimization equations for different criteria. Note complementary nature of right two columns. (Some texts and papers use other symbols for "u" exponent. It was originally picked by Dr. Leon Robinson as it was the exponent that was "unknown" prior to calibration of the well.)

Optimization region	Criteria	$\Delta P_{\text{BIT OPT}}$	$\Delta P_{\text{CIRC OPT}}$
1	JIF_{PMAX}	$\Delta P_{\text{BIT OPT}} = \left(\frac{u}{u+2}\right) \times P_{\text{MAX}}$	$\Delta P_{\text{CIRC OPT}} = \left(\frac{2}{u+2}\right) \times P_{\text{MAX}}$
2	HHP	$\Delta P_{\text{BIT OPT}} = \left(\frac{u}{u+1}\right) \times P_{MAX}$	$\Delta P_{\text{CIRC OPT}} = \left(\frac{1}{u+1}\right) \times P_{\text{MAX}}$
3	$\text{JIF}_{\text{HHPLIMIT}}$	$\Delta P_{\text{BIT OPT}} = \left(\frac{u+1}{u+2}\right) \times P_{\text{HHPMAX}}$	$\Delta P_{\text{CIRC OPT}} = \left(\frac{1}{u+2}\right) \times P_{\text{HHPMAX}}$

where.
 JIF = Jet Impact Force, pounds force
 HHP = Hydraulic Horsepower, horsepower
 $\Delta P_{\text{BIT OPT}}$ = Optimum pressure loss across the bit nozzles, psi
 $\Delta P_{\text{CIRC OPT}}$ = Optimum circulation system pressure losses, (all losses except those across bit nozzles, psi),
 P_{MAX} = Maximum stand pipe pressure, psi
 u = Exponent in the power law equation; slope of the circulation system loss on Log-Log coordinates, dimensionless
 ("u" was chosen as it is both "unique" for each well and is "unknown" until calibrated)
 API 13D, 2010, Rheology and Hydraulics of Oil-Well Fluids, API Recommended Practice 13D, sixth ed, May 2010, p 53.

Table 2.2 Percentage of available pressure to optimally spend across the bit nozzles

		JIF P_{MAX} limited	HHP P_{MAX} limited	JIF HHP limited
P_{CIRC} slope or "u"	Flow characterization	$\frac{u}{(u+2)}$	$\frac{u}{(u+1)}$	$\frac{(u+1)}{(u+2)}$
1.00	Fully laminar	33.3%	50.0%	66.7%
1.10	Transitional	35.5%	52.4%	67.7%
1.20	Transitional	37.5%	54.5%	68.8%
1.30	Transitional	39.4%	56.5%	69.7%
1.40	Transitional	41.2%	58.3%	70.6%
1.50	Transitional	42.9%	60.0%	71.4%
1.60	Transitional	44.4%	61.5%	72.2%
1.65	Transitional	45.2%	62.3%	72.6%
1.70	Transitional	45.9%	63.0%	73.0%
1.75	Transitional	46.7%	63.6%	73.3%
1.80	Transitional	47.4%	64.3%	73.7%
1.82[a]	Transitional	47.6%	64.5%	73.8%
1.85	Transitional	48.1%	64.9%	74.0%
1.86[a]	Transitional	48.2%	65.0%	74.1%
1.90	Transitional	48.7%	65.5%	74.4%
1.95	Transitional	49.4%	66.1%	74.7%
2.00	Fully turbulent	50.0%	66.7%	75.0%

[a]1.82 and 1.86 are *u* values commonly built in to "black box" software packages based on extensive field measurements taken in the 1950s. Given new mud technologies and higher mud weights today compared to the 1950s, they may not be suitable exponent values now.

from higher flow rates compared to tricones. Hence, the first step is simply to identify the bit type and use the appropriate pressure drop factor.

2.6 DRILLER'S HYDRAULIC METHODS

2.6.1 Driller's hydraulic method—PDC bits: Use hydraulic impact

For PDC bits, JIF is the preferred optimization technique. If data is not available for calibration, a power law exponent of 1.7[10] can be reasonably assumed, yielding an optimum bit pressure drop of

[10] Note that different operators, drilling fluid companies, and drilling contractors may use slightly different values of this power law exponent, depending on their experiences with particular well types and drilling fluids. Without additional data, a range of 1.6−1.9 would be most commonly used.

$$\Delta P_{\text{BIT}} = 0.46 \times P_{\text{MAX}} \qquad (2.17)$$

(Where pressure and flow rate data is available, the 0.46 in the above equation may be shifted as described in the engineer's method below.)

For example, if a rig were fitted with a 6000 psi pumping system, the optimum pressure drop across a PDC bit should be 46% of this or 2760 psi.

Then, using the desired flow rate (chosen or computed), the nozzle flow area may be calculated using the relationship:

$$\Delta P_{\text{BIT}} = \frac{\text{MW} \times Q^2}{12,775 \times \text{TNFA}^2} \qquad (2.18)$$

And its rearranged counterpart,

$$\text{TNFA} = \sqrt{\frac{\text{MW} \times Q^2}{12,775 \times \Delta P_{\text{BIT}}}} \qquad (2.19)$$

where ΔP_{BIT} is the pressure drop across the bit nozzles (psi); MW is the mud weight (ppg); Q is the flow rate (GPM); TNFA is the total nozzle flow area (in.[2]) (sometimes simply TFA).

Note: The bit pressure drop equation in its two primary forms has changed slightly over the years, as more data has become available.

When the TNFA (or TFA in some texts) is known, sizing of the nozzles may be done via a lookup table such as Table 2.3.

Note that for *identically sized nozzles*, the nozzle flow area may be calculated by the equation:

$$\text{TNFA} = \left[\frac{(\text{nozzle size})^2}{1303.8} \right] \times \text{number of nozzles} \qquad (2.20)$$

If finding the identically sized nozzle diameter when the desired TNFA is already known, use

$$\text{Nozzle size} = \sqrt{\frac{\text{TNFA} \times 1303.8}{\text{number of nozzles}}} \qquad (2.21)$$

where TNFA is the total nozzle flow area (in.[2]).

For a fuller discussion of hydraulic JIF, please see the derivations section of the Appendix at the end of this book.

Table 2.3 Conventional area of different numbers of same-sized nozzles

Diameter, 1/32 of inch[a]	Number of nozzles									
	1	2	3	4	5	6	7	8	9	10
7	0.038	0.075	0.113	0.150	0.188	0.225	0.263	0.301	0.338	0.376
8	0.049	0.098	0.147	0.196	0.245	0.295	0.344	0.393	0.442	0.491
9	0.062	0.124	0.186	0.249	0.311	0.373	0.435	0.497	0.559	0.621
10	0.077	0.153	0.230	0.307	0.383	0.460	0.537	0.614	0.690	0.767
11	0.093	0.186	0.278	0.371	0.464	0.557	0.650	0.742	0.835	0.928
12	0.110	0.221	0.331	0.442	0.552	0.663	0.773	0.884	0.994	1.104
13	0.130	0.259	0.389	0.518	0.648	0.778	0.907	1.037	1.167	1.296
14	0.150	0.301	0.451	0.601	0.752	0.902	1.052	1.203	1.353	1.503
15	0.173	0.345	0.518	0.690	0.863	1.035	1.208	1.381	1.553	1.726
16	0.196	0.393	0.589	0.785	0.982	1.178	1.374	1.571	1.767	1.963
18	0.249	0.497	0.746	0.994	1.243	1.491	1.740	1.988	2.237	2.485
20	0.307	0.614	0.920	1.227	1.534	1.841	2.148	2.454	2.761	3.068
22	0.371	0.742	1.114	1.485	1.856	2.227	2.599	2.970	3.341	3.712
24	0.442	0.884	1.325	1.767	2.209	2.651	3.093	3.534	3.976	4.418
26	0.518	1.037	1.555	2.074	2.592	3.111	3.629	4.148	4.666	5.185
28	0.601	1.203	1.804	2.405	3.007	3.608	4.209	4.811	5.412	6.013
30	0.690	1.381	2.071	2.761	3.451	4.142	4.832	5.522	6.213	6.903
32	0.785	1.571	2.356	3.142	3.927	4.712	5.498	6.283	7.069	7.854

[a]Not all sizes are available as standard nozzles.

2.6.2 Driller's hydraulic method—tricone bits: Use hydraulic horsepower

For Tricone bits drilling in moderate to hard formations, hydraulic horsepower (HHP) is the preferred optimization technique. As before a value of the power law exponent of 1.7, in the absence of calibrating data, is quite reasonable. Referring to Table 2.2 for the hydraulic power optimization technique, the optimized pressure loss across the nozzles is 63%, hence

$$\Delta P_{\text{BIT}} = 0.63 \times P_{\text{MAX}} \qquad (2.22)$$

If the same example rig with a 6000 psi pumping system were being used, the optimum pressure drop across a tricone bit should be 63% of this or 3780 psi. As with the case of jet impact, this level may or may not be entirely achievable.

For a fuller discussion of hydraulic horsepower optimization, please see the derivations section of this chapter.

As with the JIF optimization, once the TNFA has been calculated, then the sizing of the nozzles may be done via a lookup table such as Table 2.3 or with the equation previously given for identically sized nozzles.

2.7 ENGINEERS' HYDRAULIC METHOD—CALIBRATE CIRCULATION PRESSURE (ΔP_{CIRC}) TO DETERMINE EXPONENT "U"

An improvement to both of the above simplified techniques can be made by calibrating the overall exponent "u" of the nonbit portion of the flow, commonly called circulation pressure or ΔP_{CIRC}. This is the pressure required to circulate through everything except the drill bit nozzles—loosely equivalent to what the standpipe pressure would read if a drill crew tripped the BHA and drill string to bottom but had forgotten to put an actual bit on the bottom of the BHA.

No driller would ever actually trip into the hole open-ended just to calibrate a flow exponent for an engineer in the office. Hence, the solution is to mathematically remove the bit pressure drop from the total pressure drop as measured on the standpipe pressure gage or transducer, which results in the remainder being the circulating pressure drop, leaving the circulating pressure drop (ΔP_{CIRC}).

This calibration itself can be done with minimal effort with satisfactory results, or with greater effort and improved results. The simplified calibration is to simply use the slow circulation rate (SCR) flow rate and pressure obtained at least once each tour or more frequently (for well-control readiness purposes), combined with the usual operating flow rate and pressure used during drilling. These two points will define a curve[11] on a Cartesian plot or a line on a log–log plot. The slope of the line in the log–log plot becomes

$$u = \frac{\log P_{\text{OPER}} - \log P_{\text{SCR}}}{\log Q_{\text{OPER}} - \log Q_{\text{SCR}}} \tag{2.23}$$

or

---

[11] The general relationship, given by a power law approximation, is $P = k \times Q^u$. The "u" exponent must lie between 1.0 for a fully laminar flow case and 2.0 for a fully turbulent flow case. We almost never have fully laminar or turbulent flow, and the exponent "u" often falls in the range of 1.4–1.9. As measured with a linear ruler on a true log–log plot, the slope of the measured straight line would thus be expected to be between 1.4 and 1.9, and cannot physically be less than 1.0 or greater than 2.0.

$$u = \frac{\log\left(\dfrac{P_{\text{OPER}}}{P_{\text{SCR}}}\right)}{\log\left(\dfrac{Q_{\text{OPER}}}{Q_{\text{SCR}}}\right)} \tag{2.24}$$

where u is the resulting slope of the P_{CIRC} line if it were plotted on log–log paper; P_{OPER} is the operating rate standpipe pressure (psi); P_{SCR} is the SCR pressure (psi); Q_{OPER} is the operating rate flow rate (GPM); Q_{SCR} is the SCR flow rate (GPM).

This slope may also be literally measured with a ruler if the plot is reduced to an accurate log–log paper plot. If printing from a computer-generated plot, care must be taken to ensure that the vertical and horizontal axes are identical in scale on the as-printed log–log plot.

To accomplish this further improvement on the engineers' hydraulic method, we need additional and/or more accurate measurements. Given suitable data, we can very accurately determine the ΔP_{CIRC} line and can effectively calibrate out all of the uncertainties (mud properties, geometry, flow rate, etc.). The only thing that prevents us from doing so is that we do not ordinarily have an open-ended drill string in the hole. Instead, we have a drill string with a very expensive and high-technology drill bit (PDC, natural diamond, or tricone) fitted with tungsten carbide bit nozzles.

Note, however, that the wasted energy line *is the same with or without a bit.* Therefore, if we can reasonably calculate the bit pressure drop (thought to be one of the more accurate of hydraulic calculations), then we can subtract that calculated value from the total standpipe pressure and hence obtain the wasted energy line and then optimize accordingly. The effect of the bit pressure drop is calculated and removed from our measurements. In essence, we can unscrew the drill bit downhole, mathematically.

The best and most accurate way to optimize hydraulics is to "listen to the well." By this we are able to calibrate out the inherent inaccuracies of the theoretical and computational methods, resulting in optimizations that match the "real world." We call this technique the OCHO technique, which is both an acronym for Ongoing Continuous Hydraulics Optimization and a reminder that there are eight simple steps in the procedure.

Fortunately, the OCHO technique readily enables one to tailor the hydraulics program to the wellbore as it is being drilled. The eight steps are described below.

Eight abbreviated steps for Conducting an OCHO Hydraulics Calibration of the Wellbore and Selecting Nozzles and Flow rates according to the particular operating conditions of the well at hand.

1. Calibrate rig pumps to get an accurate relationship between strokes per minute (SPM) and GPM, or other units such as metric/SI. Measure the rate of liquid level drop in the slugging tank (or other convenient tank or tank partition) while pumping downhole through the drill bit. Account for air in the drilling fluid to calculate the volume of liquid moved by the rig pumps.

2. Just before tripping for a new bit, circulate at several pump rates and measure accurately the standpipe pressure and flow rate at each rate used. Note that sufficient time should be allowed for the wellbore to stabilize before taking the official data readings—depending on the drilling fluid and size of the wellbore this could be a few minutes. Note also that the data does not need to be perfectly spaced out. For example, if you asked the driller to run the pumps at 40, 60, 80, and 100 SPM, he does not have to hit those rates exactly. 35, 63, 82, and 105 SPM would be completely acceptable. This latter note is important since it may take several minutes for the well to stabilize, and we do not want the driller taking excessive time trying to tweak the pump rate to exactly what is asked.

3. Calculate and subtract the bit nozzle pressure drops from the measured standpipe pressures for each measured pair of standpipe pressures and flow rates. (This gives the circulating pressure loss through the system, except for the bit nozzles.)

4. Plot the circulating pressure loss as a function of flow rates on log—log paper.[12,13]

5. Draw the best straight line through the circulating pressure losses.[14] Measure the exponent "u" of the power law equation (or the slope of the circulating pressure line on log—log scales) with a ruler or scale.[14]

6. Adjust the placement of this circulating pressure loss line (or wasted energy) to take into account changes in depth and mud weight for the upcoming bit run.[14]

7. Calculate the optimum pressure loss and corresponding flow rate through the bit to give either the maximum hydraulic force or the maximum hydraulic power at the bit as preferred.[14]

8. Calculate nozzle sizes for the next bit.[14]

[12] These instructions are speaking to procedure. Most engineers and field personnel will eventually automate this with a suitable spreadsheet or fit-for-purpose software package or app.

[13] This is procedurally speaking. Most engineers will eventually automate this with a suitable spreadsheet or fit-for-purpose software package.

Summarizing, the OCHO technique collects standpipe pressure data for various flow rates, subtracts the bit nozzle pressure loss to yield the wasted energy line. Then the optimized operating point is computed, which fixes the flow rate and desired bit pressure drop, so that the TNFA of the nozzles can be computed and nozzles selected accordingly.

What does this "OCHO" technique involve? Basically, to implement the OCHO technique, one measures pressures, flow rates, and drilling fluid properties; and knowing what the geometry is already, one can tailor the well hydraulics operating conditions to the well's actual as–drilled conditions. In essence, one "listens" to a well in a manner not unlike how one "listens" to the gas cut to decide if the mud weight is correct. After taking the measurements, some straightforward but tedious calculations are performed, hopefully made easy by personal computers or other digital devices. The result is optimized hydraulics based on the actual wellbore, the actual rig equipment and the actual drilling fluid properties!

Properly done, this technique will correctly determine the flow rates and associated pressure drops to within the accuracy of your gages nearly every time! Rather than a theoretical approach with a given set of fluid mechanics equations that may not quite apply, have imperfect assumptions, or even be obsolete, this is a clear "Edisonian Approach" to problem solving is often stated as "One test is worth a thousand expert opinions." In the view of the author, this approach will never be obsolete and at the least can always be used to calibrate even sophisticated models successfully and accurately.

2.8 ONGOING CONTINUOUS HYDRAULICS OPTIMIZATION CALIBRATION EXAMPLE

For brevity, we assume the pumps have been calibrated and the driller has taken the data (OCHO steps 1 and 2). The collected data, with SPM converted to GPM, is shown below in the first two columns of Table 2.4.

The right two columns represent OCHO step 3, where the bit pressure drop is calculated (column 3) and then subtracted from the standpipe pressure to yield P_{CIRC} (column 4), representing P_{CIRC}, the wasted pressure loss in the system, or everything except the bit nozzle pressure drop.

To calculate column three, the ΔP_{BIT}, the equation below is used.

Table 2.4 Example OCHO wellbore hydraulics calibration data

GPM (calculated from SPM and pump efficiency)	Standpipe pressure (measured)	ΔP_{BIT} (calculated)	ΔP_{CIRC} or the wasted energy line (calculated)
140 (SCR)	480	72	408
227	1200	191	1009
314	2200	367	1833

GPM, gallons per minute; *SCR*, slow circulation rate; *SPM*, strokes per minute.
Source: Courtesy: Texas Drilling Associates.

$$\Delta P_{\text{BIT}} = \frac{\text{MW} \times Q^2}{12{,}042 \times C_D{}^2 \times \text{TNFA}^2} \tag{2.25}$$

The primary issue over recent years has been what the appropriate value of C_D should be (the coefficient that incorporates *both* the nozzle efficiency and the nozzle discharge coefficient into a single term C_D).

If the pressure recovery effect is included, the bit pressure drop equation becomes

$$\Delta P_{\text{BIT}} = \frac{\text{MW} \times Q^2}{12{,}042 \times (1.03^2) \times \text{TNFA}^2} \tag{2.26}$$

where ΔP_{BIT} is the pressure drop across the nozzles (psi); MW is the mud weight (ppg); Q is the flow rate (GPM); and TNFA is the total flow area of the nozzles, in square inches. Note that this TNFA term is squared in the equation.

This equation is slightly different from older and perhaps more familiar equations in that the nozzle coefficient of 0.95 has been replaced by a nozzle coefficient of 1.03 for the newer nozzles and bits. This is an attempt to quantify the pressure recovery effect observed from field measurements. This coefficient was also independently validated in controlled laboratory tests.[4,5] Note that in some companies, the 12,042 constant and the nozzle coefficient are combined into a single term for convenience.

$$\Delta P_{\text{BIT}} = \frac{\text{MW} \times Q^2}{12{,}775 \times \text{TNFA}^2} \tag{2.27}$$

Further, note that API RP 13D committee members did not agree on an exact value of the nozzle discharge coefficient (and associated pressure recovery) but did recognize the problems facing hydraulics designers. The API RP 13D committee modified their recommended bit pressure drop equation to

$$\Delta P_{\text{BIT}} = \frac{\text{MW} \times Q^2}{12{,}042 \times C_V{}^2 \times \text{TNFA}^2} \tag{2.28}$$

The committee stopped short of endorsing a 1.03 value for the C_V (same as C_D in this text). In the words of the API 13D subcommittee,

"The discharge coefficient C_V, varies with the diametric ratio (output diameter/input diameter) and the fluid Reynolds numbers passing through the nozzles. There is significant evidence to update the long-standing C_V, value of 0.95 to 0.98, given the flow rates, drilling fluid densities, and nozzle ratios typical to oilfield operating conditions.

$C_V = 0.98$

In field and laboratory test the flow not only through the nozzle but also the flow past the nozzle is considered when determining C_V. This results in a discharge coefficient of $C_V = 1.03$ for roller cone bits. The design of the bit has in this case an impact on the discharge coefficient. Especially for PDC bits a single C_V has not been determined yet. The reported C_V ranges between 0.89 and 0.97. Therefore, a final recommendation for the discharge coefficient considering the flow past the nozzle cannot be made. Further tests are necessary to resolve the issue." [sic][14−16]

Needless to say, additional research is needed in this area, particularly with respect to the pressure recovery effects and its relationship to mud weight, high shear rate viscosities, and drill bit/bit nozzle geometries.

OCHO steps 4−6 are shown graphically in Fig. 2.9, where the wasted energy line is plotted, a best fit straight line is drawn through the points, and where the slope of the line measured linearly (i.e., with a ruler, as is also shown in Fig. 2.9).

Note that if calculating slope numerically either with a calculator or in a spreadsheet, two cautions are in order.

First, the author strongly encourages some sort of *visible plotting of the data* be incorporated so that data integrity may be checked. Since the relationship between flow rate and pressure drop is an exponential one,

[14] API RP 13D, Rheology and Hydraulics of Oil-well Drilling Fluids, Upstream Segment, fifth ed., American Petroleum Institute, June 2006, p. 35.
[15] API RP 13D, Rheology and Hydraulics of Oil–well Drilling Fluids, Upstream Segment, fifth ed., American Petroleum Institute, June 2010, p. 34.
[16] T.M. Warren, Evaluation of jet-bit losses, SPE 17916, SPE Drill. Completion Eng. 4 (4) (1989) 335−340.

identification of spurious or outlying data points is difficult if one is simply inspecting numerical data without a graphical plot.

Second, if determining the slope numerically, one must be careful to take the log of the values to compute the slope as opposed to the values themselves. Reviewing, the conventional slope calculation would be found in a Cartesian plot using

$$\text{slope, } u = \frac{\text{rise}}{\text{run}} \tag{2.29}$$

$$u = \frac{\Delta y}{\Delta x} = \frac{y_2 - y_1}{x_2 - x_1} \tag{2.30}$$

However, for the exponential function, the slope is found by taking the log of each data pair value. If calculating based on the numeric values, the log of the values must be used.

$$u = \frac{\log y_2 - \log y_1}{\log x_2 - \log x_1} \tag{2.31}$$

or

$$u = \frac{\log\left(\dfrac{y_2}{y_1}\right)}{\log\left(\dfrac{x_2}{x_1}\right)} \tag{2.32}$$

For our example case, the slope was measured to be 1.62. This is considerably lower than the "standard" values used by many available computer software programs, which typically range from 1.8 to 1.9 or so. These larger values are artifacts of research conducted decades ago on drilling fluid systems of that day and do not accurately reflect modern drilling fluids in use today, generally speaking.

At this point, it must be reemphasized that the wasted pressure line constructed in Figs. 2.8 and 2.9 represents the entire circulation system except for the bit. It includes surface piping, all drill string components, and all return annuli. To flow at any flow rate across the x-axis (flow rate) will extract the corresponding amount of pressure (or energy) indicated on the y-axis (pressure).

2.9 OPTIMUM CONDITIONS-PRESSURE LIMITED

For most conditions of interest to most drillers, the rig will have a practical limit on pressure. If pressure drop across the bit is being
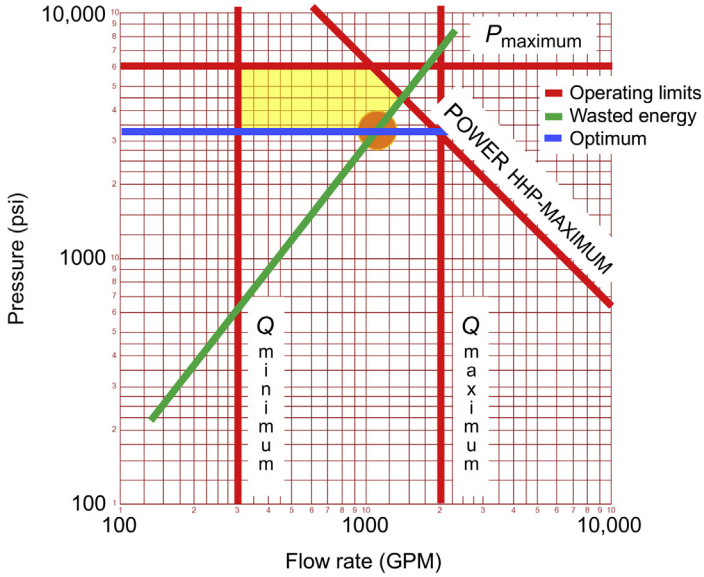
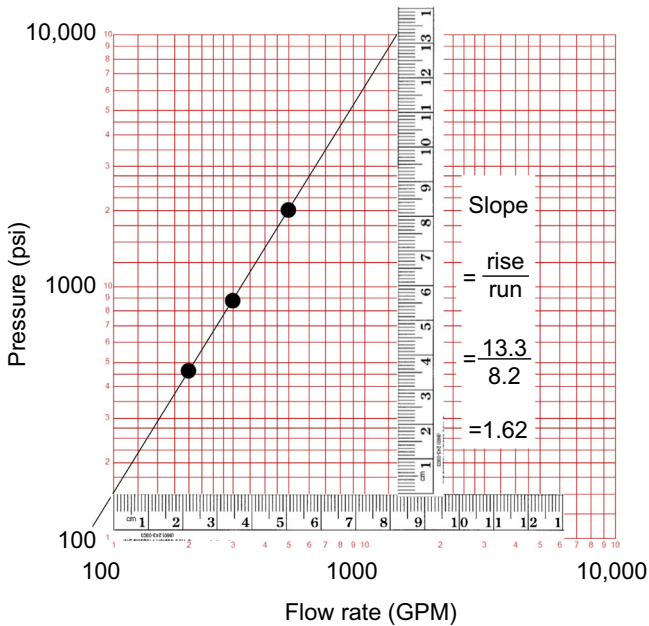**Figure 2.8** Flow rate/pressure operating space. *Courtesy: Texas Drilling Associates.*

Figure 2.9 Graphical measurement of slope (exponent *u*) on log−log data plot. *Courtesy: Texas Drilling Associates.*

optimized, both the optimum bit and the optimum wasted pressure can be calculated with the equations below, for JIF or hydraulic horsepower (HHP). For the interested reader, these are derived in the appendices and are now included in the approved API RP 13D[17].

Recall that for both the JIF and HHP approaches are two distinct regions, governed by different optimization equations. These respective optimization equations include for each case a complementary pair of equations--one equation for the optimum bit pressure drop and the second the optimum circulating system pressure losses or wasted energy. Table 2.5 shows these respective equations.

Note that the equations for any particular optimization scheme (JIF-1 and JIF-3, or HHP-1 and HHP-3) are complementary. The middle column equations give the optimum impact force or hydraulic horsepower across the bit, while the right column gives the corresponding optimum circulation system losses (i.e., the wasted energy or wasted pressure line P_{CIRC}) for the different mathematical cases.

Note also that there is a mathematical discontinuity between JIF-1 and JIF-3, that is interpolated at what has been termed the critical flow rate, or the flow rate where maximum standpipe pressure (the JIF-1 criteria) intersects with maximum available pump horsepower (the JIF-3 criteria).

Note: As a practical matter, the JIF-3 criteria are rarely met and are presented for completeness.

For OCHO step 7 illustrations, we go back to our example, where the slope (or value of the "u" exponent term in the above equations) is 1.62. The math then results in the bit optimization being 44.7% of standpipe pressure (or 1475 psi) for the JIF-1 criteria and 61.8% (or 2039 psi) for the HHP criteria. Conversely, the wasted pressure line at the optimum point would be $100 - 44.7 = 55.3\%$ and $100 - 61.8 = 38.2\%$ of standpipe pressure, respectively. Assuming the maximum standpipe pressure to be 3300 psi, these P_{CIRC} lines would be plotted horizontally at 1825 and 1261 psi. These values, along with the P_{MAX} of 3300, are shown in Fig. 2.10.

A full derivation of the optimization equations is located in the book Appendices. Additional excellent treatment is also found in the IADC Drilling Series "Drillers Knowledge Book"[18].

---

[17] API RP 13D, 2010, Rheology and Hydraulics of Oil-Well Fluids, API Recommended Practice 13D, sixth ed, May 2010.
[18] L. Robinson, J. Garcia, First Printing. Drillers Knowledge Book, first ed.IADC, 2015, 99−102.

Table 2.5 Jet impact force and hydraulic horsepower equations (note that optimum bit pressure loss and optimum circulation system loss are complementary)

Optimize type and region[a]	Optimum ΔP_{BIT}	Optimum ΔP_{CIRC} (or waste)
JIF–1	$\Delta P_{\text{BIT OPT}} = \left(\frac{u}{(u+2)}\right) \times P_{\text{MAX}}$	$\Delta P_{\text{CIRC OPT}} = \left(\frac{2}{(u+2)}\right) \times P_{\text{MAX}}$
JIF–3	$\Delta P_{\text{BIT OPT}} = \left(\frac{(u+1)}{(u+2)}\right) \times P_{\text{MAX HHP LIMIT}}$	$\Delta P_{\text{CIRC OPT}} = \left(\frac{1}{(u+2)}\right) \times P_{\text{MAX HHP LIMIT}}$
HHP–1	$\Delta P_{\text{BIT OPT}} = \left(\frac{u}{(u+1)}\right) \times P_{\text{MAX}}$	$\Delta P_{\text{CIRC OPT}} = \left(\frac{1}{(u+1)}\right) \times P_{\text{MAX}}$
HHP–3	$\Delta P_{\text{BIT OPT}} = \left(\frac{u}{(u+1)}\right) \times P_{\text{MAX HHP LIMIT}}$	$\Delta P_{\text{CIRC OPT}} = \left(\frac{1}{(u+1)}\right) \times P_{\text{MAX HHP LIMIT}}$

[a]API region or Case 3 is power limited, where standpipe pressure limit is a function of power available and flow rate. API region or Case 1 limited is maximum and constant standpipe pressure limit, as determined by equipment or contractual limits. Case 2 represents the mathematical discontinuity between these two, at the flow rate corresponding to both maximum standpipe pressure and maximum power available. JIF and HHP indicate the optimization technique, jet impact force (for PDC bits) or hydraulic horsepower (for tricones), respectively.
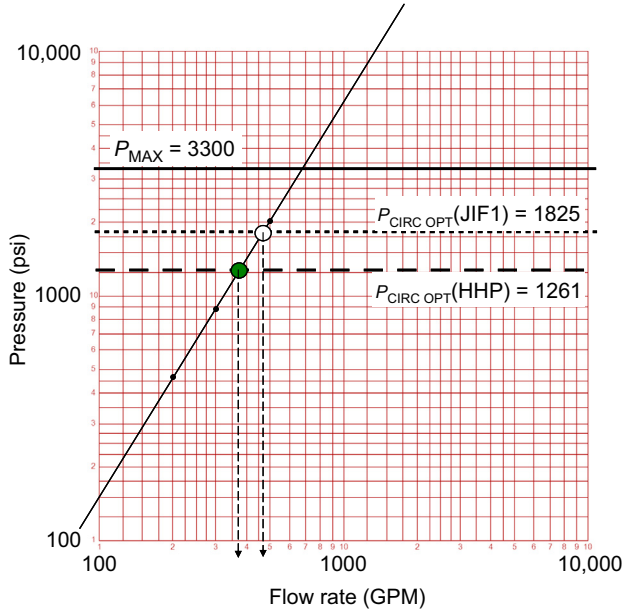
Figure 2.10 Comparison between JIF-1 and HHP-1 optimizations for maximum standpipe pressure (API region 1, Standpipe pressure limited case). *Courtesy: Texas Drilling Associates.*

For the JIF–1 criteria, the intersection of the theoretical optimum and the real–world waste pressure (P_{CIRC}) line occurs at approximately 465 GPM. For the HHP criteria, the intersection occurs at approximately 370 GPM.

2.10 SIZING THE NOZZLES

Now that the exponent "u" on the wasted energy line is known, leading us to the theoretically best place to operate, both in terms of pressure (or more precisely, velocity) and flow rates, it becomes a brief exercise to determine the actual nozzles for the next bit run, as per OCHO step 8. The bit pressure drop equation is rearranged to solve for the total nozzle flow area, TNFA, and is solved using the optimum conditions determined above.

The bit nozzle pressure loss equation becomes

$$\text{TNFA} = \sqrt{\frac{\text{MW} \times Q^2_{\text{OPTIMUM}}}{12,042 \times \left(1.03^2\right) \times \Delta P_{\text{BIT OPTIMUM}}}} \qquad (2.33)$$

or simpler,

$$\text{TNFA} = \sqrt{\frac{\text{MW} \times Q^2_{\text{OPTIMUM}}}{12,775 \times \Delta P_{\text{BIT OPTIMUM}}}} \qquad (2.34)$$

Going back to our example, for the JIF-1 criterion, this yields a TNFA of 0.3680 square inches results, and is satisfied best by a 12/32 in. and two 13/32 in. diameter nozzles.

For the HHP criterion, the TNFA is 0.2490 square inches, corresponding best to an 11/32 in. and two 10/32 in. nozzles.

Inspection of several examples such as the above, coupled with examination of nozzle size tables, will instruct the student that it is rare or perhaps truly never that a computed total nozzle flow area (TNFA) will be exactly met by nozzle combinations. This is due to the standardization and limited availability of the sizes of the nozzles, specifically, that they are manufactured only in certain standard sizes. However, the closeness of fit of the available nozzle combinations compared to the mathematically exact desired TNFA (and related flow rates and pressures) has been found to be quite sufficient by this author, and indeed, the drilling industry itself over the years.

Close examination of the Fig. 2.10 will make it clear that with the JIF-1 criteria, a higher flow rate and less pressure drop across the bit is achieved when compared to the HHP criteria. As a result, some find the JIF-1 to be most suited to conditions requiring more flow, such as PDC bits, and the HHP best suited to conditions benefiting from higher pressure loss (and hence jet velocity) across the bit nozzles, such as would be the case of roller cone bits.

2.11 PRESSURE RECOVERY DOWNSTREAM OF THE BIT NOZZLES

A phenomenon called "pressure recovery" with respect to pressure loss across downhole bit nozzles has been identified by the author. This pressure recovery effect causes the net bit pressure drop to be less than the theoretical and calculated value by a surprisingly significant amount and is not yet well understood by most drilling personnel. This effect has been measured conclusively in both laboratory and field environments. The magnitude of the pressure recovery varies with density of the drilling fluid, and/or plastic viscosity of the drilling fluid, but in the absence of

other data, the value of this recovery is assumed to be 15% (based on experimental data thus far, discussed later). This means that if the conventional calculations predict 1000 psi pressure drop across the bit nozzles, then the net pressure drop across the bit after the pressure recovery has occurred is 15% less than that, or 850 psi. Importantly, note that the additional 150 psi is additional annular pressure drop in excess of that conventionally calculated.

2.11.1 A brief history of the discovery

In the early 1980s, high speed measurements of downhole parameters were undertaken by a number of research entities, primarily led by large multinational operators. In these measurements, pressure was sometimes recorded, usually on the annulus side so that surge-and-swab pressures (fundamentally inertial in nature) and frictional pressures (increasing the ECD or in the wellbore above the hydrostatic level) could be examined. At least one group also measured internal pressure above the bit.

Prior to those measurements, it was a commonly held belief that the most accurate part of all wellbore hydraulic predictions (calculations) was that of the bit nozzle pressure drop. At that time, the bit pressure drop equation and the calculation of needed total nozzle flow area were expressed as below:

$$\Delta P_{\text{BIT}} = \frac{\text{MW} \times Q^2}{12{,}042 \times (0.95^2) \times \text{TNFA}^2} \tag{2.35}$$

$$\text{TNFA} = \sqrt{\frac{\text{MW} \times Q^2_{\text{OPTIMUM}}}{12{,}042 \times (0.95^2) \times \Delta P_{\text{BITOPTIMUM}}}} \tag{2.36}$$

Note that while the form of these equations is similar to those previously discussed, the combination of the nozzle discharge coefficient and the nozzle-efficiency coefficient was lower (0.95 in the equations immediately above). While there was slight variation here, overall, the number was lower.

As more bottom hole measurements were conducted, and follow-on laboratory measurements became available from highly controlled simulated downhole conditions, the additional measurements confirmed those of early researchers. It confirmed in essence that there were serious errors in the computed pressure drop (ΔP_{BIT}) across the bit nozzles.

Briefly, the measurements downhole were found to have less pressure drop across the nozzles than was predicted with conventional models.
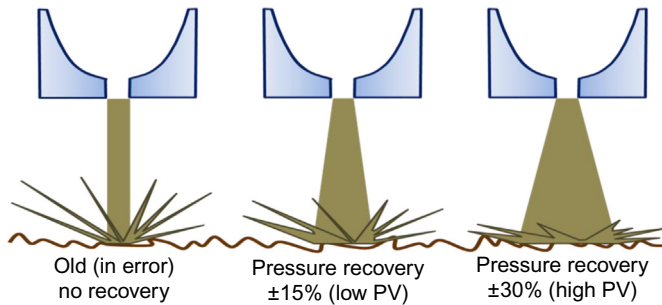
Figure 2.11 Pressure recovery effect. *Courtesy: Texas Drilling Associates.*

This lower pressure drop was thought to be a function of high shear rate viscosity, though the exact relationship was not determined at that time and remains an area rich in research potential. A higher high shear rate viscosity (typically measured as plastic viscosity or PV) would result in a higher error of actual versus predicted pressure drops across the nozzles, but the exact error versus PV was not modeled at the time.

As the researchers discovered in their investigation, the discrepancy between the measured and predicted values was traced to insufficient testing protocols dating back to the early 1950s. Pressure drops through simulated nozzles were measured in a sophisticated and exacting manner[19], but the experiments were flawed by the lack of true drilling fluid being used (the 1950s experiments used clear water), and more importantly, by the experimental setup, which caused the high velocity jet exiting the nozzles to be discharged into an air-filled chamber, rather than the one filled with liquid[21]. (One masters' student at Rice University did investigate submerged jets shortly after Eckel, but with minimal back pressure. That investigation did show a greater than 1.0 nozzle coefficient for some tests conducted, but the information was apparently not widely disseminated at the time[20].)

In the case of a submerged jet, the jet is slowed by viscous drag at the outer surface of the jet. This slowing of the velocity of the jet slows and expands the diameter of the jet as shown in Fig. 2.11, transforms some of the kinetic energy back into static pressure (compressed and stored energy) and wastes some as friction. In addition to the effects of high shear rate

[19] J. Eckel, W.J. Bielstein, Nozzle design and its effect on drilling rate and pump operation, API Drilling and Production Practice, American Petroleum Institute, 1951.

[20] William A. Kistler, May The Effect of Back Pressure on Nozzle Characteristics, Rice University Library, Houston, TX, 1953.

viscosity as mentioned above, the physical distance from the jet to the rock face also affects the magnitude of this "pressure recovery."

Further investigation revealed that this pressure recovery effect is well-known in pipeline orifice plate measurements and has been reported in that industry but previously had never been applied to drill bit nozzles.

While many additional measurements are needed to be able to accurately quantify this recovery effect and which variables have the strongest influence on it, we do know that it is quite significant. Ramsey et al. reported recovery effects ranging from nil to over 30%.[21] They suggested that if data for a particular well was not available, that an assumption of a 15% recovery effect was quite reasonable. Tommy Warren of Amoco Tulsa Research Center later refined this recommendation to 14.7%, and to the author's knowledge was the first to suggest simply using the 1.03 value for C_V (or C_D) in the bit pressure loss equation could be the most convenient way to handle this[22].

2.11.2 Bit types

The effect of bit type on pressure loss calculations is believed to be more a function of geometry than tricone versus PDC designs. Specifically, as mentioned above, since jet nozzles in PDC bits are typically closer to the rock face, the magnitude of the pressure recovery effect on those would be expected to be less than that of tricones, with their higher standoff distance from the nozzle to the rock face.

Even prior to the discovery of this pressure recovery effect on net bit pressure drop and the corresponding increase in ECD, the problem of jet velocity slowing before it reached the rock face was recognized. In general, the problem was described in terms of the ratio of the bit nozzle diameter to the height of the nozzle above the rock face[23]. Note in Fig. 2.12 the nozzle placement [in this case the nozzles have been removed (see threads)] is several inches above the bottom of the hole.

[21] M.S. Ramsey, L.H. Robinson, J.F. Miller, M.E. Morrison, February 20−23 Bottomhole Pressures Measured While Drilling, IADC/SPE 11413, Society of Petroleum Engineers, New Orleans, LA, 1983. Available from: https://doi.org/10.2118/11413-MS.

[22] T.M. Warren, Evaluation of jet-bit pressure lossesDecember SPE Drilling Engineering, Society of Petroleum Engineers, 1989, pp. 335−340.

[23] M.R. Wells, R.C. Pessier, The effects of bit nozzle geometry on the performance of drill bits, AADE-03-NTCE-51, in: Presented at the AADE 2003 National Technology Conference, Houston, TX, April 1−3, 2003.

Figure 2.12 Rock bit coming out of hole. Note nozzles have been removed.

One solution is to make the nozzle placement closer to the rock face. As mentioned, with PDC bits, this is easily accomplished.

With tricones the available design space is limited. However, success has been achieved through the use of "extended" nozzles, that essentially amount to an extension tube being welded to the bit to get the bit nozzle itself much closer to the rock face—in some bit designs within an inch or so of the rock on bottom. These, however, have in rare cases been reported to have had problems downhole, most likely tied to junk or cobblestones in the well.

Another alternative for tricones is the use of "mini-extended" nozzles. These require no bit modification or welding, but provide 1–3 in. of extension built into the nozzle design itself, permitting the discharge nozzle position to be closer to the bottom of the hole and yet maintaining original bit dimensions and interchangeability with other mini-extended nozzle sizes or conventional nozzles.

Both the fully extended nozzles and the mini-extended nozzles have been shown to improve penetration rate. Fig. 2.13 illustrates the placement of, and resulting jet shape, of three nozzle configurations commonly available for tricone bits.
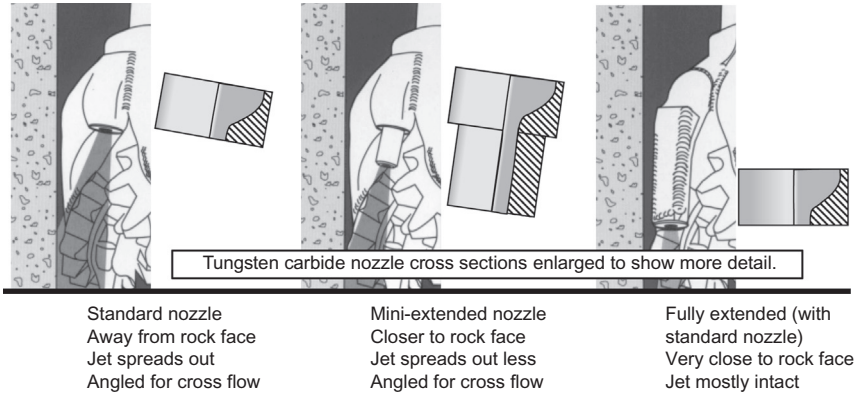
Figure 2.13 Assorted nozzle options.

2.11.3 Viscosity effects

Inspection of bit pressure drop equations readily shows that typical viscosities do not have an influence on the change in kinetic energy resulting in the pressure drop at the throat of the nozzle (or its exit point). However, in the reported data, high shear rate viscosity and/or density is thought to have a strong influence on the degree of pressure recovery experienced.

2.11.4 Remaining research

While the general tendency of the pressure recovery effect is known to be higher when nozzles are further away from the rock face and is greater when the high shear rate viscosity is higher, the exact relationship of these two items have not been thoroughly investigated at this writing.

2.11.5 Recommended practice

In the absence of data to the contrary, we recommend that a recovery factor of approximately 15% be applied to the older, conventional pressure drop calculations. One researcher (Warren) suggested a 14.7% recovery factor[24]. However, judgment is in order here and bear in mind that thinner drilling fluids will have a lower recovery and higher density drilling fluids (with correspondingly higher high shear rate viscosities) will have a higher recovery factor (reported as high as 32%). In addition, most reported data (supporting the 14.7% and 15% estimates) were with

[24] Warren, 1989, op. cit.

conventional tricone bits. Bits where nozzle exits are closer to the formation would be expected to have less pressure recovery.

2.12 EXTRAPOLATIONS AND CORRECTIONS FOR CHANGING CONDITIONS

Due to extremely long-lived drill bits available today, the well planner should consider how the hydraulics may change over the course of a particular bit run. Today's advanced bit technology has improved to the point where extremely long bit runs are not merely possible, but are common, especially offshore. If the added time and depth drilled by newer bits is not taken into account, serious errors in hydraulics estimates can result as detailed below.

Fortunately, taking these extended times, changing conditions, and depths into account is not difficult.

Drill pipe and annulus flow pressure drop equations are more complex but are affected by viscosities (particularly low shear rate viscosities such as are measured at 3 and 6 RPM Fann cylindrical rheometers as described in the Hole Cleaning chapter 3), drilling fluid density, and importantly, the length of the drill string and associated annuli.

Complicating things further could be changing drill string components and changes to managed pressure drilling procedures.

Fortunately, most of these complications are relatively straightforward and, when properly treated, are more of an accounting issue rather than one of prediction based on unknown assumptions.

2.12.1 Depth

Depth corrections or extrapolations are readily made to the wasted energy portion of the use of wellbore hydraulic pressure or energy. These corrections are linear with measured depth (MD).

If one pumps a liquid through a longer pipe, it will take more energy, measured as pressure, to move it, all other things being constant. Fortunately, this is a straightforward and linear effect, meaning that the increase in pressure to move the fluid is directly and linearly proportional to the change in length.

In drilling terms, this means that the P_{CIRC} value measured (such as above) must be corrected by a ratio of the new anticipated MD of the well when the new bit is pulled such as when dulled, a geology change,
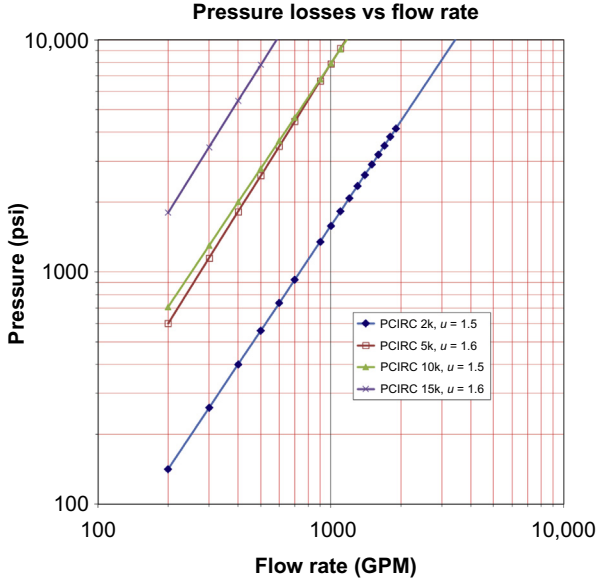
Figure 2.14 Flow rate versus P_{CIRC} as the well is deepened (measured depth). Major effect is length, but note that MW changes are also similar in nature, and that the slope ("u") of the wasted energy line can change with depth as well (cf. 5k and 10k lines). *Courtesy: Texas Drilling Associates.*

or the total depth (TD) of the hole section, divided by the MD of the well when the data was taken.

In Fig. 2.14, a typical effect of depth on the green "wasted energy" line is shown with the wasted energy line going upward from 2000 ft MD to 15,000 ft MD.

For here and the following sections, the subscript "CORR" (short for CORRECTED, e.g., $P_{CIRC\ CORR}$) will mean the value at the end of the upcoming bit run. It does not imply there is something wrong with the data obtained just prior to pulling the bit or at any other time. If the CORR is not on the subscript (e.g., P_{CIRC}), then the value P_{CIRC} refers to the data point itself.

$$P_{CIRC\ CORR} = P_{CIRC} \times \frac{MD_{CORR}}{MD} \tag{2.37}$$

For example, if the measured P_{CIRC} at a particular flow rate was 2000 psi, and the new bit would be pulled at 10,000 ft after going in the hole at 6000 ft, then the $P_{CIRC\ CORR}$ at the 10,000 ft depth would be computed to be

$$P_{\text{CIRC CORR}} = P_{\text{CIRC}} \times \frac{\text{MD}_{\text{CORR}}}{\text{MD}} \qquad (2.38)$$

$$P_{\text{CIRC CORR}} = 2000 \times \frac{10,000}{6000}$$

$$P_{\text{CIRC CORR}} = 2000 \times 1.67 = 3333 \text{psi}$$

Importantly, again referring to Fig. 2.14, note that the P_{CIRC} exponent "u" may also change as the well is deepened. This change can be up or down, depending largely on mud properties. The well designer (and mud engineer) can significantly reduce the wasted energy or pressure associated with P_{CIRC} by selecting and maintaining muds with a lower "u" value. *In the figure, a decrease of the "u" value from 1.6 to 1.5 effectively eliminates the depth penalty in going from 5000 to 10,000 ft* MD *for the operating region of flow rate!*

2.12.2 Increased depth

Most instances of depth-related corrections involve increasing depths as the well is being drilled to TD. The example given above is of such a nature and further discussion is not warranted.

2.12.3 Decreased depth

In some unusual circumstances, such as plug backs or holes cemented above an abandoned fish for sidetracking, the depth of the well may actually decrease. The same procedure applies, but the ratio of the corrected MD divided by the MD at the point of pressure measurements will be less than one rather than the more typical value greater than one.

For example, if the measured P_{CIRC} at a particular flow rate was 2000 psi, and the old bit was measured and pulled at 10,000 ft, but a plug back required putting the new bit in with a higher bottom hole of 8500 ft, the $P_{\text{CIRC CORR}}$ at 8500 ft would be computed to be

$$P_{\text{CIRC CORR}} = P_{\text{CIRC}} \times \frac{\text{MD}_{\text{CORR}}}{\text{MD}} \qquad (2.39)$$

$$P_{\text{CIRC CORR}} = 2000 \times \frac{8500}{10,000}$$

$$P_{\text{CIRC CORR}} = 2000 \times 0.85 = 1700 \text{psi}$$

If this new bit going in was expected to drill to a depth of 12,300 ft, then the expected pressure at the 12,300 ft depth would be

$$P_{\text{CIRC CORR}} = P_{\text{CIRC}} \times \frac{\text{MD}_{\text{CORR}}}{\text{MD}} \qquad (2.40)$$

$$P_{\text{CIRC CORR}} = 2000 \times \frac{12,300}{10,000}$$

$$P_{\text{CIRC CORR}} = 2000 \times 1.23 = 2460 \text{ psi}$$

2.12.4 Measured depth versus true vertical depth

Note that all depths used for such corrections, even though we are dealing with pressures, are MDs and not true vertical depth as is usually the case with pressures. The distinction here is that we are estimating and accounting for *friction losses* which are a function of length, and not hydrostatic pressures, which are a function of vertical fluid column height.

2.12.5 Mud weight (drilling fluid density)

Inspection of the bit pressure drop equation presented earlier shows that mud weight is a variable in that equation. To review, pressure drop through a bit is given by

$$\Delta P_{\text{bit}} = \frac{\text{MW} \times Q^2}{12,775 \times \text{TNFA}^2} \qquad (2.41)$$

Note that the mud weight effect through the bit is linear.

In a similar fashion, while there are numerous equations for annular and drill pipe pressure losses (most of which are woefully inadequate for describing the pressure drops themselves accurately), they are all linear with respect to mud weight.

Hence, if mud weight changes are anticipated before pulling the new bit, these are accounted for linearly as MD was above.

$$P_{\text{CIRC CORR}} = P_{\text{CIRC}} \times \frac{\text{MW}_{\text{CORR}}}{\text{MW}} \qquad (2.42)$$

Again, the subscript CORR is used to denote the revised value, in this case corrected for mud weight changes over the course of the bit run.

The example closely parallels the example of MD changes.

For example, if the P_{CIRC} pressure data was measured to be 2000 psi at a mud weight of 11.2 ppg and the next bit was expected to have mud weight of 14.5 ppg at the end of its run, the $P_{\text{CIRC CORR}}$ would be calculated to be

$$P_{\text{CIRC CORR}} = P_{\text{CIRC}} \times \frac{\text{MW}_{\text{CORR}}}{\text{MW}} \qquad (2.43)$$

$$P_{\text{CIRC CORR}} = P_{\text{CIRC}} \times \frac{14.5}{11.2}$$

$$P_{\text{CIRC CORR}} = 2000 \times 1.295 = 2589 \text{psi}$$

As in the case of depth changes, the mud weight change effect can go in the opposite direction in those unusual cases where the mud weight is decreased in a wellbore.

2.12.6 Combined effect of measured depth and mud weight

In many cases, both the MD correction and the mud weight correction should be made. To do this, the individual corrections are made as above, and then the two correction ratios of MD and of mud weights are multiplied together to obtain the combined correction ratio to be applied to the actual measured data.

$$P_{\text{CIRC CORR COMBINED}} = P_{\text{CIRC}} \times \frac{\text{MW}_{\text{CORR}}}{\text{MW}} \times \frac{\text{MD}_{\text{CORR}}}{\text{MD}} \qquad (2.44)$$

For the examples above, combining the two factors would yield:

$$P_{\text{CIRC CORR COMBINED}} = P_{\text{CIRC}} \times \frac{\text{MW}_{\text{CORR}}}{\text{MW}} \times \frac{\text{MD}_{\text{CORR}}}{\text{MD}} \qquad (2.45)$$

$$P_{\text{CIRC CORR COMBINED}} = P_{\text{CIRC}} \times \frac{14.5}{11.2} \times \frac{10,000}{6000}$$

$$P_{\text{CIRC CORR COMBINED}} = P_{\text{CIRC}} \times 1.295 \times 1.67$$

$$P_{\text{CIRC CORR COMBINED}} = 2000 \times 2.163$$

$$P_{\text{CIRC CORR COMBINED}} = 4325.3 \text{psi}$$

2.12.7 Geometry (hole diameter changes)

Somewhat more involved is the correction required when using data from one hole section to estimate pressure losses in another hole section with one or more changes in geometry. This is typically the result of finishing one hole section, running and cementing casing, and then drilling out with a smaller diameter bit. It can also occur separately or in tandem with changes to the drill string geometry.

In some cases of late, wells are designed to drill one size down to a particular depth (e.g., to an optional casing point), but a decision is made to not set the casing, and a reduced diameter bit is used below that.

The accuracy of the equations used to predict absolute values in drill string and annuli friction losses is suspected (and several different ones are in use by various software programs, companies, groups, and individuals), but the equations can be useful when correcting measured data to estimate the future parasitic pressure losses.

The basic technique is to compute a correction factor similar to those obtained above using the drill string and annuli equations of your liking and apply that correction factor to the measured data values.

As an example, we will use equations used in a popular software program[25] and companion hydraulic slide rule for drill string and annuli pressure drops as follows.

Several sections of the combined parasitic losses must be treated separately.

2.12.8 Laminar pressure losses—power law model

$$\Delta P_{\text{DP}} = \left[1.6 \times \frac{\text{AV}}{\text{HD}} \times \frac{(3 \times \text{PN}+1)}{(4 \times \text{PN})}\right]^{\text{PN}} \times \left[\frac{(\text{PK} \times \text{PL})}{(300 \times \text{HD})}\right] \qquad (2.46)$$

$$\Delta P_{\text{ANN}} = \left[2.4 \times \frac{\text{AV}}{\text{HD}} \times \frac{(2 \times \text{PN}+1)}{(3 \times \text{PN})}\right]^{\text{PN}} \times \left[\frac{\text{PK} \times \text{PL}}{300 \times \text{HD}}\right] \qquad (2.47)$$

$$\text{PN} = 3.32 \times \text{LOG}_{10}\left(\frac{Q_{600}}{Q_{300}}\right)$$

$$\text{PK} = \frac{Q_{300}}{511^{\text{PN}}}$$

where PL is the pipe length (feet); ΔP_{DP} is the Drill pipe pressure loss (psi); AV is the fluid velocity (ft/minute); HD is the hydraulic diameter (in.); ΔP_{ANN} is the pressure drop (psi); PV is the plastic viscosity (cP); $Q_{300} = \text{YP} + \text{PV}$; $Q_{600} = \text{PV} + Q_{300}$; $\text{PV} = Q_{600} - Q_{300}$; and $\text{YP} = Q_{300} - \text{PV} = 2 \times Q_{300} - Q_{600}$.

[25] Tompkins, Lee, of NOV in private correspondence February 2, 2012, referring to the "Hydraulic Slide Rule" equations and associated software.

As an example, for an annulus of 12.25 in. × 4 in., we might compute that for a given length of annulus might have a pressure loss of 25 psi for a light, thin mud, and reducing the hole from 12.25 to 8.5 in. (still with 4 in. drill pipe) would compute an annular loss 65 psi, or 2.6× higher. Assume that the drill pipe pressure loss in both cases is 300 psi. The combined P_{CIRC} would then be 325 versus 365 psi. This might be a small enough difference to neglect, or a point could be constructed/calculated on the flow versus pressure P_{CIRC} line to increase by the 40 psi (12.3% increase), and then the P_{CIRC} line for the new well geometry constructed/calculated parallel to the one in the current hole section.

2.12.9 Turbulent pressure losses

For some software packages, such as in the "Reed Rule," the following Modified Bingham Plastic Equation is used.

$$P_{TURBULENT} = \frac{PL \times 0.0002205 \times MW^{0.82} \times PV^{1.82} \times (((AF - 1) \times 2) + 1)}{1000 \times HD^{1.18}}$$

(2.48)

where $P_{TURBULENT}$ is the pressure loss (psi) (fully turbulent flow); PL is the pipe length (feet); MW is the mud weight (ppg); PV is the plastic viscosity (cP)[26]; AF = Adjustment factor = actual SPP/current SPP (dimensionless) (user input—not currently in use in the Schlumberger Reed Rule calculation package); and HD is the hydraulic diameter (in.).

Procedurally, this correction is the same as the one in the preceding section, but the equations are changed. Oftentimes we are not sure whether the mud is in turbulent flow, laminar flow, or more likely, a transitional flow. Conservative well designers would compute both the turbulent and laminar cases and choose the most conservative answer.

2.12.10 Surface equipment pressure losses

Note that the term "surface equipment" has been used historically to account for the pressure losses incurred in moving the drilling fluid from the mud pump to the drill string, which includes drops through hard piping around the rig, the standpipe, the first gooseneck, the rotary hose, the

---

[26] Plastic viscosity (PV) is calculated by mud engineers as being the Fann Rheometer (or equivalent) reading at 600 RPM outer cylinder rotational speed minus the reading at 300 RPM. As an example, if the 600 RPM reading was 80, and the 300 RPM reading was 60, the PV = Reading$_{600}$ − Reading$_{300}$ = 80 − 60 = 20 cP.
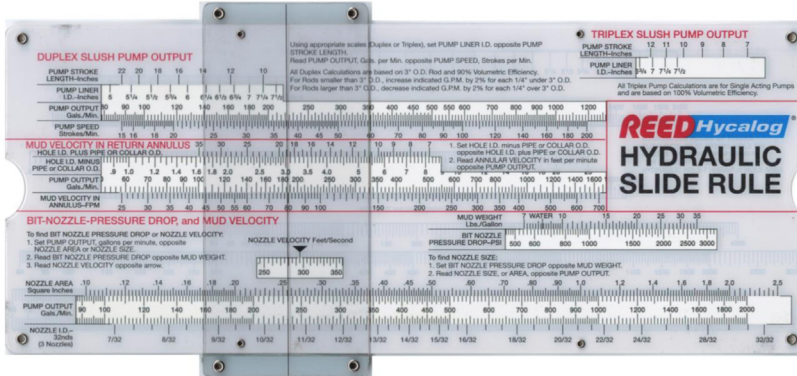
Figure 2.15 Reed rule hydraulic slide rule (front shown).

second gooseneck, the swivel, and the kelly or top drive depending on the rig. Reed Tool Company, as part of their hydraulic slide rule, adopted a convenient practice that divided various sizes of surface equipment into five types as shown below. This was initially empirical as reported in Lapeyrouse.[27]

Not all rigs will fit into one of the previously standard four identified case numbers (1–4). The idea is for the well designer to pick the "case number" that best fits those listed in the table. Case 5 was introduced at the suggestion of this author a few years ago. For newer high pressure rigs with taller derricks/masts and equipped with a top drive system, a new "Case 6" might be something to consider, as was Case 5 recently! (Original calculations of the surface equipment "case number" only included 1–4.)

To account for surface equipment losses, one has three options. The first involves using the "Reed Rule" (at this writing provided by NOV in software CD-ROM or a physical "slide rule"), the second involves an approximating technique relating to these case numbers, and the third inherently includes this as part of the "OCHO" technique described later in this chapter.

2.12.10.1 Slide rule

One tried and true way to estimate surface equipment and other pressure losses involves the use of a "hydraulic slide rule." In the case of the popular "Reed Rule" (shown in Fig. 2.15), the procedure is to select a group

---

[27] N. Lapeyrouse, Formulas and Calculations for Drilling, Production and Workover, first ed., 1992, Gulf Publishing, Houston (now Elsevier), p. 195.

or "case" of surface equipment that most closely matches the rig being evaluated and then follow the instructions printed on the hydraulic slide rule itself to find the pressure loss. This gives a quick estimate in a minimal amount of time. For Case 5 applications, Case 4 may be used with minimal error concerns as the values are small by comparison to others and the difference between Case 4 and 5 is largely inconsequential.

2.12.10.2 Approximate correlations

A second technique (which can be used in a large number of otherwise unusual calculations) is to use an equivalent length of pipe of a standard diameter to represent the surface (or other) equipment. The idea is to represent the unknown and perhaps difficult to calculate component or components with a hydraulically equivalent length of pipe yielding to easier computation.

Surface equipment may be similarly represented, some estimates of the equivalent length of 3 in. inside diameter pipe given in Table 2.6 for various surface "case" combinations.

Alternately, but with similar results, API 13D[28] gives the equation

$$P_{SC} = C_{SC} \times \rho_S \times \left(\frac{Q}{100}\right)^{1.86} \tag{2.49}$$

Similarly, using the Blasius approximation, the graph (Fig. 2.16) provides a quick estimate of pressure drop in psi per foot of 3 in. ID pipe at various flow rates and densities.

Note that except for extremely high flow rates, the total pressure losses through today's modern rigs' surface equipment are quite small, and the error introduced by neglecting these entirely is not large. Similarly, note that as flow rates increase, the wasted energy or pressure through the pipe increases exponentially, and the reader can think about how this would affect available pressure drop for use by the bit or reamer nozzles thousands of feet below the rotary.

2.12.11 Embedded measurement with ongoing continuous hydraulics optimization

A third way to handle surface equipment losses once the well is spudded is to simply include them as part of the P_{CIRC} measurement at the rig site. This technique, discussed in detail later in this chapter, explicitly

---

[28] API 13D, 2010, op. cit. p. 26.

Table 2.6 Various components—length and inside diameter[a]

	Case number	Standpipe	Kelly hose	Swivel	Kelly	Equivalent 3 in. pipe length[b]	Coefficient of surface connections, C_{SC}[c]
Surface equipment combination type or case number	1	40 ft × 3 in.	45 ft × 2 in.	4 ft × 2 in.	40 ft × 2.25 in.	650	1.0
	2	40 ft × 3.5 in.	55 ft × 2.5 in.	5 ft × 2.5 in.	40 ft × 3.25 in.	250	0.36
	3	45 ft × 4 in.	55 ft × 3 in.	5 ft × 2.5 in.	40 ft × 3.25 in.	150	0.22
	4	45 ft × 4 in.	55 ft × 3 in.	6 ft × 3 in.	40 ft × 4 in.	100	0.15
	5	100 ft × 5 in.	85 ft × 3.5 in.	22 ft × 3.5 in.	n.a. (top drive)	100	0.15
	6				Top drive		

Proposed, as currently recommended in API 13D, p. 28.
[a]After Reed Rule ©Reed Tool Company, now ReedHycalog, a subsidiary of NOV (c.2017).
[b]As calculated from the NOV ReedHycalog Hydraulics Software, version 3.0, ©2012.
[c]C_{SC} from Table 4 of API 13D.
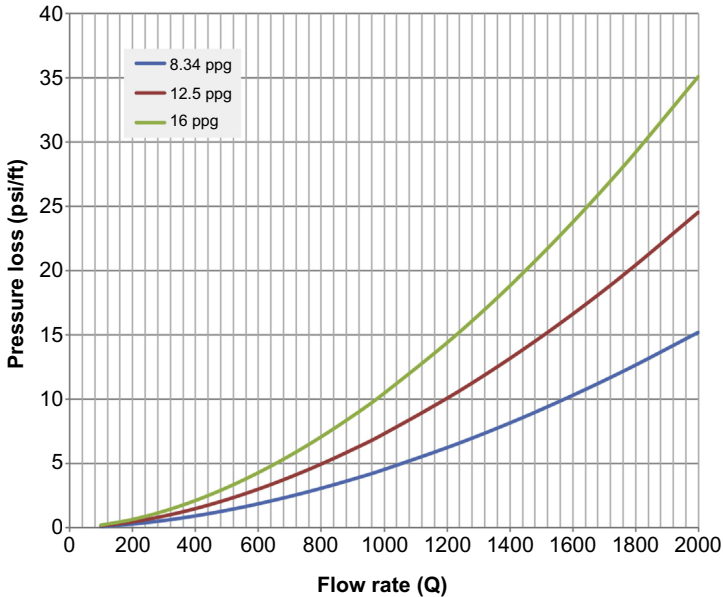
Figure 2.16 Pressure loss in 3 in. ID pipe. For estimation purposes (using Blasius approximation for f_F and turbulent flow assumptions.)

measures all pressure drops in the system and is used to divide the pressure losses of the bit nozzles from those of everything else. Simply including these as part of the "everything else" works quite well in this author's experience.

2.13 BIT "RECOVERY EFFECT," MW, AND THE BIT TYPE ITSELF

To review, pressure drop through a bit is given by

$$\Delta P_{\text{bit}} = \frac{\text{MW} \times Q^2}{12,775 \times \text{TNFA}^2} \tag{2.50}$$

Note that the mud weight effect through the bit is linear. Increasing the MW by 10% will have a corresponding 10% change in the pressure drop across the bit, all other variables remaining fixed. This single effect is likely the most important factor when standpipe pressure seems to vary slightly as a hole is drilled or circulated. Even though the bit (and nozzles) is constant, the mud weight is almost never perfectly homogeneous, and hence when heavy or light spots of mud pass through the nozzles, the pressure loss across the bit increases or decreases accordingly.

Hence, if mud weight changes are anticipated before pulling the new bit, these are accounted for linearly as MD was above, or by simply recalculating using the bit pressure drop equation.

To a lesser extent, as described previously, the solids content and resulting plastic viscosity affect the amount of pressure recovery, as does the placement of the nozzles in the bit. Nozzles positioned further from the rock face (such as on a tricone bit) will tend to have a higher pressure recovery than those placed closer to the rock face (such as in a PDC bit). However, published data is somewhat lacking at this writing, and in the absence of data, no specific correction for the bit type is presented.

2.13.1 Other drilling fluid properties

For pressure drops through the nozzles, drilling fluid rheology, especially low shear rate viscosity, is not especially important, due to the high shear rate environment of the bit nozzle flow. However, there is an apparent effect of high shear rate viscosity on the bit pressure drop as discussed above. A high plastic viscosity (representing the high shear rate viscosity and usually accompanied by high mud weight) will tend to result in a higher bit recovery factor.

For system pressure losses, low and high shear rate viscosities are more important, and some effort should be made if, for example, the yield point or plastic viscosity will be changed significantly from one run to another. The general approach used before would be employed here—that is, a correction factor that would account for the anticipated changes to rheologies be computed and applied to the measured well-circulation data.

As an example, the Blasius correlation for the Fanning friction factor is a function of the reciprocal of the Reynolds raised to the 0.25 power. Embedded in the Reynolds number for a power law or Bingham Plastic fluid such as a drilling fluid is the plastic viscosity. Hence, a correction factor for changing plastic viscosity could simply be

$$\text{Correction}_{PV} = \frac{PV_2{}^{0.25}}{PV_1{}^{0.25}} \tag{2.51}$$

and hence a measured circulation system pressure loss, P_{CIRC1}, would be adjusted by this ratio to get the new prediction of circulation system pressure loss, P_{CIRC2}.

$$P_{CIRC2} = P_{CIRC1} \times \text{Correction}_{PV} \tag{2.52}$$

2.14 OPERATING LIMITS CHANGES

If operating limits change, perhaps from some change in rig equipment or equipment availability, a reoptimization may be required. If minimum or maximum flow rate limits change, but these were not the deciding factor anyway, then no reexamination is warranted. However, if standpipe pressure limits change, or if available power limits change, then the optimization usually will be obsolete and should be recalculated.

2.15 PUMP-OFF FORCES

With diamond bits of all types, and to a lesser extent PDCs with very shallow rib designs, the effect of what has been called "pump-off force" should be considered. Briefly, in diamond designs, the flow of drilling fluid typically exits the bit in the center, and then radially flows outward toward the OD or gage of the bit, providing cooling and cuttings removal from the individual diamond cutters. The small clearance between the bit face and the rock (made smaller as weight is applied and the cutters "depth of cut" increases) results in high pressure drilling fluid acting across the cross-sectional area of the diamond bit, effectively producing a force opposite to the driller's applied WOB.

This force could be investigated as a "drill off test" in the field (i.e., until this force is overcome, the bit will not drill fast or at all) or can be estimated in advance. The API gives the approximate formula[29] for calculating this force as

$$\text{HPO} = [0.942 \times P_{\text{BIT}} \times (d_B - 1.0) \times 0.001] \qquad (2.53)$$

where HPO is the hydraulic pump-off force, 1000 lb (opposite applied WOB); P_{BIT} is the pressure drop across the bit (psi); and d_B is the diameter of bit (in.).

While this pump-off or "lift-off" force can be significant for natural diamond and diamond impregnated type bits, it is usually of little consequence for tricones or PDCs. In these latter types, the effect is limited to one similar to that of the reaction force of a fireman's hose, albeit with higher pressure drops and flow rates, and not the "pressure times area" calculation of the diamond bit case. As such, the reaction forces associated

---

[29] API 13D, 2010, op. cit. pp. 52−53.

with PDCs and tricones are typically small enough that they may be not be discernible on the driller's weight indicator and hence can be safely ignored.

2.16 NON-OPTIMUM CONDITIONS

There are, of course, cases where optimum combinations of flow and nozzle sizes simply cannot be achieved. This condition is commonly caused by

- Downhole equipment power requirements;
- Poor nozzle sizing to begin with;
- Insufficient data available;
- Large and unforeseen changes to the circulation system;
- Operational or engineering supervisors failure to run hydraulics in optimum conditions, usually due to not understanding it properly or not realizing its importance to drilling efficiency.

In such cases, the goal of the hydraulics designer should be to optimize the hydraulics as best as possible under the circumstances.

Graphically, an example is given below of a case such as this (Fig. 2.17).
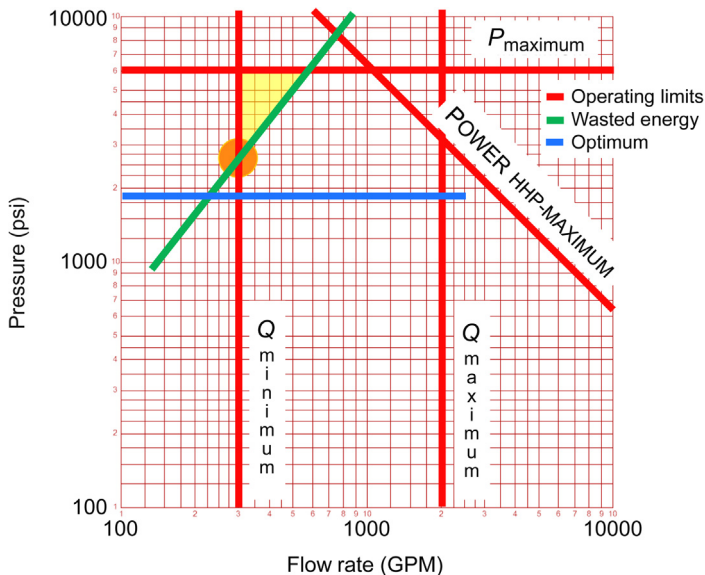
Figure 2.17 Non-optimum pressure losses across the bit nozzles. *Courtesy: Texas Drilling Associates.*

In this example, the parasitic losses have increased until it is impractical if not impossible to circulate at the previous rate, shown by the blue lines' intersection and the red dot. However, the parasitic losses (P_{CIRC}) at that flow rate are now nearly 100% of the available pump pressure.

The answer in this case is counterintuitive, requiring that the hydraulics designer decrease the flow rate all the way to the minimum flow rate.

Note that if it were not for the minimum flow rate line, the optimum flow rate and pressure loss would be at the intersection of the green wasted energy line and the blue ΔP bit optimum line.

Since the green line intersects the minimum circulation rate line above the blue line, this means that there is *less than optimum* stored energy (pressure) available to use across the bit. This *available* pressure for the bit is depicted by the yellow zone.

In the example, there is approximately $6000 - 2750 = 3250$ psi available for use across the bit. Hence, the flow rate to use when sizing nozzles is the minimum flow rate, and the pressure drop to use across the bit is the 3250 (or a little less to be conservative), rather than the optimized values based on the *u* equations in previous tables.

2.16.1 No remaining pressure available for the bit

Inspection of Fig. 2.17 shows that as the well is deepened or mud weight is increased, or both, the green line representing the circulation system exclusive of the bit rises—wasted energy (or pressure)— at a given flow rate. This increase in the P_{CIRC} line will continue on a deep and/or high mud weight well until the line crosses the intersection of the red $P_{MAXIMUM}$ and the $Q_{MINIMUM}$ operating limit lines. At this point, the pressure available for the bit (yellow region) diminishes to zero.

When the available bit pressure drop is at zero, the well designer has two options. First, maximum sized nozzles (or no nozzles at all) are put in the bit, effectively giving no significant pressure drop across them. Second, that red line intersection must be moved up or to the left, by either increasing the available maximum pressure (if this is an option, such as by changing pump liner sizes) or by reducing the minimum flow rate line (which is almost always possible given sufficient planning for mud-carrying capacity and MWD and other downhole tool adjustments needed.)

Note that this second option may well require rejetting downhole motors, reamers, MWD, or other downhole tools that use hydraulic energy for activation or power, and that drilling fluid rheology may require changing in order to ensure good hole cleaning.

2.16.2 Designated flow rate (including minimum flow rate)

Similarly, there are times when a flow rate must be fixed. This can be due to situations such as

- a narrow window between minimum and maximum flow rates;
- a clear impingement against either the minimum or maximum flow rate limits;
- specific inflexible requirements of downhole equipment; or
- inflexible field or office supervisors or clients.

In this case, once again, the approach is to use what is available for the bit, good or bad. In the previous example the yellow shaded area showed the available operating region for the bit. If the flow rate is fixed, this two dimensional area becomes a vertical yellow one-dimensional line segment. All (preferably) or part of that line segment can be used for the desired pressure drop across the bit.

2.16.3 Designated nozzle sizes

If nozzle sizes are fixed, then the approach becomes how to get the best drilling benefit out of the nozzles that are required in the bit. In this case, there is very little flexibility for the designer, being limited to changing the flow rate only. Generally speaking, rigs with nozzles that are fixed are usually fixed too large, and the only improvement that might improve drilling performance is to pump faster and obtain a higher flowrate.

However, note that in pumping faster, the ECD friction losses up the annulus also increase, thus leading to higher effective drilling fluid density overbalance. This in turn can result in *slower* drilling rates or even lost returns.

This effect of increasing flow rate causing increased ECD that decreases penetration rate is especially evident when the mud weight and the formation pore pressure are closely matched (as well designers increasingly do today).

2.16.4 Designated bit pressure drop

With a designated bit pressure drop, the procedure is identical to that described in above sections, except that no determination of the available bit pressure drop is necessary—that is a given in this scenario (e.g., if an MWD or other hydraulically powered downhole tool required a specific pressure drop in order to function properly.)

2.17 FOUNDER POINT DETERMINATION

Once the hydraulics (or any other parameter affecting penetration rate) is optimized, the founder point may be affected. Hence, it is necessary to conduct a drilling test to evaluate the new founder point for efficient drilling operations. Two techniques to do this are discussed in the Drilling Efficiency chapter.

One of the many benefits of OCHO on-site optimization is improved rates of penetration. The idea is that when the bit chips the rock, it should only have to do this one time. If the hydraulics are sufficient, they will blast that chip out from under the bottom of the bit, and the chip will be gone and one will never worry about it again. If one has insufficient hydraulics, that chip will remain on the bottom of the hole, and hence it will be redrilled. In essence, the hole will be drilled two or three or four times instead of one time.

Referring to Fig. 2.18 nearby, note that as bit weight is increased, the drilling rate increases, but the improved penetration rate per 1000 pounds of bit weight added decreases, perhaps flattening to even zero. Why does it level out? It is because the bit is foundering due to insufficient cleaning of the bottom of the hole! At point B the bottom of the hole is not being cleaned and is, in essence, being drilled more than one time since freshly cracked rock is being reground into smaller cuttings. At point B the hydraulics are clearly failing to clean the bottom of the hole and the bit is balling up. If higher bit hydraulics are used (i.e., more HHP or JIF across the bit nozzles through optimization or running the pumps harder), one
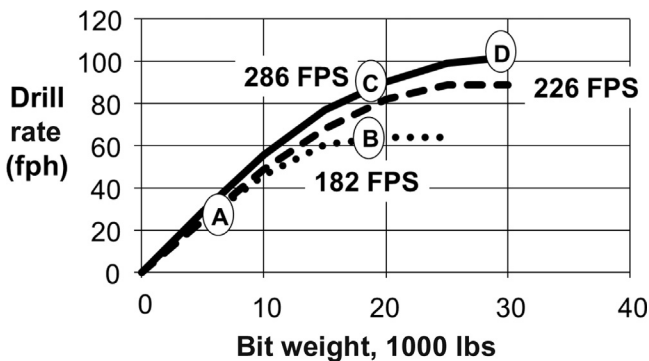
Figure 2.18 Effect of hydraulics and WOB optimization on drilling rate. *WOB*, weight on bit. *Courtesy: Texas Drilling Associates.*

gets a substantial increase in penetration rate, as shown at point C. A further increase is seen with still higher hydraulics. But a very important part about this figure is not just the increase one gets from going from point B to point C. The importance is in going from point A and then being able to load the bit more and get all the way up to point D! By ensuring maximum cleaning, optimizing hydraulics permits maximizes drilling rate!

Surprisingly, ECD can usually be *reduced* through optimized hydraulics. The reason for this is that most drillers will use a "seat of the pants" calculation technique, or perhaps no calculations at all, and the result will typically be a higher flow rate than is actually needed. When one optimizes the hydraulics properly, then one often finds that you may actually be able to reduce the flow rates and, hence, get a lower ECD. The bit hydraulics will be higher, the ECD lower, ROP faster, and the total flow rate lower.

2.17.1 "John Wayne" company man inefficiency example

To illustrate, let us assume that we have a company man whose operating style is "my way or the highway" so to speak. Let us further assume he does not have a robust understanding of how bit and wellbore hydraulics optimization works, but he/she does recognize the benefit of better hydraulics. Let us further assume that this company man does not like, as a matter of a rule-of-thumb and his personal preference, to run nozzles smaller than 16's (16/32 of an inch).

Imagine a bit has dulled and this Company Man John arrives just as the new bit is being fitted with nozzles to run in the hole. The MWD engineer has already done calculations and determined that four 11's will be optimized. (The reader will recall that refers to 11/32nds of an inch diameter.) John announces these are too small and promptly orders that 16's be run instead (16/32nds). The rig crew complies.

Unwittingly, Mr. Wayne has completely destroyed the good work the MWD engineer has diligently done. The TNFA, in going from 11's to 16's, has increased from 0.371 to 0.785 square inches—a little more than doubling the TNFA.

When the improperly jetted bit is on bottom and the pumps are turned on, the bit pressure drop is lower than the MWD engineer planned—perhaps even too low to run the MWD tools correctly. Inspection of the ΔP_{BIT} equation shows that the TNFA term is squared and is in the denominator. Since Mr. Wayne more than doubled the TNFA, the effect on ΔP_{BIT} is to reduce the bit pressure drop value by a little over 75%.

The solution Mr. Wayne and others immediately seek is to simply run the pumps faster. This does indeed increase the standpipe pressure and the bit pressure drop. However, inspection of the log—log hydraulics plot shows that running the pumps faster mostly increases wasted energy (or pressure)—the green line representing P_{CIRC} is intersected by the new flow rate and pressure combination much higher and a correspondingly smaller amount of pressure at that flow rate is actually being used across the bit nozzles!

The final insult is that Mr. Wayne sometimes has the nozzles so large that the -1 sloped power limit line is crossed before the maximum standpipe pressure is reached. Hence, if 4000 psi was desired, and the power limit is reached when the standpipe pressure is only 3500 psi, Mr. Wayne may now think that the 16's were too small and want even larger nozzles on the next bit run!

Of course, the correct optimization procedure would be to reduce flow rate and use smaller nozzles as the MWD engineer had already calculated! Depending on the BHA configuration, this might be accomplished by dropping a suitably sized ball to plug one nozzle, but this can only safely be done when there are no obstructing BHA components (mud motors, MWD tools, etc.), and the bit is a tricone type is being used. Dropping a ball to plug a PDC nozzle should never be done, as the cutters affected by the reduction of flow near them could heat up and suffer accelerated wear or premature failure.

2.18 REVIEW AND ENERGY SAVINGS

Significant energy savings may be achieved through proper optimization of hydraulics since, at its core, the optimization involved minimizing wasted energy (or pressure) in order to maximize useful expenditure of energy (or pressure).

A rig site parable, based in fact and supported by data, illustrates this best. Consider the following.

You are walking around location one day and discover a leaking valve. It is hooked onto a diesel tank, and the stream of diesel is about 1/4 in. in diameter in size. A rough estimate is that your leak is about 500 gal/day, and from the look of the small lake of diesel on the ground, it has probably been doing this for several hours. Knowing that this is wasteful, costly, polluting, and potentially unsafe, you quickly fix the valve and stop the leak.

Drilling engineers are concerned about many issues. In reality, however, there are not many issues that drilling engineers can actually influence after the well is spudded. You had influence over the leaking valve. However, your casing program is now fixed. The drilling fluid system, at least generally speaking, has been decided. The drill string has been designed. The rig and equipment have been selected. In most technical areas, we do not really even adjust these decisions made "prespud." Wellbore and bit hydraulics, however, is one of the technologies that we can and should influence and optimize *after* the well spuds.

To quickly review, there are three primary users of hydraulic energy in a well after the pumps energize the fluid. The hydraulic energy generated by the pumps is consumed by the drill string, the bit, and the annulus. With the proviso that one must have sufficient velocity to clean the hole, the only one of these three that is really of any significant value to drilling efficiency is the bit pressure drop. The other two consumers of hydraulic energy are basically waste. Once one obtains sufficient annular velocity to clean the hole, good engineers and foremen should try to minimize waste. They should stop the leaks.

Current hydraulic technologies start with a simple seat-of-the-pants approach, which is probably what is used in at least 90% of the wells drilled. In this method, the drilling superintendent or toolpusher may know that if he runs #12 nozzles at a certain depth that he can get 300 GPM and 3000 psi out of his pumps. He knows this because he has used this combination of pump rates, pressures, and jet sizes before and that is what he is going to do again. There is no real analysis that goes into where the hydraulic energy is being consumed.

A better technique consists of using either modern software or the older hydraulic slide rules (i.e., the "reed rule") for calculations. Other bit and MWD and other service companies have software and smart-phone "apps" as well.

The third (and in this author's opinion the best) method does not yet enjoy widespread use. I refer to this technique as the OCHO technique. The problem with the previously mentioned more conventional techniques, such as the seat of the pants approach and the Reed Rule software, is that they are conducted prespud hence do not take into account changing well conditions. Well plans are going to change before spud. There may be a last minute change in drilling fluid types or drilling fluid densities.

The rig equipment may change. The rig may not even be picked until one has designed the well. Geometries may actually change in many cases.

Most importantly, plans will change after one spuds the well. Generally, when any of these changes take place, the drilling engineer does not have time to go back and recalculate the hydraulics, and hence there are many problems with hydraulics initially.

In addition to design–related problems, actual downhole drilling fluid properties are not known when one is planning or even while drilling the well. We typically measure drilling fluid properties at 120°F. We do not usually know what the rheological properties actually are downhole. Drilling fluid is affected by both pressure and temperature. Bentonite may be flocculating downhole. Drilling fluid additives are being consumed or destroyed outright, and various things are happening downhole that we really do not fully understand and that are very expensive to try to understand on the rig site. Further, the actual well geometry is not known. The well will contain enlarged areas (not true "washouts"!) and the other rugose places in the open hole.

The OCHO advantage is not just an improved ROP. One can also experience substantial fuel savings. Fig. 2.19 shows fuel used by a rig for mud pumping. In this case, the engineer had gone on vacation shortly after the well spudded. His drilling foreman knew he watched hydraulics very, very closely, and when the engineer returned from vacation, the rig was using over 2100 gal/day in diesel strictly for the pumps.

Instinctively, the engineer looked at the way they were running the hydraulics and knew it was not optimized. The engineer worked with the
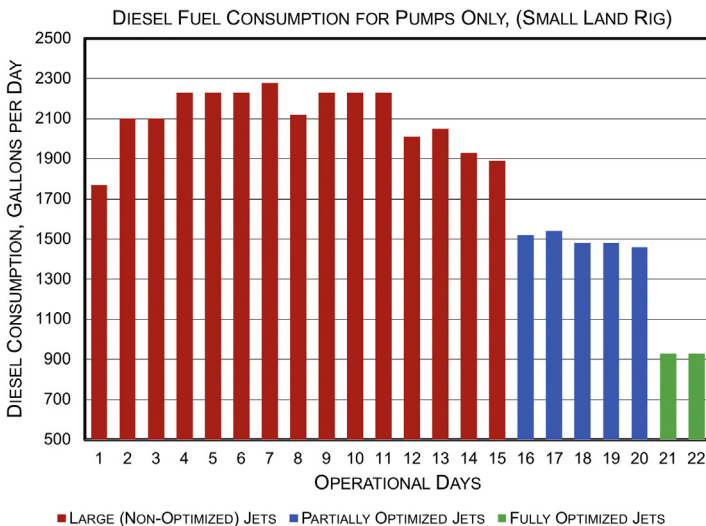
Figure 2.19 Fuel savings without loss of rate of penetration (ROP) with optimized hydraulics. *Courtesy: Texas Drilling Associates.*

Figure 2.20 QR to TNFA calculator.

drilling foreman to optimize the hydraulics using the OCHO technique on one trip, which was on day 31. As seen in Fig. 2.19, the fuel usage immediately dropped by several hundred gallons a day! This was a relatively small land rig; and the engineer optimized hydraulics again at the next bit trip. The fuel usage dropped substantially more! The difference between the initial nonoptimized point and the second optimized point was about 1100 gal of diesel a day!

Not obvious, but of great importance for drilling contractors, this reduction in diesel fuel usage translates into a decrease in wear-and-tear and maintenance requirements in a direct percentage of the fuel savings. Inspection of Fig. 2.19 shows that the diesel consumption dropped by over 50%. In wear-and-tear and maintenance-related items, this means that all components involved in providing hydraulic pressure to the drilling fluid system are decreased by the same percentage, over 50%! Put another way, equipment life is over doubled!

Fix the leak. Optimize your hydraulics.

A nozzle size calculator for up to eight jet nozzle sizes is located online at http://www.texasdrillingassociates.com/hydraulics/NozzleCalculator.htm or for an online table, http://www.texasdrillingassociates.com/hydraulics/hydraulics.htm (Fig. 2.20).

2.19 EXERCISES

2.19.1 Nozzle sizing exercise

Equations for convenience:

1. $\Delta P_{\text{BIT}} = \frac{\text{MW} \times Q^2}{12{,}775 \times \text{TNFA}^2}$

2. $\text{TNFA} = \sqrt{\frac{\text{MW} \times Q^2}{12{,}775 \times \Delta P_{BIT}}}$

Note: The above forms of the bit pressure drop equation include approximately 15% pressure recovery.

1. Complete the following table of total nozzle flow areas using the tables:

Nozzles	TNFA
12–12–12	_____
13–13–14–14	_____
16–16–16	_____
5 × 14	_____
3 × 11	_____

2. Using a maximum rig pressure of 6000 psi and a u exponent value of 1.7, calculate the pressure drop that should be across the bit.

	HHP or JIF?	Percent	psi
PDC bits?	____	____	____
Tricone bits	____	____	____

3. For the 50% PDC case above, a mud weight of 14 ppg and a flow rate of 800 GPM, calculate the total nozzle flow area (TNFA) needed for optimum hydraulics. Note that the terms TNFA and TFA are synonymous or interchangeable.

4. For the TNFA found in step 3, determine the sizes of the nozzles for a bit with

Two nozzles	_____
Three nozzles	_____
Four nozzles	_____
Six nozzles	_____

Hole Cleaning

Contents

3.1 INTRODUCTION

With the advent of modern synthetic muds and advanced performance water–based mud systems, one of the nemesis of drillers, stuck pipe, has been on the decline. At the same time, the use of directional

wellbores, and the lengths and complexities of wellbores, has increased. In addition, penetration rates of the drill bit have improved dramatically over the past 10 years or so.

As a result, one of the more troublesome challenges facing modern drillers is how to efficiently clean the hole of the drill cuttings in order to minimize or eliminate trouble costs associated with the inability to do so.

Hole cleaning is a two-part process of removing drilling cuttings from the hole. The first part involves moving cuttings from the very bottom of the well (beneath the bit), and the second part is to get those cuttings up the annulus and to the surface. The similarly used term "cuttings transport" more accurately addresses only the latter of the two—the movement of the cuttings up the wellbore in the annulus and is the subject of this chapter. Bit hydraulics and the cleaning under the bit are addressed in Chapter 2, Bit Hydraulics.

Annular velocity (AV) (a function of both pump rate and hole geometry) is the main variable influencing hole clearing for both vertical and inclined/horizontal wells. Fluid rheology can be significant in hole cleaning. Depending on the field conditions, there are other notable variables including density [mud weight (MW)], drill pipe rotation, drill pipe eccentricity, and hole angle.

The drill cuttings first need to be removed from the bottom of the hole after the cuttings have been generated by the bit. This avoids the cuttings being ground up further which results in smaller particles that increase the viscosity (specifically the plastic viscosity, PV) which may make the particles more difficult to remove from the mud later with solids control equipment. Bit nozzle sizing is influenced by the overall hydraulics system and is an important design key to efficiently remove newly formed cuttings from underneath the bit.

Inadequate hole cleaning also can cause other drilling problems including stuck pipe, excessive downhole circulating pressure [equivalent circulating density (ECD)], slow drilling rates of penetration (ROP), high rotary torque (which ultimately will limit horizontal drilling reach) hole pack off and bridging, and many more. After drilling to total depth, poor hole-cleaning troubles can include poor well logging performance, trouble running steel casing in the well, and difficult or lower quality cementing operations.

Keeping the hole clean is nearly as important as keeping it full. How to do it is considerably differs between low-angle and high-angle wells. The worst location in the well for hole cleaning is right between the two extremes, in the intermediate hole angle sections between 20 and 70 degrees.

How to keep the wellbore clean of drill cuttings, sloughing shale, and other solids is question that has plagued drillers for nearly 100 years. With the advent of highly deviated drilling becoming both accepted and widespread, we have learned the "hard way" that the same practices and drilling fluids that worked well in vertical wellbores simply failed to do so in highly deviated ones. Further, the near horizontal wellbores present yet another challenge.

Fortunately, there are tools available to help use do a reasonable job in each category today.

Practical guidelines and techniques will be discussed first. Toward the end of the chapter some more technical subtleties will be presented.

3.2 HOLE-CLEANING FACTORS

There are many parameters that influence hole cleaning. These include but are not limited to
- AV,
- rotation and size of the drill pipe,
- rheological properties (the viscosity in whatever form it is defined),
- fluid and particle densities (relating to the buoyancy effect),
- hole inclination angle,
- hole size (or casing inside diameter size),
- cutting size and concentration (dependent on the drilling rate),
- mud type (water or oil–based mud), and
- pipe-in-hole or pipe-in-casing eccentricity.

In short, hole cleaning is dependent on the intrinsic and extrinsic properties of the fluid doing the transporting, the cuttings, and the well geometry itself. Nearly everything ties to hole cleaning (or conversely, problems associated with poor hole cleaning) in some fashion.

3.3 VERTICAL AND DEVIATED-FROM-VERTICAL HOLE-CLEANING DIFFERENCES

Typically, hole clearing is treated differently in vertical wells and inclined wells, including horizontal wellbores. While these are discussed

and applied separately, the well designer should take note that while all deviated wellbores include a vertical section the reverse is not true. Hence, all wells need to be evaluated on vertical hole cleaning, while only deviated wells (loosely defined as being over 30 degree deviation from vertical) must also be checked for directional hole-cleaning concerns.

One of the major forces that hinders hole cleaning is gravity. Gravity naturally opposes the transport of the drilled cuttings in several ways. In vertical wells, it acts directly opposite the cutting movement from the bottom of the well to the surface. In horizontal wells, it acts perpendicular to the movement, while in inclined wells, it acts at an angle. Especially in the case of the latter two, gravity can rapidly move the cutting from the flowing annular mud to the low side of the hole where the *velocity of the mud is zero* (see Figs. 3.10−3.14). This means that once the cutting is resting on the low side of the hole, it is extremely difficult (i.e., nearly impossible) to get it back into the moving flow stream without additional mechanical action such as rotation of the drill string.

Further, it is important that the well designer understand that cleaning cuttings in deviated hole sections is not simply a matter of applying the same techniques successfully used for decades in vertical wellbores. There are fundamental flow regime differences that require separate treatment in each hole section.

3.4 VERTICAL WELL INTERVALS

Drilling fluid must perform many functions as described initially in almost any course or introduction to drilling fluid theory. One of the important functions is transporting cuttings and sloughings to the surface. Usually drilling fluids are non-Newtonian, and hence very complex from a rheological perspective. This non-Newtonian nature is by design. It cannot only enhance the carrying capability of a drilling fluid but it also makes it difficult to develop theoretical guidelines to adequately describe parameters necessary to clean a borehole.

Three discussions are presented here. The first is a "field-useable" empirical correlation for holes drilled almost vertically. This correlation has been successful for boreholes up to 35 degree from vertical. The second is a series

of guidelines for holes from about 35 degree deviated from vertical to fully horizontal. Third is a simple trend analysis technique to monitor cuttings bed buildup in highly deviated wells. These have been evaluated in the laboratory but, more importantly, validated through extensive field use.

3.4.1 Robinson's Cuttings Carrying Index

One important component of a good drilled solids management philosophy is the drilling fluid carrying capacity. As drilled solids enter the well bore (both sloughings and drill-bit-generated), they should be brought to the surface as soon as possible. If these drilled solids are tumbled and slowly brought to the surface, they have time to fracture, divide into smaller pieces, and continue to disintegrate and increase the low gravity solids content of a drilling fluid.

This relationship was developed by Leon Robinson, PhD and later published for use by our great industry. His goal was to develop a "field-friendly" way of quickly determining whether a well might be adequately cleaning the well or, conversely, was in danger of stuck pipe or other problem due to insufficient hole cleaning.

In developing the empirical correlation, multiple wells in a wide variety of overall drilling situations were used. Early work showed that MW was a very important factor, as was AV. MW affected the force required to move the cutting (via the increased buoyancy decreasing the effective weight of the cutting as MW increased.) AV increases imparted more energy to the cutting to lift the cutting out of the hole. If other properties are equal, higher velocity means higher shear forces are available to transport the cutting, whether the fluid is highly viscous or not.

The intuitive third major factor was of course viscosity. During the time the empirical field-friendly relationship was developed, the yield point [YP, the low shear rate viscosity (LSRV) in the Bingham Plastic model, discussed later], was almost universally used as a measure of how well the mud would clean the hole in the annulus.

However, some wells still experienced problems cleaning the hole even with relatively high YPs.

Multiple mathematical functions of YP as the independent variable were examined, but to no real satisfactory conclusion.

Coincidentally, much laboratory work was being done with various LSRV measurements and proxies (discussed later in this chapter).

In addition, it seemed that drilled solids also affect the drilling fluid properties that control carrying capacity in vertical and nearly vertical (up to 35 degree) wells. While this was not intuitive at the time, it was related to slip velocities of the cuttings.

This last observation proved to be a key to developing the field-friendly equation. As it became clear that the *quantity of solids already in the mud* affected the ability to lift additional solids, a new approach to the traditional YP seemed appropriate.

The LSRV, K, seemed to fit the bill.

K is a function of *both* the YP and the PV (described later). Since PV is affected primarily by the size, shape, and quantity of solids in the mud (along with the liquid–phase viscosity), it seems to capture the essence of what was needed. Though strongly dependent on the YP (which remains the most important single characteristic of the mud for lifting cuttings), it is tempered by the PV, which serves in this case as a convenient proxy for the solids in the mud. Solids content can be difficult and time-consuming to accurately measure at the rig site.

Any given mud will have a limited quantity of solids it can physically transport at a given velocity in the annulus. A highly viscous mud may have a higher transport ability than a lower viscosity one, but both have limits. Any excess solids will fall out to the low side of the hole. The ability to lift solids is not unlimited, even as pump rate is increased. (The pump rate itself is also limited by the pump hardware and rig hydraulic considerations.)

To illustrate the effect of solids on the ability of the mud to lift additional solids, assume that a given barrel of mud has the ability to lift 100 lb of solids, as illustrated in Fig. 3.1. If the mud is densified, 60 lb of that capacity might be "used up" by the barite used to achieve density. Yet another 15 lb might be used up by clays and viscosity modifiers designed to ensure the barite stayed in suspension and to give the mud some initial gel strength. Still another 20 lb might be used up by colloidal and other small-sized drill solids that the solid-removal equipment at the surface has been unable to remove from the mud. With these illustrative numbers, only 5 lb of capacity for new solids, that is, the new cuttings formed at the drill bit, to be carried out of the hole. Furthering the difficulty, the cuttings are almost always larger in size than the other categories of solids, making them even more difficult to transport.
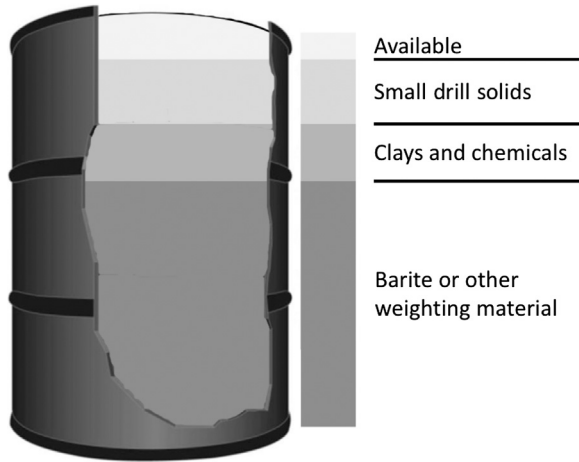
Figure 3.1 Illustration of use of solids lifting ability for a mud.

So, with the third major factor relating to YP and viscosity identified (and tempered by solids content already in the mud via the PV), the exact relationship needed to be solved. After many years of field observation and reports, using traditional oilfield units, Dr. Robinson realized that for most of the hundreds of wells examined, that if one took the MW multiplied by the AV and multiplied by this new *K* viscosity, and the result was numerically 400,000 or greater, the well was unlikely to have experienced hole cleaning—related nonproductive time problems. Conversely, if the computed multiplication result was less than 400,000, the chance of having problems increased, and the further under 400,000 the result was then the more likely the chance of well problems.

This criterion (simply ensuring that MW $\times$ AV $\times$ *K* greater than 400,000) was conveyed to some drilling engineers and used with enthusiasm by them for a few years. However, widespread adoption by company engineers and later all of industry did not occur until the concept was fine-tuned (by defining the Cuttings Carrying Index or CCI as the above product divided by 400,000) that the use became widespread.

That relationship has been published relating a CCI to the product of the MW, AV, and a characteristic viscosity (*K*).

The equation is

$$CCI = \frac{MW \times AV \times K}{400,000} \tag{3.1}$$

where CCI is the Cuttings Carrying Index, dimensionless; MW is the mud weight, pounds per gallon (ppg); AV is the annular velocity, ft/minute; and K is the viscosity, equivalent centipoise.

The 400,000 constant was empirically determined by observing hole-cleaning conditions on many rigs over an 8−10-year period. A CCI value of unity seems to indicate good hole cleaning in both water-based and oil-based drilling fluids. The constant is probably not accurate to more than one significant figure.

The K viscosity can take different forms, but for this purpose was chosen by Dr. Robinson as the viscosity from the power law rheological model, expressed as equivalent centipoise. It can be related to the PV and YP through the pair of equations:

$$n = 3.322 \times \log\left[\frac{(2 \times PV + YP)}{(PV + YP)}\right] \tag{3.2}$$

or more simply,

$$n = 3.322 \times \log\left[\frac{(Fann_{600})}{(Fann_{300})}\right] \tag{3.3}$$

and

$$K = (511)^{(1-n)} \times (PV + YP) \tag{3.4}$$

While these equations can be tedious by hand calculation, they work well in spreadsheets or programmable devices of all types.

An alternate, and what many consider to be an easier method of finding the LSRV K value, is to use the graph following in Fig. 3.2. In this graph, one can simply find the intersection of the PV curve (a separate curve is given for various common values of PV), and the YP lines. The YP lines are vertical lines.

Any interpolation between PV curves or YP vertical lines may be done visually with excellent results.

Referring to Fig. 3.2, a PV of 15 and a YP of 25 intersects at a K value (read off the vertical axis to the left) of about 1200. If PV is not exactly a multiple of 5, simply estimate where the value falls between the two lines and pick the K value accordingly.

It is not necessary to be accurate to three decimal places (or even one decimal!) in order for this technique to be helpful. Inspection of the equations and the graphical representation in Fig. 3.2 shows that at a constant YP value, increasing the PV (i.e., increasing the solids content of the
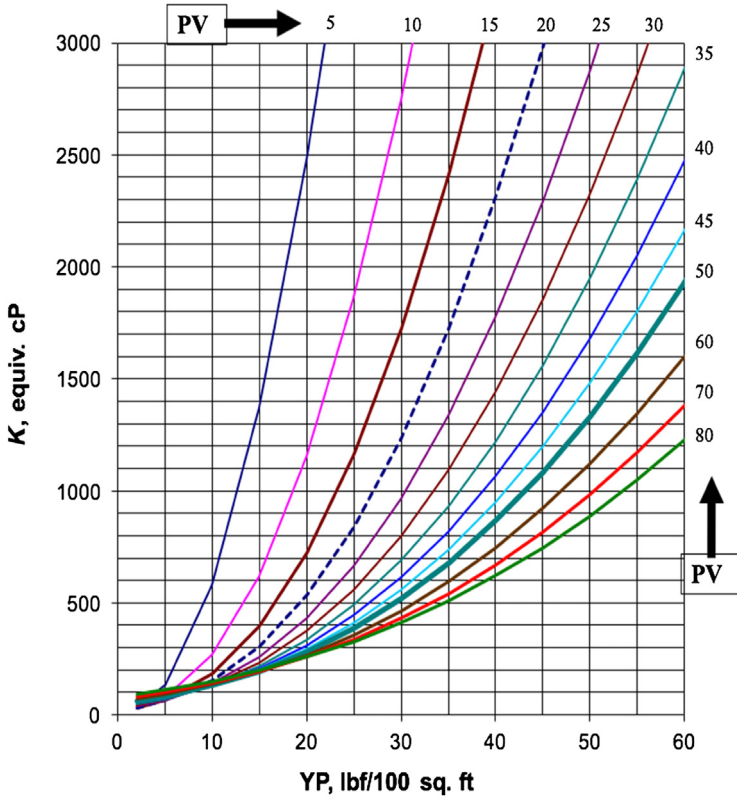
Figure 3.2 Equivalent viscosity (*K*) as a function of PV and YP. *PV*, plastic viscosity; *YP*, yield point. *Courtesy: IADC.*

mud), decreases the value of the *K* viscosity and by extension, the overall ability of that mud to clean the hole[1]. Note that a graphical solution to finding the LSRV *K* as a function of PV and YP is sufficiently accurate and more convenient for most people as shown nearby.

Note also that the desired value of the CCI is 1.0. However, if a cracker–jack operation with good people, supplies, and equipment has a history of trouble free operation with a particular mud system at a lower value, for example, 0.9, that may be sufficient. The well designer should note that risk associated with stuck pipe increases proportionally as the CCI falls further under 1.0. That is, a CCI of 0.5 would be considerably riskier than a CCI of 0.8. Similarly, values in excess of 1.0 convey further

[1] L. Robinson, J. Garcia, Drillers Knowledge Book, IADC, 2015.

Table 3.1 Cuttings appearance and CCI

CCI value	Cuttings description
1.0	Sharp edges
0.5	Well rounded
0.1	Grain sized

CCI, Cuttings Carrying Index.

minimizing risk of hole trouble associated with hole cleaning, up to a point. In excess of a value of 2.5, additional benefit is lacking (discussed later).

Further refinements and study also showed that there was a qualitative but observable correlation between values of CCI and the appearance of cuttings back to the surface, as shown in Table 3.1[2].

Inspection of the table coupled with field experience confirms that hole cleaning would be satisfactory with CCI = 1.0, while it would be correspondingly poor at a CCI value of 0.1, putting the well drilling operation at great risk.

Theoretical solutions of the carrying capacity can become very complex and is a fruitful area for graduate students to develop their analytical skills. Most of the correlations and certainly the flow equations are much too complicated to be satisfactorily used on a drilling rig. The rules of thumb presented here are workable but in no way are intended to diminish the excellent theoretical and empirical work that has been done and continues to be pursued by many scholars and researchers.

3.4.2 "Cuttings block" effect

Importantly, the success of the CCI also yields potential insight into real world cases where good hole cleaning eludes the well-construction team even though design and execution seem adequate or even robust. The success of the CCI helps in evaluating even unusual hole-cleaning failures. The key may lie in the AV term and what may happen in severely enlarged hole sections.

For example, assume that we are drilling a 12.25 in. hole with a 5 in. drill string. We have computed the AV to be 85 ft/minute, and know that the MW is 13.2 ppg and the *K* viscosity is 850 cP. With these parameters, we calculate the CCI value to be 2.4. We are having no hole-cleaning problems.

[2] L. Robinson, M. Morgan, Effect of hole cleaning on drilling rate and performance, in: AADE Drilling Fluids Conference, Houston, Texas, April 6—7, 2004. AADE-04-DF-HO-42.

After drilling a few hundred more feet, cuttings coming back across the shaker decrease and then stop completely even though full mud returns are still reporting to the surface and flow rate, drilling rate and mud properties are the same.

What happened?

An enlarged wellbore may be the culprit. Let us assume the wellbore for 50 ft or so has enlarged (usually due to either unconsolidated rock or the more common case of a "chemical attack" on the formation rock by the mud) to about 22 in. from the original 12.25 in. This raises the cross-sectional flow area *in that 50-ft length enlarged wellbore section* by a factor of 3.7, which in turn reduces the CCI value for that section to 0.6! While the CCI in the 12.25 in. section is robust, the ability of the mud to lift cuttings through and past the 22 in. enlarged section is very poor.

In extreme cases of hole enlargement, this can lead to a de facto "cuttings block" effect where cuttings will have accumulated and tumbled and degraded until small enough to be lifted out of the wellbore.

3.4.3 Sifferman's transport ratio

Prior to Leon Robinson's work, Tom Sifferman, PhD, conducted experiments on vertical hole cleaning in a simulated wellbore[3]. In general, the procedure was to inject cuttings into the bottom of the simulated wellbore (made of casing of different internal diameters) and record the speed of cuttings that reported to the top (or "surface") of the wellbore as a function of various mud types and properties and flow rates of that mud (Fig. 3.3).

His experimental design examined multiple controlled variables. In his observations, several were found to be of major importance. The top two parameters influencing the transport ratio were the AV and the rheological properties of the mud, with simulated chip size and mud density also having important contributions.

In most cases, the cuttings velocity upward would not be the same as the annular mud flow velocity, and the difference represented the tendency, especially in turbulent flow, for the cuttings to "slip" back down the hole.

The relationship reported was

$$V_C = V_A - V_S \tag{3.5}$$

---

[3] T. Sifferman, et al., Drill cutting transport in full scale vertical annuli, in: SPE 4514 Presented at the SPE 48th Annual Fall Meeting in Las Vegas, Nevada, Sep 30−Oct 3, 1973.
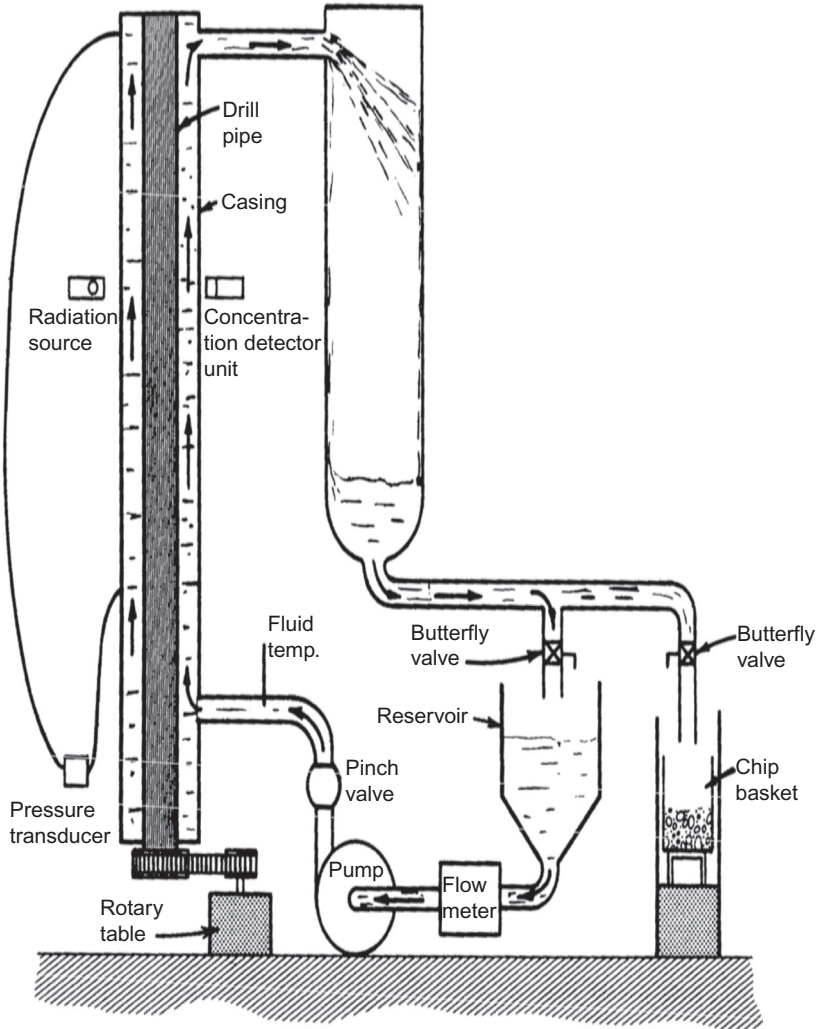
Figure 3.3 Sifferman's transport ratio apparatus [2].

where V_C is the velocity of the cuttings, upward; V_A is the bulk average AV; and V_S is the slip velocity of the cuttings, downward.

Dividing both sides by V_A, the transport ratio (TR) was then obtained,

$$\text{Transport ratio} = \frac{V_C}{V_A} = 1 - \frac{V_S}{V_A} \tag{3.6}$$

or
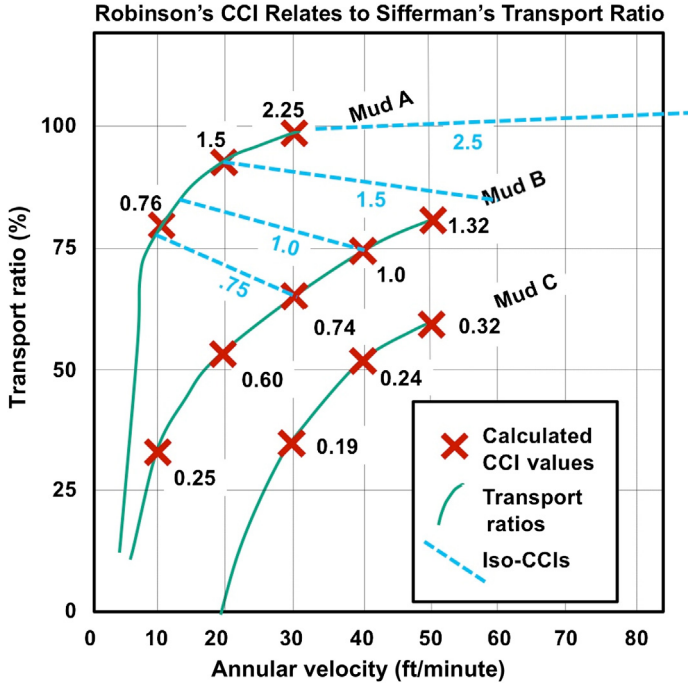
Figure 3.4 Comparison of Robinson and Sifferman approaches.

$$\text{Transport}\% = \frac{V_C}{V_A} \times 100\% \qquad (3.7)$$

Dr. Sifferman's transport percent was defined such that if the cuttings reported to the surface at the same velocity as the mud, one was said to have 100% hole cleaning. Any delay in the time or volume of the cuttings reported to the surface was less than 100%, as shown in Fig. 3.4.

3.4.4 Robinson and Sifferman comparison

Neither work was "theoretical"—both investigations relied on data, one from actual drilling wellbores (with little control over extraneous variables) and the other in laboratory conditions with rigorous controls.

However, both investigations, divergent in nature as they were, came to similar conclusions. Hence, it was inevitable that they would be, and should be, compared (Table 3.2).

The comparison was made, and the two are compared in Fig. 3.4.

Table 3.2 Reported and computed data for Fig. 3.4

Mud	PV	YP	K	V, CCI = 0.75	V, CC1 1.0	V, CCI 1.5	V, CCI 2.5
A	16	37	2520	9.9	13.2	19.8	33.1
B	14	21	825	30.3	40.4	60.6	101.0
C	8	8	213	117.4	156.5	234.7	391.2

PV, plastic viscosity; *YP*, yield point; *CCI*, Cuttings Carrying Index.

At first blush the comparison, while nominally in the right direction for each, does not quite match up. That is, a CCI value of 1.0 (thought to be the value desired in that calculation) occurs considerably lower than a TR of 100%—somewhere between 75% and 85% for muds A and B. Note that at least for mud A, and perhaps extrapolated for mud B, 100% TR is achieved at or below a CCI value of around 2.5.

Initially this was somewhat perplexing until it was realized that Robinson and Sifferman essentially had different criteria for defining successful hole cleaning. Sifferman's 100% TR indicated perfect hole cleaning, which is not necessary to drill a well and is even so indicated by Sifferman. Robinson's 1.0 criteria for designing CCI was predicated on the absence of trouble—not having hole cleaning–related hole problems such as stuck pipe—and said nothing about whether that degree of hole cleaning was perfect or not.[4]

When this distinction is understood, the two efforts are very complementary, not discordant! Combining the two means that for the CCI check at the rig site or in the office, one does not need a CCI greater than 2.5 since that represents perfect hole cleaning or 100% transfer ratio.

So, this author now suggests that the CCI be kept in a nominal range between 1.0 and 2.5. Allowing CCI to go higher than 2.5 is generally a waste of pump pressure, energy, and equipment. Running the pumps too fast also unnecessarily increases the friction loss up the annulus, resulting in higher ECDs and bottom hole pressure. Though normally reported and categorized as lost returns (usually assumed to be a formation strength issue), in cases where pumps were running too fast, even this could be attributed to incorrect design for hole cleaning. In cases where it is found that the CCI is substantially over this value, consideration should be given to

---

[4] The Sifferman tests compared to the CCI were run at low annular velocities in a 12 in. ID by 3.5 in. ID annulus with no pipe rotation, a 12 lb/gal (ppg) mud weight, and with the medium size artificial cuttings (1/8 in. by 1/4 in. by 1/8 in.). As noted earlier, based on these results, annular velocities less than 120 ft/minute are adequate for many muds.
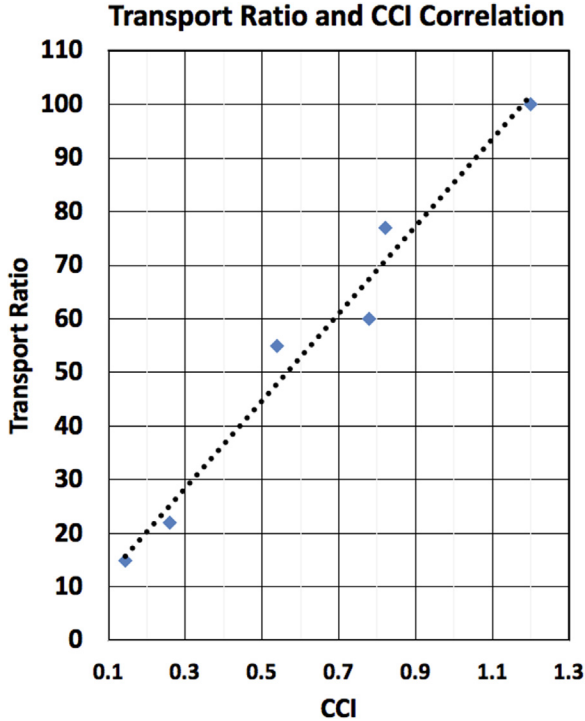
Figure 3.5 Linear correlation of transport ratio with CCI (data points and linear fit). *CCI*, Cuttings Carrying Index.

slowing the pump speed, reducing the rheology, or perhaps both to bring the CCI back into the suggested range. In addition, there is good correlation between the CCI and the TR[5] (Fig. 3.5).

Last, due to the rapid appreciation of the CCI as an effective technique for monitoring hole cleaning, it was rapidly incorporated into API 13D in 2006, merely 2 years after it was first formally reported by Robinson.

CCI example: Consider a mud with a PV $=22$ and YP $=13$. Based on Fig. 3.2 previously, the mud would have an effective viscosity K value of 220 cP. If it was a 13.6 ppg mud (MW) flowing at 62 ft/min (AV), then the CCI is calculated as

$$\text{CCI} = \frac{K \times \text{AV} \times \text{MW}}{400,000} = \frac{(220)(62)(13.6)}{400,000} = 0.464 \qquad (3.8)$$

---

[5] L.H. Robinson, M. Morgan, Effect of hole cleaning on drilling rate and performance, in: AADE Drilling Fluids Conference, Houston, Texas, April 6–7, 2004. AADE-04-DF-HO-42.

★★★Therefore, this will not provide adequate hole cleaning, since the CCI is about one half. For CCI being 1 (good hole cleaning), the above equation can be rearranged to determine the needed value of K:

$$K = \frac{400,000 \times CCI}{AV \times MW} = \frac{(400,000)(1.0)}{(62)(13.6)} = 474 \text{cP} \qquad (3.9)$$

For the same PV of 22 and the new value of $K = 474$ cP, the YP from the figure above becomes about 20. This then provides adequate hole cleaning by increasing the YP from 13 to 20.

3.4.5 Summary (vertical intervals)

The CCI or the Sifferman TR techniques described above, when combined, can give a very satisfactory measure of whether hole cleaning is sufficient to avoid trouble in most cases. Recall that the TR was thought to be sufficient at about 75% or higher. The CCI is thought to be sufficient at 1 (or higher).

However, an unlimited TR (well above what is needed for 100% hole cleaning) or a very high CCI would be counterproductive. Too much hole-cleaning ability results in higher ECDs, lower penetration rates, and in general, wasted energy, and poor efficiencies.

Referring back to Fig. 3.4, CCI values are superimposed on the plot of TR for mud systems, one mud achieves a near perfect TR at a corresponding CCI value of 2.25.

At first, this seems like discordant results, until one realizes that the two measures are looking at different points of perfection. The TR is looking at cutting slippage on its way out of the wellbore relative to the drilling fluid. The Cuttings Carrying Capacity is looking at what it takes to stay out of trouble, based on years of observation—a decidedly Edisonian approach to hole-cleaning issues.

Rather than being discordant, the results are highly complementary. A CCI of 1.0 is reached at a TR of around 75% or so, rightly confirming what any driller knows intuitively that some cuttings in the annulus are acceptable. (If this were not true, then we would have to drill a foot or a few feet, and then circulate bottoms up to remove those cuttings completely before proceeding to drill deeper.)

So what should drillers do when the CCI is already greater than 1.0? Again, the TR gives valuable guidance. Since in Fig. 3.4 TR is nearing

100% when the CCI is computed to be 2.25, it is safe (and conservative) to assume that a CCI value of 2.5 is more than sufficient.

The author proposes that this 2.5 constitutes an upper limit to the design requirements of CCI for ensuring adequate hole cleaning yet not being wasteful in doing so.

Hence, depending on relative risk of a wellbore, a range of CCI values, from 1.0 to 2.5, represents the minimum (or necessary) and maximum (not overly inefficient or wasteful) range for hole cleaning both to stay out of trouble without undue stress on the bottom of the hole (due to ECDs) or on the rig equipment (due to higher pumping rates).

Should a hole be deemed not particularly risky, a value closer to 1.0 can be the target for the mud engineer. Should a hole (or nearby offsets) have a history of stuck pipe or other hole-cleaning related problems, a value of 2.5 might be more appropriate. This latter case would essentially put an extra safety factor on the hole-cleaning parameters, without being wasteful.

Note that the charting techniques in API RP 13D do not show this range of values nor explicitly connect the charts to the Robinson CCI or the Sifferman TR, though these are all obviously quite closely related.

3.5 HIGH-ANGLE HOLE CLEANING

While the CCI has been thoroughly confirmed in vertical wells (those less than 30 degree deviation from vertical), and all wellbores include this vertical and near vertical section, additional constraints should be put on the mud in order to ensure good hole cleaning in the deviated sections.

3.5.1 Boycott settling: the crux of the problem

With the advent of advanced mechanical techniques to accurately drill highly directional wellbores in the 1980s and 1990s (and continuing improvements through today), drillers faced an unanticipated challenge. While the bit could be efficiently steered in the direction desired, trouble costs escalated dramatically in wells drilled more than around 30 degree deviation from vertical.

In particular, problems associated with cleaning cuttings out of the hole increased. For several years, mud engineers were often blamed for

these failures, since the mud formulations had been successfully used for decades in other (mostly less than 30 degree deviated) wells. Efforts were focused initially on doing more of the same things better—improved quality control of the mud, with little to show for it in real cost savings, reduced trouble rates, or less stuck pipe.

After years of industry investigations, trial and (mostly) error, and research, M-I Drilling Fluids (at this writing part of the Schlumberger family of companies) set up a clear plastic inclined wellbore simulator to study the problem. In the course of their investigations, they rediscovered something first reported in literature in 1920, now commonly referred to as the "Boycott Effect" or "Boycott Settling."

During World War I in 1919, a medical doctor, A.E. Boycott, attending to wounded soldiers, made a major discovery that affects the way we design wellbores and fluid in them in order to efficiently remove cuttings. Dr. Boycott, not having a centrifuge to separate white and red blood cells from patients' blood samples, had to simply let gravity do the separation as the blood was held in test tubes. This separation generally took from 8 to 24 hours. As such, he and his staff had developed a standard procedure of collecting new blood samples from wounded soldiers in the morning, putting anticoagulant in the test tubes, and going to lunch. After returning in the afternoon, they would begin testing the blood taken from the *previous day*, since it by then had settled into the denser red blood cells on bottom and less dense white blood cells on top.

One day after coming back from lunch, a test tube rack had been accidentally bumped and was lying at an angle deviated from vertical. To Dr. Boycott's and his staff's amazement, the blood in those inclined test tubes was already separated, even though it had been collected only a few hours earlier that same day.

He noted the angled test tube separation effect—this could help with treating the wounded soldiers—and a year or so later reported the phenomenon in the British journal, Nature[6].

Briefly, in an inclined test tube, the denser red blood cells separate to the low side of the test tube, the white to the high side. This sets up a gravity-driven circulation that then accelerates the separation by density.

The same Boycott Effect occurs in directional wellbores, leading to cuttings bed formation and barite sag.

---

[6] A.E. Boycott, Sedimentation of blood corpuscles, Nature 104 (1920) 532.
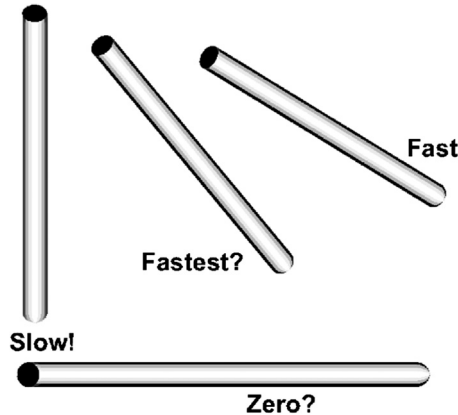
Figure 3.6 Boycott Effect can affect gas kick migration rates. *Courtesy: Texas Drilling Associates.*

It seems that in an inclined wellbore, just like Dr. Boycott's inclined test tubes, the flow characteristics of the mud, gas, and higher density solids is dramatically different in that a gravity-driven circulation system is established that does not exist in a vertical wellbore due to more-or-less randomized mixing of the particles as they are pulled downward. In an inclined wellbore, as the particles settle to the low side of the wellbore, the lower portion of the drilling fluid is heavier while the upper portion is lighter. This segregated fluid distribution in turn permits gravity to establish a circulation along the high side and low side of the wellbore, with some fluid moving up and some moving down, even with the pumps shut off!

In the case of a gas kick, the Boycott Effect works in a similar fashion to rapidly separate what may initially be entrained microbubbles of gas into larger bubbles on the high side of the hole. Whereas the entrained microbubbles may migrate very slowly—especially in a vertical wellbore—the coalescing of microbubbles and subsequent breakout of larger bubbles may migrate very rapidly by comparison in a deviated wellbore. Some reports indicate that the difference in migration speeds can be an order of magnitude larger for the Boycott Effect separated gas bubbles (Fig. 3.6).

A simple physical metaphor for this difference between vertical and deviated flow can be found in a simple "glitter tube" commonly found in toy stores and the like. If the tube is inverted vertically, the velocity of the gas bubble traveling to the top is counterintuitively slower than in the

inclined tube case. The motion of the glitter particles making their way to the bottom is slower than in an otherwise similar inclined tube case. By this analogy, the rate at which solids might settle out of a mud column in a deviated wellbore might be similarly accelerated.

3.5.2 Rules of thumb—guidelines

One approach to addressing these somewhat counterintuitive effects is to apply some time-tested rules of thumb that operators have found useful since the explosion of highly directional drilling occurred in the early 1990s. It was realized by industry, in part due to a video produced by the M-I drilling fluid research group in Houston, Texas, that low shear rate viscosities played a much larger role in cleaning highly deviated wellbores than was previously thought (or at least practiced) by the industry. As part of that groundbreaking work, M-I reported that several mainstream mud systems that had performed well in vertical wellbores for decades simply did not have sufficient low shear rate viscosities to clean the wellbore.

While the guidelines used by industry have changed (and undoubtedly will continue to change with improved knowledge and products), the 3 RPM and 6 RPM Fann viscometer dial readings have been a good proxy for mud engineers. The guideline for the 3 RPM Fann reading has been to maintain a minimum reading of 10 for all hole sizes. The guideline for the 6 RPM Fann reading, long taken to require a value of 1.3 times the hole diameter in inches, has in recent years been "thickened" somewhat to a value of 1.6 times the hole diameter in inches.

As technology has developed, some companies are going back to a thinner mud at high angles, recently reported to be as low as 0.8 times the bit diameter for the 6 RPM reading.

A hybrid LSRV reading has also been used with some success, calculated by multiplying the 3 RPM reading by 2 and then subtracting the 6 RPM reading from that.

$$LSRV = 2 \times (3 \text{ RPM Fann}) - (6 \text{ RPM Fann}) \qquad (3.10)$$

The report is that if this LSRV hybrid number is in the range of 16−18, the muds are thick enough to pick up cuttings and prevent redeposition of cuttings, yet not so high as to cause harmful ECD effects.[7]

As with all rules of thumb, they continue to evolve with time as more experience is gained using them in field operations.

[7] Unpublished private correspondence.

Table 3.3 Rules of thumb for 3 RPM and 6 RPM Fann dial readings for good hole cleaning

	3 RPM Fann reading	6 RPM Fann reading (c.1995−2000)	6 RPM Fann reading (c.2000−15 +)	6 RPM Fann reading (c.2010 +)	Combined or hybrid LSRV (c.2010−19 +)
Hole size (in.)	Minimum 10	1.3 × bit diameter (in.)	1.6 × bit diameter (in.)	0.8−1.0 × bit diameter (in.)	[(2 × 3 RPM) −6 RPM] dial readings (*maximum*)
8.5	10	11	14	7−9	16−18
12.25	10	16	20	10−12	16−18
14.75	10	19	24	12−15	16−18
17	10	22	27	14−17	16−18
26	10	34	42	21−26	16−18

LSRV, low shear rate viscosity.

1. To reduce "sag" of barite and help suspend cuttings, the 3 RPM Fann reading should be larger than 10. (Caution should be exercised to ensure that the 30-minute gel does not show an excessive increase above the 10-minute gel.)
2. To clean horizontal holes, the 6 RPM Fann reading should be as large or larger than 1.3 times the hole diameter in inches. In recent years, some operators have opted to increase this to 1.6 times the hole diameter in inches.
3. Still others have used different relationships and values as the best for cleaning high-angle holes. Table 3.3 summarizes some of these practices. As with all drilling issues, what may work well with one set of equipment, mud, and geology may not be the best for all, so final decisions will rest with the drilling team to determine the best solution for their case.

These assorted rules of thumb are summarized in Table 3.3, and examples given for selected hole sizes. Note that in recent years, some investigators have concluded that a thinner 6 RPM viscosity is a better solution than a thicker one, due to this thinner fluid producing a more turbulent flow regime.

In a high angle well, solids need only fall a few inches to reach the bottom of the hole. In vertical wells, the settling distance is thousands of feet. With simpler drilling fluid systems of many years ago, most drilling contractors subscribed to the concept that the fluid velocity was the only parameter that would prevent settling in pipes.

For example, in the lower large diameter back–flow lines between mud tanks, if the velocity was less than 5 ft/second, barite would settle. Generally, the barite would settle and plug the lower part of the line until the velocity was greater than 5 ft/second. (They also tried to prevent the velocity from exceeding 10 ft/second to decrease the likelihood of turbulent flow.) The wisdom of that era was that nothing could prevent settling except velocity. Fortunately, rheological means have been found that will allow several thousand feet of horizontal hole to be cleaned. These techniques are still improving.

3.6 TREND ANALYSIS IN HIGH-ANGLE WELLBORES

In addition to formal analysis and rules–of–thumb guidelines, trend analysis can be an effective way to monitor whether hole cleaning is sufficient. Tried and true items to monitor include

- cuttings' size,
- cuttings' shape,
- cuttings' volume,
- mud properties, and
- pressures related to cuttings loads.

The last item on the list can be accomplished in a variety of ways. Some operators have used standpipe pressures or better downhole pressure while drilling (PWD) tools to warn when cuttings load is building up in the annulus. This works since cuttings build up effectively makes the annulus mud denser, in the same manner that barite does, but less efficiently (since the specific gravity of cuttings is lower than that of barite.) This pressure monitoring can effectively warn of cuttings buildup in the annulus when done holding other variables affecting pressure constant as explained in the following section.

3.6.1 Cuttings bed measurement and management

Particularly in the regions of a well that exceed 30 degree inclination from vertical, care must be taken to actively manage the formation, stability, and removal of beds of cuttings that inevitably form at various locations.

First, these beds must be broken up, put back into the active flowing section of the wellbore annulus fluid, and removed from the well. Usually this can only efficiently be accomplished by rotating the drill string, though some other techniques have proved helpful at times, including

- spiral rigid blade centralizers,
- high density (HD) mud "pills" (for higher buoyancy) followed by high-viscosity pills,
- low density mud "pills" (for higher turbulence) followed by high-viscosity pills,
- rotating the drill string,
- increased AV, and
- wiper trips.

A particularly helpful trend analysis available to highly deviated wellbores (hole angle greater than 30 degree from vertical) is to monitor the magnitude of the annulus friction loss changes when going from the drill string rotating to nonrotating or vice versa. This was first noticed in one of the first commercial uses of PWD (not even named that at the time) conducted and analyzed by Amoco Offshore Stavanger Norway in the mid-1990s. A highly deviated well was being directionally drilled using what at the time was the standard "slide-rotate" directional drilling method utilizing a bent housing mud motor. It was noticed that there was a significant, yet not constant, variation in the bottom hole ECD when the drill string was rotated as compared to the nonrotating "sliding" mode. Investigation revealed that when a cuttings bed was present, as is almost always the case in a highly deviated well such as the one being drilled, rotation of the drill string "stirred up" the cuttings bed, thus putting more cuttings in the bulk mud and making it slightly, yet measurably more dense. When the rotation of the drill string is stopped, some cuttings fall back to the low side of the hole, effectively reducing the bulk density of the annulus mud (in much the same way barite sag reduces density, as describe previously in this chapter).

Referring to Fig. 3.7, one can see that the difference between the left side of the grayed area data points (taken during slide drilling times in the well) and those of the right side of the grayed area (taken during times of rotary drilling) are very consistent. The rotary drilling points are higher ECD than the static (sliding drilling) data points at nearby depths. Other variables to ECD were kept nearly constant during this hole interval, except in a few cases where flow rate was adjusted in order to control ECD.

In this particular type of trend analysis, the macro trend, such as the one where ECD is rising steadily from about 1900 to 2200 m (a clearer
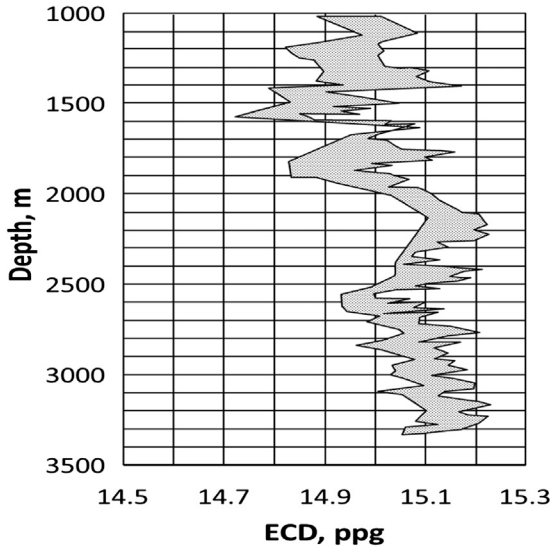
Figure 3.7 Measured ECD in highly deviated well. Left edge of shaded area is sliding mode while right edge of shaded area is rotating mode. *ECD*, equivalent circulating density. *Courtesy: Texas Drilling Associates.*

trend on the rotating than the nonrotating data), does not matter so much as the trend of the difference between the rotating and nonrotating data at a given depth. As an example, the data at about 1650 m shows a relatively small separation of only about 0.1 of a ppg difference, but by 1800 m this difference has rapidly widened to nearly 0.3 ppg difference. An alert driller, toolpusher, company man, mud engineer, or other personnel should be trained to rapidly recognize this difference and take remedial action to remove the rapidly building cuttings bed.

The action to remove the bed may vary with operator and rig site personnel preferences. The remedies could include

- Faster pump rate.
- Rotation coincidental with sweeps or pills. A viscous pill can be very effective when used with rotation but is not effective used by itself. Some personnel believe that a very thin pill, a weighted pill, or both, preceding the viscous pill can also improve remedial hole cleaning, but data supporting this is largely anecdotal in nature.
- Back-reaming.[8]

[8] Back-reaming has recently been shown to sometimes cause problems, and hence many operators are now discouraging its use as a routine way of handling cuttings beds. See Appendix in this chapter for more information.

- Increasing the LSRV of the drilling fluid (where ECD considerations on open hole fracture pressure permit).
- Decreasing the LSRV, with the thought that the increased turbulence of the thinned fluid may help pick up at least smaller cuttings.

As is readily evident from the variety of possible remedies as well as the opposite nature of the last two bulleted points, there is much work remaining to be done on how to best design and use mud systems for high-angle wellbore cleaning.

Note that in wells where a PWD tool is not being utilized, the same effect, albeit somewhat attenuated, can usually be seen on most standpipe pressure measurements. If the driller simply notes in his trip book the difference between rotating and nonrotating pressures, he can quickly spot the effect of a cuttings bed buildup, in most cases before significant risk of trouble or actual trouble develops.

Note that pumping a high-viscosity mud "pill" will generally not be effective by itself in removing cuttings beds. This is due to the shear-thinning nature of the mud. In the region adjacent to the cuttings bed, the mud is subjected to a relatively high shear rate, and hence a pill that is highly viscous at low shear rates will be locally thin just adjacent to the bed of cuttings (where high shear rates occur).

Note also that this skepticism of the ability of viscous pills to not be effective in high angle and horizontal wellbores should not impugn on their ability to remove cuttings from a vertical wellbore. The use of viscous pills or sweeps to remove cuttings in vertical wellbores is well established.

In any high-angle wellbore, trend analysis is also important. The trend is your friend. This may be quantitative or qualitative and may involve multiple variables such as size and shape of cuttings, volume of cuttings reporting to the surface as a function of ROP, and even pumping or PWD pressures.

The illustration in Fig. 3.7 is not hypothetical. It is based on one of the first times drillers were able to directly observe cuttings bed buildup in a wellbore, at least in a qualitative sense. As the difference between rotating and nonrotating pressure increased (at any given depth), the largest contributor to the increase is the presence of a cuttings bed on the low side of the hole.

As the cutting bed increases, so does the variation in pressure between rotating and nonrotating conditions. The wider the difference in nonrotating and rotating pressures (gray area of Fig. 3.7), the deeper the cuttings bed is at least in a relative sense.

Note that Barite Sag is somewhat similar, and a brief discussion is included in this chapter's appendix.

3.7 HORIZONTAL WELL HYDRAULICS

In horizontal and nearly horizontal wellbores, a curious discovery was made by Henry Nickens of Amoco Production Research Company in Tulsa, Oklahoma. Dr. Nickens was investigating pressure drops through annuli, particularly at high angles in simulated wellbores and flow loops.[9] He found that, counterintuitively, it was possible at times to change the flow rate in the horizontal test section without appreciably changing the pressure drop through that test section. In some flow rate comparison cases, the relationship between flow rate and pressure drop was actually negative—the faster he pumped, the less pressure drop he got!

In terms of conventional fluid mechanics, this was not possible. Increasing flow rate, implying higher velocities, should result in higher pressure losses. In fluid mechanics terms, the link between fluid velocity pressure losses is a well-established part of the physics of fluid flow.

The solution to this apparent paradox found by Dr. Nickens lies in the behavior of the cuttings beds themselves as shown in Fig. 3.8. Fluid velocity itself was changed by the cuttings beds and vice versa.

Dr. Nickens found that the cuttings beds acted as a regulator on pressure drop or, more accurately, on fluid velocity which controls that
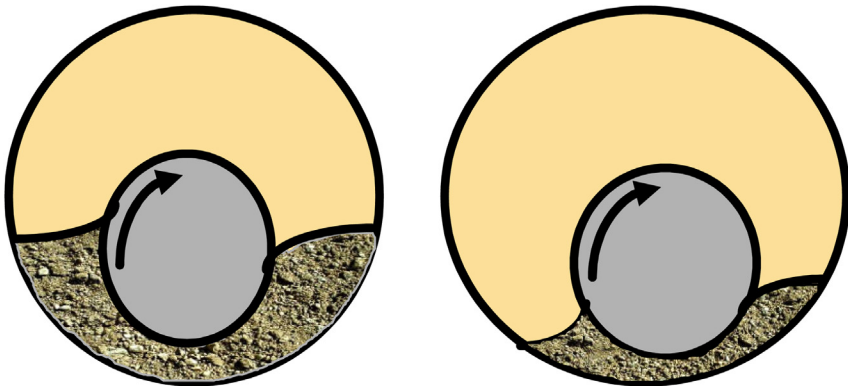
Figure 3.8 Poor and better hole cleaning as seen by cuttings bed thickness in horizontal wellbore section. *Courtesy: Texas Drilling Associates.*

---

[9] Nickens, Henry, PhD, private correspondence August 1, 2018. Dr. Nickens work was based on analysis and simulation models based on cuttings transport data from the Tulsa University Drilling Research Project (TUDRP).

pressure drop. When the pumps were run faster, the cuttings bed would erode as shown on the right drawing. This erosion of the bed resulted in a larger cross–sectional area above the bed and the pipe, resulting in a lower velocity and hence lower pressure drop.

Conversely, if the pumps were slowed, more cuttings would fall out of the slurry to the low side of the hole as shown on the left side of the drawing, reducing the cross–sectional area resulting in a higher velocity and hence higher pressure drop.

Once equilibrium was reached after a pump rate change, the equilibrium velocity of the fluid was essentially unchanged, and hence the pressure drop itself was unchanged!

Effectively, the cuttings bed buildup served to adjust the flow velocity to match the fluid's ability to transport cuttings.

3.8 INSTRUCTIVE VIDEO

M-I, one of the premier drilling and completion fluid companies with a robust research program, produced an excellent video that examined effects of various parameters on hole cleaning of various geometry wells. To do this, they constructed laboratory-sized but properly scaled flow loops. These flow loops had clear plastic sections so that it was possible to see and hence videotape the fluid in motion in the simulated wellbore.

Note several factors that are varied by the M-I investigators in the video:
- mud type,
- drill string eccentricity (see Fig. 3.9),

Concentric   Partially   Fully
                    eccentric   eccentric
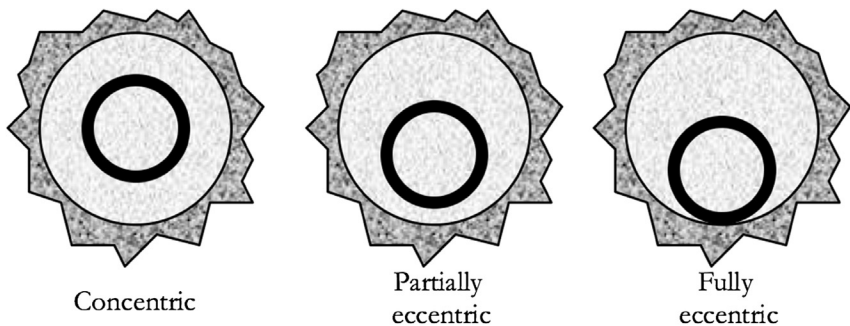
Figure 3.9 Representative pipe placements in wellbore. *Courtesy: Texas Drilling Associates.*

- drill string rotation,
- hole angle,
- hole geometry, and
- fluid velocity.[10]

Several test series examined the effect of pipe eccentricity on the removal of cuttings beds. They refer to pipe as being concentric, partially eccentric (sometimes giving the amount of eccentricity), and fully eccentric, which would be typical of a drill string lying on the low side of a wellbore. Fig. 3.9 illustrates this.

3.9 CHAPTER APPENDICES

3.9.1 Blank *K* (plastic viscosity, yield point) chart (for use in problems)

A blank K viscosity chart is provided by Fig. 3.10 below, for use in exercises or for use by field personnel.

3.9.2 Exercise with Cuttings Carrying Index

Using the $K-PV-YP$ chart nearby, find the K value for the PV and YP values in the table. Then use the equation for CCI shown below to find the value of CCI for the following mud properties:

Part One: Calculating the CCI directly

$$\mathrm{CCI} = \frac{\mathrm{MW} \times \mathrm{AV} \times K}{400,000}$$

No.	PV	YP	K	AV	MW	CCI
1	10	20	1160	100	12	
2	20	20		100	12	
3	20	10		150	12	
4	30	25		180	18	
5	40	20		180	15	

PV, plastic viscosity; *YP*, yield point; *AV*, annular velocity; *MW*, mud weight; *CCI*, Cuttings Carrying Index.

---

[10] In lieu of flow rate for the scaled size tests.
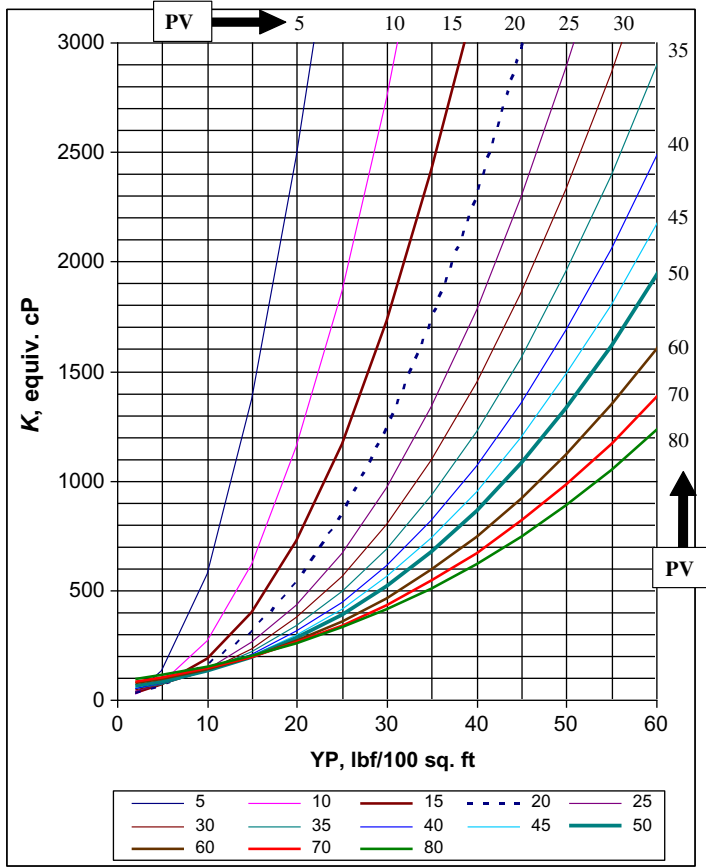
Figure 3.10 Blank K–PV–YP (low shear rate K viscosity) chart (Texas Drilling Associates, IADC). *PV*, plastic viscosity; *YP*, yield point.

Part Two: Calculate the needed K viscosity and then look up the required YP on the graph. Hint: To find the K viscosity needed to make the CCI = 1.0, 2.5, or something in-between, the CCI equation is rearranged as shown below:

$$K = \frac{\text{CCI} \times 400,000}{\text{MW} \times \text{AV}}$$

No.	PV	YP	K	AV	MW	CCI
6	20			80	9	**1.0**
7	15			100	10	**2.5**

PV, plastic viscosity; *YP*, yield point; *AV*, annular velocity; *MW*, mud weight; *CCI*, Cuttings Carrying Index.

Substitute **1.0** in no. 6 or **2.5** in no. 7 for CCI and the MW and AV in order to calculate K viscosity. Then find that K viscosity on the left axis of the chart and go across until you cross the curved PV line. (PV cannot be quickly adjusted since it is due almost entirely to solids content.) Then drop down vertically to read the YP needed on the horizontal axis.

3.9.3 Slip velocities

When a particle falls though a static or quiescent fluid of infinite volume (to avoid wall effects), the particle eventually attains its maximum and final velocity called its "terminal settling velocity." It is also often called the slip velocity, v_s, too since it is the velocity at which the particle falls (slips) relative to the remainder of the fluid. In hole cleaning, the concept is often used for a cutting slipping in a moving fluid.

There are several equations that have been proposed to calculate slip velocities.

Chien (1972)[11] developed slip velocity equations, the simpler one is given in the following equation:

$$v_S = 86.5 \sqrt{d_C \left(\frac{\rho_C}{\rho_M} - 1 \right)} \tag{3.11}$$

where v_S is the cutting slip velocity in ft/minute, d_C is the equivalent diameter of the cutting in inches, while ρ_C and ρ_M are the cutting and mud densities in ppg.

The concept of equivalent diameter is introduced since most cuttings are not perfect spheres. There are various ways to determine the equivalent diameter, but this is beyond the scope of this book. For instance, it can be based on geometry (the diameter that has the same volume or surface area) or hydrodynamics (such as the same settling velocity). The terms sphericity or shape factor are often used in these discussions also.

If the particle is not spherical and has a longer "length" than other dimensions, the particle will fall at different settling velocities depending on its orientation to the force of gravity. In fact, some particles will "wobble" (move back and forth almost horizontally) as they fall.

[11] Chien, Sze-Foo, "Annular velocity for rotary drilling operations", Int. J. Rock Mech. Min. Sci. 9: 403-416, 1972.

3.9.4 Velocity profiles (cuttings movement)

After the cuttings are generated at the bottom of the hole by the drill bit, they move up the annulus between the wellbore and the bottom hole assembly (BHA). As the cuttings travel out of the hole, the annuli change (wellbore by drill pipe, casing by drill pipe, etc.). If the drill pipe/BHA is perfectly centered in the wellbore, there is no eccentricity, and both sets of centerlines lie along the same line. This, however, is unusual and there is usually some eccentricity (offset of the centerlines) which results in more flow (and therefore higher velocities) on one side of the eccentric annulus. More importantly, the velocity profiles in the annulus are not the same as in a circular pipe but are skewed as well. They are not symmetric. However, for this discussion, we will assume that the AV profiles are similar to those in a circular pipe such as the drill pipe to simplify our discussion.

For laminar flow, in the ideal case, all the fluid is moving in parallel layers like playing cards sliding over each other in a deck-of-cards fashion as shown in Fig. 3.11.

For a circular pipe, the maximum fluid velocity is at the centerline of the pipe. However, at the wall, the fluid is not moving due to the "no slip at the wall" condition, which states that the fluid at the wall is stationary. The velocity profile has the shape of a symmetric parabola for Newtonian fluids as shown in the following equation:

$$V_r = \frac{\Delta P \times R^2}{4 \times \mu \times L} \times \left[1 - \left(\frac{r}{R} \right)^2 \right] \tag{3.12}$$

where V_r is the velocity along the pipe, R is the inside pipe radius, r is the distance along the radius from the centerline, L is the length of the
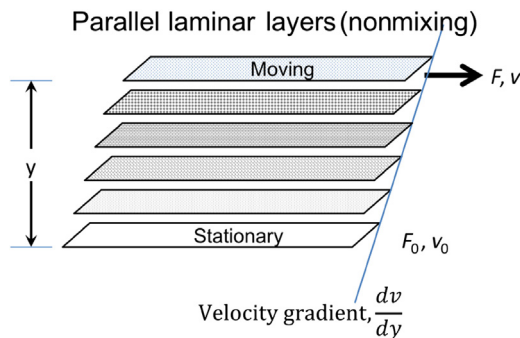
Figure 3.11 Laminar flow concept (nonmixing).
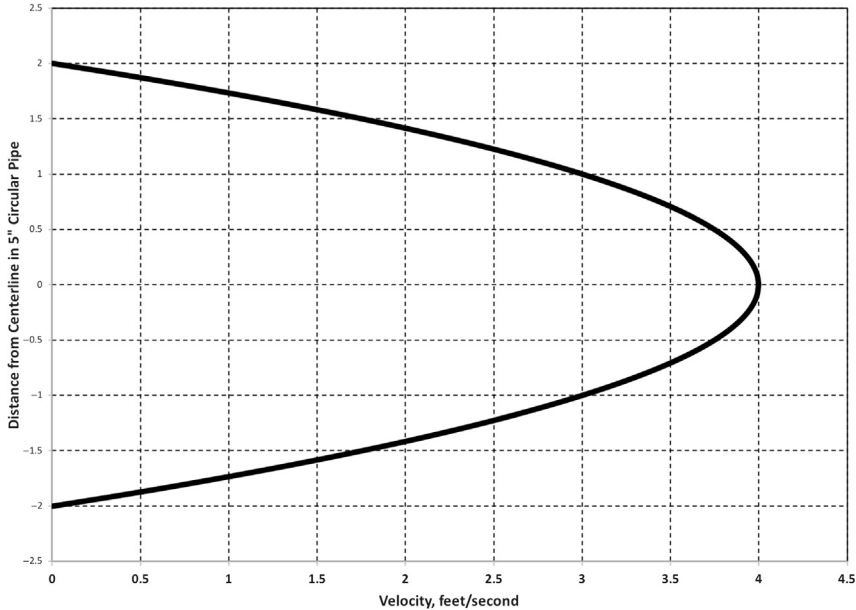
Figure 3.12 Parabolic laminar flow in circular pipe, maximum velocity in center.

pipe over which the pressure drop (ΔP) is measured, and μ is the Newtonian viscosity.

If this parabolic equation for velocity V_r is plotted for various values of the distance r along the radius from the centerline, Fig. 3.12 shows the results, where the maximum velocity is at the centerline of the pipe and there is zero at the pipe wall (no slip condition). The figure could be considered for the case of laminar flow of a Newtonian fluid down the drill pipe.

For flow up the annulus, such as between the drill pipe and either the wellbore or casing, the velocity profile is skewed toward the centerline due to slightly less drag on the inside compared to the outside of the flow cross section due in turn to the smaller zero velocity surface on the inside as shown in Fig. 3.13.

The velocity profile equation for annular flow is more complicated than the one above for a circular pipe. It is given by

$$V_Z = \frac{1}{4\mu}\frac{dP}{dz}\left[r^2 - r_o^2\right] - \frac{V_C + \left(\left(\frac{1}{4\mu}\right)\left(\frac{dP}{dz}\right)\right)\left[r_o^2 - r_i^2\right]}{\ln\left(\frac{r_o}{r_i}\right)} \times \ln\frac{r}{r_o} \qquad (3.13)$$

where r_o is the pipe radius, r_i is the core radius, and r is the radius being investigated in annulus.
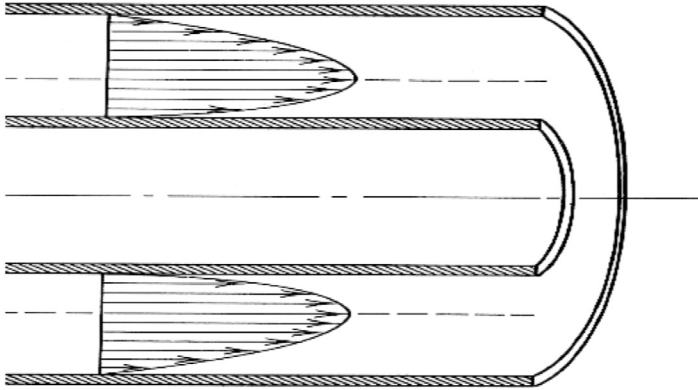
Figure 3.13 Laminar flow in concentric annulus skewed slightly toward inner surface.

But the annular flow equation reduces to the case of a circular pipe when the inner pipe is removed (i.e., the inner pipe diameter shrinks to zero).

If a drill cutting stays at the point of the maximum velocity, it will reach the surface in less time than the average time based on the average velocity. However, a drill cutting often falls off the peak velocity and moves to a point of lower velocity and therefore takes more time to get to the surface. The movement has often been called "tumbling" or "slipping" since the drill cutting may actually be falling down opposite the flow (moving backward) at times.

When such slippage or tumbling occurs, the cuttings TR (discussed earlier in this chapter) will necessarily be less than 100%. However, the TR is a very conservative measure to design to be 100%, and a smaller value is usually sufficient, perhaps in the 70%−80% range, checked for efficacy with the CCI (also discussed earlier in this chapter).

If the fluid follows a Bingham plastic model, the fluid in the center area of a circular pipe moves as a plug (a relatively flat velocity profile with little variation in velocity), while in the outer areas, the velocity decreases from the maximum plug velocity to zero at the outside wall as shown in Fig. 3.14. The fluid near the centerline has a shear stress less than the YP. In the outer area toward the pipe wall, the shear stress is greater than the YP.

Since the velocity profile is flat in the center (middle) area, the cuttings that are present can be transported efficiently by the peak (maximum) velocity.

Finally, for a power law fluid, the velocity profile depends on the power law index n.
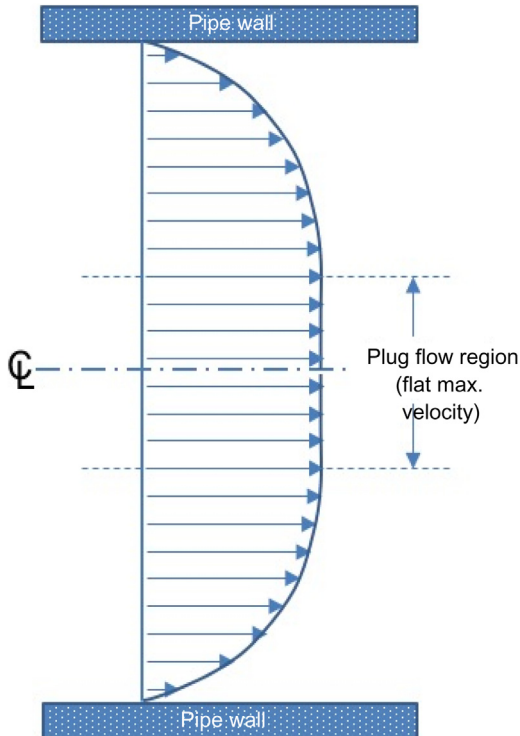
Figure 3.14 Idealized flow profile for a Bingham fluid.

$$V_r = V_{\text{MAX}} \times \left(\frac{(3 \times n) + 1}{n + 1} \right) \times \left[1 - \left(\frac{r}{R} \right)^{\frac{(n+1)}{n}} \right] \qquad (3.14)$$

where R is the radius, V_r is the local velocity being investigated, and V_{MAX} is the maximum velocity found along the centerline (Fig. 3.15).

Note that when the power law index n is equal to 1 ($n = 1$), the fluid is Newtonian and the velocity profile is parabolic as shown in Fig. 3.14.

Note also that when n is 1/3, the velocity profile looks somewhat similar (yet slightly different) compared to the Bingham plastic velocity profile.

3.9.5 Viscoelasticity, elastic modulus, viscous modulus

Some interesting work is underway regarding the viscoelastic behavior of drilling fluids. The difference between a liquid and a solid seems rather clear
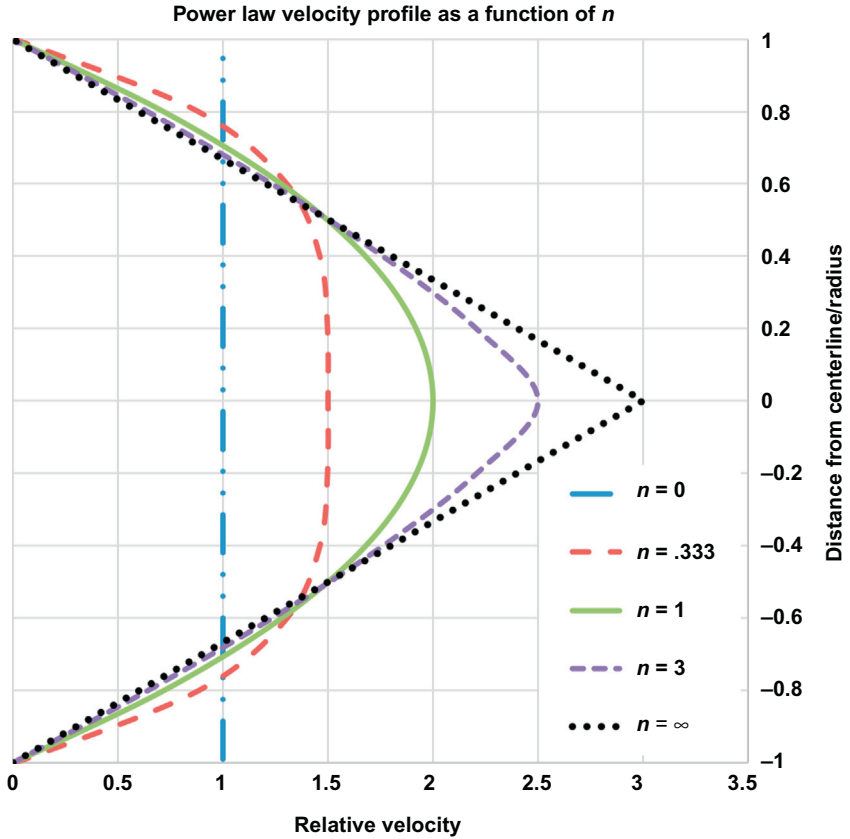
Figure 3.15 Power law fluid velocity profile as a function of radial location and *n*. (Note that calculations are relative to maximum velocity.)

on the surface or from a superficial examination. Consider, however, the addition of Jello to hot water. The initial slurry is liquid. After a short time, the mixture sets into a gelled structure. Is it a solid? At what point does the liquid become a solid? Many complex mixtures are described mathematically by examining the relationship between shear stress, shear, and shear rate. A simple liquid which has a shear rate directly proportional to the shear stress is called a Newtonian liquid. The constant of proportionality is called the viscosity. An elastic solid has a shear displacement directly proportional to the shear stress. Hooke's law describes the solid by stating that the strain is directly proportional to the stress.

Some materials exhibit characteristics of both liquids and solids. If such materials are subjected to an oscillatory stress, the measured strain would not be either exactly in-phase with the applied stress (like an elastic solid) or exactly out-of-phase with the applied stress (like a liquid). The measured strain would be some intermediate angle between 0 and 90 degrees out of phase. Some energy would be stored in each cycle, and some energy would be dissipated as in a liquid. So the material acts as a viscous material for part of the cycle and an elastic material for part of the cycle. This provides the term "viscoelastic."

The rheological equation which describes this behavior involves relating the shear stress, τ, to a complex shear relaxation modulus, G. The stress on the material under oscillation at a frequency of $\acute{\omega}/2\pi$ with maximum amplitude, γ could be represented with the equation

$$\tau = \gamma \times (G' \times \sin(\omega \times t) + G'' \times \cos(\omega \times t)) \tag{3.15}$$

where G' is the shear or elastic modulus (the in-phase component) and G'' is the viscous modulus (the out-or-phase component).

The problem with the above concepts is that the equipment is not yet adaptable to field measurements. These concepts are still being developed and refined. The exploration of the behavior of various polymers and clay blends indicate that the YP, the gel strength, and the 3 or 6 RPM rheometer readings do not predict the responses from viscometers that measure the G' and G'' components. These measurements will probably be eventually used to aid in prediction of horizontal hole cleaning.

Horizontal holes can be cleaned effectively if the drilled solids are prevented from falling from the drilling fluid. If the fluid does not have reasonably large elastic component of viscosity, drill solids will settle. For example, drilled solids suspended in molasses will eventually fall to bottom. Drilled solids suspended in grape jelly will not fall. Why? The elastic component of viscosity of the molasses is zero. It is a Newtonian fluid (the viscosity is constant no matter what the shear rate is). The grape jelly has a very high elastic component of viscosity arid will suspend solids. The question has always been the following: "how to produce a fluid that flows easily and has a very high gel structure (or high elastic component) when the flow stops?" High concentrations of XC-polymer or Dow Chemical's MMH (mixed metal hydroxide, see below) are known to perform like this.

Some of the benefits of such fluids compared with conventional fluids include the following:

- Pump pressures will be lower for the same flow rates.
- Circulation lag time is reduced.
- Torque and drag is reduced due to improved hole cleaning.
- Fewer problems running logging tools, casing, or liners.

The second development that has been achieved recently is the use of the MMHs fluid. MMH is a highly positively charged man–made additive that creates some unusual drilling fluid properties. An MMH drilling fluid in a well in East Texas had a funnel viscosity of only 45 seconds yet it would support a 2-in. diameter rock picked up on location. The turnkey contractor claimed that they were sinking record wells because of several benefits of the fluid—primarily better hole cleaning. MMH behaves differently from most fluids that exhibit such a high gel structure. Ordinary water-based mud formulations rely on "Wyoming Bentonite," (sodium montmorillonite), but this in turn usually requires the application of high shear rates to loosen the gel structure. MMH breaks with shear strain; therefore, very low standpipe pressures required to initiate flow after a trip. The MMH fluid will also provide a very large elastic component of viscosity.

However, though the fluid performance is exemplary when run correctly, the formulation is very sensitive to chemical treatments on the surface, and competent mud engineers are an absolute necessity. The system can be essentially ruined by relatively small concentrations of organic acids, for example. As organic acids are common on rig sites and used as mud additives; the danger of accidentally ruining the MMH mud system is very real.

3.9.6 Barite sag

The topic of barite sag is very closely related to hole cleaning. Some of the first papers on barite sag were actually based on hole-cleaning concerns.

In reality, a more general term for barite sag is "weight-material sag" as used by ISO and the American Petroleum Institute (API) in their document. Hematite and calcium carbonate should also be included.

Barite sag has been defined as the "density variation observed in directional wells observed when circulating bottoms up after operations where the drilling fluid has been exposed to near static conditions."[12].

---

[12] J.C. Rojas, B. Daugherty, et.al. "Increased deepwater drilling performance using constant rheology synthetic-based mud", AADE-07-NTCE-20, 2007, presented at the 2007 AADE National Technical Conference and Exhibition in Houston, Texas, April 10-12, 2007.

This variation is due to settling of the weighting material which is typically barite.

Two key findings of early work on barite sag were as follows[13]:

- The density variations are caused by slumping of the beds on the low side of the hole.
- Most of the bed formation occurs while the pumps are on and the mud is still flowing. Little occurs once the pumps are turned off.

The concept of sag factor, defined below, was introduced to help highlight and track barite sag[14].

$$\text{Sag factor} \quad = \frac{\text{Density at bottom hole}}{(\text{Density at bottom } + \text{density at surface })} \qquad (3.16)$$

Zero sag gives a sag factor of 0.5. If the sag factor is >0.54 in the North Sea, there is concern and steps should be made to lower this sag factor.

For dynamic barite sag, a device was built by Schlumberger Cambridge Research and is described in the Appendix. The term "excess density," which is 1000 times the density difference before and after the sag test, was used as a descriptor of barite sag in this case.

OFI Testing Equipment has a barite sag procedure that seems somewhat similar to the proposed ISO procedure given below. It uses a "sag shoe" insert in the bottom of a viscometer to measure barite sag. Several years ago, Zamora et al.[15] were issued a US Patent on a sloping insert for a viscometer called a "shoe" that is used in testing for barite sag with a procedure they called the Viscometer Sag Test (VST).

Subsequently, the Viscometer Sag Shoe Test (VSST) was developed. The OFI "Viscometer Sag Shoe Test (VSST) is a well site and laboratory

---

[13] P.M. Hanson, T.K. Trigg, Jr., G. Rachal, M. Zamora. 1990. "Investigation of barite sag in weighted drilling fluids in highly deviated well" in: paper SPE 20423 Presented at the 65th Annual Technical Conference and Exhibition of the Society of Petroleum Engineers held in New Orieans, LA, 23-26 September. *(PDF)*.

[14] E. Gao, M. Booth, N. MacBeath, Continued Improvements on High-Pressure/High-Temperature Drilling Performance on Wells With Extremely Narrow Drilling Windows - Experiences From Mud Formulation to Operational Practices, Shearwater Project, Society of Petroleum Engineers, 2000, January 1. Available from: https://doi.org/10.2118/59175-MS.

[15] M. Zamora, M. Baranowski, "Methods and apparatus for measuring sag properties of a drilling fluid using a rotary viscometer", US Patent # 6931916, Assigned to M-I L.L.C., Issued August 23, 2005.

test that measures the weight–material sag tendency of field and lab-prepared drilling fluids under dynamic conditions."

Both the VST and VSST remain somewhat controversial. One criticism is that the geometry of the VST/VSST is so different from that of a well that they cannot be used to determine absolute values of the potential for barite sag problems.

Last, as the industry has learned to deal with Boycott settling and develop different rules of thumb to be used to clean cuttings out of inclined wellbores, the noted incidences of barite sag seem to also be declining in frequency.

3.9.7 Back-reaming

Back-reaming is the process of pulling the bit out of the hole while simultaneously pumping the drilling fluid and rotating the drill pipe. It has been referred to as "drilling while coming out of the hole." Back-reaming became popular about 50 years ago for use in deviated holes after top drives were introduced.[16] Unfortunately, back-reaming can cause problems instead of solving them if done improperly. Stuck pipe, wellbore stability issues, and higher ECDs are some of the potential problems.

3.9.8 Sweeps

Both high and low viscosity, HD MWs, fibers, and combinations (or in series/tandem) of these drilling fluids have been used as hole-cleaning aids. These "sweeps" are often small volumes of fluid (sometimes called "pills") that can be used to help remove more of the cuttings from the hole/wellbore. Unfortunately, although hole-cleaning aids such as sweeps have been discussed for many years, there is not much information in the public technical literature about them.

High-viscosity fluids are thought to remove the cuttings better due to the movement of the sweep as a "plug" that carries the cuttings out of the hole. The obvious advantage of weighted sweeps is the lower density difference (buoyancy effect) of the cuttings for more effective removal.

---

[16] Prior to top drives, it was very difficult to back-ream using Kelly rigs. With the hardware setup of a Kelly rig, one can only back-ream a joint of pipe at a time, and the process is very slow. In addition, many older land rigs do not have sufficient prime mover power to run the rotary, pumps, and drawworks simultaneously. Any combination of two of the three major functions is done, but not all three simultaneously.

Factors that need to be considered for the use of sweeps include "hole angle, fluid density, formation, cuttings diameter, drill pipe rotation, and fracture gradient."[17].

High-viscosity sweeps work better in vertical and near vertical wells, while HD sweeps work better in deviated wells. Fibrous aids which include typically used as lost circulation materials can often be incorporated to help remove large particles, as well as help to erode the cuttings bed more effectively.

Experience and lab work both have shown that in high-angle holes, sweeps alone rarely if ever are sufficient. They must be accompanied by some mechanical means of getting the low-side-bedded cuttings moving and in the flow stream. The most common and one of the most effective mechanical means is to rotate the drill string.

The exact rate of rotation needed has been reported to range from 40 to in excess of 180 RPM. While the latter should certainly be sufficient for hole cleaning, RPMs greater than 120 tend to create whirl-related vibrations that damage BHA components. Hence, this author prefers a rule of thumb of 80 RPM or less if this is sufficient based on careful observation of the particular well-being drilled.

There are numerous types of sweeps that have been tried and continue to be used by various operations that seem pleased with their results. These include the following:

- Low-viscosity sweeps (LV pill) in which an unviscosified base fluid or a fluid having a lower viscosity than the base fluid or mud is used.
- High-viscosity (HV), in which a volume of drilling fluid is viscosified to a level higher than the base fluid or mud.
- HD, in which the density of a volume of drilling fluid is increased to a level higher than the base fluid density, thus improving buoyance assistance.
- HV/HD, in which a volume of drilling fluid is both viscosified and increased in density.
- Tandem sweeps (two consecutive sweeps) composed of any of those listed above.

---

[17] T. Hemphill, J.C. Rojas, Drilling fluid sweeps: their evaluation, timing, and applications, in: SPE 77448 presented at the 2002 SPE Annual Technical Conference and Exhibition, San Antonio, Sept. 29—Oct 2.

3.9.9 Turbulizers/spiral centralizers

Spiral–bladed centralizing devices, both rotating and nonrotating, have been used with success in both drill string (cuttings beds) and cementing (cleaning wellbore for cement bonding) applications. They are purported to cause a swirling action around the wellbore and tubular while in the case of drill pipe, allowing the drill pipe to rotate without dragging on the low side of the hole. This results in reduced drag and a swirling of the mud (or cement) up the wellbore for a short distance.

Qualitatively, the author has viewed videotaped demonstration of the spiral turbulence inducing ability of the helical turbulizers and is convinced that they produce very good effects over a limited length of wellbore.[18] Hence, if a short distance of helical turbulence is helpful (around 10 ft) they are excellent. However, after the 10 ft or so the helical turbulence has dissipated and additional devices would be used as required for the desired length.

The turbulizers under various company names have long been and continue to be commonly employed in casing running and cementing operations to improve cement job performance, especially in critical areas such as the casing shoe or to isolate hydrocarbon bearing zones.

---

[18] The visualization experiments were conducted by the Arco research department in Plano, Texas. Videos were produced that the author has viewed that clearly demonstrated the helical turbulence inducing capability of the spiral blades. It is unknown at this writing what may have become of these videos.

Effects on Drilling Efficiency and Rate of Penetration

Contents

In this chapter, we hope to pull together much of what you have already learned into a fast and efficient way of determining and applying the best possible combination of weight on bit (WOB) and revolutions per minute (RPM) to drill the best, most efficient wellbore possible.

4.1 INTRODUCTION

Combining of all factors affecting rates of penetration (ROPs) into a single closed–form set of equations to enable economic optimization has long been a goal of drilling visionaries. While individual pieces of the puzzle have been satisfactorily solved (bit hydraulics for example), the combined effect on all factors on the overall economics remains elusive and an area rich for more research and engineering.

Though hydraulics is an important part of improving ROP and should where possible be optimized, there are cases where pump horsepower is limited and other uses for the hydraulic energy are more advantageous. This could be in cases where a mud motor consumes most of what hydraulic energy is available with little left over for bit nozzles. Even in those cases the available energy should be utilized. Optimization, includ–ing a reiterative optimization of flow rates, mud motor parameters, and bit nozzles remains a productive endeavor.

In a similar vein, local operations may find that for hole cleaning pur–poses a maximum flow rate is preferred, without any nozzle restrictions. These variations in operating practices, as we search for better ways to drill, are of course what makes drilling efficiently both challenging and enjoyable when improvements are achieved.

Some of those factors include site costs, mobilization and demobiliza–tion costs, mud costs, cementing costs, casing capital costs, wellheads, dril–ling fluids expense, waste disposal, and of course actual day rate drilling

operations costs. The bits themselves are yet another, and while arguably they are *the* most important piece, their costs tend to be forgotten in the analysis as they are typically small in number compared to others.

Most of these costs are beyond the scope and mission of this book. However, there are some aspects of efficiency that can be reasonably addressed.

4.2 THEORETICAL CONSIDERATIONS

4.2.1 Kinematic and absolute viscosity effects

Absolute viscosity μ (defined as the ratio of shear stress to shear rate) and its cousin kinematic viscosity ν [defined as absolute viscosity divided by density (μ/ρ)] have two main effects on drilling efficiency. For the interested reader absolute viscosity and kinematic viscosity are discussed further in this text's Rheology chapter six.

The first effect is that as the viscosities become higher (due to base liquid viscosities or additives or contaminants increasing the viscosities), it becomes more difficult to pump the mud down the drill string and back up the annulus. More correctly, this pumping requires more energy as pressure to pump the mud at the same rate, other factors being equal. This results in additional pump horsepower being used for this transfer of mud, or as described in the previous chapter, the P_{CIRC} or wasted energy line is higher. This in turn reduces the available hydraulic power and/or jet impact force available for the bit.

The second effect is that the higher viscosities in turn result in higher equivalent circulating densities (ECDs) at the bottom of the hole where the rock is being broken by the bit. Especially when a minimal overbalance is desired in order to increase ROP, this effect can be quite strong.

In addition, in areas where the rock is weak and prone to losses, the added ECD can be the tipping point that extends fractures in the rock and causes partial or full lost returns.

4.2.2 Solids content and plastic viscosity

Solids content and its proxy plastic viscosity not only have similar effects on pumping pressures as do absolute and kinematic viscosities but also affect the fluid behavior as it exits the bit nozzles. A higher plastic viscosity will result in a higher pressure recovery and therefore reduce the force or

power of the jet striking the bottom of the hole. This in turn results in lower penetration rates as the bottom of the hole is not cleaned as efficiently. A detailed discussion of pressure recovery is found in the previous chapter dealing with bit hydraulics.

4.2.3 API fluid loss

Standard API fluid loss test results have little impact on ROP. The test is largely instructive as a measure of the degree of invasion of a base liquid of a mud into a formation over time. The test is usually administered for 30 minutes and the filtrate collected in a graduated cylinder. Some mud engineers have found it helpful in noncritical wells to run the test for 7.5 minutes and double the result.

4.2.4 Dynamic filtration loss (aka "spurt loss")

In running the standard API fluid loss test, after the mud and the filter press are assembled, the start of the test is when pressure (usually from a rig or portable compressed gas source) is applied. During the first, second, or third second of time, there is a rapid—nearly instantaneous—"spurt" of mud filtrate through the filter medium prior to filter cake solids being deposited and the filtrate transmission dropping to near zero for the remainder of the 30 minutes.

This near instantaneous spurt loss is highly correlated with drilling rate (see Fig. 4.1[1]).

The exact causal link remains under investigation. Referring to Fig. 4.2, it is thought that a high spurt loss fluid has the effect of bringing the near-wellbore rock pore pressure to or close to that of the mud pressure. In the figure, the near-wellbore rock pore pressure gradient is the same as the mud density gradient of 12 ppg. If so, even for a small distance under the bit, it implies that the bit is drilling at "balanced" pressure, again only near-wellbore, while the far-field or undisturbed pressure in the formation might be considerably lower. A low or zero spurt loss mud, on the other hand, could prevent or slow the filling of small cracks in the rock made by the bit, lowering the pressure in those cracks,

---

[1] M.S. Ramsey, J.A. Shipp, B.J. Lang, A. Black, D. Curry, Cesium formate—the beneficial effects of low viscosity and high initial fluid loss on drilling rate—a comparative experiment, IADC/SPE Asia Pacific Drilling Technology Conference, September 9—11, 1996, Kuala Lumpur, Malaysia.

Dynamic fluid loss and drilling rate
(15k WOB, 60 RPM, Berea)
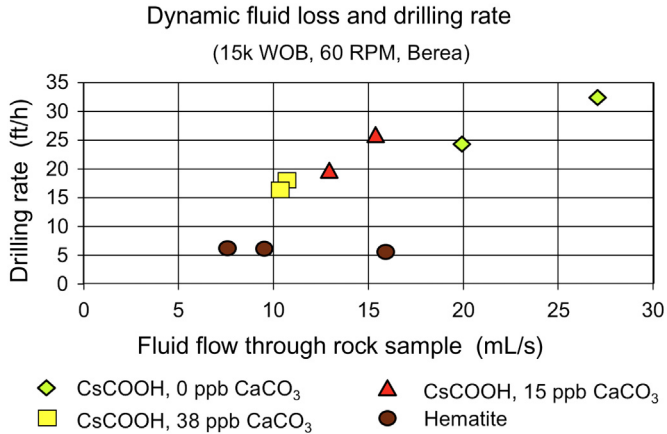
Figure 4.1 Higher spurt loss improves penetration rate.
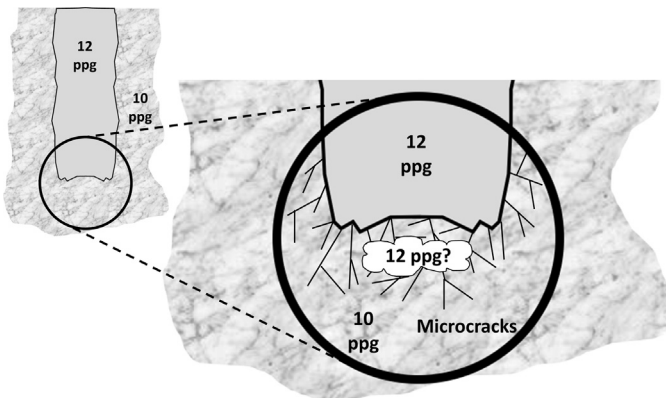
Figure 4.2 Near bit pore pressure of rock with high spurt loss fluid.

resulting in a localized severely overbalanced situation. This would be particularly pronounced in tight formations or relatively impermeable shales.

Note, however, that some mud companies have promoted the use of "zero spurt loss" muds as an aid to wellbore stability problems when drilling sensitive formations. Those may be preferred in cases where penetration rate is not as important as other considerations. In most cases, especially for land well drilling, economics of the drill well will be highly dependent on penetration rates achieved, and in wells with marginal or thin economic returns, this effect can make or break the economic success of the well.

4.3 PRACTICAL CONSIDERATIONS

4.3.1 Drill-off tests

No credible optimization of drilling rate can be complete without some sort of drill-off testing designed to empirically test the effect of RPM, WOB, and other drilling parameters on ROP being conducted. These can be accomplished several ways, three of which are briefly described below. A detailed discussion is contained in Section 4.9, and a more succinct discussion is presented immediately below.

4.3.1.1 Conventional drill-off tests

With conventional drill-off tests, a matrix of RPM and WOB settings is set up, and ROP over a drilled distance of 3 ft or so is averaged for each RPM/WOB combination. After each cell of the matrix is completed, a different RPM/WOB is then started and the process continued. Once the matrix is complete, it is usually clear approximately what RPM and WOB to run, or at least the combinations that deserve further refinement. The inefficient combinations can be ruled out.

Conventional matrix style drill-offs yield excellent quality data but can take much time, and by the time the evaluation is complete, the bit may be in a new rock formation, necessitating repeating the test.

4.3.1.2 Expedited drill-off tests

In the expedited form of the drill-off test, the bit is loaded to the maximum WOB that it is designed for or that the driller is willing to run on the bit. At that point, the brake is locked (preventing drill string vertical motion at the surface), and the weight that has been applied is "drilled off." Upon maximum applied WOB, the drill string length shrinks as compared to free-hanging length off bottom. As the hole bottom is deepened (but the surface remains locked in vertical space by the drawworks brake), the drill string stretches a little as the WOB is reduced.

There is no vertical motion to monitor at the surface; so, the time that it takes for a fixed increment of weight to drill-off is monitored and recorded (perhaps 2000 lb, 4000 lb, or whatever increment is convenient for the rock that is being drilled).

Once a test is complete for the first RPM, other RPMs are investigated similarly as required.

This technique represents a vast improvement in both time and footage required to be drilled in order to determine the better ranges of RPM and WOB to run for most efficient or fastest ROPs.

4.3.1.3 Automated

Some rigs have been equipped with automated systems either tied to the automatic driller or standalone. In such systems, the computer-driven rig data recording software and associated hardware will record (and typically graph in real time) the drill-off for each RPM. When the weight has drilled off to a level clearly inefficient to drill, the test can then be repeated at a different RPM.

4.3.2 Recommended practices

After any major change to the operating parameters, a drill-off test of some sort should be run to ensure that maximum and/or the most efficient penetration rate is being achieved with the new parameters. This is true of hydraulic optimization and any flow changes, since these flow rate changes can affect the ECD and hence the overbalance and therefore also affect the ROP.

4.4 HYDRAULIC EROSION OF THE WELLBORE

4.4.1 Historical

For decades, some have cautioned that excessive hydraulics can erode the hole. This is done largely by observing hole enlargement in some wellbores and believing that the most likely culprit is the jet nozzles or annular velocity—usually without any real data to back up that assumption. The next several paragraphs will seek to dispel the notion that hole enlargement (or "washouts") is caused by jet nozzles or annular velocity.

4.4.2 Measurements of borehole diameters

Several types of measurements are used in an attempt to gage the borehole wall. These will be described below.
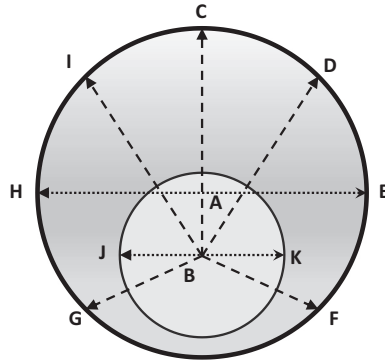
Figure 4.3 Positioning problem with acoustic and mechanical calipers.

4.4.2.1 Fluid caliper

The simplest and least precise way to measure the average borehole size is with a fluid caliper. The idea is to insert a suitable marker or tracer in the mud and count the pump strokes required to pump the tracer down the drill string (a known volume) and then back up the annulus (not known well). The borehole was drilled with a known bit size but may have experienced an unknown degree of hole enlargement after drilling. Such tracers might include paint, carbide, radioactive markers, rice, popcorn, peanut shells, walnut shells, or anything else that the mud engineer finds to work.

4.4.2.2 Measurement while drilling/Logging while drilling

Measurement while drilling (MWD), logging while drilling (LWD), pressure while drilling (PWD) and other tools that transmit downhole-collected data to the surface in near real time, usually through sound waves, have been used for measuring the borehole for about three decades at this writing. The fundamental principle for borehole diameter measurement is to emit a sonic signal and accurately measure the two-way travel time as the signal travels from the tool to the borehole wall and back again—akin to timing the echo in a canyon to estimate its width. There are numerous downhole complications, such as not being centered in the wellbore (see Fig. 4.3), but most of these are handled well by the tools' averaging algorithms. A high level of gas in the mud can alter the travel time significantly, giving an erroneous measurement in that case.
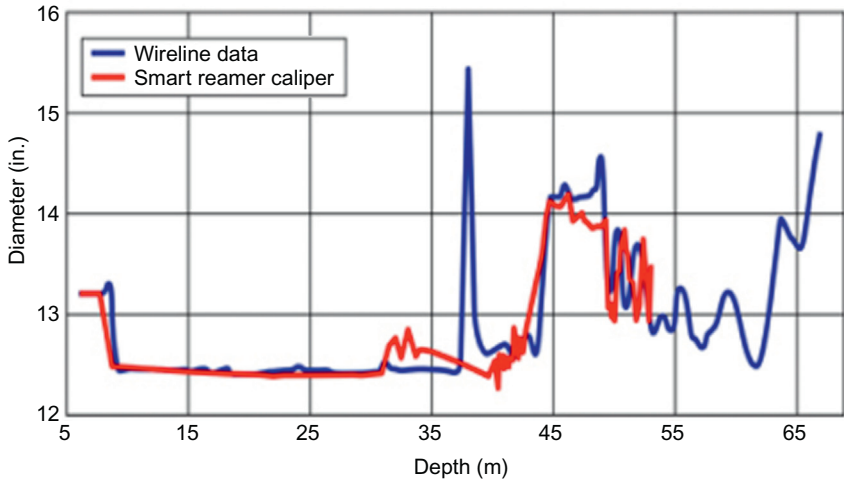
Figure 4.4 Comparison of acoustic and mechanical caliper in test section. *Courtesy: World Oil.*

However, in cases like that, the sonic sensors would generally provide an early warning that a gas kick may have been taken[2].

4.4.2.3 Wireline

The most accurate way to measure the borehole is with a mechanical caliper. These come in a variety of types, mostly distinguishable by the number of caliper arms they contain. A simple caliper may have 1−4 arms, while a high resolution one may have 16 or more. More caliper arms minimize the positioning problem as more spring-loaded arms tend to center the tool better.

Comparison of wireline, considered the most accurate, and MWD acoustic tools has improved over the years. In Fig. 4.4, a recent comparison of the two is presented[3]. While there are individual section measurements that vary significantly, the well engineers and operations personnel are usually concerned more with the overall average hole diameters over

[2] C. Maranuk, Acoustic MWD caliper improves accuracy with digital-signal technology, Oil Gas J. (1998). <http://www.ogj.com/articles/print/volume-96/issue-9/in-thisissue/general-interest/acoustic-mwd-caliper-improves-accuracy-with-digital-signaltechnology.html. > (accessed 20.09.16).

[3] W. Rasheed, S. Zhou, N.M. Al-Khanferi, Smart caliper qualified for measurementwhile-drilling operations, World Oil Mag. 235 (2) (2014). <http://www.worldoil.com/magazine/2014/february-2014/features/smart-caliper-qualified-for-measurementwhile-drilling-operations. > (accessed 20.09.16).

relatively long intervals, for example, when calculating excess cement volumes to pump after a casing string is placed.

4.4.3 *Perceived* hydraulic hole enlargement cause

Some propose that mud annular velocity and bit jet velocity can cause hole enlargement or "washouts". They envision that the mud, containing abrasive solids, can erode rock in much the same way that a high pressure sand laden water jet can cut through steel.

4.4.4 Objections

There are numerous independent objections to the idea that either annular velocities or jet velocities can cause hole enlargement in competent consolidated rock. These are fully discussed in the Pressure Losses chapter but are listed below for initial consideration. Note that these are applied to consolidated rock, not "mud-line mush" usually found on the sea floor or unconsolidated soils found near the surface on land locations. In the shallow unconsolidated sediments, erosion is possible.

These independent objections to the notion of hydraulic erosion of the rock include the following:

- Annular velocities are actually very *low*—as slow as walking.
- It takes expensive high technology hardened steel or diamond to crush the rock.
- Oil muds do not erode the hole as they would if mechanical erosion were the problem.
- Cutting beds are very difficult to erode with flow rate alone.
- We have difficulty in eroding even the soft filter cake with the drilling fluid itself prior to cementing operations.
- Experimental tests do not confirm any *significant* hole erosion.
- At worse it is a mathematically self-limiting problem as the hole enlarges.

These are each discussed at some length in the Pressure Losses chapter, including that the typical caliper of Fig. 4.5 is best explained as chemical attack of water-sensitive formations by water in the drilling mud over time discussed below.

4.4.5 Explanations for hole enlargements

The above is not to say that hole washouts do not occur. Quite the contrary, they are a continuing issue well designers must consider. However, with the exception of the unconsolidated sediments, the problem is
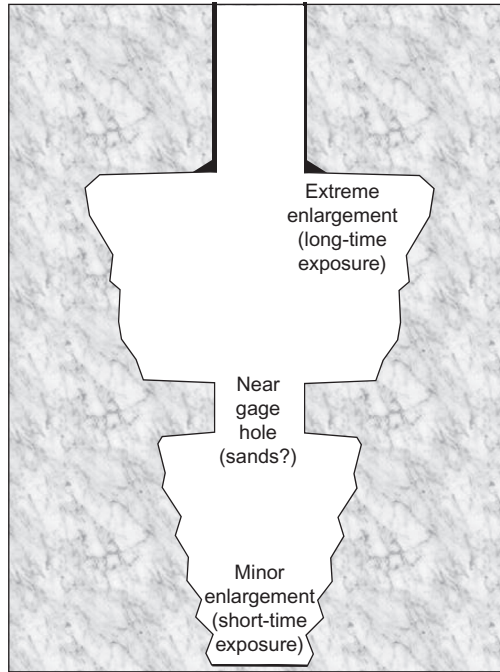
Figure 4.5 Typical caliper log (not to scale-exaggerated horizontally and compressed vertically).

chemical in nature. The most common reason for hole enlargement is that water–sensitive formations absorb water, swell, become weak, and at some point the weakened rock sloughs into the wellbore. Caliper logs often show a funnel–like character (see Fig. 3.5) from just beneath the last casing shoe to the total depth (TD) of the hole section thousands of feet below. This is indicative of the time of exposure of the water–based mud to the open formation. The upper most sections of the open hole have been exposed to the water the longest, and hence the water absorption, weakening, and sloughing have occurred there more than toward the bottom of the hole section.

4.5 DRILL PIPE SIZE EFFECTS

The selection of the drill pipe to use for a hole section is often given little or no consideration, with the "decision" being whatever size

pipe the rig has that will work in that hole section. The geometries, available pipe, and economics may dictate that answer. However, in cases where a range of drill pipe sizes is available for a hole section, an intriguing twist to the economics occurs.

Due to the life of the pipe and the influence of the inside diameter of the pipe on the pressure loss through the pipe, size permitting, it is more economic to rent or buy larger diameter pipe. The economic savings of buying or renting more expensive pipe over its lifetime are due to the savings in diesel fuel needed to run the pumps. The savings of diesel fuel over the life of the pipe will more than pay for the increased pipe costs.[4] In some areas, notably long-lateral shale wells in Texas and elsewhere, special pipe has been fabricated with unusual tool joint and pipe combinations in order to put the largest possible pipe in the hole.

Aside from the straight up economic cost benefit, using larger pipe will of course have more available hydraulic power or impact force available at the bit. This is due to the annulus pressure drop not increasing as much as the drill pipe inside pressure losses decrease, resulting in an overall lower P_{CIRC} and more available for the bit.

As an added benefit, the larger pipe is also not going to buckle under compressive loads as severely as a smaller diameter pipe.

4.6 ROCK FAILURE

A drill bit's function is to break rock. Efficiently breaking rock is a secondary goal, but one necessary for world class performance and high efficiency.

Achieving high efficiency typically will require that the rock fail in a brittle fashion.

At the surface (under atmospheric pressure), rocks appear hard and brittle. If a cylinder of rock is compressed to failure in a laboratory compression machine, the rock will fail abruptly and in a brittle manner. Under controlled conditions of confining and pore pressure, however, the

---

[4] When this author originally did this analysis, energy costs were substantially lower than at this writing. Economics favor the use of larger pipe now even more clearly than before. Use 6.625 in. instead of 5.875 in.

Figure 4.6 Rock sample ready for compression testing at downhole conditions. *Courtesy: IADC.*

same rock will behave in a totally different manner and, in the extreme, may not fail in a conventional brittle fashion at all.

To examine the pressure effects on rock failure, sample rock cylinders, 3/4 in. in diameter and 1.5 in. long, were jacketed with plastic in order to separate internal pore pressure inside of the rock from the confining pressure applied to the inside of the outer cylinder and the outside of the flexible plastic.

A picture of such a test apparatus (sans outer pressure housing) and a cross-sectional diagram of similar are found in Fig. 4.6[5] and Fig. 4.7[6], respectively.

Some rock types, such as Carthage marble (a limestone) can, under different conditions, fail in both malleable and brittle fashion. A cylinder before compression is shown on the top of Fig. 4.8. The brittle failure in the middle of the figure occurs when the rock is compressed with the piston when the pore and confining pressures are equal. The sample on the bottom is a typical plastically failed sample when the pore pressure is much lower than the confining pressure.

Similarly, three cylinders of Bedford (Indiana) limestone are shown in Fig. 4.9[5]. The cylinder shown in the middle of the figure is a typical plastic failure for a rock sample (as opposed to brittle). For this case, the

[5] L. Robinson, J. Garcia, Drillers Knowledge Book, IADC, 2015.
[6] S. Rees, Introduction to triaxial testing. <https://www.gdsinstruments.com/__assets__/pagepdf/000037/Part%201%20Introduction%20to%20triaxial%20testing.pdf.> 2018 (accessed 09.07.18), used by permission.
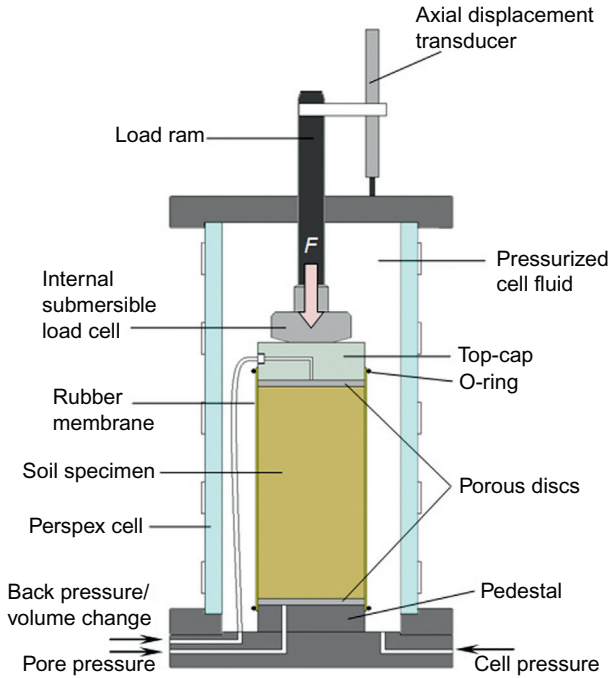
Figure 4.7 Triaxial compression testing test apparatus for rock testing at downhole loading conditions. *Schematic courtesy: GDS Instruments.*

Figure 4.8 Carthage marble tests. Pretest (top), brittle (middle), and malleable (bottom). *Courtesy: IADC.*
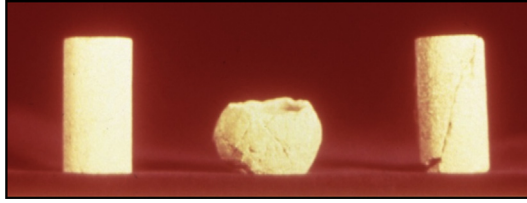
Figure 4.9 Indiana limestone tests: pre, plastic, and brittle. *Courtesy: IADC.*
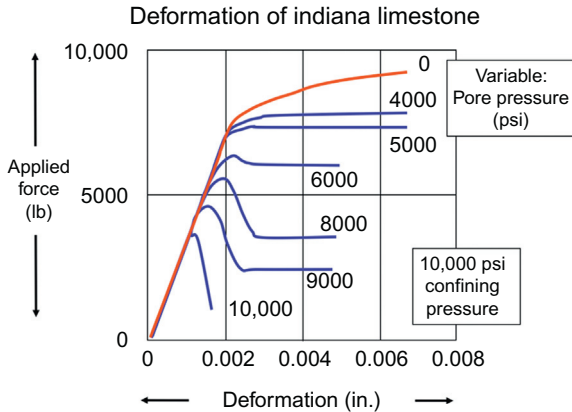
Figure 4.10 Force-deformation diagram for Indiana limestone. *Courtesy: IADC.*

confining stress was 10,000 psi, while the pore space pressure was regulated to 5000 psi—a difference of 5000 psi between pore pressure and confining pressure.

An approximate force/deformation/pore pressure/confining pressure diagram for Indiana limestone is shown in Fig. 4.10.

When the confining and pore pressures were equal, 10,000 psi, the rock fails in a brittle manner. A single shear plane traverses the cylinder with a loud noise. Before failure, however, the force on the top of the cylinder initially deforms the cylinder in an elastic deformation. At a force or load of 2000 lb, the rock would return to its original length if the load was removed. At a force around 4000 lb, the force/deformation curve becomes nonlinear. At this point, the yield strength is reached. Further deformation requires a slight increase in force and then the rock fails in shear. The maximum force is called the point of ultimate strength. When the confining and pore pressures are equal, the magnitude of the pressure has no significant effect on the ultimate

strength. The rock is as strong at atmospheric pressure as it is at 10,000 psi. The failed rock also has the same appearance. A shear plane is created diagonally across the cylinder. The failure plane generally passes between the grains.

As the pore pressure decreases, the rock requires higher loads before failure. In the Indiana limestone when the pore pressure is 8000 psi with the 10,000 psi confining pressure, the failure profile changes significantly. The ultimate strength and yield strength is higher than before. At the point when the ultimate strength is reached, several shear planes diagonally cross the specimen.

Counterintuitively, the pore space then increases dramatically. To maintain a constant 8000 psi pore pressure, pore fluid must be pumped rapidly into the sample. The shear planes create additional pore space within the sample that causes the pore pressure to diminish.

Sandstones behave in a similar manner to limestones except the transition from brittle to malleable failure requires a much higher pressure differential. This should be anticipated because the quartz grains are much stronger than the calcium carbonate grains in the limestone.

As the pore volume increases, the need for fluid to rapidly fill the increased pore volume is amplified, again arguing for using a high spurt loss fluid unless compelling wellbore concerns dictate otherwise.

The strongest limestone shown in Fig. 4.11 is the Carthage marble. The weaker limestone is the Indiana limestone. The sandstones are samples of Berea and a core from the Four Corners area of New Mexico.
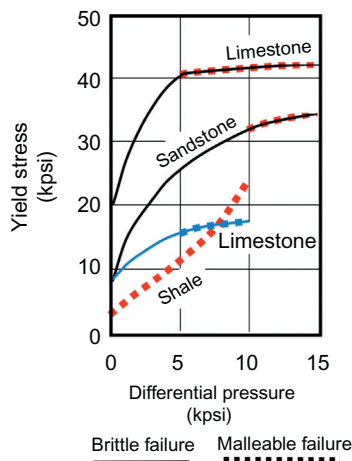
Figure 4.11 Yield stress of several different rocks. *Courtesy: IADC.*

The shale is from Belly River, Canada. The shale strength is significantly lower than the sandstone.

Shales deform and fail in a similar manner but the strength properties are much more difficult to determine. The clay surfaces within a shale react with water and salts to change the internal pressure within the shale. Pore pressures applied to shales require long times to equilibrate due to much lower permeabilities. At failure, liquid cannot be supplied to the failure planes fast enough to maintain a constant pore pressure. The permeability of the Indiana limestone was around a millidarcy, whereas shales have permeability of the order of a micro-millidarcy. In laboratory conditions, as many as 7 days were required to transmit pressure from the bottom of a 1.75 in.–long shale core to the top of the cylinder. The reactive nature of the clays within shale cores and how to best handle it for investigations continue to plague researchers. Results published in the literature vary greatly depending upon the shale handling and history. Shales exposed to the atmosphere gain or lose water. Attempts to maintain shale samples in a controlled relative humidity that matches their desire for water generally result in air intrusion into the core. Drying the cores drastically changes their reaction to water. Shale strength information should be evaluated within the context of the handling and sampling procedures used.

This is one of the reasons that so many researchers attempt to continuously improve on predicting wellbore stability stresses. If the failure stress for the rock is unknown, failure in a wellbore cannot be accurately predicted. Hence, if the handling procedure changes the failure mode and criteria, then the estimated in situ failure stresses are probably not accurate. Other known weaknesses in analyzing cores include the following:

- Most failure models use cylinders of rock and few use true wellbore-shape configurations.
- Questions concerning intermediate principal stresses and equivalency conditions cast doubt on the validity of most measured failure conditions, even ones such as shown above.
- Even when cores have been preserved at the well site (e.g., by wrapping in aluminum foil and sealing with paraffin), concerns arise. If pore pressure was applied by introducing a brine solution, the brine solution may not the same mixture of ions as was present in the shale downhole. Consequently, the introduction of the brine solution itself could affect the results obtained.
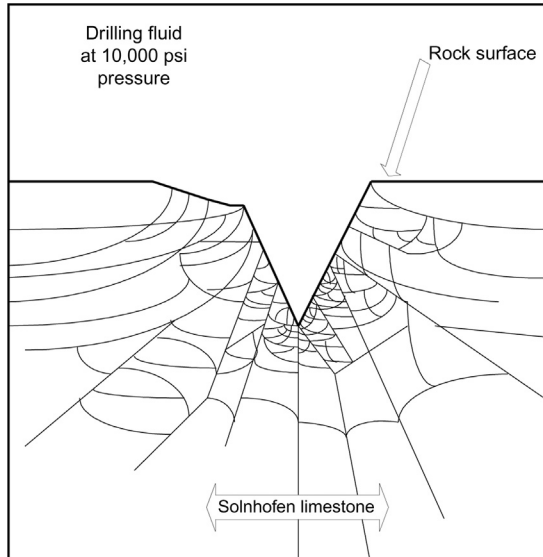
Figure 4.12 Indentation of a simulated sharp bit tooth impacting Solnhofen lime-stone under 15,000 psi confining pressure. *Courtesy: L. Robinson, Ph.D., Private Correspondence, 2018.*

4.6.1 Rock and bit tooth/rock interaction

When a 60 degree tooth impacts Solnhofen limestone, a network of fractures is created beneath the surface. Solnhofen limestone is a relatively impermeable rock. Pore pressure within such a formation would not be measurable. The cracks create a permeable zone beneath the drill bit.

These cracks tend to be filled with fluid from the drilling fluid. Drilling fluid is often designed deliberately to prevent those cracks from filling. High spurt losses from drilling fluid filtration would help fill these cracks. Filling these cracks rapidly increases drilling rates, by balancing the pressure in the new cracks with the wellbore (Fig. 4.12,[7]).

Cross–section of Solnhofen limestone after a 60 degree chisel has impacted while subjected to 15,000 psi pressure.

This limestone is relatively impermeable and has very low porosity. The cracks emanating from the impact probably resemble the cracks in a formation drilled with a roller-cone bit.

The failure mechanism of the cylinders helps explain the failure mechanism beneath this chisel. The zone of failure has a high confining pressure

[7] L. Robinson, Ph.D., Private correspondence, 2018.
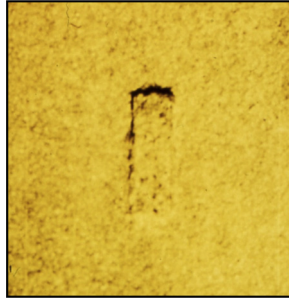
Figure 4.13 Limestone with 3000 psi drilling fluid pressure applied to top of rock. The pore pressure is open to the atmosphere, so a differential pressure of 3000 psi exists across the surface of the rock. The failure is malleable or plastic in nature.
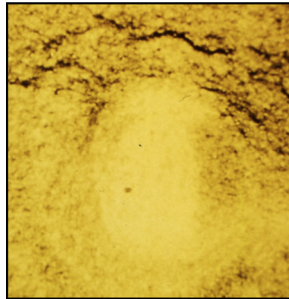
Figure 4.14 Limestone with 3000 psi water pressure applied to the top of the rock. The pressure is transmitted into the pore space of the limestone so confining pressures and pore pressures are equal. The failure is brittle in nature.

(the bottom–hole drilling fluid pressure) and a low pore pressure (newly formed cracks that must be filled with fluid). This increases the strength of the rock and makes the rock appear to be malleable or plastic.

The plastic nature of the rock is only a downhole condition. When the chips, cuttings, sloughings, or cores arrive at the surface, the pore pressure and the confining pressures are equalized. The rock becomes brittle. The rock downhole may also retain some of its abrasive characteristics even though it does fail in a plastic manner.

A vivid visualization of this behavior can be observed by placing a limestone sample in a pressure vessel containing drilling fluid. Pressure can be applied to the drilling fluid, and a filter cake will be formed to separate the pore pressure from the confining pressure. If a rectangular tooth (imperfectly simulating a roller-cone bit tooth) is placed beneath the piston in the triaxial compression vessel, the tooth impact can be determined with either pore pressure equal to the confining pressure or significantly lower than the confining pressure (Figs. 4.13 and 4.14).

A bit tooth (or any other compressive device) only leaves its clear imprint when Indiana limestone fails malleably—the first picture. Brittle failure removes much more material much more efficiently—the second picture. (Photos courtesy IADC[5].)

The question is sometimes asked, when drilling with roller-cone bits and water-based muds, "Why do shales drill so much slower than sandstones, when they have about the same or even much lower compressive strength in surface testing?" The answer should now be obvious from the discussion above. The description of the series of events that happened as a bit tooth is forced into a shale surface should explain the effect, which is depicted in Fig. 4.15.
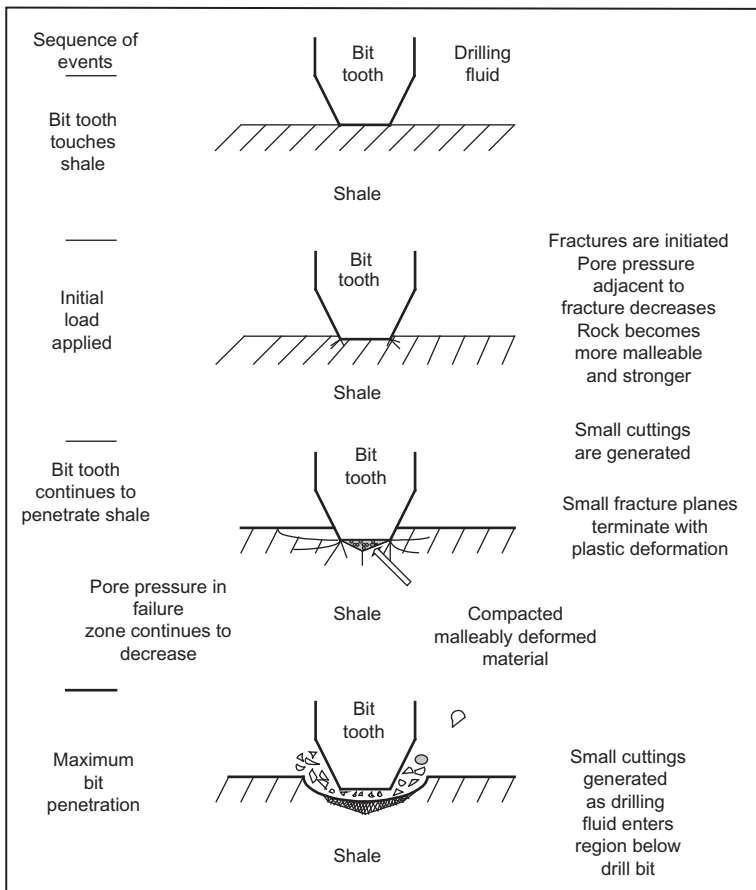
Figure 4.15 Sequence of events as a bit tooth penetrates shale. *Courtesy: L. Robinson, Ph.D., Private Correspondence, 2018.*

To drill, material from the crater must be removed by the drilling fluid. These pictures above portray the events as a bit tooth penetrates shale.

When the pore pressure is maintained at the same pressure as the confining pressure, the failure is brittle and large chips fly from the surface.

Cracks below the tooth impact zone tend to fill with fluid. In a permeable rock, or a rock with gas in the pore space, fluid may be supplied from the formation. In impermeable rock, the pore space must be filled with drilling fluid or filtrate. Drilling fluid is designed to have a low fluid loss; therefore, the cracks are not filled rapidly. The lack of fluid to fill the pore space results in a significant decrease in pore pressure. The increase in rock strength and the change from brittle to malleable failure is a well-known effect in rock mechanics. As the cracks are generated, the pore pressure in the region decreases. The rock becomes stronger and fails more plastically as the next tooth impacts the area. The artificially created permeability and porosity also cause a filter cake to be formed on the surface of the crushed zone. This filter cake makes it difficult for the chips to be removed. In cases like this, increasing the rotary speed on "soft-formation" bits tends to scrape the filter cake away and will increase the founder point (Fig. 4.16).

Conversely, if a drilling fluid has a high "spurt loss," the incipient cracks in the rock are quickly filled with fluid, thus equalizing pressure across the chip and helping it fail in an efficient, brittle fashion.

As the fracture starts beneath the bit tooth, it must be filled with fluid.
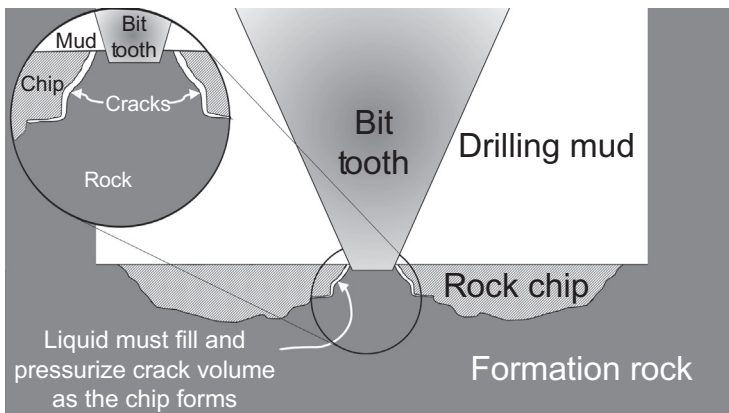
Figure 4.16 New voids created as cracks propagate must be filled and pressurized for efficient drilling.

If no fluid is available to fill the crack, the pore pressure around the fracture decreases. The rock becomes stronger and starts to fail malleably. Cuttings will become much smaller and drilling rate will decrease.

The plastic nature of the rock is only a downhole condition, caused by the imbalance between wellbore pressure and rock pore pressure. When the chips, cuttings, sloughings, or cores arrive at the surface, the pore pressure and the confining pressures are equalized. Under equalized conditions, as discussed previously, the rock fails in a brittle fashion.

Interestingly, the rock downhole, even if failing in a plastic mode, may retain its abrasive characteristics.

Extended nozzles have the effect of increasing the jet velocity at the bottom of the hole. High jet velocities assist removal of the crushed material adhering to the bottom of the hole.

Feenstra and van Leeuwen[8] describe "... bottom balling in hard rock drilling. The bottom becomes covered with a layer of crushed material, which is clearly visible on inspection." These were laboratory tests with full-scale bits drilling under pressure. "This phenomena is most pronounced when non-friable rock is drilled with an insert bit, which has a crushing action."

Referring again to Fig. 4.15, small rock chips shown at the bottom of the crater in Step 4 may not be efficiently removed by the drilling fluid. These chips and smaller sized debris have been observed in laboratory drilling tests and are usually described as rock flour. Drilling rates of the order of 10 ft/h with a rotary speed of 100 RPM mean that the bit is advancing about

$$\frac{(10 \text{ ft}/h)(h/60 \text{ min})(12 \text{ in.}/\text{ft})}{(100 \text{ Rev}/\text{min})} = 0.02 \text{ in.}/\text{Rev} \tag{4.1}$$

where Rev is the one revolution of the bit or 360 degree.

New drill bit teeth are always longer than 3/8 in. Clearly, the drill bit teeth do not remove 3/8 in. of rock with each revolution. This layer of crushed rock and mud solids certainly would inhibit the drilling rate of an insert bit. The existence of a "cake" on permeable sandstone is easily visualized even with a clean surface at the bottom of the borehole. The fractures

[8] R. Feenstra, J.J.M. van Leeuwen, Full scale experiments on jets in impermeable rock drilling, in: Presented at the SPE Annual Fall Meeting in New Orleans, 1963. W. Moore, How to dull a bit for fun and profit. Drilling (March, 19

caused in the rock by the action of the bit apparently create void space—or porosity and permeability—at the surface of even impermeable hard rock.

4.6.2 Variables that affect drilling rate

A borehole advances because a drill bit fails the rock beneath the bit and drilling fluid removes the resulting debris. With a roller-cone bit, rock failure depends upon a bit tooth penetrating the formation. WOB provides the force to cause the tooth penetration and rotary speed controls the number of impacts received by the rock. Obviously, drilling rate should depend upon both WOB and rotary speed. As observed in the previous section, the rock failure mode also depends upon the pressure differential (between the wellbore pressure and the pore pressure) at the bottom of the hole. This pressure differential not only changes the mode of failure and the failure strength of the rock but can also tend to hold cuttings in place. This latter effect is sometimes referred to as the "hold down" effect.

Regardless of the subtleties, cuttings must be removed from the hole bottom so that that fresh rock can be exposed and attacked by the bit without a protective covering layer of rock chip debris.

In some places (like recent sediments beneath some oceans) drilling rate can be increased to a speed that is limited by how fast the drill pipe can run into the hole and new drill pipe added to the drill string. In these cases the problem is one of "keeping" the hole that is drilled. The drillers' saying of "It's not how much hole you drill but how much hole you keep…." comes readily to mind.

Too many cuttings in the annulus will increase the drilling fluid density enough to cause downhole formations to fracture and drilling fluid to leave the wellbore (lost circulation). Obviously in these situations, drilling rate improvements are not of concern. The primary focus should be on drilling a borehole at the lowest cost per foot. If the drilling rate is 1000 ft/h, 3000 ft can be drilled in only 3 hours. If, however, 3 days must be spent solving the lost circulation problem, the net cost of the 3000 ft will be very high. Suppose, instead, the drilling rate is controlled to 200 ft/h. Fifteen hours will be required to drill the 3000 ft, but the net cost will be lower. Sometimes the fastest drilling rate is not always the most economic way to drill in terms of cost per foot.

Drilling at the lowest cost per foot requires proper bit selection, proper mud weight, and proper WOB and rotary speed. Bit selection is discussed in another chapter. In this chapter, the focus will be selecting the best

WOB (W) and the best rotary speed (N) to produce the lowest cost per foot. The effect of pressure differential will also be discussed.

4.6.3 Drilling rate equation

Before the bit founders, drilling rate can be predicted from the equation:

$$\text{ROP} = \frac{K\left(N^\lambda\right)\left(\frac{W^2}{D}\right)}{m + \Delta P} \tag{4.2}$$

where K, m, and λ are constants; N is the rotary speed (rpm); W is the weight on bit (lb); D is the bit diameter (in.); and ΔP is the pressure differential across the bottom of the hole, meaning pressure inside the borehole at the bottom versus the pore pressure immediately below the bit.

This equation can be used to describe data published in the literature. Much laboratory data are available in which the pressure differential is carefully controlled and the WOB and rotary speeds are accurately measured. In the field, the effect of these variables is somewhat more elusive, particularly the pressure differential across the bottom of the hole.

Each of the variables in the drilling rate equation will be discussed individually to illustrate the validity of the components of the equation.

4.6.4 Effect of rotary speed on drilling rate

Rotary speed effects on drilling rate vary with the type of drill bit. Generally, doubling the rotary speed does not double the drilling rate. Below the founder point, an increase in drilling rate will be observed as the rotary speed is increased. This exponent, one in this case, is usually less than one. A value of $0.7-0.8$ seems to fit the majority of situations for both insert and milled-tooth bits.

From some laboratory data there is some indication that the exponent may also be functionally dependent on the pressure differential across the bottom of the hole. This effect may be accounted for by performing drill-off tests at the rig site (Fig. 4.17).

4.6.5 Effect of differential pressure

Most bottom–hole pressures are higher than the formation pressures. Usually an excess pressure of $200-300$ psi is designed into the drilling fluid program. This prevents entry of unwanted formation fluid into a wellbore. This pressure differential is usually not known very accurately.
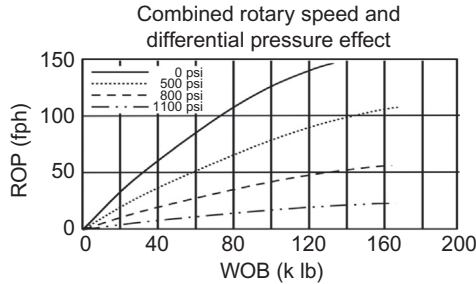
Figure 4.17 Combined effect of bit differential pressure and WOB at constant rotary speed. *WOB*, weight on bit.

When a chip or cutting is made, fluid must fill the fracture space below the chip. If insufficient fluid is available, a full vacuum can exist under the chip. This means that the pressure holding the chip in place is the bottomhole pressure and not just the differential pressure.

The differential pressure has two effects at the hole bottom:
- it forces the chip against the formation (the "hold down" force) and
- it changes the rock properties themselves (increasing the strength and causing some rocks to fail malleably).
  Fluid to fill the cracks below the chips can come from three sources:
- drilling fluid entering the cracks from the wellbore,
- filtrate flowing through the cake at the bottom of the hole or the chip, or
- formation fluid flowing through the pores of the rock.

Obviously, in shale or an impermeable rock, formation fluid will not usually be available to fill the crack. This effect was discussed in the section above. The spurt loss of the drilling fluid or the quantity and type of filtration control ingredients in the drilling fluid control the entry of fluid into the cracks in impermeable rock. This may be the most compelling reason that the relaxed fluid loss oil-based drilling fluids drill faster now than the very low fluid loss oil-based fluids used decades ago.

The effect of differential pressure on ROP appears to be an exponential decay. The exponential relationship does not fit all of the data in the literature or all unpublished data the author has seen nor match the standard reciprocal relationship between ROP and $(m + \Delta P)$.

A simple interpretation of the value of m is that it is the negative differential pressure that will produce an infinite drilling rate. The value

should approximate the tensile strength of the formation. Tensile strengths of rock are on the order of 200−500 psi. This seems to match with values observed when developing equations to describe drilling data.

4.6.6 Effect of weight on bit on drilling rate

As more weight is applied to the drill bit, the drilling rate increases. As the bit is turned faster, the drilling rate increases. Both of these factors have limits as to their effect.

Rotating a roller-cone bit too fast may result in excessive tooth breakage. Also, cuttings must be removed from the bottom of the hole before they are reground by the next cone's teeth. If they are not removed, further increases in weight of bit or rotary speed will not result in the same increase in drilling rate as experienced before. This condition is called "foundering" or "floundering" and is illustrated in Fig. 4.20 for three sets of bit loading and hydraulics conditions. ."

As the WOB is increased, the drilling rate increases as a square of the WOB, up to the founder point. In the graph above, drilling rate reaches a value slightly above 30 ft/h at 27,000 lb WOB while circulating 200 gpm. An incremental increase of the WOB no longer increases the drilling rate as much as before. The drilling rate still increases, but at a much lower response to the increased WOB.

Increasing the flow rate to 260 gpm increases the apparent founder point significantly. A drilling rate of 50 ft/h is attained before reaching the new founder point.

Notice in these experiments that the drilling rate at 20,000 lb of bit weight is the same whether the circulation rate is 200 or 260 gpm. This would indicate that no cuttings are available to be removed with the higher circulation rate. Some data in the literature report increase in drilling rate at any bit weight when the hydraulics are increased. This would hold true if the drilling fluid is not removing all of the cuttings from the bottom of the hole.

Consider an argument between two drillers on the effect of hydraulics on drilling rate if one driller is using 23,000 lb on the bit and the other is using 35,000 lb. The first driller would not see much difference in drilling rate because either 200 or 400 gpm will remove all of the cuttings generated at the bottom of the hole. The second driller would observe an increase in drilling rate from about 32−34 ft/h to rates around 46−48 ft/h. Does hydraulics affect drilling rate? "Yes" and "no"
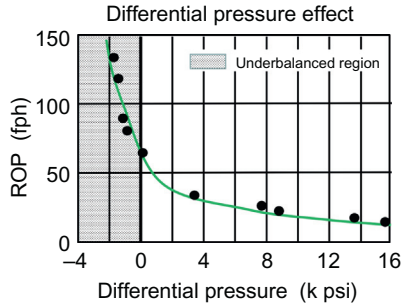
Figure 4.18 Effect of differential pressure between borehole and formation pressure on drilling rate in limestone.
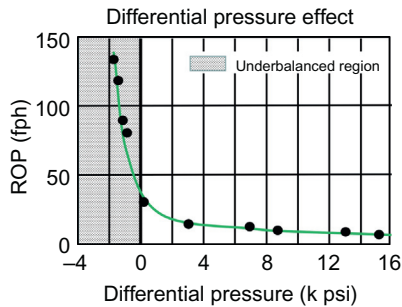
Figure 4.19 Effect of differential pressure between bottom hole and formation pressure on drilling rate in Mancos Shale.

may both be correct answers in the absence of any other drilling parameter changes.

In the Feenstra and van Leeuwen report, the founder point increased as the flow rate was increased to 400 gpm. Since they controlled the pressure differential independently from the circulation rate, they did not duplicate downhole conditions. At the higher circulation rates, the pressure drop in the annulus would be higher. This would increase the bottomhole pressure, which would decrease the drilling rate. Referring back to Figs. 4.18 and 4.19, the increased flow rate and associated increased ECD would have the effect of moving to the right on the plot. At the bit, the effective differential pressure across the rock would be increased and have the same effect as if the mud weight itself was higher (Fig. 4.20).
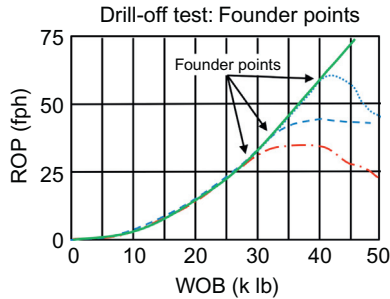
Figure 4.20 Illustrating founder points.

4.7 FOUNDER POINTS

Founder points are determined by the condition of the bit teeth and the hole cleaning beneath the bit. If the plastic viscosity of the drilling fluid is decreased, the founder point will be raised.[9] As the circulation rate is increased, the cuttings below the bit are removed more efficiently, and the founder point increases. More weight can be applied to the bit and the drilling rate will increase.

Drill bits with a large skew and offset can increase the founder points by increasing rotary speeds. Drilling with an 8.5 in. IADC code 111 b increasing the rotary speed from 75 to 135 RPM increased the founder point from 30,000 to 50,000 lb. At 30,000 lb, the drilling rate increased from 58 to 63 ft/h when the rotary speed was increased. At 50,000 lb, however, the drilling rate was 70 ft/h in the foundered condition at 75 RPM and 115 ft/h for the 135 RPM condition. This test was conducted in the Texas Gulf Coast region at 7802 ft. The circulation rate was 380 gpm, the nozzle velocity was 205 ft/s, mud weight was 11.6 ppg, and the hydraulic impact was 467 lb.

4.7.1 Exercises to determine the founder point using drill-off data

1. A drill-off test with a drill bit without hydraulic optimization procedures was performed just after the drill bit reached bottom.

---

[9] The reader will recall that the plastic viscosity (PV) is a function of the size, shape, and number of solids in the mud along with the base liquid viscosity. Since the latter is not generally adjustable in any way, the solids content controls the PV. Low PV is always better than high PV, and hence low solids content is superior to higher solids content.
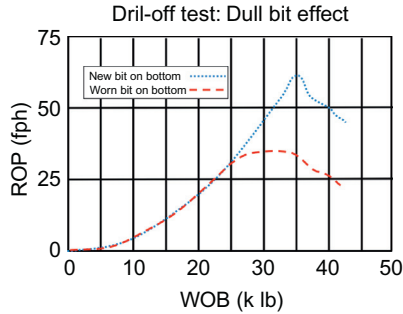
Figure 4.21 Drill-off data showing bit effect.

Table 4.1 Example drill-off test data table

WOB 1000 lb	ΔT (s)	Test #1 ROP (ft/h)	ΔT (s)	Test #2 ROP (ft/h)
50				
48	35.8		18.4	
46	32.3		17.4	
44	30.0		16.5	
42	28.0		15.0	
40	26.0		15.2	
38	25.8		16.8	
36	26.0		18.7	
34	26.3		20.8	
32	26.7		23.5	
30	27.1		26.3	
28	30.0		30.0	
26	33.9		34.9	
24	40.3		40.3	
22	48.0		47.8	
20	58.6		58.6	
18	70.1		70.1	
16	80.6			
14	99.2			
12	129.0			
10	184.3			
8	322.5			

WOB, weight on bit; *ROP*, rate of penetration.

At this depth, with the drill string in the well, the pipe stretches 2.15 in. per 2000 lb change in bit weight. The time to drill–off 2000 lb is presented below. Find the founder point (Table 4.1).

2. Just before this bit was pulled out of hole (POOH), a series of hydraulic optimization tests were performed to determine the correct nozzle sizes and flow rate to use on the next bit. The drilling fluid properties had remained constant during the dulling of bit #1. When the newt bit reached bottom and bottoms circulated up, another
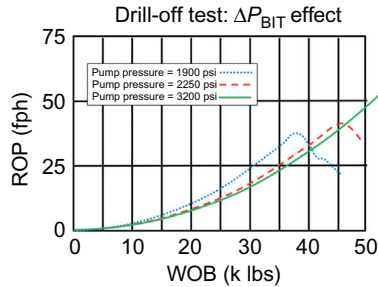
Figure 4.22 Drill-off tests as standpipe pressure is changed.

drill–off test was performed. Compare the founder points and explain any difference noted (Fig. 4.21).

One negative aspect of increasing the flow rates is that the pressure drop in the annulus will increase. The pressure at the bottom of the bore-hole is determined by the hydrostatic pressure from the drilling fluid column and from the pressure loss in the annulus. The increase in pressure drop across the bottom of the borehole will cause the drilling rate to decrease. The ROP will be higher for the low flow rates, but the shape of the ROP curve will still be a square function of the WOB. This is observed primarily when the differential pressure across the bottom of the hole is almost zero. This is the pressure region where the response of ROP is most sensitive to pressure differential (Fig. 4.22).

While drilling a well very close to balanced (i.e., the pressure differential is close to zero), the standpipe pressure was reduced from 3200 to 1900 psi. Drill-off tests indicated that the founder point was lower. At the lower WOB values, the drilling rate was higher at the lower standpipe pressure.

4.8 EFFECT OF HYDRAULICS

One of the purposes of drilling fluid is to remove the cuttings from the bottom of the hole. Hydraulics can be designed so that the maximum hydraulic horsepower is expended across the nozzles or so that the fluid strikes the hole bottom with the maximum force. This will be discussed in another chapter. In the drilling rate equation [Eq. (4.1)], no term is included for hydraulics. This equation is valid for WOB and rotary speeds *below the founder point*.

If the drill bit will not make hole without putting some WOB, and the bit is *not* in a founder condition, hydraulics will *not* improve drilling rate. If the fluid impacting the bottom of the borehole does not make the rock fail, no term for hydraulics should be included in Eq. (4.1).

Hydraulics will make a significant impact on the drilling rate behavior after the founder point. Drilling fluid properties and hydraulics will determine how many cuttings remain on the bottom of the hole after the founder point is reached. Laboratory experiments that indicate causality or functional relationships between drilling rate and hydraulic horsepower (or hydraulic impact) occur in conditions that are past the founder point threshold.

4.9 DRILL-OFF TESTS

The founder point can be found in the field using drill–off tests. As early as 1958, Arthur Lubinski suggested doing a drill–off test by applying the maximum weight possible to the drill bit and timing how long it takes the weight to "drill-off." With the brake locked in place, the top part of the drill string does not move. As the drill bit drills ahead, the drill pipe stretches. The drill pipe may be considered an elastic string. Every change of 2000 lb will change the string length by the same amount. The drill collars are large and do not change in length as much as the drill pipe. The change in drill collar length is ignored.

The change in length of the drill pipe may be approximated from the stretch constants (at end of chapter and also available from stuck pipe calculations, or it can be measured on the rig floor). Stop the rotation and place the bit on the bottom of the hole with about 5000 or 10,000 lb b load. Place a mark on the kelly or the joint of drill pipe about 5 ft above the rig floor. Add about 10,000 lb to the bit weight and measure the movement at the surface. Add an additional 10,000 lb b weight and repeat. Repeat the measurements as the weight is removed from the bit. Divide the average distance moved at the surface by the change in bit weight in thousands of pounds. This will be the stretch constant for this drill string. [*Note:* An accurate stretch constant is needed if prediction of actual drilling rates is needed. If, however, only the founder point is needed, the shape of the curve and the founder point will not change if

an incorrect value—or even an arbitrary constant—is used. In fact, the simple reciprocal of time to drill-off may also be plotted on suitable axes with similar results.]

4.9.1 Drill-off procedure

Drill-off tests may be performed with the following procedure:

- Choose a rotary speed and a maximum weight to be applied to the bit. The rotary speed will affect the maximum weight selected. The maximum weight may be either determined from the drill collar weight available or from the maximum weight recommended by the bit manufacturer.
- Set the rotary speed and apply the maximum weight. Drill for a short time at these values. (The rotary speed may decrease slightly as weight is applied.)
- Set the brake and record the time.
- Record the WOB and time for every 2000 lb decrease in WOB.
- Continue the procedure until about 25% of the original WOB remains. (After some experience, the procedure may be halted with 50%−60% of the original WOB.)
- If the formation seems to change during the tests (observed by significant discontinuities in the data), repeat the test—particularly in the higher weight ranges.
- Repeat the procedure for three rotary speeds.
  Calculate the ROP from the equation:

$$\text{ROP} = \frac{\left(\frac{((\text{SC})(\text{DP Length})(\Delta\text{WOB}))}{((1000)(1000))}\right)\left(3600 \ \text{s/h}\right)\left(\text{ft}/12 \ \text{in.}\right)}{\Delta T} \tag{4.3}$$

or more simply

$$\text{ROP} = \frac{(\text{SC})(\text{DP Length})(\Delta\text{WOB})}{\Delta T} \times 0.0003$$

where SC is the stretch constant (in. per 1000 lb per 1000 ft) for drill string. If calculated, assume that the bottom hole assembly (BHA) does not stretch. Drill pipe (DP) length is the length of drill pipe (feet). ΔWOB is the weight on bit increments associated with time measurements. ΔT is the time to drill WOB increments (s).

Note: If using thousands of pounds instead of pounds, and using thousands of feet instead of feet, the 0.0003 constant in (4.4) becomes 300 instead of 0.0003.

$$\text{ROP} = \frac{(\text{SC})(\text{DP Length})(\Delta\text{WOB})}{\Delta T} \times 0.0003 \qquad (4.4)$$

Stretch constants for common drill pipe sizes are presented in Table 4.2 of this chapter.

Note that for values not listed, the stretch constant may be estimated with the equation:

$$\text{Stretch constant} = \frac{1}{(\text{Cross} - \text{sectional area of steel pipe} \times 2.5)} \qquad (4.5)$$

Table 4.2 Drill pipe stretch constants (approximate values based on new pipe dimensions-correct for actual dimensions of pipe in use)

Outside diameter (in.)	Nominal weight (lb/ft)	Inside diameter (in.)	Wall area (in.^{2})	Stretch constant (in./1000 lb/1000 ft)
2.375	4.85	1.995	1.304	0.30675
	6.65	1.815	1.815	0.21704
2.875	6.85	2.441	1.812	0.22075
	10.40	2.151	2.858	0.13996
3.5	9.50	2.992	2.590	0.15444
	13.30	2.764	3.621	0.11047
	15.50	2.602	4.304	0.09294
4	11.85	3.476	3.077	0.13000
	14.00	3.340	3.805	0.10512
4.5	13.75	3.958	3.600	0.11111
	16.60	3.826	4.407	0.09076
	18.10	3.754	4.836	0.08271
	20.00	3.640	5.498	0.07275
5	16.25	4.408	4.374	0.09145
	19.50	4.276	5.275	0.07583
	25.60	4.000	7.069	0.05659
5.5	21.90	4.778	5.828	0.06863
	24.70	4.670	6.630	0.06033
5.875	23.40	5.1 approx.	6.7 approx.	0.05988 approx.
	26.30		6.9 approx.	0.05780 approx.
6.625	25.20	5.965	6.526	0.06129
	27.7	5.632 (Prem)	9.56 approx.	0.04184 approx.
	34			
	50			

As an example, if a rig is drilling with 17,000 ft of 4.5 in. 16.6 ppf drill pipe, the incremental weight that is "drilled off" for each time measurement is 2000 lb, and a particular measurement shows that it takes 5 seconds to do so; the calculation would be as follows:

Pipe stretch constant = 0.09076 [from Table 4.2, toolpusher manual, or calculation of Eq. (4.6)]

$$ROP = \frac{(0.09076)(17,000)(2000)}{5} \times 0.0003$$

$$ROP = 185 \ ft/h$$

Note: If using thousands of feet and pounds, the example becomes

$$ROP = \frac{(0.09076)(17)(2)}{5} \times 300 = 185 \ ft/h$$

These calculations are more easily performed if a computer spread sheet (like Excel or Google Sheets) is set up on a computer at the rig site.

In 1968, Stanley Moore published an article on "How to Dull A Bit for Fun and Profit"[10]. Several have tried this technique but obtained erratic results. Many of the drill-off curves were unintelligible that caused the procedure to be abandoned. The problem has been resolved by averaging the time of drill-off over bigger changes in weight. Drilling times are measured ever 2000 lb change in bit weight. If the drill string experiences significant drag forces, the time may not be sufficient for the weight indicator to properly indicate the bottomhole condition. The time may be extended by averaging the drill times over a 4000 lb WOB change. A significant amount of "smoothing" can be achieved if the averages are taken sequentially in 2000 lb increments.

If the curve is still erratic, the WOB averaging interval may be increased to 6000 lb. For example, as the bit weight indicated on the surface changes from 50,000 lb down to 40,000 lb, the time for each 2000 lb change is measured. The time change from 50,000 to 44,000 lb is calculated by adding the three times from 50,000 to 48,000, 48,000 to 46,000, and 46,000 to 44,000 lb. The drilling rate is then calculated as though the bit weight change was from 50,000 to 44,000 lb. This will be the drilling rate at an average weight of 47,000 lb. The time change from 48,000 to 42,000 lb is calculated by adding the three times from 48,000 to 46,000, 46,000 to 44,000, and 44,000 to 42,000 lb. Drilling rate for the average bit weight of

---

[10] W. Moore, How to dull a bit for fun and profit. Drilling (March, 1968).
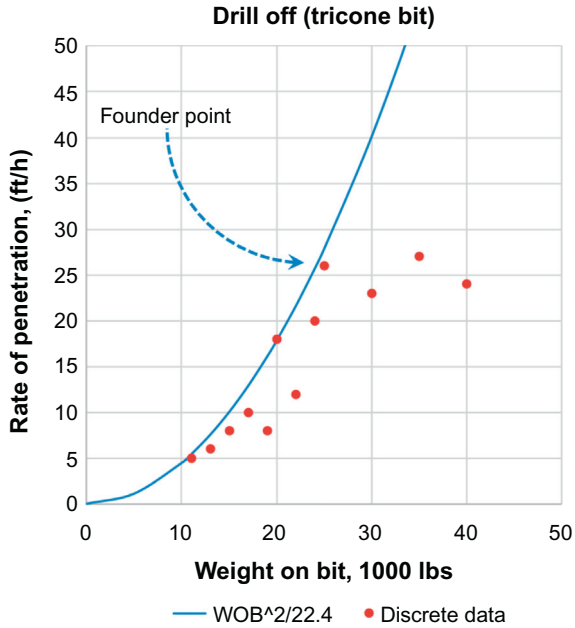
Figure 4.23 Typical drill-off test during a bit run.

45,000 lb is calculated as though the bit weight change was from 48,000 to 42,000 lb. By using the overlapping time intervals, minor perturbations are smoothed to represent more clearly the true drilling rates.

The drilling rate equation was then calculated using a single black data point and the line drawn using the calculated drilling rates.

In Fig. 4.23, the drilling rates increase until the bit weight reaches about 25,000 lb. Above 25,000 lb WOB, the drilling rate remains about the same or even decreases. After the drill-off test, the data can be confirmed by selecting the conditions at the founder point and drilling 10−15 ft. The WOB can be increased by a few thousand pounds to confirm that the apparent founder point is correct. Care should be taken, however, to ensure that polycrystalline diamond compact (PDC) bits are not balled up in soft formations during this additional WOB (Figs. 4.24 and 4.25).

From the drilling rates presented in the graph above, a straight line may be used to connect the drilling rates below the founder point. This would make the functional relationship:

$$ROP = K(W - W_0) \tag{4.6}$$
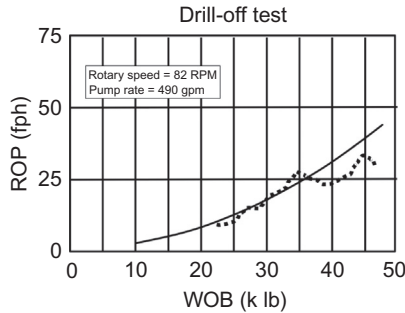
Figure 4.24 Continuous measurement. *Courtesy: Texas Drilling Associates.*
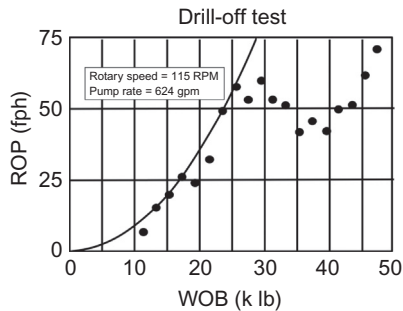
Figure 4.25 Discrete measurement points. *Courtesy: Texas Drilling Associates.*

where K is the proportionality constant; W is the WOB; and W_0 is a threshold bit weight.

Even though the data presented in this graph may support this equation, drilling tests using WOB below the threshold bit weight indicate that the squared term matches better with the true bit behavior. However, these slow drilling portions of the drilling curve require a very patient driller and rig supervisor because the drilling rates are very low, and the rig time is very long. Usually these tests are performed in the upper weight ranges so that the drilling rate remains as high as or higher than routine operations.

Watching the weight indicator closely as the weight indicator hand slowly moves reveals some interesting hidden facts. Frequently the hand starts moving uniformly and slowly until an apparent resonance is reached. At this point the weight indicator hand vibrates. Sometimes the vibration is so extensive that the time cannot be measured as the hand passes the next

mark on the weight indicator. Usually the vibration only lasts over a 4000 lb weight drill–off range. After that, the drill string appears to cease vibration. This vibration sometimes occurs two or three times during a drill–off test. It is reproducible if the drill–off test is repeated. The vibration occurs at different weight ranges if the rotary speed changes. (There is also an implication here that should not be bypassed. A rotating drill string can vibrate at resonance with no weight applied to the bit. These equations have been well documented in the literature for years. However, equations should recognize that the drill string vibrates at different WOB values for different rotary speeds. This means that any equation that describes resonant frequencies should have both a speed and WOB dependence.)

4.9.2 Computer-assisted drill-off tests

Totco developed a computer-assisted program that converts the hook-load decrease during a drill-off test into a drilling rate curve for the driller. The drillers that have tried this have found it to be easy, instructive, and fun to use. Preliminary results indicate a substantial decrease in drilling costs.

A computer is used to collect and process data. Results of the drill-off tests are displayed in real time at the driller's console. Automation of the tedious manual calculations allows implementation of this well-known, but seldom applied, technology. The driller drills several inches with the maximum selected WOB and locks the brake, and the computer is activated. The change in drill string weight is recorded as a function of time. A video screen mounted at the driller's console allows the driller to monitor the progress of the test in terms of penetration rate as the weight is drilled off.

This device has been easily accepted by drillers when it gave coherent results. The system was installed on nine wells in one old field in Texas. The field has had drilling activity almost continuously for the past 25 years. The "learning curve" had flattened many years ago. Drilling programs had become copies of each other and costs were very predictable. Almost 1000 drill-off tests were run while drilling these 9 wells. About 57% of the tests indicated that significant adjustments were needed in the rotary speed or the WOB. The results were averaged to show a net 10% reduction in total cost per foot for the wells. Each well was cheaper. Average rotating
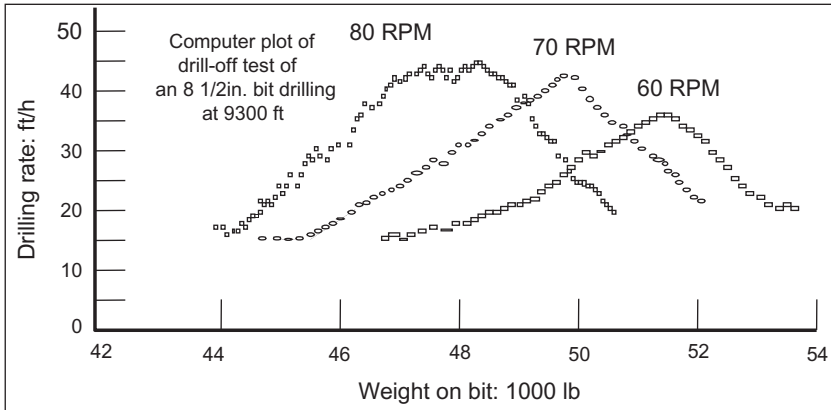
Figure 4.26 Computer display for drill-off test. *Courtesy: Texas Drilling Associates.*

hours were reduced by 17% for these wells. Remember this was a very mature field.

Conscientious drillers ran several tests during their tour. A typical set of curves usually made it easy to find the founder point and the best WOB for the rotary speed selected. The drilling rates during these tests were generally in the same range as the maximum penetration rates. This means that very little time is lost on the rig because of these tests. Generally drillers would select three rotary speeds for their suite of tests. Three curves can be displayed simultaneously on the screen (Fig. 4.26).

Several difficulties are inherent in the technique. Several times in offset wells, the data were not interpretable. False results quickly kill a driller's incentive to use a procedure. One difficulty with the on-site display unit is the small time intervals used to calculate drilling rates. With high coefficient of friction—where the weight indicator does not faithfully follow the WOB—the computer time intervals may be too short to deliver meaningful curves. In hand calculations the time intervals frequently must be several minutes long before the curve is smooth enough to be interpretable. A computer makes many drilling rate calculations in 1 minute. Sometimes these time intervals are much too short for meaningful calculations.

If a resonance point is captured within the weight range, the data will also make no sense. Negative drilling rates have been observed on some computer displays because of the vibration. The computer may interpret that the WOB

Table 4.3 Drill-off exercise data

Drill-off from 1000 lb	Weights to 1000 lb	Average WOB (for plotting)	Time (s)	ROP (ft/h)
70	68	69	17	30.8
68	66		16	
66	64		15	
64	62		14	
62	60		12	
60	58		15	
58	56		18	
56	54		16	
54	52		14	
52	50		12	
50	48		11	
48	46		12	
46	44		11	
44	42		10	
42	40		9	
40	38		8	
38	36		10	
36	34		12	
34	32		15	
32	30		19	
30	28		23	

has decreased to a certain value when the drill string is vibrating. At the next time slot, the WOB may be read as a larger number from the vibration. The computer may interpret this as the bottom of the hole moving upward.

4.9.3 Drill-off problem

While drilling a 12.25 in. diameter well, a drill–off test was conducted. The drill pipe was 4.5 in., 20 lb/ft, and 12,000 ft long. The maximum drill collar weight available is 70,000 lb.

Calculate the drilling rate and find the founder point for the hydraulics being used for the well. The first line is calculated so you can check your calculation technique (Table 4.3).

$$\text{ROP} = \frac{(\text{SC})(\text{DP Length})(\Delta \text{WOB})}{\Delta T} \times 0.0003 \tag{4.4}$$
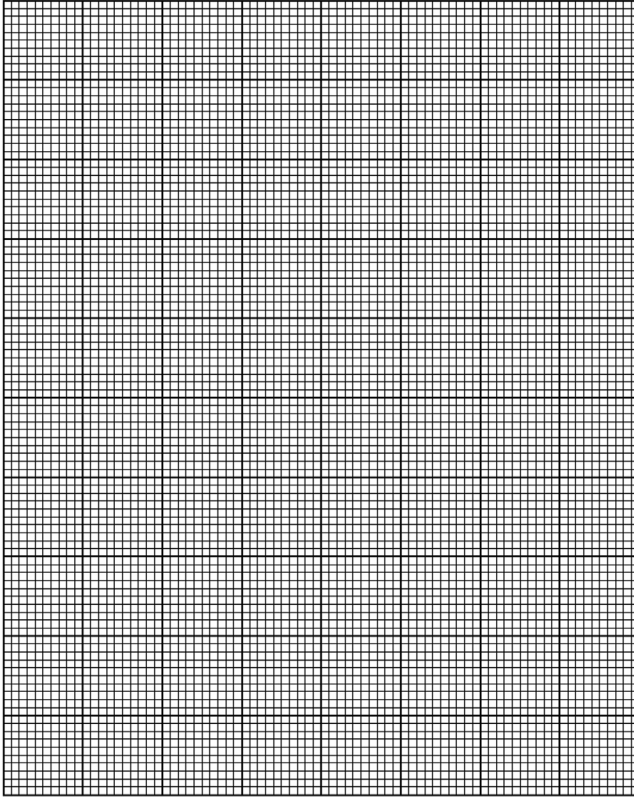
4.10 *D*-EXPONENT

ROP using the *d*-exponent is one of the primary indicators of abnormal pressure. As pressure in a formation increases, and mud weight is held constant, ROP will typically increase. The increase is especially prominent when the total overbalance is less than 0.5 ppg. Hence, close monitoring of penetration rate is often used to detect the impending onset of high pressure and hence help to identify the correct depth to set the next casing string.

In May, 1966, Jorden and Shirley[11] presented the *d*-exponent that has become an important parameter to identify the overpressure formations

---

[11] J.R. Jorden, O.J. Shirley, Application of drilling performance data to overpressure detection, J. Pet. Technol. (1966) 1387−1394.

from interpretations of drilling-performance data. Bingham[12] described the basic drilling rate equation that was used:

$$\mathrm{ROP} = a \times N \times \left(\frac{W}{D}\right)^{b} \tag{4.7}$$

where a and b are constants; N is the rotary speed; W is the weight on bit; and D is the bit diameter (ft).

When abnormal pressure is encountered, drilling rates tend to increase even though the rotary speed and the WOB are held constant. Grant's equation did not include a term related to the pressure effect that was known at that time. Jorden and Shirley made the assumption that the D was not a constant but a variable. The variability of D was assumed to be caused by the differential pressure.

To derive the Jorden and Shirley equation, take the logarithm of both sides:

$$\log\left(\frac{\mathrm{ROP}}{N}\right) = \log a + (b)\log\left(\frac{W}{D}\right) \tag{4.8}$$

Solving for the value of b:

$$b = \frac{\log\left(\frac{\mathrm{ROP}}{N}\right)}{\log\left(\frac{W}{D}\right)} - \frac{\log a}{\log\left(\frac{W}{D}\right)} \tag{4.9}$$

Jorden and Shirley disregarded the second term in the equation and inserted numerical constants to *create* their equation for the d-exponent:

$$d = \frac{\log\left(\frac{\mathrm{ROP}}{60N}\right)}{\log\left(\frac{12W}{10^{6}D}\right)} \tag{4.10}$$

The value of d normally is between 1.0 and 2.0. Jorden and Shirley use the value of bit diameter in inches rather than feet as used the Bingham's equation.

Curiously, Jorden and Shirley in their paper state: "It has also been shown that this equation does not describe drilling performance under field conditions." Although Jorden and Shirley credit Bingham with identifying the existence of a laboratory relationship between drilling rate and differential pressure, they admit that, under field conditions,

[12] Bingham, M.G., A new approach to interpreting rock drillability, Oil Gas J., November 2, 1964—April 5, 1965.

drilling rate is not necessarily influenced by differential pressure in the same manner.

Their final conclusion is perhaps the most interesting.

A correlation between normalized rate of penetration and differential pressure is recognizable from the available data. Although a trend is indicated in the d *exponent differential-pressure curve..., the scatter of data is too great for quantitative application...*

Yet the *d*-exponent is used extensively in the field today because it is believed by many field personnel that it somehow "works." Even though the value of the exponent of the WOB term is now known to be a constant value of 2, the exponent can be made into a variable if the pressure term does *not* appear in the drilling rate equation. An equally valid argument could have been made for an exponent on the *N* term in the drilling rate equation. *Any* added term on the right side of the drilling rate equation could be used to explain the fact that the ROP increases even though *W* and *N* are held constant.

4.11 CORRECTED *D*-EXPONENT (D_C)

Recall from Section 3.6.5 that differential pressure can affect penetration rate. As the bottomhole differential pressure gets close to balance with the formation, drilling rate increases. However, the well can also start "talking to you" with various other indicators (ROP, connection gas, gas cut mud, temperature, etc.) that warn of approaching balanced pressure, causing the on-site field personnel to raise the mud weight. This raising of the mud weight can mask the effects of watching the "*d*-exponent," rendering it less useful or even completely useless.

If the mud weight is changed during a casing seat hunt or other investigation of drilling rate, a straight ratio correction has been used by many. Its accuracy has never been definitively confirmed, in part due to the same concerns expressed by Jordan and Shirley over the original *d*-exponent. However, the corrected *d*-exponent d_c is expressed by the simple equation:

$$d_{\text{corrected}} = d \times \frac{\text{MW}_1}{\text{MW}_2} \tag{4.11}$$

where d is the regular d-exponent as defined above; $d_{corrected}$ is the corrected d-exponent, or d_c; MW_1 is the original mud weight; and MW_2 is the new mud weight.

4.11.1 Exercises

Two illustrative exercises are presented below to supplement those in the main body of the chapter.

4.11.2 Corrected *d*-exponent example

Assume that the "d-exponent" has been found to be relatively constant at a value of 1.282. The rig crew becomes concerned when connection gas goes from a relative constant value of 50 gas units to 200 gas units over three connections, and the mud is starting to get a little "gas cut." They weight up the mud from 10.2 to 10.5 ppg. What should the new baseline d-exponent be?

Answer:

$$d_{corrected} = d \times \frac{MW_1}{MW_2}$$

$$d_{corrected} = 1.282 \times \frac{10.2}{10.5} = 1.282 \times 0.97143 = 1.245$$

4.11.3 DP stretch drill-off test exercise

In conducting a drill–off test while drilling at 12,500 and using a 500 ft BHA, the following data were obtained. The stretch constant for the drill pipe was 0.10512 in./1000 lb/1000 ft. Calculate ROP and graphically determine the optimum weight in order to drill faster.

Note: Recall that ROP can be calculated from the equation:

$$ROP = \frac{(SC)(DP\ Length)(\Delta WOB)}{\Delta T} \times 0.0003$$

Start weight	End weight	Average weight	ΔT, Time in seconds	ROP
30,000	28,000	29,000	25	
28,000	26,000	27,000	29	
26,000	24,000	25,000	26	
24,000	22,000	23,000	25	

(Continued)

Start weight	End weight	Average weight	ΔT, Time in seconds	ROP
22,000	20,000	21,000	26	
20,000	18,000	19,000	35	
18,000	16,000	17,000	45	
16,000	14,000	15,000	60	
14,000	12,000	13,000	90	

Which in *this problem* works out to be ROP $= 756.9/\Delta T$.

For plotting, use the *average weight* (WOB) versus the calculated ROP (two grayed columns)

The solution is left to the reader.

Drill-off Test
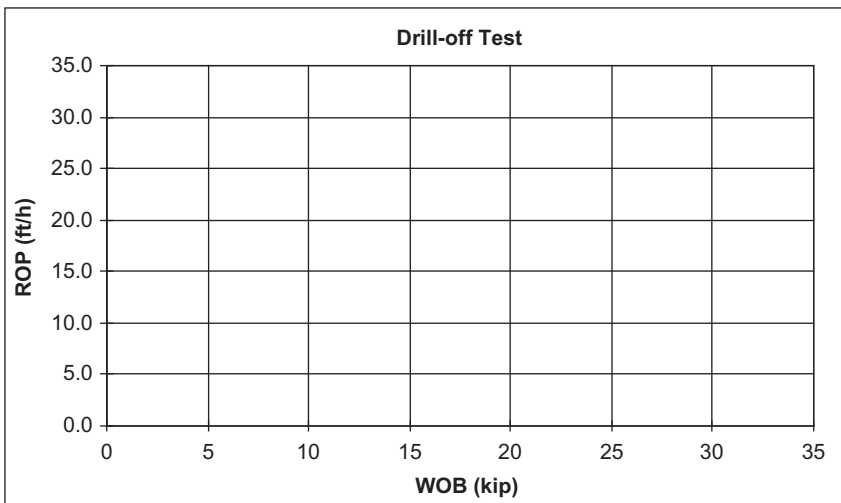
4.12 MECHANICAL SPECIFIC ENERGY

To evaluate the overall efficiency of the drilling operation, the concept of mechanical specific energy (MSE) has been developed and successfully used. Briefly, the concept is to compute the total energy input and divide by the footage drilled. The more successful implementation by

operators incorporates real time graphing and associated trend analysis. To compute MSE, the following equation may be used[13]:

$$\text{MSE} = E_m \times \left(\frac{4 \times \text{WOB}}{\pi \times D^2 \times 1000} + \frac{480 \times N_b \times T}{D^2 \times \text{ROP} \times 1000} \right) \qquad (4.12)$$

where MSE is the mechanical specific energy (kpsi); E_m is the mechanical efficiency (ratio); WOB is the weight on bit (lb); D is the bit diameter (in.); N_b is the bit rotational speed (rpm); T is the drill string rotational torque (ft lb); and ROP is the rate of penetration (ft/h).

For a full discussion on MSE, please refer to the Driller's Knowledge Book (another in this series) by Robinson and Garcia[5], or the original papers by Koederitz[13] or Dupriest[14].

4.13 ADDITIONAL REFERENCES

Several additional references are worth noting for the interested investigator that were not explicitly referenced in this chapter. They include the following:
- Preston Moore's classic "Five factors that affect drilling rate"[15],
- Ramsey and Robinson's "Onsite Continuous Hydraulics Optimization"[16],
- Robinson, L.H., "On site nozzle selection increases drilling performance"[17],

[13] W.L. Koederitz, J. Weis, A real-time implementation of MSE, in: AADE–05–NTCE–66, AADE National Technical Conference and Exhibition, April 5–7, 2005.

[14] F.E. Dupriest, W.L. Koederitz, Maximizing drill rates with real-time surveillance of mechanical specific energy, in: IADC/SPE Paper No. 92194 Presented at SPE/IADC Drilling Conference, February 23–25, 2005, Amsterdam, The Netherlands.

[15] P.L. Moore, Five factors that affect drilling rate, Oil Gas J. (1958).

[16] M.S. Ramsey, L.H. Robinson, Onsite Continuous Hydraulics Optimization (OCHOt), AADE–01–NC–HO–31, AADE 2001 National Drilling Conference, March 27–29, 2001, Houston, TX.

[17] L.H. Robinson, On site nozzle selection increases drilling performance, Pet. Eng. Int (1982).

- Ramsey, M.S., Robinson, L.H., Miller, J.F., Morrison, M.E., "Bottomhole Pressures Measured While Drilling"[18],
- Warren, Tommy M., "Evaluation of Jet–Bit Pressure Losses," SPE Drilling Engineering, December, 1989 pp. 335−340[19],
- Lapeyrouse, N.J., Formulas and Calculations for Drilling, Production, and Workover[20],
- Tompkins, Lee, ReedHycalog Hydraulics Program v2.2.3 or later[21],
- API Recommended Practice (RP) 13D, Rheology and Hydraulics of Oil–well Drilling Fluids[22], and
- Jet Nozzle Flow Area Calculators and tables located online.[23]

[18] M.S. Ramsey, L.H. Robinson, J.F. Miller, M.E. Morrison, Bottomhole pressures measured while drilling, in: IADC/SPE Paper No. 11413, Presented at the 1983 IADC/SPE Drilling Conference, February 20−23, 1983, New Orleans, LA.

[19] T.M. Warren, Evaluation of jet–bit pressure losses, SPE Drill. Eng. (1989) 335−340.

[20] N.J. Lapeyrouse, Formulas and Calculations for Drilling, Production, and Workover, Gulf Publishing, Houston, TX, 1992.

[21] L. Tompkins, ReedHycalog Hydraulics Program v2.2.3, February 2006, (or newer versions).

[22] American Petroleum Institute, API Recommended Practice (RP) 13D, Rheology and Hydraulics of Oil–well Drilling Fluids, American Petroleum Institute, 2006 and 2010 ed.

[23] Jet Nozzle Flow Area Calculators, such as the ones located online at www.tdaweb. com/TNFA.calculator.htm and http://www.texasdrillingassociates.com/hydraulics/ NozzleCalculator.htm.

Pressure Drop Calculations

Contents

5.1 INTRODUCTION

The optimization of bit hydraulics has been the subject of much discussion over the years. Unfortunately, due to the inability to understand the various flow regimes, coupled with the lack of knowledge about the downhole and time-dependent values of variables important to calculating pressure (or energy) losses, accurate modeling is somewhat elusive (see Chapter 6: Rheology, Viscosity, and Fluid Types on downhole property changes). Further, drilling fluids are notoriously non–Newtonian in nature, and their particular shear stress vs shear rate curves are difficult to predict and expensive to measure and do not extrapolate easily to other wellbores and drilling fluid systems. One industry expert has described the task as "Mission Impossible."

Broadly speaking, the energy stored in the drilling fluid as pressure (stored via fluid compression) by the triplex pumps is utilized in four broad areas:

- Surface equipment pressure losses in transporting the fluid from the pumps to the top of the drill string;
- Drill string component pressure losses (including mud motors, measurement while drilling (MWD), logging while drilling (LWD), pressure while drilling (PWD) equipment, etc.);
- Bit nozzle pressure losses; and
- Return wellbore, casing, and riser annuli pressure losses.

Of these four categories, the only one that directly and significantly affects drilling rate, good or bad, is the bit nozzle pressure loss. For the purposes of hydraulics optimization, the others can be thought of as necessary, yet wasted, energy or pressure. [Note that the flow up of the return annulus has a secondary effect on drilling rate, related to the equivalent circulating density (ECD), that affects drilling rate, especially when drilling at or near balanced pressure compared to the formation

pore pressure. This was addressed in some detail in Chapter 3: Hole Cleaning.]

In addition to the storage and use of energy (as pressure), calculation of pressure at any point in the wellbore also requires computing the hydrostatic pressure caused by the fluid density and the fluid column height.

Other issues related to pressure, including surge and swab pressures and the issue of the hole "washing out," are also addressed in this chapter.

5.2 CONCEPTS

The general term fluid can be divided broadly into gases and liquids. As air drilling is omitted from our consideration, liquids remain as our focus.

A brief review from Chapter 1, Introduction, is in order. Liquids in general can be classified as either being Newtonian (named after Sir Isaac Newton who studied their behavior nearly three centuries ago) or non-Newtonian.

Newtonian fluids exhibit a constant viscosity regardless of shear rates. (*Note:* With all liquids, Newtonian or non-Newtonian, the viscosity usually varies as a function of temperature, pressure, and some other influences.) For the Newtonian case, Fig. 5.1 shows a graph of shear stress vs shear rates in a straight line, going through the origin, with the slope being that of Newtonian viscosity as shown. Low-viscosity fluids have a lesser slope, with high-viscosity liquids exhibiting a steeper slope on such a graph.
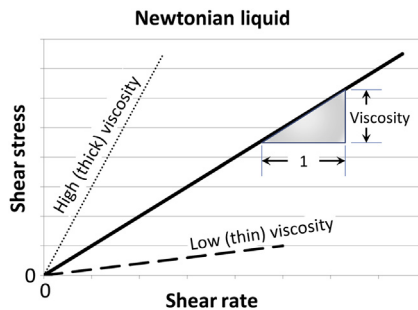
Figure 5.1 Classical Newtonian viscosity is the slope of the line defining the relationship between shear stress to shear rate (and is constant for all shear rates).

5.3 SURFACE AND BOTTOM-HOLE PRESSURES

At any point, surface pumping pressure (i.e., "standpipe pressure" for a drilling rig) will consist of frictional losses (including sometimes time-dependent fluid properties) and inertial effects.

Friction losses can be further broken down into surface piping losses, drill string losses, bottom-hole assembly (BHA) losses, bit nozzle pressure losses, downhole tool losses, and losses through various annuli as the drilling fluid returns up to the surface flow line.

Inertial losses can include effects of accelerating or decelerating the fluid, as well as accelerating or decelerating the drill string and BHA itself. Often ignored, these inertial losses, while transient in nature, can be the highest additions or subtractions from bottom-hole pressures of any effect. Important mud properties include viscosities (usually as a function of shear rate, time, temperature, and pressure), density of the fluid, gas content, and gel strengths. Transient acceleration and gel strength–related effects can decline quickly (in seconds) or persist for several minutes.

Further, pump pressure (and associated flow rate) can be intentionally changed if the surface annulus pressure, usually taken to be 0 psig, is altered through the use of managed pressure drilling equipment or by closing the blow-out preventers (BOPs) and circulation through a back-pressure choke. Further, note that the annulus fluid density is also a function of the ability to clean the hole of higher density rock cuttings and, therefore, also the rate of penetration (ROP).

Combining all of these effects in a generalized fashion yields

$$
\begin{aligned}
P_{\text{standpipe}} = {} & \Delta P_{\text{surface\_friction}} + \sum \Delta P_{\text{drillpipe\_friction}} + \sum \Delta P_{\text{BHA\_friction}} \\
& + \sum \Delta P_{\text{tools}} + \Delta P_{\text{nozzles}} + \sum \Delta P_{\text{annulus\_hydrostatic}} \\
& - n \sum \Delta P_{\text{drillpipe\_hydrostatic}} + \Delta P_{\text{backpressure}} \\
& + \sum \Delta P_{\text{annulus\_friction\_pumps}} \\
& \pm \sum \Delta P_{\text{annulus\_friction\_drill\_string\_motion}} \pm \Delta P_{\text{accelerations}}
\end{aligned}
$$

$$(5.1)$$

Bottom-hole pressure, meaning the pressure inside of the borehole at the bottom of the hole outside of the bit, is somewhat simpler, though it is also a function of the ability to clean the hole of higher density rock cuttings and, therefore, also the ROP.

$$P_{\text{bottomhole}} = \sum P_{\text{annulus\_hydrostatic}} + \sum \Delta P_{\text{annulus\_friction\_pumps}}$$
$$+ P_{\text{backpressure}} \pm \sum P_{\text{annulus\_friction\_drill\_string\_motion}} \pm P_{\text{accelerations}}$$

(5.2)

Note that the annulus hydrostatic pressure is a function of the volume and density of cuttings being carried in the mud, as well as flow rate and associated hole cleaning. This effect is discussed more fully in the Downhole Properties chapter, Section 7.7. For brevity, suffice for now to recognize that both the hydrostatic pressure (a function of mud density and cuttings load) and the friction pressure (a function of flow rate and fluid properties) combine to exert pressure on the bottom of the hole. The cuttings load is also a function of the drilling rate and cuttings density. A generalized graph illustrating this is shown in Fig. 5.2.[1]

The annular pressures consist of hydrostatic pressures and friction losses. [Friction losses include ordinary circulation as well as "surge" and "swab" pressures.] When pumps are off, pressures on bottom are hydrostatic only (no friction pressure), though some trapped pressure and
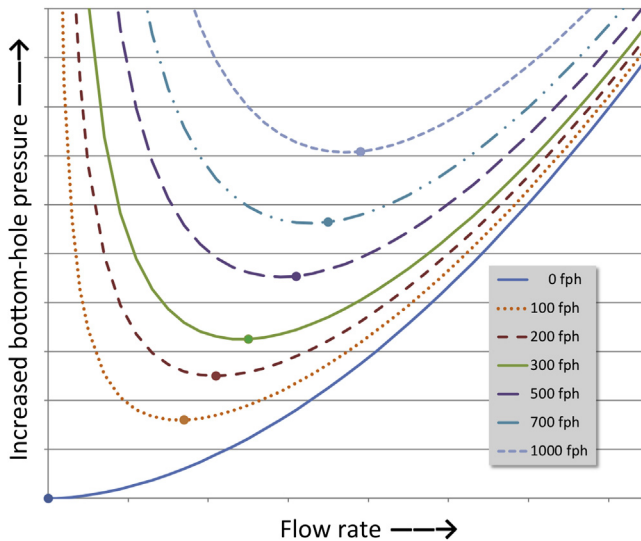
Figure 5.2 Combined flow, drilling rate, and hole cleaning effect on bottom-hole pressure.

---

[1] While this type of combined effects plot has been presented in various drilling texts before, recent advances in bit and other technologies have required redrawing to include up to 1000 ft/hour penetration rates!

hydrostatic imbalances have been observed. The reader should note that mud properties including density change downhole as described in the Downhole Properties chapter.

5.3.1 Hydrostatic pressure

What causes pressure in a wellbore? What causes pressure in the formation? How do we calculate it and deal with it in a convenient fashion, given changing mud weights as we deepen the well?

To begin, one might think of pressure in terms we have all experienced "first hand." When diving to pick up a silver dollar or quarter on the bottom of the deep end of a swimming pool, you will notice that the pressure on your ears goes up—sometimes even to a painful level—depending on how deep you dive. Why? We will address this and how to do the calculations in this chapter (Fig. 5.3).

Fundamentally, hydrostatic pressure, or the pressure exerted by the fluid itself, without any external influences such as pressure losses, surges, or swabs, is caused by gravity acting on the mass of the liquid mud. To illustrate, imagine that we had a cubed container filled with fresh water. The container measured 1 ft $\times$ 1 ft $\times$ 1 ft as shown in Fig. 5.4. Since water weighs 8.321 ppg and there are 7.4805 lb per cubic foot, the total weight of the 7.4805 gal of water in the cubic foot would be 62.25 lb. To evaluate the pressure at the bottom of the cube, we could take the fact that the bottom has 144 in.^{2} of area (12 in. $\times$ 12 in. = 144 in.^{2}). This means that the 62.25 lb of weight is distributed evenly on the 144 in.^{2}. Put another way, each square inch is supporting 0.432 lb of the water.
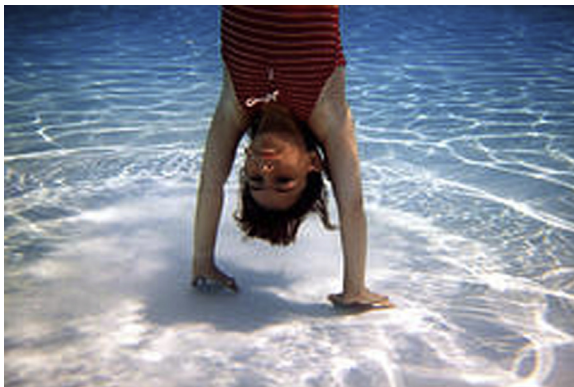
Figure 5.3 Deep end of the swimming pool.
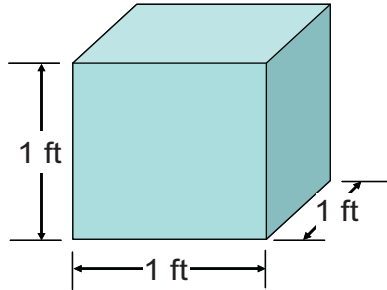
Figure 5.4 62.25 lb of water.
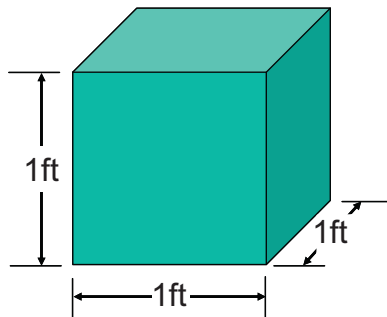
Figure 5.5 64.0 lb of seawater.

If the height of the water was doubled, the pressure would likewise double. If the height were tripled, the pressure would triple as shown nearby in Fig. 5.6. In fact, we could determine the pressure of a fresh water column by taking the pressure of 1 ft of water and multiplying it by the number of feet. This equation would take the form of

$$P = 0.432 \times \text{height} \tag{5.3}$$

However, since we do not often drill with just fresh water, nor do we do so for very long, this equation would not be very useful to drillers. To illustrate, let us say we were drilling with seawater instead of fresh water. Since seawater has about 35,000 parts per million salt plus some small amounts of other dissolved minerals, it has a slightly higher density than does fresh water[2]. Referring to Fig. 5.5, we see that the exact same 1 ft^3 volume of seawater weighs slightly more than fresh water, 64.0 lb.

[2] CRC Press, Handbook of Chemistry and Physics, 56th ed., CRC Press, 1976.
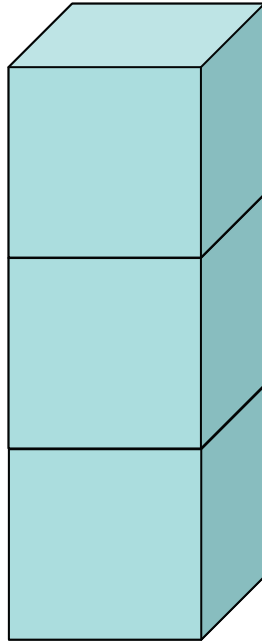
Figure 5.6 Three-feet fresh water column.

Repeating the calculations that we did for fresh water, we find that the pressure on the bottom of the 1-ft cube of seawater is 0.444 lb per square inch, or about 1.03 times as much pressure as fresh water. We could also express the pressure of a column of seawater as before, only the equation would change slightly to

$$P = 0.444 \times \text{height} \tag{5.4}$$

Formation water is even of higher density (more dissolved salt and minerals), and its density is usually rounded to 67.324 lb per cubic foot, and a repetition of this procedure would give us

$$P = 0.468 \times \text{height} \tag{5.5}$$

We could do this for every density of mud that we might use, but it would be far more convenient to have a single equation that would work for all cases. By taking the constant we got for fresh water, 0.432, and dividing it by the density of water, 8.321 ppg, we obtain 0.05192, usually rounded to 0.052. Similarly, if we take the seawater constant 0.444 and divide by the density of seawater, 8.56 ppg, we also get 0.052. Repeating

Table 5.1 Example liquid densities and pressure gradients

(1) Liquid type	(2) Liquid density (Sg)	(3) Liquid density (ppg)	(4) Liquid pressure gradient (psi/ft)
Fresh water	1.0	8.321	0.432
Seawater	1.03	8.56	0.444
Formation water	1.082	9.0	0.467
Red Seawater (upper layer)	1.173	9.76	0.507
14.5 ppg synthetic mud	1.743	14.5	0.753
18.5 ppg completion brine	2.22	18.5	0.96
22.0 ppg kill mud	2.64	22.0	1.14

for the formation water, we also get 0.052. Other examples of gradients are shown in Table 5.1.

Ordinarily, it has been found *most convenient* for rig-site drillers land office engineers and others to work with pressure in terms of pounds per gallon (ppg) which is, more accurately, the most common density measurement used to indicate a pressure gradient rather than a pressure.

This means that a simple equation is needed to convert the pressure gradient to a pressure at a given depth. In US Oilfield customary units, that pressure at a given depth may be found by

$$P_{\text{HYDROSTATIC}} = 0.052 \times \text{MW} \times \text{TVD} \tag{5.6}$$

where $P_{\text{HYDROSTATIC}}$ is the pressure at the bottom of the static wellbore in pounds per square inch; MW is the mud weight in ppg; TVD is the true vertical depth in feet; 0.052 is a conversion factor to make the units come out correctly when using US Oilfield units and lets us use a single equation for all mud densities. Further discussion on its value in other unit systems is found below.

●●●──

Example:

As an example, a vertical well with 12.2 ppg mud, drilling at a depth of 15,600 ft, would have a bottom-hole pressure of

$$P_{\text{HYDROSTATIC}} = 0.052 \times \text{MW} \times \text{TVD}$$
$$P_{\text{HYDROSTATIC}} = 0.052 \times 12.2 \times 15,600$$
$$P_{\text{HYDROSTATIC}} = 9897 \text{ psi}$$

Table 5.2 Assorted unit systems and their respective pressure conversion factors

	Type	Pressure units	Conversion factor	Mud weight units	Vertical depth units
United States	1	PSI	0.052	ppg	Feet
	2	PSI	0.1706	ppg	Meters
	3	PSI	0.432	Sg	Feet
	4	PSI	1.4196	Sg	Meters
Canada	5	kPa	0.00981	kg/m^3	Meters
Russia	6	Atmospheres	0.09678	Sg	Meters
	7				
	8				
	9				
	10				

Exercise:

Find the hydrostatic pressure at the bottom of the well if the mud weight is 16.0 and the true vertical depth of the well is 18,000 ft.

Note that in some countries, other units of height and mud weight are used. In those countries, the constant 0.052 changes as shown in Table 5.2.

5.3.2 Dual-gradient systems

Though still under development and considered mostly experimental at this writing, numerous attempts to design and, in some cases, build, working prototypes of so-called dual–gradient systems have been attempted. Conceptually, these would permit casing to be set deeper in a formation without as much risk of lost returns higher in the hole. This concept will be addressed more fully in Section 5.15.

5.4 FLOW REGIMES

Much has been written over years on flow regimes in boreholes and much debate has been over laminar and turbulent flow and just where a crossover or transition from laminar to turbulent flow occurs in a wellbore. While it is beyond the scope of this book to settle those debates,

the authors would be remiss without briefly addressing them. This has been discussed in Chapter 1, Introduction, but a brief review is in order.

5.4.1 Laminar, turbulent, transitional flow

When viscous forces are higher than inertial forces, a Newtonian (or even non–Newtonian) fluids will flow in layers—laminar flow—from the Latin *laminae*—where there is very little if any mixing of particles between layers.

Though difficult to achieve, even in controlled laboratory conditions, this is the most efficient flow type, where doubling of the flow rate only requires doubling of the associated pressure required (Fig. 5.7).

When the flow is more like a jet engine exhaust, or perhaps like water out of a fireman's nozzle, it is said to be fully turbulent. This is the least efficient flow type, and when it occurs, the pressure required to pump the

Figure 5.7 Laminar, transitional, and turbulent flow above a candle. (By Gary Settles—Own work, CC BY-SA 3.0, https://commons.wikimedia.org/w/index.php?curid = 29522249.)

fluid rises as a square of the flow rate. To double the flow rate requires four times the pressure under turbulent flow conditions.

Transitional flow is as its name implies, intermediate between fully laminar and fully transparent. For the purpose of calculating downhole pressures, suffice for here to say that most of our flow regimes are transitional and that the corresponding exponent of a power law or Herschel—Bulkley flow is in between 1.0 (fully laminar) and 2.0 (fully turbulent). Hindering the development of laminar flow is the fact that all or part of our drill string is rotating and moving vertically, and geometries at any given point in the flow are changing throughout the flow path. Solids, both microscopic and larger (rock cuttings from drill bit action at the bottom of the hole) also hinder fully laminar flow.

5.4.2 Newtonian

As mentioned previously, viscosity is not a function of flow rate or more correctly, shear rate, for Newtonian flow. Fluids such as water, gasoline, oil, and others—especially other clear liquids—generally behave in a Newtonian fashion, while solid-laden fluids such as drilling fluids, latex paints, ordinary tomato ketchup, or toothpaste do not. These latter liquids and gels exhibit a nonlinear viscosity as a function of shear rate.

5.4.3 Non-Newtonian

Bingham plastic fluids flowing in a *pipe* have a Reynold's number comparable to that of the Newtonian fluid,

$$R_e = \frac{\rho_{\text{cons}} \times \overline{V}_{\text{cons}} \times D_{\text{cons}}}{\mu_{\text{PVcons}}} \qquad (5.7)$$

where the cons subscript denotes "consistent units," or again in US Oilfield units with an appropriate conversion factor,

$$R_e = \frac{\rho \times Q}{\mu_{\text{PV}} \times D} \times 378.92 \qquad (5.8)$$

where ρ is the mud density (ppg); μ_{PV} is the plastic viscosity (centipoise); D is the hydraulic diameter (in.). This varies from the Newtonian case only in that with a Bingham plastic fluid, the viscosity is not constant with shear rate and is therefore specified to be the plastic viscosity (PV).

Similarly, in the *annular* case,

$$R_e = \frac{\rho_{\text{cons}} \times \overline{V}_{\text{cons}} \times (D_{\text{hole,cons}} - D_{\text{pipe,cons}})}{\mu_{\text{PVcons}}} \tag{5.9}$$

And for US Oilfield units,

$$R_e = \frac{\rho \times Q}{\mu_{\text{PV}} \times (D_{\text{hole}} - D_{\text{pipe}})} \times 378.92 \tag{5.10}$$

Power law fluids flowing in *pipes* have Reynold's number given as[3]

$$R_e = \frac{D^n \times v^{(2-n)} \times \rho}{8^{(n-1)} \times \left[\left(\frac{(3 \times n + 1)}{(4 \times n)} \right) \right]^n \times k} \tag{5.11}$$

where n is the flow behavior index (dimensionless) and k is the consistency index [(m/L s^{2-n}), lbf s^n/ft^2, or Pa s^n].

For a discussion of the calculation procedure and uses for n and k, please review the Chapter 3, Hole Cleaning

5.4.4 More on transitional flow and pressure losses

The transition between fully laminar flow and fully turbulent flow is neither well defined nor abrupt. This is especially true for non-Newtonian fluids such as drilling mud. Hence, the reader must be aware that somewhere between a full laminar flow regime and a fully turbulent flow regime, there exists a transition zone (with commensurate ill-defined "edges"), where neither flow regime dominates nor whose models would yield accurate calculations.

A conservative practice is to calculate for both the laminar and turbulent cases and use the worst for design purposes when planning the well.

Once the well is being drilled, data–driven measurements and subsequent calibrations can be undertaken readily to correct the initial prespud assumptions.

5.4.5 Reconciliation and recommendations

The way the debate has classically been addressed is to calculate both ways (i.e., using both a laminar flow and turbulent flow model) and then design based on the worst case. While this may nominally work, a superior way is to calibrate the models using actual wellbore data, which was covered previously in Chapter 2, Bit Hydraulics, dealing with optimum bit hydraulics.

[3] R. Mitchell, S. Miska, SPE Textbook Series Fundamentals of Drilling Engineering, vol. 12, 2011, p. 258.

In addition, it is possible that, due to the drill string being eccentrically positioned in the wellbore, the flow regime may be different in different sections of the wellbore cross-section[4]. The difference might or might not be from being nearly or fully laminar in some regions of the annulus to fully turbulent in other regions but may be very likely to contain different portions of the transition zone flow.

Similarly, it is possible that the flow could be turbulent (fully or nearly so) in the BHA by open hole annulus, be transitional further up hole in a drill pipe by casing inside diameter annulus, and then be either closer to laminar or turbulent in the marine riser depending on whether a boost line was being used (yet still transitional in all cases).

This consideration, too, supports the idea that the better way to handle the problem is rig site and wellbore-specific calibrations as detailed in Bit Hydraulics chapter.

5.5 FRICTION FACTORS

In attempts to deal with the friction losses caused by the wetted surfaces in fluid flow, engineers and scientists working on government municipal water projects developed the concept of using friction factors to better calculate pressure losses (or head losses), for different types of pipes that possessed varying degrees of roughness to them.

5.5.1 Brief history

As early as the era of the American Revolution, 1775, M. Chezy investigated pipe flow and determined that pressure losses in flow were a function of the circumference divided by a fraction of the pipe area[5].

Henry Darcy (who later developed the famed "Darcy's Law" used for reservoir fluid flow), in his early career, worked on municipal water supplies for Dijon, France, and developed an equation for pressure loss, which after refinement some years later with help from the German Julius

---

[4] F. Akgun, R. Jawad, Determination of friction factors of fluids flowing turbulently through an eccentric annulus, 1 (1) (2007) 37−49. ISSN 0973-6328. Available from: <http://www.ripublication.com/ijpst/ijpstv1n1_3.pdf>, 2009 (accessed 23.07.09).

[5] J.T. Fanning, Practical Treatise on Hydraulic and Water–Supply Engineering, sixteenth ed., D. Van Nostrand Company, New York, 1906. 644 pp., p. 229.

Weisbach in the mid-19th century became known as the Darcy−Weisbach equation, still in widespread use today.

$$\Delta p = f_D \times \frac{l \times \rho \times V^2}{2 \times d} \tag{5.12}$$

where Δp is the pressure loss; f_D is the Darcy friction factor; l is the length of pipe; ρ is the density of fluid; V is the flow velocity; and d is the inside diameter of pipe.

Note that with the V term being squared, this equation is dealing with turbulent flow.

After Osborne Reynolds identified the transition between laminar and turbulent flows using the dimensionless number bearing his name, the calculation of the friction factor for laminar flow as a function of the Reynolds' number had become common by the early 1900s, being the simple equation,

$$f_D = \frac{64}{R_e} \tag{5.13}$$

For the case of turbulent flow, the calculation, even since the mid-1800s, had been tedious at best, with various empirical equations being used for hand calculations as the slide rule was not yet on the scene. Most research had been done in a limited range of pipe sizes, types, water velocities, etc., and hence, the various empirical equations for f_D tended to be accurate over that particular researcher's scope of work and less so in a general sense.

J.T. Fanning undertook to solve this in his book, which debuted in 1877, by compiling all known good experimental data into tables, identifying the pipe type (e.g., "sheet−iron asphaltum-coated pipes," "cast−iron pipes," "lead pipes," "iron pipes," "wrought−iron cement-lined pipe," "glass pipes slightly rounded at the end," "smooth pipe," etc.)[6]. Cumbersome as this may seem, it represented a major manual calculation breakthrough, as the design engineer could simply look up his tubular type and size and read his tabulated friction coefficient from the table itself.

---

[6] J.T. Fanning, Practical Treatise on Hydraulic and Water-Supply Engineering, sixteenth ed., D. Van Nostrand Company, New York, 1906, pp. 236−246.

However, in what eventually became a huge source of confusion to this day,[7] Fanning used in his calculations the hydraulic *radius*, rather than *diameter*, but other investigators (notably Moody, et al.) used hydraulic *diameter*. This meant that Fanning's friction factor, which we will designate f_F in this book (though in Fanning's books he called it *m* in his tables), had a value one-fourth of what was needed to satisfy the Darcy−Weisbach equation from decades earlier.

Adding to the confusion is that subsequent to Fanning, others used a generic "friction" factor or coefficient *f*, without identifying which one of the two it represented, and a reader must carefully evaluate the context of the particular author to infer which one.

5.5.2 Friction factor approximations

For the laminar portion of the Moody diagram, the friction factor may be calculated in a straightforward manner as

$$f_D = \frac{64}{R_e} \tag{5.14}$$

Recalling that the Darcy friction factor is related to the Fanning friction factor by

$$f_D = 4 \times f_F \tag{5.15}$$

and hence we may calculate the laminar Fanning friction factor just as easily with

$$f_F = \frac{16}{R_e} \tag{5.16}$$

Turbulent flow presents more difficulties. Over the next few decades, others sought to provide a direct calculation of the turbulent friction factor, usually focusing on the Darcy form, not Fanning's smaller one.

---

[7] We found that confusion on these friction factors continues to the present, including at least one university-level textbook that used the Fanning factor when they should have been using the Moody one. So long as one recognizes that the Fanning factor is only one-fourth the value of what today is termed the Moody friction factor, and equations reflect the proper use, there is no harm. Several major disciplines today, notably HVAC, chemical engineering, and some public water works, along with much of the oilfield, choose to stay with the Fanning factor rather than the Moody one, which has become far more common in most other disciplines.

Paul Blasius in 1913 published that for smooth pipes (typical of today's drill pipe and casing),

$$f_D = \frac{0.3164}{R_e^{0.25}} \tag{5.17}$$

This remains valid for Reynolds' numbers from 4000 to 80,000.

Johann Nikuradse provided data that resulted in a slightly improved function for friction factor, sometimes referred to as either the von Karman's or Prandtl's

$$\frac{1}{\sqrt{f_D}} = 2 \times \log_{10}\left(R_e \times \sqrt{f_D}\right) - 0.18 \tag{5.18}$$

In 1939 Colebrook[8] (with acknowledgment to White) published what today is called the Colebrook−White equation, which used the Moody ratio of roughness to diameter, ε/d, as

$$\frac{1}{\sqrt{f_D}} = -2 \times \log_{10}\left(\frac{\varepsilon/d}{3.7} + \frac{2.51}{R_e \times \sqrt{f_D}}\right) \tag{5.19}$$

or in terms of the Fanning factor

$$\frac{1}{\sqrt{f_F}} = -4 \times \log_{10}\left(\frac{\varepsilon/d}{3.7} + \frac{1.255}{R_e \times \sqrt{f_F}}\right) \tag{5.20}$$

or equivalently

$$\frac{1}{\sqrt{f_F}} = -4 \times \log_{10}\left[\left(0.269 \times \frac{\varepsilon}{d}\right) + \left(\frac{1.255}{R_e \times \sqrt{f_F}}\right)\right] \tag{5.21}$$

Though not a particularly difficult problem for today's "goal-seeking" spreadsheet functions, at the time, this required a manually tedious and iterative solution. Hence, the hunt for an easier-to-compute solution for f_D (or f_F) continued, and the Haaland equation[9] approximating the turbulent portion of the Moody[10] diagram is

[8] C.F. Colebrook, Turbulent flow in pipes, with particular reference to the transition region between the smooth and rough pipe laws, J. Inst. Civ. Eng. (London, England) 11 (1938−1939) 133−156. Available from: <http://www.engineering.uiowa.edu/ ~me_160/lecture_notes/ijoti.1939.13150.pdf>, 2013 (accessed 11.07.13).

[9] Robert W. Fox, Alan T. McDonald, Philip J. Pritchard, Introduction to Fluid Mechanics, John Wiley & Sons, 2009, p. 332.

[10] L.F. Moody, Friction factors for pipe flow, Trans. ASME 66 (8) (1944) 671−684.

$$\frac{1}{\sqrt{f_D}} = -1.8 \times \log_{10}\left(\left(\frac{\varepsilon/d}{3.7}\right)^{1.11} + \frac{6.9}{R_e}\right) \tag{5.22}$$

or better

$$f_D = \left\{\frac{1}{\left[-1.8 \times \log_{10}\left(\left(\frac{\frac{\varepsilon}{D}}{3.7}\right) + \left(\frac{6.9}{R_e}\right)\right)\right]}\right\}^2 \tag{5.23}$$

Note that Haaland's is only an approximation of the Colebrook[11] and White equation (which is itself an empirical formula that tracks the underlying data imperfectly), but Haaland compares with Colebrook and White well and does not require an iterative solution.

Though the Colebrook and White equation is also not difficult with today's "goal-seeking" functions in modern laptop spreadsheets, it has more recently been approximated by the Swamee—Jain equation[12],

$$f_D = \frac{0.25}{\left[\log_{10}\left(\left(\frac{\varepsilon}{(3.7 \times D)}\right) + \left(\frac{5.74}{R_e^{0.9}}\right)\right)\right]^2} \tag{5.24}$$

Referring back to Eq. (5.21), if one assumes that the ε/D ratio is 0 (a good approximation for most oilfield tubulars, i.e., "smooth pipe"), then this reduces to

$$\frac{1}{\sqrt{f_F}} = 4 \times \log_{10}\left(R_e \times \sqrt{f_F}\right) - 0.3946 \tag{5.25}$$

In addition, Blasius approximates this further in the range of Reynold's numbers from 2100 to 100,000, as a straight line (on log—log diagrams) from the equation,

$$f_F = \frac{0.0791}{R_e^{0.25}} \tag{5.26}$$

---

[11] C.F. Colebrook, Turbulent flow in pipes, with particular reference to the transition region between smooth and rough pipe laws, J. Inst. Civ. Eng. (Lond.) (February 1939).

[12] P. Swamee, A. Jain, Explicit equations for pipe-flow problems, J. Hydraul. Div. (ASCE) 102 (5) (1976) 657—664.
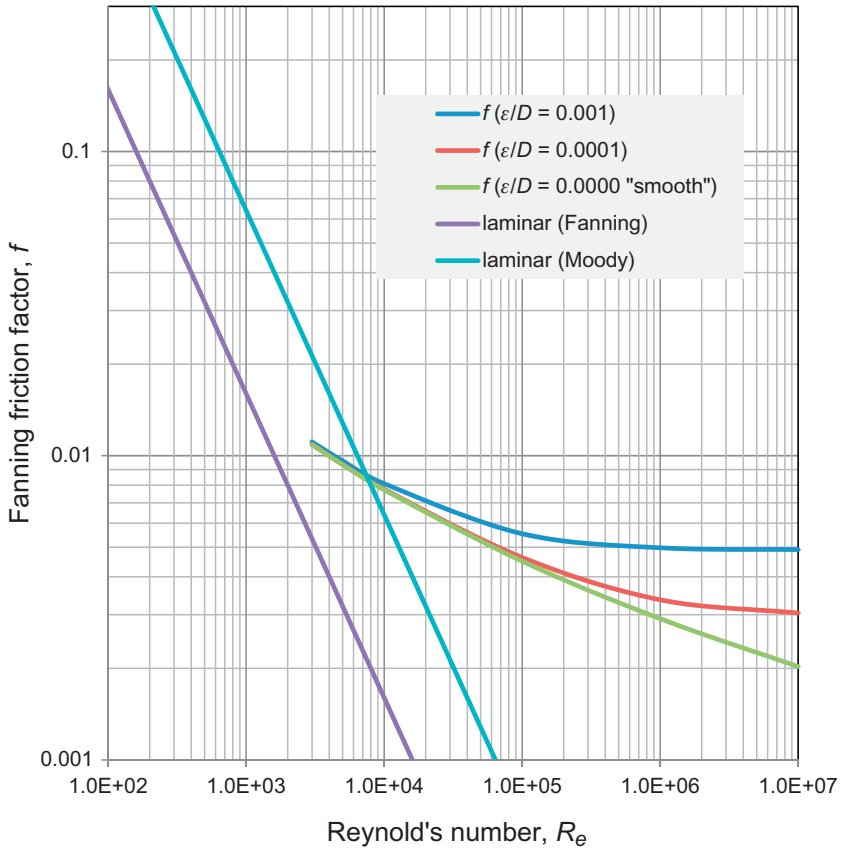
Figure 5.8 Stanton chart—approximately one-fourth of the friction factor as shown on the Moody diagram. Chemical engineering (and the oilfield) tends to use the Fanning friction factor, f_F, while civil and mechanical disciplines tend to use the Darcy−Weisbach (Moody) friction factor, f_D.

Note that the Fanning friction factors are sometimes presented in a chart form similar to the Moody diagram (see Appendix), but in the case of the Fanning friction, factor is called a Stanton Chart as presented in Fig. 5.8.

Note that the use of the Fanning or Moody diagrams carries the same caveats previously noted with regard to Newtonian solutions being used for non-Newtonian fluids such as drilling mud and is only accurate for water, seawater, and base oil.

As mentioned above, the inside of casing and drill string pipe may be thought of as "smooth pipe." However, borehole walls and the effect of

internal and external upsets of drill string components, as well as casing coupling effects, may not meet this criterion.

The second friction factor mentioned above by Fanning, f_F, is *not* as common in textbooks but used more commonly in the oilfield.

The Fanning equation for friction is defined as

$$f_F = \frac{D}{2 \times \rho \times v^2} \times \frac{dp}{dl} \tag{5.27}$$

However, this requires prior knowledge of the pressure loss per unit length of pipe, data that are not usually available during the planning of the well, especially if a different drilling fluid or wellbore geometry is contemplated compared to what was present when available data were collected.

More commonly, the friction factor is assumed or estimated from prior data and models as above, and the resulting pressure loss is computed from

$$\Delta p = f_F \times \frac{2 \times \rho \times v^2 \times l}{d} \tag{5.28}$$

Note that this is identical to the Darcy—Weisbach equation [Eq. (5.12)], when the one-to-four relationship between the Fanning friction factor f_F and the Darcy (or Moody) friction factor f_D is taken into account.

Note that which equation is used is largely a matter of preference and convenience, since in most oilfield conditions of turbulent flow, they all yield acceptable results. The nearby figure compares both Darby friction factors, f_D, and Fanning ones, f_F, for both cases of the Colebrook—White equation (considered most accurate over the widest range of Reynold's numbers) with some other approximations.

The Blasius equation is clearly the simplest but has more limited range than some of the others. This more limited range is more obvious when compared to the Darcy, due to scaling effects. The best estimation among the more complicated equations overall at this writing is the Swamee—Jain equation (Fig. 5.9).

For a more detailed examination of the various estimation equations in common use, Kiijärvi[13] has published an excellent paper.

---

[13] J. Kiijärvi, Darcy friction factor formulae in turbulent pipe flow, in: Lunowa Fluid Mechanics Paper 110727, July 29, 2011, 11 pp.
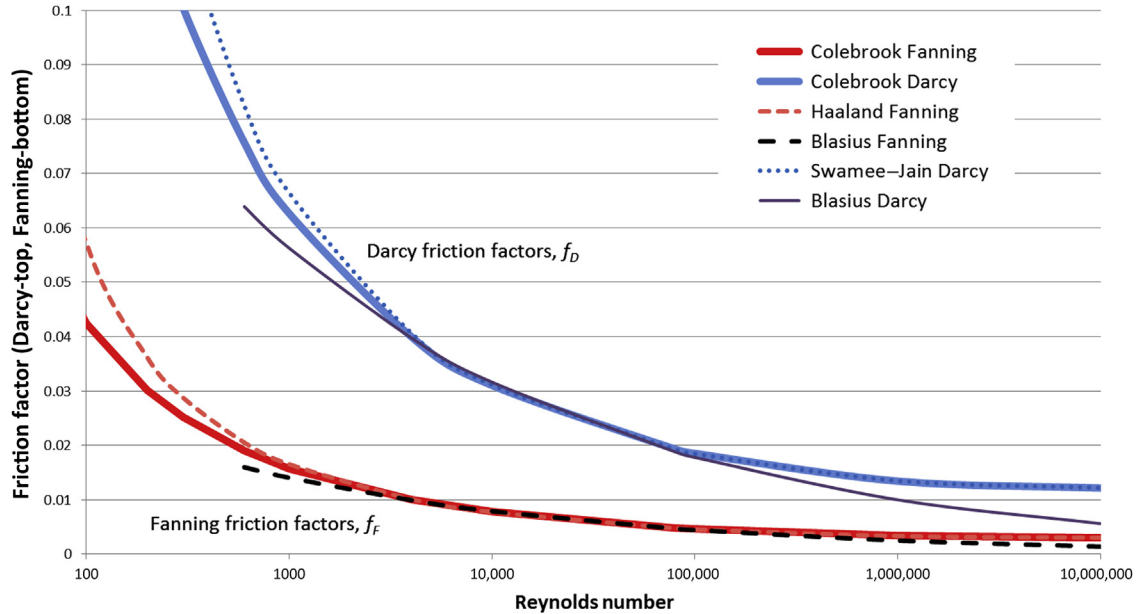
Figure 5.9 Comparison of friction factors (Colebrook) with estimations of same.

5.5.3 Pressure loss calculations in wellbores

There are several ways to examine prediction of pressure losses in the circulating system. Note that for non-Newtonian modeling, both the friction factor estimation and the transition to turbulent flow are more difficult, leading to the use of largely empirical equations for pressure loss calculations. These predictive equations are helpful, but sometimes result in large errors, and *should be calibrated with data from the actual well* once drilling has commenced.

Note that some portions of the circulation system can be calculated with greater accuracy than others. Bit pressure losses are generally thought to be the most accurate component, followed by surface system losses and then inside-drill string losses. The least accurate predictions are those used in the annular pressure losses.

There are two primary geometries and four fluid models to consider. The geometry is that of a pipe for flow inside the drill string traveling to the bit and an annulus (which can also be either concentric or eccentric to varying degrees). The fluid models commonly used for prespud design include Newtonian, Bingham Plastic, and Power Law. These can be further expanded as the designer desires to look at laminar flow and turbulent flow conditions.

To summarize, the different geometries, fluid models, and flow characteristics to be used, most with a separate formula for computing pressure loss, are listed in Table 5.3.

Note that in the absence of a compelling reason to use something else, the power law models will generally give more accurate results and are

Table 5.3 Flow geometries, models, and regime combinations

Geometry	Flow model	Flow regime
Pipe	Newtonian	Laminar
Pipe	Bingham plastic	Laminar
Pipe	**Power law**	**Laminar**
Pipe	Newtonian	Turbulent
Pipe	Bingham plastic	Turbulent
Pipe	**Power law**	**Turbulent**
Annulus	Newtonian	Laminar
Annulus	Bingham plastic	Laminar
Annulus	**Power law**	**Laminar**
Annulus	Newtonian	Turbulent
Annulus	Bingham plastic	Turbulent
Annulus	**Power law**	**Turbulent**

recommended. However, the Newtonian and Bingham plastic equations are given for completeness.

The well designer should determine the geometry he/she is dealing with, estimate whether the flow is laminar or turbulent, and then use the power law equation for that pair of criteria.

Equations for these different cases will be given without much discussion below. For a full discussion of any of these equations, please refer to the chapter endnote references themselves. Due to increased importance of the bit nozzle pressure losses, these will be examined separately in Chapter 2, Bit Hydraulics.

5.5.3.1 Pipe

Velocity is the relevant term for computing pressure loss, so conventional units of flow must be converted to velocity, feet per second in US units. In all models, the average pipe velocity is given by

$$\bar{v} = \frac{Q}{2.448 \times d^2} \tag{5.29}$$

where $\bar{v}$ is the average velocity (feet per second); Q is the volumetric flow rate (gallons per minute); d is the pipe inside diameter (in.).

The derivation of the conversion constant 2.448 for the use of customary US Oilfield units is given in this book's Appendices.

For *laminar pipe flow* with a *Newtonian* fluid model, the pressure drop per length is given as[14]

$$\frac{\Delta P}{\Delta L} = \frac{\mu \times \bar{v}}{1500 \times d^2} \tag{5.30}$$

For *laminar* pipe flow with a *Bingham plastic* fluid model, the PV (μ_{PV}) must be substituted for the Newtonian viscosity μ, and the yield point effect must be added. Doing these substitutions yield[15]

$$\frac{\Delta P}{\Delta L} = \frac{\mu_{PV} \times \bar{v}}{1500 \times d^2} + \frac{\tau_{YP}}{225 \times d} \tag{5.31}$$

where μ_{PV} is the plastic viscosity (cP); v is the average fluid velocity (fps); τ_{YP} is the yield point (lbs/100 sq. ft); d is the inside diameter (in.).

---

[14] B. Adam, C. Martin, K. Millheim, F.S. Young, Applied Drilling Engineering, SPE Textbook Series, vol. 2, 10th printing, 2005, p. 155.
[15] Ibid, p. 155.

For *laminar* pipe flow with a *power law* fluid model, the pressure drop per length is given as[16]

$$\frac{\Delta P}{\Delta L} = \frac{K \times \bar{v}^n \times \left(\frac{\left(3 + \left(\frac{1}{n}\right)\right)}{0.0416}\right)^n}{144{,}000 \times d^{1+n}} \tag{5.32}$$

As a reminder, K is the consistency index and n is the flow behavior index.

Another popular equation for laminar pipe power law calculation is[17]

$$\frac{\Delta p}{\Delta l} = \left[1.6 \times \frac{\bar{v}}{\left(d_{\text{IDpipe}}\right)} \times \frac{(3 \times n + 1)}{(4 \times n)}\right]^n \times \left[\frac{K}{300 \times \left(d_{\text{IDpipe}}\right)}\right] \tag{5.33}$$

For turbulent flow, there are multiple different accepted predictive equations that are in use for Newtonian and Bingham plastic models, and yet another for the power aw model case. These are presented below and simply numbered where multiple accepted equations are used. Note that in these, a friction factor, as discussed above, is sometimes used.

Turbulent pipe flow—Newtonian, Bingham plastic, and power law model #1[18].

$$\frac{\Delta P}{\Delta L} = \frac{f_F \times \rho \times \bar{v}^2}{25.8 \times d} \tag{5.34}$$

This equation is derived from the very definition of the Fanning friction factor, as shown in Chapter 9, Appendices, Section 9.4. Note that while these are oilfield units, the velocity of the mud in this form of the equation is in feet per second, rather than feet per minute, another common US Oilfield customary unit.

Note also that the Fanning friction factor f_F must be used in this equation. Care must be taken to use the best-known computation of what could be called an equivalent Reynolds number for non-Newtonian fluids, which we shall indicate as R_{eNN}, to distinguish it from the ordinary Reynolds' number calculation. R_{eNN} is computed by first determining the apparent viscosity μ_a (see Appendix), then using that in the classic Reynolds' number equation, and then determining if the flow can be treated as turbulent using the Hanks correlation between critical

---

[16] Ibid, p. 155.
[17] Reed-Hycalog Hydraulics Software package, per private correspondence with author.
[18] Bourgoyne, op cit., p. 155.

Reynolds' number R_{eC} (i.e., the Reynolds number where flow becomes turbulent) and the Hedstrom number (see Appendix for a discussion of this). Once turbulence is confirmed, then the Fanning friction factor form of the Colebrook−White equation [Eq. (5.20)] may be used.

Turbulent pipe flow—Newtonian, Bingham plastic model #2[19].

$$\frac{\Delta P}{\Delta L} = \frac{\rho^{0.75} \times \bar{v}^{1.75} \times \mu^{0.25}}{1800 \times D^{1.25}} \tag{5.35}$$

For the Newtonian flow case, and similarly,

$$\frac{\Delta P}{\Delta L} = \frac{\rho^{0.75} \times \bar{v}^{1.75} \times \mu_{PV}^{0.25}}{1800 \times D^{1.25}} \tag{5.36}$$

for the Bingham plastic case, the difference between the two being the use of the absolute viscosity μ for the Newtonian case and the PV, μ_{PV}, in the latter case.

Without using the friction factor at all, these equations may be used with good results, provided turbulent flow is present.

For derivations for those interested readers, we refer you to *Applied Drilling Engineering*[20] as reference.

Yet another popular relationship is given by[21]

$$\frac{\Delta p}{\Delta l} = \frac{0.002205 \times \rho^{0.82} \times \mu_{PV}^{0.18} \times v^{1.82}}{1000 \times d^{1.18}} \tag{5.37}$$

5.5.3.2 Annulus
In an annulus, the equations used for pipe pressure loss must be modified for the different geometry. This is commonly done through the use of substituting a hydraulic diameter in place of the pipe diameter. The hydraulic diameter is defined as

$$d_{hydraulic} = \frac{4 \times cross-sectional\ area}{wetted\ perimeter} \tag{5.38}$$

or

---

[19] Ibid, p. 155.
[20] Ibid, p. 155.
[21] Reed-Hycalog Hydraulic Software, private correspondence from author.

$$d_H = \frac{4 \times A_{ann}}{P} \qquad (5.39)$$

or

$$d_H = d_2 - d_1 \qquad (5.40)$$

(API 13D uses this without comment[22]. Details of derivation are in this book's Appendix.)

When an annular area is desired, such as when using an average velocity, it is computed as

$$Area_{annulus} = Area_2 - Area_1 \qquad (5.41)$$

or

$$Area_{annulus} = \frac{\pi}{4} \times \left(d_2^2 - d_1^2\right) \qquad (5.42)$$

And hence velocity, with conversions to use conventional US Oilfield units of GPM and inches for diameters, becomes for the case of annuli,

$$\bar{v} = \frac{Q}{2.448 \times \left(d_2^2 - d_1^2\right)} \qquad (5.43)$$

For *laminar annulus* flow with a *Newtonian* fluid, the pressure drop per length is given as[23]

$$\frac{\Delta p}{\Delta l} = \frac{\mu \times \bar{v}}{1000 \times (d_2 - d_1)^2} \qquad (5.44)$$

For *laminar annulus* flow with a *Bingham plastic* fluid model, the pressure drop per length is given as[24]

$$\frac{\Delta P}{\Delta L} = \frac{\mu_{PV} \times \bar{v}}{1000 \times (d_2 - d_1)^2} + \frac{\tau_{YP}}{200 \times (d_2 - d_1)} \qquad (5.45)$$

For *laminar annulus* flow with a *power law* fluid model, the pressure drop per length is given as[25]

---

[22] API 13D, Rheology and Hydraulics of Oil-well Fluids, sixth ed., API Recommended Practice 13D, 2010, p. 27. May 2010.
[23] Bourgoyne, op cit., p. 155.
[24] Ibid, p. 155.
[25] Ibid, p. 155.

$$\frac{\Delta p}{\Delta l} = \frac{K \times \bar{v}^n \times \left(\frac{\left(2+\left(\frac{1}{n}\right)\right)}{0.0208}\right)^n}{144{,}000 \times \left(d_{\text{IDhole}} - d_{\text{ODpipe}}\right)^{1+n}} \tag{5.46}$$

Another popular calculation for *laminar annulus power law* calculation is[26]

$$\frac{\Delta p}{\Delta l} = \left[2.4 \times \frac{\bar{v}}{\left(d_{\text{IDhole}} - d_{\text{ODpipe}}\right)} \times \frac{(2 \times n + 1)}{(3 \times n)}\right]^n$$
$$\times \left[\frac{K}{300 \times \left(d_{\text{IDhole}} - d_{\text{ODpipe}}\right)}\right] \tag{5.47}$$

For turbulent annulus flow, as with pipe flow previously, there are different accepted predictive equations that are in use for Newtonian and Bingham plastic models, and another for power law case.

Newtonian Turbulent Annulus #1[27]

$$\frac{\Delta p}{\Delta l} = \frac{f_F \times \rho \times \bar{v}^2}{21.1 \times \left(d_{\text{IDhole}} - d_{\text{ODpipe}}\right)} \tag{5.48}$$

Newtonian and Bingham Plastic Turbulent Annulus #2[28]

$$\frac{\Delta p}{\Delta l} = \frac{\rho^{0.75} \times \bar{v}^{1.75} \times \mu^{0.25}}{1396 \times \left(d_{\text{IDhole}} - d_{\text{ODpipe}}\right)^{1.25}} \tag{5.49}$$

As with pipe, the reader is directed to *Applied Drilling Engineering*[29] for more information.

Yet another accepted relationship is[30]

$$\frac{\Delta p}{\Delta l} = \frac{0.002205 \times \rho^{0.82} \times \mu_{\text{PV}}^{0.18} \times v^{1.82}}{1000 \times \left(d_{\text{IDhole}} - d_{\text{ODpipe}}\right)^{1.18}} \tag{5.50}$$

---

[26] Reed-Hycalog Hydraulic Calculator Software (and slide rule), per private correspondence from author.
[27] Bourgoyne, op cit., p. 155.
[28] Ibid, p. 155.
[29] Ibid, p. 155.
[30] Reed–Hycalog Hydraulic Software, private correspondence from author.

5.5.3.3 Eccentric annulus

The reader should also be aware that for a wellbore with a drill string or other pipe inside of it, the above annulus equations are idealized in that they assume the inside pipe is concentric with the wellbore. The pipe is assumed to be centered. This is not of course what one would expect in a deviated wellbore, and nearly all wellbores are deviated at least a small amount. This eccentricity of the pipe-in-hole affects the pressure loss, but no suitable relationship is known to this author to accurately account for this in an unknown downhole situation. (There are of course laboratory studies that have examined this for known conditions.) Even if an accurate model did exist, one would rarely if ever know the degree of eccentricity that actually existed downhole.

5.5.4 Wellbore hydraulics design and operational considerations

Where possible, the drill string designer should take into consideration what a particular drill pipe design may do for hydraulic pressure losses. A larger diameter pipe requires less pressure (energy) to pump a given flow rate through it than does a smaller diameter. This translates into savings in terms of improved ROP, improved hole cleaning, and even a significant diesel fuel savings.

Specifically, if a rental string of drill pipe is required, or if there are choices available as to which drill string to buy or to use, the larger diameter pipe will be chosen. The reason is that the added cost of the larger pipe will be more than offset by the savings due to reductions in pressure losses through the pipe. This is not just abstract but will be measured in reduced diesel usage, reduced wear and tear on mud pumps (mechanical and fluid ends), diesel generators, and so forth.

Cursory inspection of Table 5.4 and Fig. 5.10 shows clearly that as nominal pipe size is increased, the inside-drill pipe pressure loss decreases

Table 5.4 Comparison of pipe sizes and pressure losses, for illustration, based on NOV software Vers 3.0, MW = 13, 10,000 ft of 12.25 in. hole

Nominal drill pipe size (in.)	Drill pipe equiv. ID[a] (in.)	Drill pipe PSI/k′ at 300 GPM	Annulus PSI/k′ at 300 GPM	Combined PSI/k′ at 300 GPM	Drill pipe PSI/k′ at 600 GPM	Annulus PSI/k′ at 600 GPM	Combined PSI/k′ at 600 GPM
4	3.34	890	16	906	3142	113	3255
5	4.23	292	84	376	1029	209	1238
6.625	5.581	57.3	51	108	202	1112	1314

[a]Halliburton "Redbook" application for Apple iPhone, version 2.0.1.
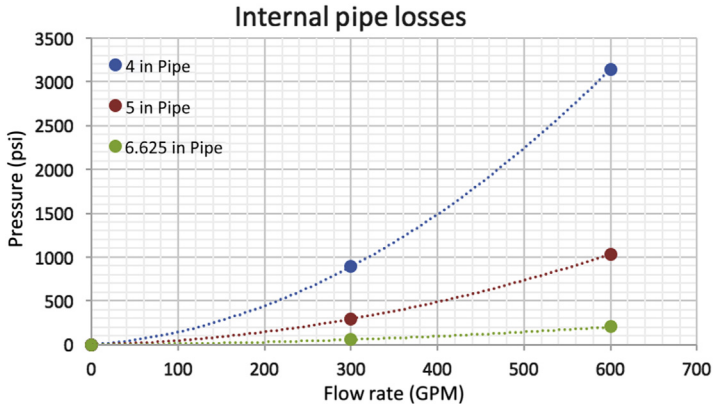
Figure 5.10 Internal pipe losses for representative pipe. (Software package generated.)

much more rapidly than the corresponding increase in the annular pressure drop as the velocity lowers inside the pipe but does not increase much in the annulus.

This has profound implications for wellbore hydraulics efficiencies. In practice, it has been reported that when renting drill strings, the added cost of renting a larger diameter drill pipe is *more than offset in diesel savings alone* by the lower pumping costs.

Importantly, this has led to innovative drill string designs in recent years as efforts to improve efficiencies in the "shale plays" have occurred. To improve both hole cleaning and stability of the pipe against buckling under compression, it is now relatively common in those high-efficiency drilling areas to use 4.5 in. pipe fitted with tool joints that historically have been for 4 in. pipe, such as 4.5 in. 16.6 ppf pipe with NC-40 connections.

5.6 CASING DRILLING

When casing is used as the drill stem, transmitting fluid power and rotational energy from the surface to the bit, the splits between how energy (or pressure) is utilized change, but the main components remain similar. The inside of the drill string losses are typically higher than inside of the casing losses, and the annular losses due to the smaller annulus tend to be higher, roughly offsetting each other. Equations discussed above for

pipe and annulus losses remain applicable, but of course the diameters are vastly different. Any pressure drop through whatever bit is used on the bottom of the casing will be calculated similar to any regular bit, though casing drilling nozzles, if any, tends to be so large as to not cause much pressure loss.

5.6.1 Underreamers

Underreamers, along with some other downhole tools, commonly have jets similar to bit nozzles. Their pressure loss is computed in the same manner as bit nozzles, and their flow area must be accounted for when sizing the actual bit nozzles.

Depending on design, note that to work properly, the underreamer hydraulics must be done correctly or the underreamer will fail to fully open. Hence, the underreamer hydraulic design may drive the effective minimum flow rate through the tool and/or the minimum pressure losses across the bit (Table 5.5).

As an example, Weatherford, a major underreamer supplier, published that a differential pressure (at the tool) of 500 psi is recommended and that flow rates through the three nozzles of their tool can range from 105 to 618 GPM depending on tool size and mud properties (at 75 ft/s velocity, which loosely equates to a pressure drop of 50−55 psi for 12 ppg MW.)

Put another way, with these pump-out underreamers, some amount of pressure drop is required to activate the cutting arms to move outward. In Tesco's case, another supplier, this is 200 psi minimum.

Table 5.5 Sample underreamer flow rates
Typical target flow rates

Csg size and hole size (in.)	GPM		FPM[a,b]	
	Max	**Min**	**Max**	**Min**
4.5 × 6.25	280	155	365	200
5.5 × 6.75	265	145	425	230
5.5 × 7.5	275	150	260	140
7 × 8.5	325	185	340	195
9.625 × 12.25	585	365	250	155
13.375 × 16	800	525	255	165
13.375 × 17.5	880	580	170	110

[a]Between casing and open hole per Tesco *Casing Drilling Manual*, Section V–3, page 11, 2004.
[b]Tesco Casing Drilling Manual, Section V–3, page 11, 2004.

5.7 COILED TUBING OPPORTUNITY

Coiled tubing (CT) drilling, a niche market for many years, is marked by lower flow rates (due to smaller inside diameter "drill string" of the continuous coiled pipe) and *constant drill string losses with increasing depth.*

In conventional jointed pipe drilling, the pressure losses through the inside of the drill string increase with depth, as do the annular losses. In CT drilling, since the full coil is used from top to bottom, regardless of how much of the coil is actually utilized in the wellbore, only the annular losses increase with depth—the drill string losses of the coil are constant with all depths.

While this is very inefficient from the use of hydraulic power and energy, it does offer interesting opportunities for some researcher to further study annular pressure losses without employing relatively expensive downhole measuring equipment.

5.8 BIT NOZZLES

Bit nozzle sizes and the corresponding flow rates and resultant pressure drops across those nozzles are a major influence on drilling rate. For this chapter's purposes, we simply note this, as a full discussion is contained in Chapter 2, Bit Hydraulics (Fig. 5.11).
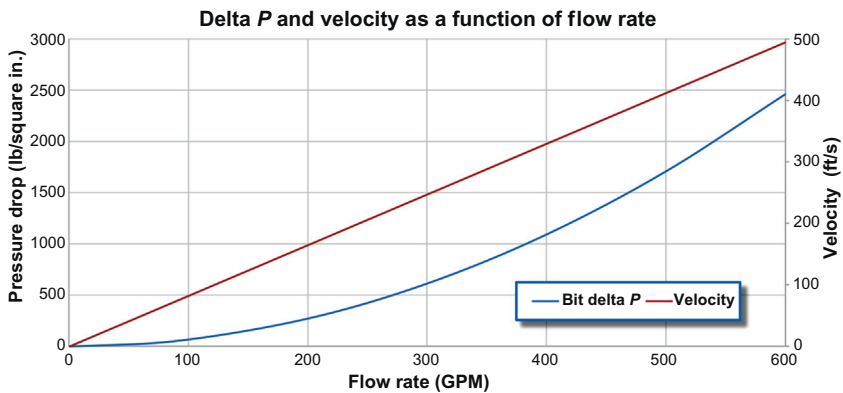
Figure 5.11 Pressure loss and velocity vs flow rate (for TNFA = 0.3889 in.^{2} and MW = 13.2 ppg).

5.9 OTHER GEOMETRY EFFECTS SUCH AS CENTRALIZERS, REAMERS, PIPE JOINTS, HOLE RUGOSITY[31], ETC.

Other minor effects, while all contributing in their small way to pressure drops in the annulus, are usually not explicitly accounted for in planning a well. This is in part due to the fact that many of the equations used for planning are empirical in their origin and hence have some of these effects somewhat built into them.

Of course, as more computing horsepower and engineering time is available, more of these small effects might be suitably modeled, though the authors believe that with current technology limits, this would not be a productive use of available time.

These uncertainties and unknowns are why it is important to use the rig, the drill string in the hole, and the well itself essentially like a "real-world rheometer" to get pressure loss readings at different rates and then optimize nozzle and flowrate selections accordingly.

Note also that if an unusually high number of these assorted tools were used, the most likely unusual situation might be a large number of roller reamers or nonrotating/bearing type drill pipe centralizers, then the added annular losses could be quite significant and should be estimated or better measured when drilling the well.

5.10 EQUIVALENT CIRCULATING DENSITY CALCULATION

Once friction losses have been measured or predicted, the conversion to ECD is straightforward

---

[31] Rugosity, or roughness factor of a surface is defined as the ratio fr = Ar/Ag, where Ar is the real (true, actual) surface (interface) area and Ag is the geometric surface (interface) area. This can relate to small surface irregularities or in the case of use for describing open hole wellbores, can refer to the degree of enlargement of the borehole from the original drilled diameter, or both. International Union of Pure and Applied Chemistry, (IUPAC), Compendium of Chemical Terminology, 2nd ed. (the "Gold Book") (1997). Online corrected version: (2006—) "Roughness factor (rugosity) of a surface", located at: http://goldbook.iupac.org/R05419.html and accessed August 17, 2015.

$$ECD = MW + \frac{\text{Annulus friction loss}}{0.052 \times TVD} \qquad (5.51)$$

All terms are defined as before. Note that if other than US customary units are involved, the 0.052 conversion factor changes accordingly.

5.11 SURGE AND SWAB PRESSURES

In the next series of charts (on the following pages), we will attempt to first orient the reader to various effects taking place downhole as they relate to pressures. The charts start out simple (and unrealistic) and are made slightly more complex (and more realistic) at each step. While the illustrations are necessarily simplified to illustrate principles, the last charts in the series are based on high-speed downhole measurements and hence are quite real in their implications and magnitudes of the surge and swab pressures experienced in wellbores.

The first chart (Fig. 5.12) is simply to orient the reader as to the layout of the charts themselves. The *x*-axis is *time*, while the vertical or *y*-axis is *pressure*. *Time* increases to the right and *pressure* increases toward the top.

The horizontal line represents pressure exerted on a point in the well by the fluid column itself, without any influence of fluid motion. This static fluid pressure is referred to as *hydrostatic* pressure.

Note that if the *hydrostatic* or any pressure exceeds the strength of the rock (depicted at the top of the chart), the result can be a *fracture* of the
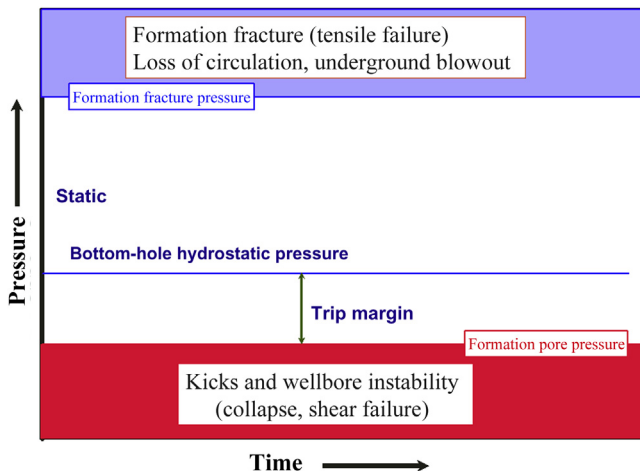
Figure 5.12 Basic layout of surge−swab figure series.
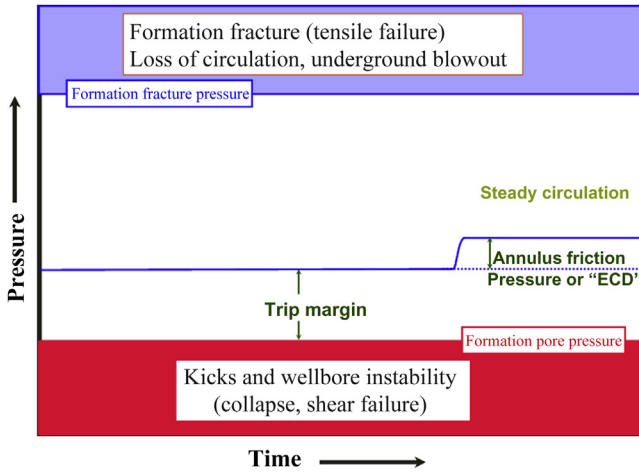
Figure 5.13 Effect of circulation on bottom-hole pressure.

formation, leading to loss of circulation and perhaps cascading to eventually cause an underground blowout.

If the pressure is reduced below the pore pressure of the rock (depicted at the bottom), the result can be shear failure of the rock or an influx of formation fluids (or "kick").

The first addition of reality is that for fluid to do work for us it must move. This fluid movement requires energy. Loosely speaking, we can measure this energy in a fluid by measuring pressure.

Hence, shown on the right side of Fig. 5.13 is the effect of a constant level of circulation. Fluid mechanics considerations require that this circulation requires a pressure drop. For the case of drill wells, this pressure drop is often referred to as the *annulus friction pressure*, or the combined effects of the hydrostatic pressure with this friction pressure are referred to as the *equivalent circulating density*, or ECD for short.

Note that the term "trip margin" is shown to represent how much design margin exists between the mud hydrostatic pressure and the formation pore pressure.

To improve our chart series, we now add the effects of pipe movement (Fig. 5.14) commonly referred to as *swab* (pipe coming out of the hole) and *surge* (pipe running into the hole). Our steady circulation friction pressure portion on the right remains unchanged.

When pipe is run into the hole, fluid must move out of the way. If a barrel of steel is added to the hole, a barrel of mud must come out. If a
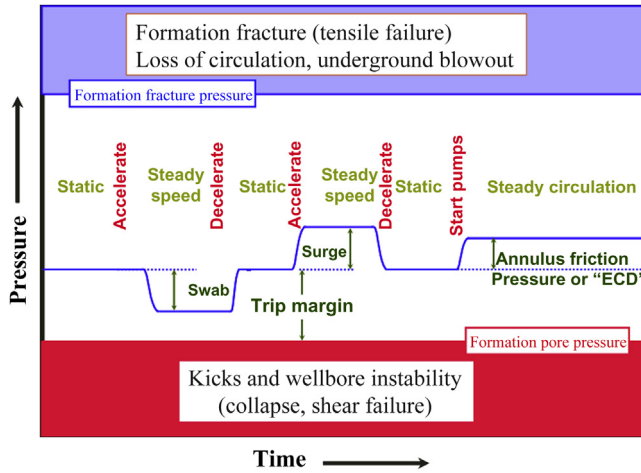
Figure 5.14 Surge and swab are similar to pumping in nature.

bit is in the hole and flow through the nozzles is restricted, either by the nozzles themselves or by a drill string "float" valve or by nozzle protectors (sometimes called "grasshoppers"), the displacement is not merely the steel but effectively includes the inside volume of the drill string. As this mud comes out of the hole, it is moving. In exactly the same fashion as the steady circulation on the right, moving fluid (in this case caused by pipe motion) requires a pressure drop. This pressure drop is exacerbated by the pipe physically moving in the opposite direction of the fluid motion.

Removing pipe from the hole causes the same effect, but since the direction of fluid movement is reversed, the pressure effects are reversed. In this case a barrel of steel is being removed from the hole, so a barrel of mud must flow in to take its place. The magnitude of the pressure change is the same if the pipe motion is the same. Only the plus or minus direction changes. Note also that the general "shape" of the curves for the *surge* and *swab* pressures are similar to the shape for the steady circulation by the pumps. This is simply due to the fact that the drilling fluid does not care what is making it move. In the case on the right, we are moving the fluid with triplex pumps. In the cases to the left, we are pumping the fluid with the drill string.

Next we note (Fig. 5.15) that there is a short transition that exists when fluid starts to move, or conversely, when moving fluid begins to stop and return to a static situation. The change from static to flowing or flowing to static does not occur instantaneously.

This is loosely analogous to starting or stopping your automobile. It takes some time to go from a complete stop to 60 MPH. Likewise, it
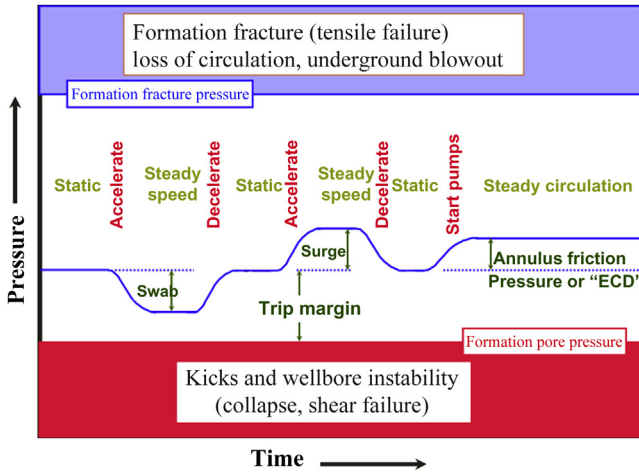
Figure 5.15 Changes to fluid flow are spread out over a transition time.

takes some time (and distance) to apply the brakes and go from 60 MPH to a complete stop.

Now our chart is complicated further (Fig. 5.16) with the addition of overshoots in pressure (plus or minus) during the transition or acceleration phase.

Concentrating on the "steady circulation" at the right, we point out that the pressure ramps up rapidly to a value above the steady-state friction pressure, before settling down to a steady-state value. This is *not* due to running the pumps too fast initially, but due primarily to acceleration effects.

A similar effect on pressures when breaking circulation may be observed if the mud possesses relatively high gel strengths. In such cases, it may take a considerable amount of pump pressure to break the gel structure and initiate flow in the first place. The inertial effects will still be there, as can be evidenced when circulation is established when the drilling fluid is fresh water or seawater (with zero gel strengths).

Sir Isaac Newton observed that an object at rest tends to remain at rest and an object in motion tends to remain in motion[32]. It takes more

---

[32] I. Newton, Principia. The Mathematical Principles of Natural Philosophy (A. Motte Trans. from the original Latin), First American Edition, 1846. It's phrasing is *"The vis insita, or innate force of matter, is a power of resisting, by which every body, as much as in it lies, endeavours to persevere in its present state, whether it be of rest, or of moving uniformly forward in a right line."* (p. 79 of 594 as accessed August 9, 2013 at the public domain digital library of the University of California at <http://ia600300.us.archive.org/8/items/newtonspmathema00newtrich/newtonspmathema00newtrich.pdf>.
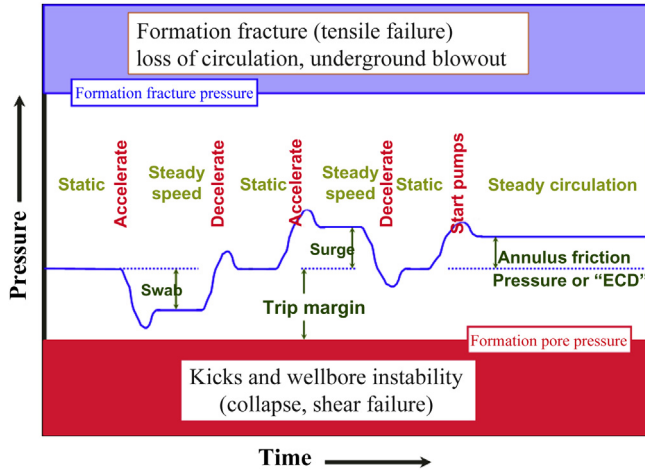
Figure 5.16 Inertial effects—illustrative only.

energy to make an object accelerate from rest to moving. Our "object" is the mud column. In terms of fluid mechanics, it takes more pressure to get a fluid moving than it takes to maintain its motion in a steady fashion.

Returning to our automobile analogy, it takes more gasoline (and power) to accelerate the car up to 60 MPH than it does to keep it cruising at a uniform constant speed of 60 MPH. Note that in the center case of the *surge* pressures, the pressure actually dips *below* the hydrostatic line as the pipe motion is slowing down. This is not due to the pipe bouncing (though that can happen and have a similar looking result) but is due to the latter part of Newton's observation. It takes energy (measured as pressure) to slow down our "object" (or drilling mud) after it has been moving. This is analogous to energy being dissipated by the automobile brakes when stopping.

Finally, our plot is made fully realistic (Fig. 5.17).[33] Note the very large swings in pressure that occur during the transition or acceleration/deceleration phases of fluid motion.

Note that while time periods are short, sometimes on the order of a few seconds, the pressure "spikes" can often reach into the upper (formation fracture) region, or the lower (well kicks and wellbore collapse) regions.

Note further that to minimize these acceleration spikes, it is more important that the *accelerations* be minimized than that the *steady speed*

---

[33] This diagram is based on actual high-speed wireline pressure measurements made by the author and others on real drill wells, not theoretical or laboratory work.
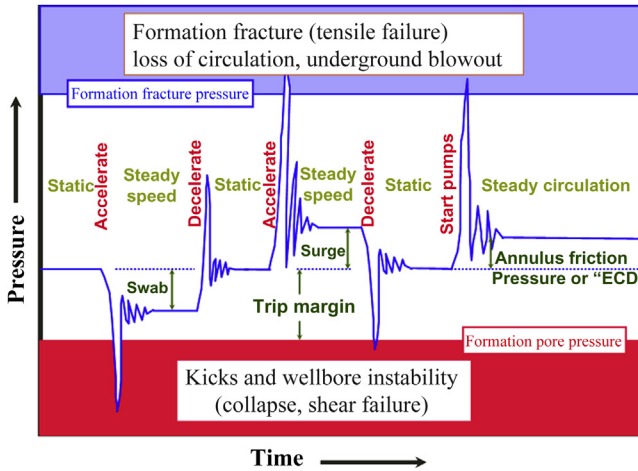
Figure 5.17 Representative surge and swab spikes in pressure due to inertial effects, based on downhole measurements.

during the middle of the pipe movement (i.e., the "middle joint time") be reduced. Put in more oilfield terms, it is far more important to have an "easy off, easy on the slips" practice than to slow down that middle joint speed of a stand.

Similarly, when pumps are brought up after a noncirculating time, the ramp up in pump speed should be sufficiently slow so as to not induce high pressure spikes as gels are broken and mud is accelerated.

To illustrate in a different manner, refer to Fig. 5.18. The leftmost shaded area represents the pore pressure in the rock being drilled; the rightmost area represents the fracture pressure of the rock. The dashed vertical line roughly in the center is the hydrostatic pressure exerted by a static mud column.

If the pumps are turned on and quickly ramped up to full speed, very large pressure spikes can be caused, as shown on the top portion of the plot. This immediate spike in pressure has been measured at several hundreds of psi and has the potential to at least momentarily extend fractures into the rock. This initial spike in pressure can be in part due to breaking of the gel strength just discussed, but a significant portion can be the simple inertial effect first described by Sir Isaac Newton.

The transients typically die down in 30 seconds or less.

After the transients are gone, the remaining increased pressure at the bottom of the hole is due to the friction in the annulus, and the net combined bottom–hole pressure (hydrostatic plus friction loss) is the ECD.
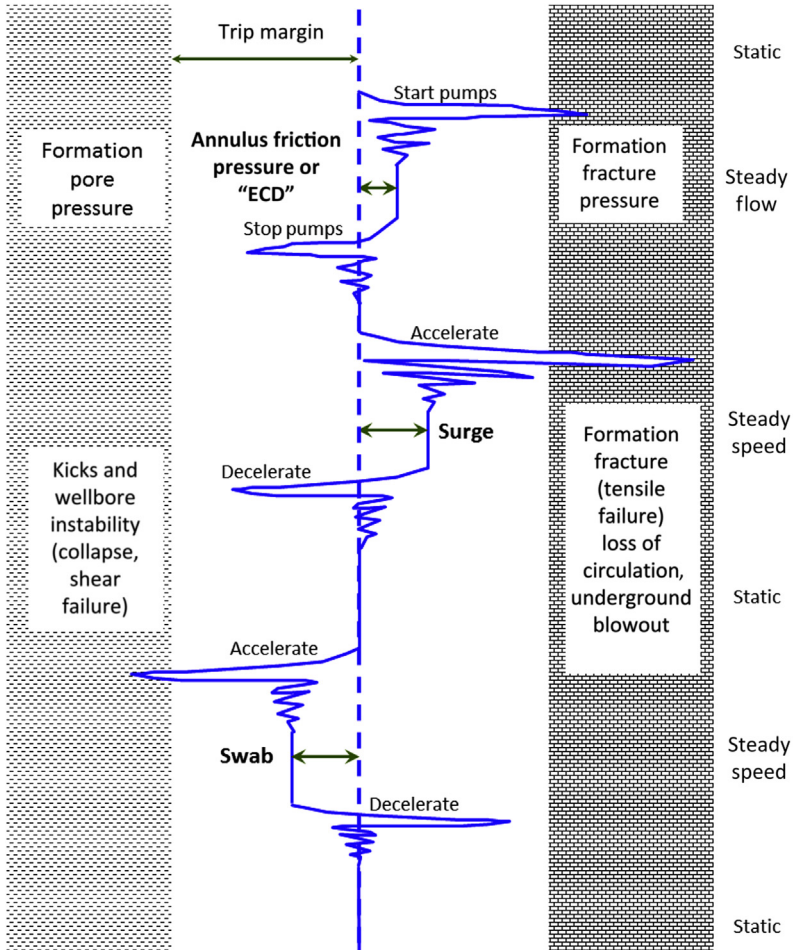
Figure 5.18 Effects of breaking circulation and pipe movement on bottom-hole pressure. *Illustration courtesy Texas Drilling Associates.*

Sudden stopping of the pumps can also cause pressure transients, which as shown can dip below the hydrostatic pressure level.

Moving the pipe in or out of the wellbore is essentially an alternative manner of pumping the mud and, not too surprisingly, can have similar effects on the bottom–hole pressure as shown in the bottom two events depicted (surge and swab).

Fortunately, most of the inertial forces can be minimized during pump start up and pipe movement by adopting an "easy on—easy off" operational policy, for both pump changes and pipe movement. Though the inertial effects cannot be eliminated 100%, they can be minimized as illustrated in Fig. 5.19.
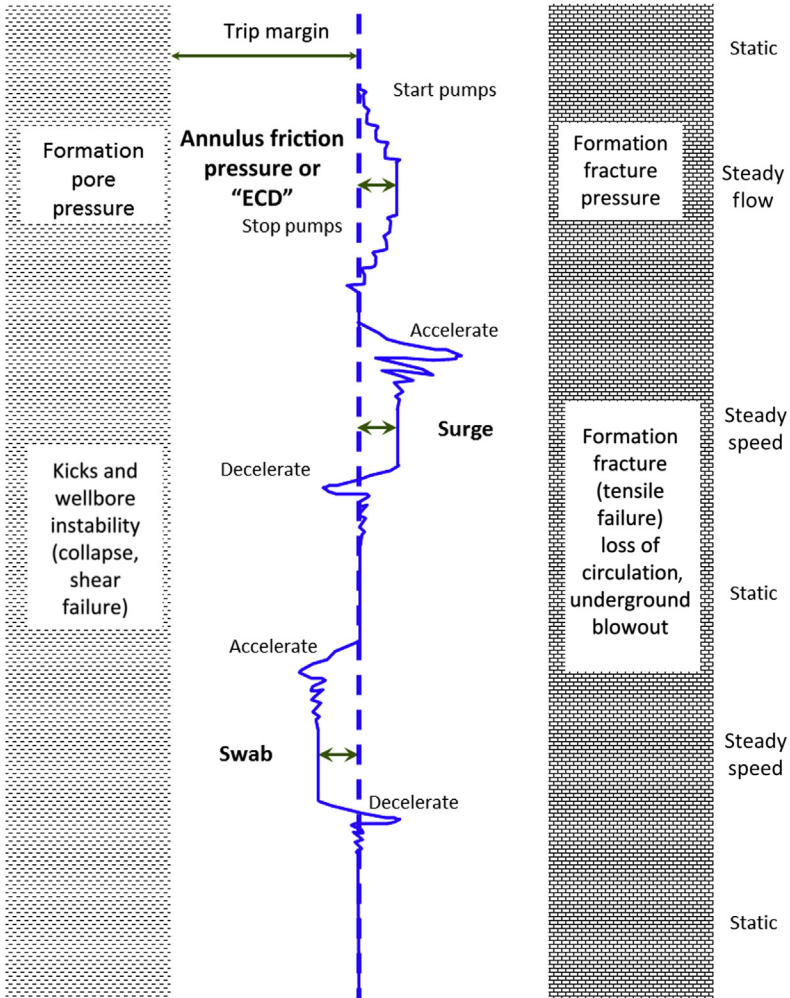
Figure 5.19 Transient pressure effects minimized by slowly ramping pump speed up and minimizing acceleration effects of pipe movements. *Illustration courtesy Texas Drilling Associates.*

5.11.1 Trapped pressures

Depending on the mud properties and the operational practices being used, some pressure, above and beyond the hydrostatic pressure, may remain trapped in the wellbore after pipe movement stops or pumps are shut down. This pressure is small but in critical areas may remain an important consideration.

5.11.2 Combined effects are *more* than additive

Very importantly and little noted, if the pumps are turned on or are already running when pipe in being put into the wellbore (causing surge), the effects of pumping and surging the pipe are combined and the combined pressure effect is *greater than the sum of the two components*. This combination is not merely additive, though that may be serious enough, but are governed by the power law exponent. Hence if pipe movement created the equivalent of 200 GPM flow, the pumps were running at 200 GPM when pipe was moved, and the power law exponent was 1.8, the pressure loss in the annulus would change from:

$$\Delta P_{\text{ANNULUS}} = k \times 200^{1.8} = k \times 13,863 \tag{5.52}$$

to

$$\Delta P_{\text{ANNULUS}} = k \times 400^{1.8} = k \times 48,273 \tag{5.53}$$

or nearly 3.5 times the flowing only pressure.

For additional derivations and explanations, please consult the API 13D document.

5.11.3 Deepwater—supercharging, flowback, and fingerprinting

Unfortunately, many wells being drilled in the world today, particularly in deepwater basins, have a much narrower operating range. The working area between the pore pressure in the rock and the fracture pressure of the rock may be very close together, sometimes less than 1 ppg. In such a case, the pressure transients are identical to the previous chart, but the safe operating window is greatly reduced. This window is sometimes so narrow that virtually any pipe movement or fluid movement induces a problem with the formation. In these extreme cases, the solution may call for extremely delicate fluid movements, a change out of the fluid system (to reduce friction losses), or setting casing to isolate formations with insufficient strength or high pore pressures.

It is situations such as these that may lead to a well being described by the unfortunate term of "ballooning," where the appearance is that the well is expanding when the pumps are turned on (and thus taking on more fluid) and then relaxing back when the pumps are turned off (and thus giving fluid back).
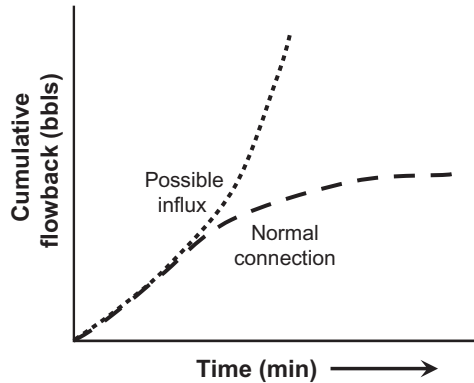
Figure 5.20 Fingerprinting. Comparing each connection flowback characteristics with the trend from previous trouble-free ones.

More properly, this behavior should be referred to as "supercharging" and "flowback," or some similar pair of terms that more accurately reflect what is happening. Fluid is actually being lost to the formation when the pumps are on, and the formation is flowing back when the pumps are off, in a manner somewhat analogous to the charging of a hydraulic accumulator and its subsequent discharge when used. Extreme caution must be exercised by the drilling team in such a situation, since it is nearly impossible to distinguish between such "flowback" and a bona fide formation flow or "kick" situation.

The primary technique used today to attempt to distinguish between a kick and ordinary flowback when pumps are off in such a situation is called "fingerprinting." This refers to the careful monitoring of flowback in all situations and comparing the current well behavior with that of prior ones. If the current flowback characteristics match the prior ones where no kick was occurring, it may be inferred that no kick is occurring. However, if the flowback of the current event is higher *or* does not reduce over time in the same fashion as prior ones, then the conclusion would be that the well could be flowing and it should be shut–in (Fig. 5.20).

5.12 HOLE WASHOUTS

Do high flow rates cause hole "washout"? Drilling engineers often get accused by geologists of washing out holes with aggressive hydraulics. While commonly believed, it is wrong. One can strongly believe a false doctrine. Below are seven independent reasons why such beliefs are not accurate.

Note that these reasons are independent. If you find you can agree with *any* of them, then the result is that aggressive hydraulics do *not* cause hole washout—at least not to any significant extent that could cause hole problems.

1. Annular velocities are *low*—as slow as walking. When we speak in terms like "aggressive" and "maximum" and "optimized" hydraulics, we paint a picture in our mind of a high pressure jet capable of cutting through steel. Nothing could be further from the truth. In the annulus, where the supposed washouts occur, the velocities are actually quite low—on the order of a leisurely walk or slow rivers like the Mississippi or Nile rivers.

2. It takes hardened steel or diamond to crush the rock. Our industry spends tens of millions of dollars on R&D and hundreds of millions of dollars on bits themselves every year. If rock could be eroded, we would simply do this.

3. If it was hydraulics that was responsible, then oil muds would also erode the hole. They do not. If it was really due to mechanical energy levels being too high with the drilling fluid, it would not matter what type of fluid we used—similar hydraulics would still erode the hole.

4. When we are trying to clean the hole, cutting beds are very difficult to erode with flow rate alone, and the rocks in that case (the cuttings) are already broken.

5. In cementing operations, we have great difficulty in eroding even the soft filter cake with the drilling fluid itself.

6. This author once conducted a test on an experimental bit equipped with "Extended Nozzles." These nozzles were only about 3/4 in. above the face of the rock, a soft shale. At the end of the bit test, the bit was kept on bottom, without rotating, but full pumping, for 30 minutes. At the end of the test the rock was examined. Even in this extreme case, not driven by annular velocity but with high velocity nozzle flow, the rock only eroded about 1/2 in.

7. At worse it is a self-limiting problem as the hole enlarges. The cross-sectional flow area that the fluid flows in goes *up* as a *square* of the "washout." What this means is that if the diameter goes up even a little, the flow rate goes *down* a *lot*, until it quickly returns to the preoptimized condition. Even if the annular velocity was responsible for some limited erosion, it would be self-limiting at an inch or so of hole diameter washout, and never lead to the massive washouts the geologist is concerned about.

In summary, except in truly unconsolidated formations or very unusual situations, washouts are *not* caused by high flow rates. Optimized hydraulics are good for drilling.

One might reasonably ask what does cause hole washout, since the phenomenon does occur? There are numerous reasons why washouts occur, but aggressive hydraulics are not among those. Some known causes include the following:

- Bit and BHA vibrations.
- Bit whirl, especially if bit is stationary vertically in the hole.
- Tectonic stresses/wellbore instability.
- Chemical attack of mud liquid degrading rock (water is the prime culprit). The most common manifestation of this is shale swelling and caving into the wellbore when water-based muds are used.
- Unconsolidated formations.
- Insufficient mud weight, also causing shale (and other rock type) cavings.

5.13 RISER BOOST

In offshore floating drilling environments, it is common to employ a riser boost pump. This permits additional mud to be injected into the flow stream at the mud line in order to keep the mud velocity in the large inside diameter riser sufficient to clean cuttings out of the hole.

This riser boost is typically achieved by running a separate pump using a separate 3—4-in. diameter boost line down the riser to the injection point.

Due to the large annular cross-sectional area, the added pressure loss in the riser caused by this can usually be safely ignored as it is small. The pump pressure at the surface may be significant, but nearly all of this is friction loss through the boost line itself (i.e., the "wasted energy" or pressure from the OCHO discussion in the Bit Hydraulics chapter), and very little is expended up the riser annulus.

5.14 CUTTINGS BED EFFECT

For highly deviated wells the effect of the cuttings bed on ECD may be diagnostic of how well the hole is being cleaned of cuttings in the first place.

Briefly for this chapter, it has been observed that when the drilling string is rotated after having reached a steady-state circulation pressure (without rotation), the circulating friction loss goes up. This is due to the
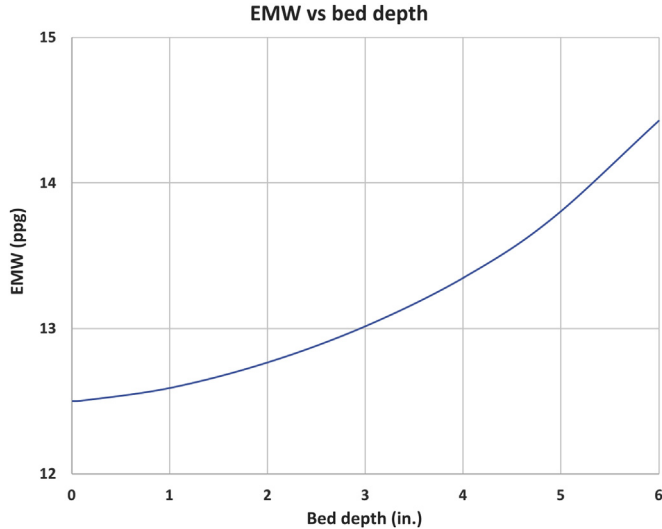
Figure 5.21 EMW due to stirring cuttings bed (12.5 ppg MW, 2.5 Sg cuttings, 0.6 packing factor). *EMW*, equivalent mud weight.

slightly lengthened flow path of the helical vs earlier straight flow lines, a slightly higher degree of turbulent flow (in the transition from laminar to turbulent flow continuum), and most importantly, the effect of stirring and suspending the cutting in the flow stream. While the first two effects may be relatively constant over time and linear with increasing depth, the latter changes depending on the mass of the cuttings bed itself go from lying on the low side of the hole to being suspended in the mud.

As the bed grows in depth, the difference between the nonrotating and rotating circulating pressures grows accordingly as illustrated in Fig. 5.21. Note that this figure does NOT include the effects of flow rate, which will drive the overall ECD even higher.

This is thoroughly discussed in Chapter 3, Hole Cleaning.

5.15 DUAL-GRADIENT SYSTEMS

As mentioned previously, a considerable amount of engineering design and experimentation has gone into dual-gradient drilling systems. These systems, if ever fully working, will permit drilling to progress in longer intervals before casing must be run. The "way they work"

Table 5.6 Water column effect on fracture gradients

Well depth (ft)	Land (ppg)	5000 ft water (ppg)	9000 ft water (ppg)
2000	14.0	10.0	9.5
8000	17.5	14.0	12.5

conceptually is to have a light fluid or even seawater in the riser of an off-shore floating operation, and the below-mud-line section is a more typical mud weight, or even a higher mud weight, than would ordinarily be used. The formation at any given depth experiences a "TVD-weighted" average of the two mud weights involved.

5.15.1 Discussion

As water depths increase in offshore drilling, the fracture gradient and the pore pressure gradient values become closer and closer together. This is caused by the fracture gradients being considerably lower as the water depth increases. Fracture gradients depend upon the overburden stress. When rock is replaced by seawater, the average overburden density (and corresponding stress) decreases. For example, the effect of water depth for two different water depths is shown in Table 5.6.

If a 2000 ft well is drilled in land, the fracture gradient would be around 14.0 ppg if no tectonic forces were present. If the 2000 ft well was drilled below the mud line in 9000 ft of water, the fracture gradient would be 9.5 ppg. This effect is caused by replacing 9000 ft of rock with 9000 ft of water. The horizontal stress (which controls the fracture gradient) would be considerably smaller because the overburden stress is so much lower.

If wells are drilled with risers and a uniform density drilling fluid, many more casing strings will be required. This may require larger blowout preventer stacks and larger risers. Both of these requirements will greatly increase the well cost because of the new larger equipment and the cost of rig time to run casing strings. Expandable casing will be a large part of any ultimate solution, but another possibility is to use a dual density system. In a dual density system, mud weight above the stack would be kept at a seawater gradient, or 8.5 ppg. This allows wells to be drilled almost as they would on land. A comparison of the effect is shown in Fig. 5.22.

Conventionally, wells are cased when the required mud weight (pore pressure) approaches within 1 ppg of the fracture pressure. For a 4000 ft water depth with an assumed pore pressure gradient as shown in the chart,
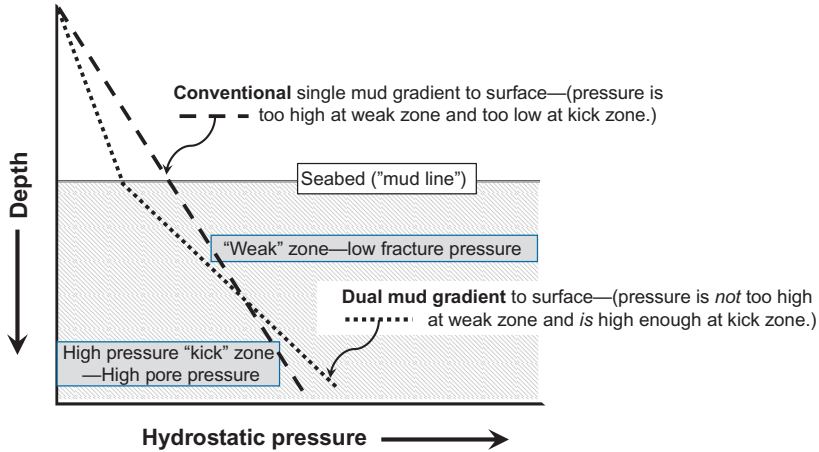
Figure 5.22 Conventional and dual-gradient mud circulating systems.

six strings of casing would be required to reach a target depth of 20,000 ft below mud line. With a dual density system, only three strings of casing would be required to reach a 20,000 ft reservoir.

Placing a lift pump on the ocean floor is one way to achieve a dual density system. Three major efforts are underway to develop this type of system: a JIP (joint industry project) by Conoco and Hydril with nine participants in the second phase; Shell; and the Baker Hughes/ Transocean SedcoForex (with BP and Chevron) DeepVision project. All of these projects are well funded and have different approaches for the same result.

The Conoco group plans to use positive displacement, diaphragm sub-sea mud lift pumps. The other two approaches use turbines. All pumps must move drilling fluid that contains cuttings. The Shell system has a novel approach to eliminating some of the larger solids from the system before they reach the subsea pumps. A large box with an open bottom will be filled with nitrogen. Drilling fluid leaving the well will pass through a solids slide with large openings. The very large solids will drop to the ocean floor and the drilling fluid with the remainder of the cuttings will fall into a funnel to be directed to the lift pumps. Solids may consist of not only drilled solids and those that fall into the wellbore from side of the hole but also large junks of cement that fall in from casing seats. Solids as large as 10 in. in diameter can reach the surface. The Shell system pro-vides an excellent solution to that problem. Both other approaches are addressing the problem and actually pumping cuttings during the
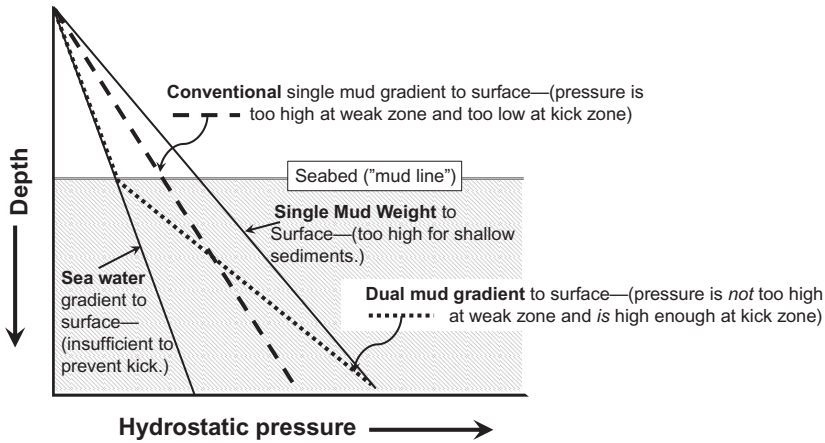
Figure 5.23 Effect of dual gradients on hydrostatic pressures.

development phase of the projects. (Fig. 5.23) further illustrates how having a sea water gradient to the mud line and a higher gradient below that more closely matches the pore and fracture pressures versus a single mud weight all the way to the surface. Implied in this is that as water depths increase, the benefit of a dual–gradient system increase.

Many problems, including significant ones relating to detecting and circulating formation influxes out of the well, must be solved before any of these systems can be used routinely. Their solution is imperative, however, if we plan to continue drilling in deepwater.

5.15.2 Illustrative exercise—dual gradient

Use Fig. 5.24 to work the exercise steps below. Note that the mud line (ML) is 5000 feet below sea level for this exercise.

1. Pick casing points using the stair–stepped top–down approach (like drilling the well down), from the shoe of the last string shown.
2. If a dual–gradient system is used, and the MW in the riser from surface to the mud line (5000 ft) is 8.6, what is the pressure inside the riser *at the mud line*?
3. Complete the table below and plot the dual gradient–equivalent mud weight (DG–EMW) on the graph, again picking casing points but using the DG–EMW.

Depth	Dual-gradient heavy MW	Dual-gradient pressure, including 8.6 MW from surface to mud line, plus 10.5 MW below mud line	Dual-gradient equiv. MW (DG-EMW)
5000	10.5		
7500	10.5		
8000	10.5		
9000	10.5		
10,000	10.5		
Light mud from surface to mud line now increases to 9.8 ppg.			
(_____ psi to ML)			
11,000	10.5		
12,000	10.5		
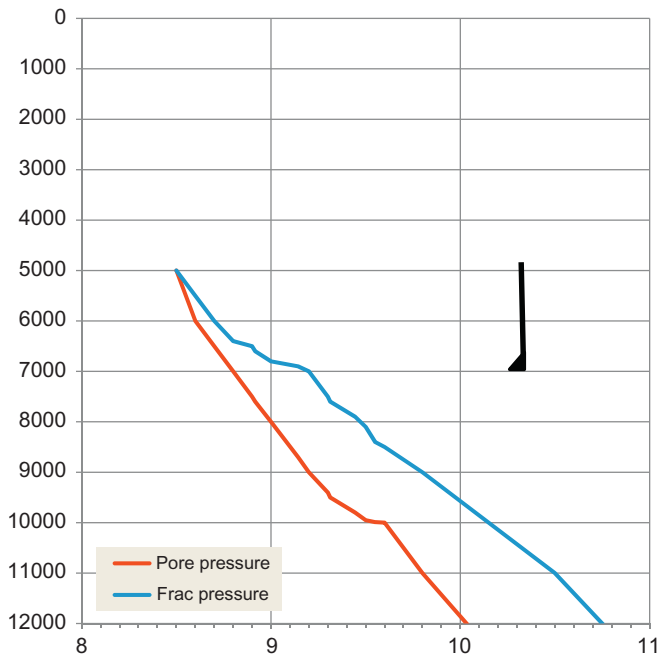
Figure 5.24 Pore Pressure and Fracture Pressure estimates for use in the dual gradient illustrative exercise.

As should be evident if worked correctly, the combination of the two mud weights enables casing string setting to be delayed until approximately 10,000-ft depth. The DG-EMW will plot between the pore pressure and fracture pressure line to approximately 10,000 ft,

where it will risk intersecting the pore pressure line if drilling is continued. However, even though the DG-EMW at 10,000 ft is well above the prior casing shoe pressure, the DG-EMW at the prior casing shoe is *not increasing*.

After casing is run, the wellbore is strengthened, and the weak point would become the new casing shoe, as is the case with traditional systems. With the hole down to 10,000 ft now "behind pipe," the riser mud weight can now be increased, and the well deepened to TD without even changing the circulating mud weight.

5.15.3 Pressurized mud cap

While likely *not* a preferred method of drilling in most wells, the concept of a mud cap in the annulus and top of the wellbore above a loss zone, coupled with drilling taking place with a low-cost mud such as seawater, has been proposed and successfully used in some geologic applications. This is the reverse of the concept usually thought of as dual gradient, but it does, in fact, have two gradients as well. The cases where this is known to work well are where severe loss zones occur and the cuttings can literally be pumped into that formation.

A severe disadvantage of this technique is that no returns report to the surface—it is assumed that all of the seawater or fresh water and whatever cuttings it brings up are shunted out to the loss zone.

However, as with any high spurt loss and/or low viscosity, low-density fluid, drilling rate is improved. In addition, when compared to a loss of hydrostatic pressure in the annulus, well control is improved somewhat.

5.15.4 Dual mud weight system

Another novel system being developed involves the use of two separate mud weights, pumped separately and mixed at the mud line (Fig. 5.25). The higher density mud weight is pumped through the drill string and the lighter mud is pumped down a separate line to the mud line, where the two densities are mixed in a mixing valve.

Returns of the mixed system are taken up the riser in a conventional manner. When the mud reaches the rig, it is processed through solids removal equipment and then run through centrifuges to separate the high density from the low density.
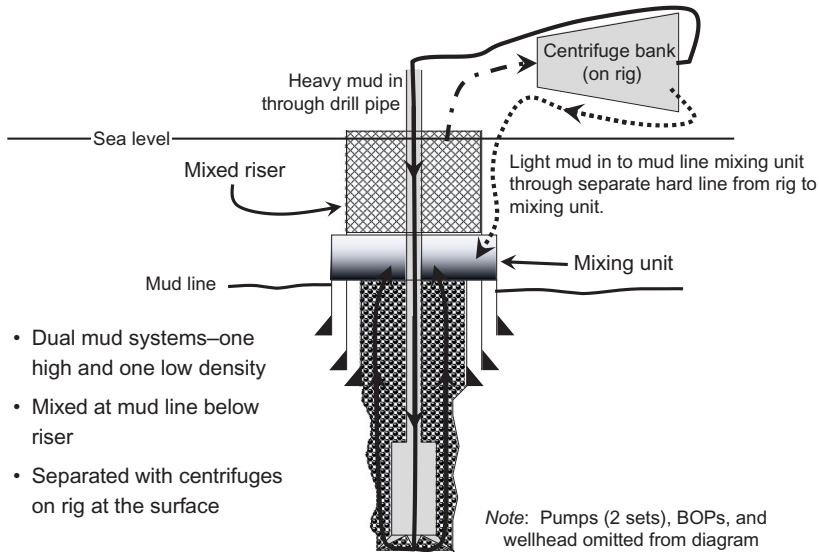
Figure 5.25 Dual mud dual gradient system.

This system requires essentially two circulating systems, two pumping systems, two solids removal systems, two chemical additions sections, and double the personnel to run the two mud systems.

Nonetheless, other than the doubling of surface requirements, this system is simpler downhole than are most others.

5.15.5 Mud line pumping system

Some work has been done in developing a mud line pumping system. By setting a pump at the mud line, along with suitable sealing elements much like a rotating BOP (RBOP) at the subsea stack, the mud hydrostatic pressure in the annulus of the riser is eliminated or reduced.

At least one version of this system contemplates including all solids control equipment subsea—certainly a daunting task.

5.15.6 Suspended "riserless" pump system

A variation on the subsea mud pump concept is to suspend a booster pump on a pipe below the floating rig, but not extending all the way to the mud line, and pumping the returns up a separate line, eliminating the need for a riser (Fig. 5.26).

While not achieving all the benefit of a full subsea system, the riserless system is by some estimates simpler. The riserless system has also been
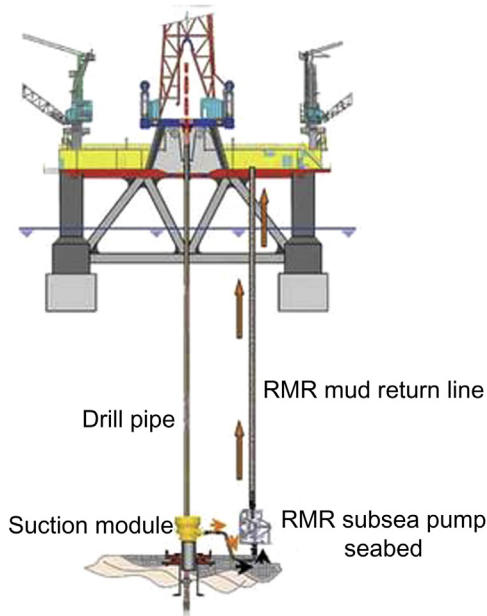
Figure 5.26 Riserless mud return system. *Courtesy: Enhanced Drilling.*

tested in the Caspian Sea. While encouraging results are reported, the water depth is not very deep in the test locations.

One major operator reported having run a riserless mud return system in the former Soviet Union 21 times in the Caspian Sea[34] and has continued to do so since then. The technology has been developed as part of a JIP. The technology is said to have advantages that include the following:

- Return top hole mud to the rig where "pump and dump" is currently the only option.
- Reduced well construction costs.
- Eliminate large volumes of mud needed for pump-and-dump operations.
- Minimize discharge to the environment.
- Lessen operational dependence on weather.
- Extended shallow casing depths.
- Improved hole quality.
- Wider choice of drilling fluids.
- Recovery of drilling fluids.
- Potential replacement for marine riser.

[34] BP, October 2006.

Though tests to date have been in relatively shallow water, the technology is planned for deeper water depths in the near future.

5.15.7 Mud line "riserless" pump system

The system described above, though workable, at this writing has a younger sibling whereby the pump is located on the mud line on a skid package rather than suspended from hard piping. This system, run by the Enhanced Drilling company of Norway[35], has been successfully used in several wells, including in the Caspian Sea and the US Gulf of Mexico.

5.16 COILED TUBING DRILLING

For nearly all cases, CT drilling is not economical when compared with conventional jointed pipe drilling, due primarily to high fatigue loading on larger diameter tubes limiting their lifetime. However, there are niche applications where it is justified for a variety of reasons, including the following:

- very shallow wellbores (primarily onshore),
- limited site footprint available.
- limited platform space,
- limited platform deck load available,
- transportation considerations, and
- completed well interventions.

Note that in the deepwater arena, there is little competitive advantage at all to CT drilling. For ultra-deepwater drilling, it is not technically feasible due to high pressure losses and limited tubing diameters.

Currently, CT is used, however, in completion and workover operations, including deepwater applications. As coil tubing diameter increases,

---

[35] R. Stave, R.R. Brainard, J.C. Cohen, Enhanced Drilling (formerly AGR Subsea, Inc.), Riserless mud recovery moves into deepwater, Offshore Magazine, 05/01/2008. Available from: <https://na01.safelinks.protection.outlook.com/?url = https%3A%2F%2Fwww.offshore-mag.com%2Farticles%2Fprint%2Fvolume-68%2Fissue-5%2Fdrilling-completion%2Friserless-mud-recovery-moves-into-deepwater.html&data = 02%7C01%7CDavidP%40PennWell.com%7Cbf27f4574de3485c5b2108d5e5d1978d%7C5bbf75da8a3f493c8343e6cd0cb0e070%7C0%7C1%7C636667610712292858&sdata = 2FVBYdkKOv6pdZ%2FLS4Bm97gds7NilmX2%2BtRBAGJQGzM%3D&reserved = 0>, 2018 (accessed 16.07.18).

the research continues, but this author believes that the above restrictions on widespread use of CT drilling equipment will continue indefinitely.

5.17 EXERCISES

Calculate the pressure gradient for the liquids shown.

(1) Liquid type	(2) Liquid density (Sg)	(3) Liquid density (ppg)	(4) Liquid pressure gradient (psi/ft)	(5) Pressure gradient divided by density	(6)
Fresh water	1.0	8.321	0.432		
Seawater	1.03	8.56	0.444		
Formation water	1.082	9.0	0.467		
Red Seawater (upper layer)	1.173	9.76	0.507		
14.5 ppg synthetic mud	1.743	14.5	0.753		
18.5 ppg completion brine	2.22	18.5	0.96		
22.0 ppg kill mud	2.64	22.0	1.14		

Rheology, Viscosity, and Fluid Types

Contents

6.1 RHEOLOGY

Broadly speaking, rheology is the study of how materials move or flow. This movement, flow, or perhaps deformation of materials is applicable to a number of disciplines, but has been studied extensively for flow through pipes, annuli, and other conduits of liquids such as drilling fluids. Rheology differs from viscosity in which viscosity is a measure of the "thickness" of the fluid that describes the resistance of the fluid to deformation caused by stress. Rheology encompasses the entire field of studying how matter moves. While this at first blush seems overly broad for a text dedicated to wellbore hydraulics, the field indeed includes movements of semisolids and even what nonrheologists call solids themselves.

Table 6.1 Viscosity comparison [1,2]

Material	Viscosity (cP)	Viscosity (Pa s)
Water	1	10^{-3}
SAE 60 motor oil	1000−2000	1−2
Honey	2000−3000	2−3
Hershey chocolate syrup	10,000−25,000	10−25
Peanut butter	150,000−200,000	150−200
Crisco shortening	1,000,000−2,000,000	1000−2000
Pitch (Tar)	10^{10}	10^{7}
Mantle rock	$10^{24}-10^{27}$	$10^{21}-10^{24}$

To a true rheology aficionado, nothing is completely rigid. What seems to be a solid, such as a rock, is merely a material having an extremely high viscosity!

Not to put too sharp a point on it, but the entire earth's crust and mantle layers (along with surfaces of other planets studied and modeled now by NASA), complete with planet development and continental movements, have been successfully modeled with rheology concepts and appropriate viscosity terms for the solid rock. For illustration, the values of viscosity are given in Table 6.1 for some common materials.

While the entire field of rheology is beyond the scope of this chapter, we will endeavor to highlight those concepts and flow types relevant to wellbore hydraulics and hole-cleaning considerations. Note that some of the concepts are suitable for computer modeling and prediction, while others are more suited as descriptive and find use as quality control tools.

6.2 VISCOSITY

Fluids in general and liquids in particular exhibit a wide range of behavior when moved from one point to another. In general, for flow through a pipe, frictional resistance to flow will require energy as pressure to overcome.

---

[1] U. Walzer, R. Hendel, J. Baumgardner, Mantle viscosity and the thickness of the convective downwellings. <http://web.archive.org/web/20060826020002/http://www.chemie.uni-jena.de/geowiss/geodyn/poster2.html>, 2015 (accessed 18.08.15).

[2] Viscosity Comparison Chart, The Composites Store, http://www.cstsales.com/viscosity.html (accessed 18.08.15.).

The forces present in this environment are "shear stresses (SSs)," that arise from the force vector component parallel to the fluid's flow cross section. The deformation that in turn results from an SS is a steady state "shear rate (SR)." Conversely, imposition by external forces of an SR results in an SS.

In the simplest case, a liquid has a linear proportional relationship between SR and SS. That is, if SS is plotted (*y*-axis) as a function of SR (*x*-axis), the result will be a straight line. The SS increases linearly with increasing SR. To pump such a liquid through a pipe at twice the SR, the SS will be similarly doubled.

Such a liquid may be very thin, exhibiting low viscosity, such as water, or be very thick, such as honey. The viscosity for any SR with such a liquid is the slope of the line plotted on the SS versus SR axis. The slope of the thin low-viscosity fluid would have a low slope, the thicker high viscosity fluid a higher one, as shown in Fig. 6.1.

Fluids with such straight-line (or constant) viscosity are said to be Newtonian fluids, after Sir Isaac Newton. Many clear (solids free) liquids exhibit this Newtonian behavior, including water, brines, pure oils, and many others.

However, while Newtonian fluids lend themselves to simple modeling, pressure loss predictions, and the like, such fluids would generally not be optimum for use in drilling wells. In order to drill wells efficiently, the ideal fluid would, at a minimum

- be very thin (low viscosity) as it passed through the bit (high SR through the nozzles) and struck the bottom of the hole where newly formed rock cuttings were. This thin-in-high-shear condition will enable the mud to more efficiently blast those rock cuttings (or "chips") off the bottom;
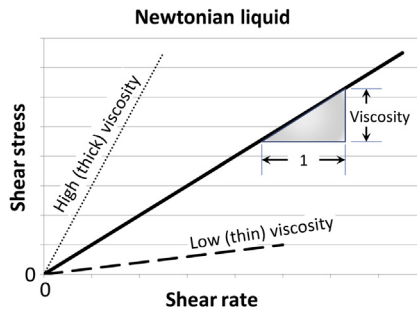
Figure 6.1 Newtonian fluids (straight-line relationship between shear stress and shear rate and going through the origin).

- thicken immediately after exiting the bit, as the fluid velocity slowed in the annulus, [low SR (LSR)], in order to continue to lift the cuttings up the annulus and out of the wellbore; and
- become a semisolid (possess a "gel strength" and "yield stress") when the flow is stopped, so those cuttings would not fall to the bottom side of the wellbore—perhaps hundreds or thousands of feet away in a vertical wellbore but only a few inches away in a highly deviated one.

Note there are numerous other functions we also require of the drilling fluid, such as the ability to protect valuable pay zones from fluid invasion, minimize trouble or nonproductive time costs, possess a low-friction coefficient, be stable at downhole temperature and pressure, etc., but these functions are beyond the scope of this chapter.

To satisfy the bullet points in terms of our SR/SS diagram, the slope (or tangent) at LSR should be steep (annulus), the slope at high SRs should be relatively flat (bit nozzles), and the y-intercept at zero SR should be nonzero (positive).

Viscosity itself is a term used in two forms, the more commonly used being "absolute" (or "dynamic") viscosity and the less commonly used being "kinematic" viscosity. Dynamic viscosity is customarily designated with the Greek μ "mu" or the Greek η "eta." In the classic textbook definition, we refer to Fig. 6.2. The two flat plates are separated by y distance, and the top plate is moving in the x direction at some speed relative to the bottom plate. A Newtonian fluid fills the gap between the two flat plates.

Constant motion (velocity, v) of the top plate relative to the bottom requires a force, F, which is distributed over the area, A, creating an SS that transmits through the fluid to the bottom plate. SS and SR are quantified as shown in Fig. 6.2. Sir Isaac Newton observed that for straight and parallel flow, the relationship between the SS, τ and the SR, v/h, or $\delta x/\delta y$ at a point could be expressed as

Parallel plate shear rate

$$\text{Shear rate} = \frac{v}{h} \qquad \text{Shear stress} = \frac{F}{A}$$
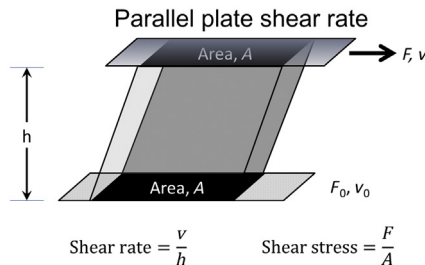
Figure 6.2 Parallel plate shear rate illustration.

$$\tau = \mu \frac{\partial x}{\partial \gamma} \qquad (6.1)$$

Rearranging:

$$\mu = \frac{\tau}{\frac{\partial \gamma}{\partial x}} \qquad (6.2)$$

Hence, viscosity, μ, is the ratio of SS divided by SR. That means that viscosity, μ, is the slope of the line as in Fig. 6.1.

A thin or low viscosity Newtonian liquid such as water or alcohol would have a line with a small slope closer to horizontal, while a thick or high viscosity Newtonian fluid such as honey would have line with a greater slope closer to the vertical. In both cases, the viscosity, μ, *does not change with a change in SR*. To point out an obvious but important point, in terms of Fig. 6.1, the *slope* of the SS versus SR line (which is the Newtonian viscosity) *remains constant at all values of SR*.

Kinematic viscosity, ν, is defined as the ratio of absolute viscosity divided by density ρ. This is sometimes utilized in fluid mechanics problems due to its relationship to the ratio of viscous forces to inertial forces.[3] This ratio is, effectively, the kinematic viscosity:

$$\nu = \frac{\mu}{\rho} \qquad (6.3)$$

As noted previously, unless otherwise noted in this text, the term "viscosity" will refer to the absolute or dynamic viscosity, μ, and *not* the less commonly used kinematic viscosity, ν.

Last, note that in the (SS/SR) plot of Newtonian fluids, all viscosity lines originate at the origin (0,0), meaning that the liquids at rest (zero SR) will not support an SS (as would be required to suspend particulates). This inability to generate an SS at zero flow (or zero SR) is part of the very definition of a Newtonian fluid.

Summarizing characteristics of Newtonian liquids, we find that they
- do not generate an SS at zero SR,
- have a constant viscosity with changing SR, and
- are *usually* "clear" liquids (in contrast to those containing suspended solids).

Non-Newtonian fluids are those that do not possess these characteristics. A non–Newtonian fluid may have a viscosity (or slope on SR SS plot) that

---

[3] B.S. Massey, Mechanics of Fluids (1970) 19.

varies with SR, a nonzero intercept, or both. Drilling fluids containing solids and/or polymers are generally non-Newtonian and may be described by a variety of flow equations. The most popular of these has been the Bingham Plastic model, but others, such as the power law and the Herschel−Bulkley models, have received much attention in recent years.

Bingham plastic fluids are modeled with the familiar straight line:

$$y = mx + b \qquad (6.4)$$

For the case of a Bingham plastic fluid, this becomes

$$\text{Shear stress} = \text{plastic viscosity} \times \text{shear rate} + \text{yield point} \qquad (6.5)$$

or more succinctly and symbolically:

$$SS = PV \times SR + YP \qquad (6.6)$$

Practically speaking, PV represents the viscosity at a high SR, such as through the bit nozzles, and YP is typically associated with annular flow (LSR).

Mud engineers measure actual viscosities of drilling fluids at two to six different SRs (depending on the well, mud, and application) and then compute the PV and YP.

6.3 ROTARY VISCOMETER

The most common instrument used for viscosity measurements is the Couette viscometer (or viscosimeter). Several well-known manufacturers are established, including the Fann,[4] Chandler,[5] OFITE,[6] Vindum,[7] Rheosys,[8] and others. This type is described as a "true Couette coaxial cylinder rotational ...." viscometer.[9] The speed of the outer rotating

---

[4] Fann Instrument Company, https://www.fann.com/fann/default.html.

[5] Chandler Engineering, http://www.chandlereng.com/.

[6] OFI Testing Equipment, Inc., http://www.ofite.com/.

[7] Vindum Engineering, http://vindum.com/.

[8] Rheosys, LLC, http://www.rheosys.com/index.html.

[9] Description of Fann 35A Viscometer by the Fann Instrument Company, located online at URL: http://www.fann.com/products/Default.aspx?navid = 224&pageid = 439& prodid = FPN%3a%3aJJN5QT4NQ, accessed June 19, 2013.

cylinder is controlled from 3 to 600 RPM run at various RPMs, corresponding to the SRs in reciprocal seconds as shown in the following table:

Cylinder speed (RPM)	Shear rate (s^{-1})
3	5.11
6	10.22
100	170
200	341
300	511
600	1022

The SS imposed on the internal, spring-restrained, and nonrotating "bob" is read out on a dial indicator when the apparatus is run at those speeds. According to industry standards, using an instrument such as the Fann 35A pictured nearby (Fig 6.3), each 1-degree movement of the dial indicator (connected to a "bob" and connecting shaft and restrained by a clock spring) represents an SS of approximately 1 lbf/100 ft^2 (actually

Figure 6.3 Fann 35A. *Courtesy: Fann/Halliburton.*

1.065 lbf/100 ft^2, or 0.511 Pa), and one RPM of the rotor equals an SR of 1.7023 second^{-1}. [10]

Due to the instrument design, the dial reading at 300 RPM corresponds to the viscosity in centipoise at 511 second^{-1}.[11,12]

To convert the other RPM readings to centipoise, the more general conversion formula, with conversion factors suitable for other Fann rotational speeds, is

$$\text{Viscosity} = \frac{\text{dial reading}}{\text{RPM}} \times \frac{511}{1.7} \qquad (6.7)$$

which reduces to

$$\text{Viscosity} = \frac{\text{dial reading}}{\text{RPM}} \times 300 \qquad (6.8)$$

And as mentioned above, at the special case of 300 RPM reduces further to

$$\text{Viscosity} = \text{dial reading} \qquad (6.9)$$

where the "dial reading" is the actual reading from the Fann 35A (or similar) instrument, the "RPM" is the operating speed of the outer continuously rotating cylinder, the constants are conversion factors, and the "viscosity" is the absolute viscosity (μ) in centipoise.[13]

The PV and YP computations themselves are straightforward due to the design of the instruments. The PV is *defined* as the R_{600} dial reading minus the R_{300} dial reading, and the YP is *defined* as the R_{300} dial reading minus the PV.

As an example, consider the following readings from the Fann viscometer (Table 6.2):

For this example data set, the PV and YP calculate to 15 and 65, respectively, and the dial readings and viscosity versus SR (Fann speed) are plotted in Fig. 6.4. Note that the two lines intersect at the 300 RPM point, consistent with the instrument design as described previously.

---

[10] IBID

[11] In metric units the *poise* is the standard unit for viscosity. It is defined as the stress required (dyn per cm^2) to result in velocity (1 cm per second) between layers 1 cm apart. Most oilfield uses are in *centipoise*, 1/100 of a *poise*.

[12] Generally, second^{-1} is pronounced "reciprocal seconds."

[13] Texas Drilling Associates, Drilling Technology & Practices, 2010 ed., pp. 10−15.

Table 6.2 Representative Fann readings and cP

Fann speed (RPM)	Fann dial reading	Absolute viscosity (cP)
600	95	47.5
300	80	80
200	67	100.5
100	45	135
6	4	200
3	3	300
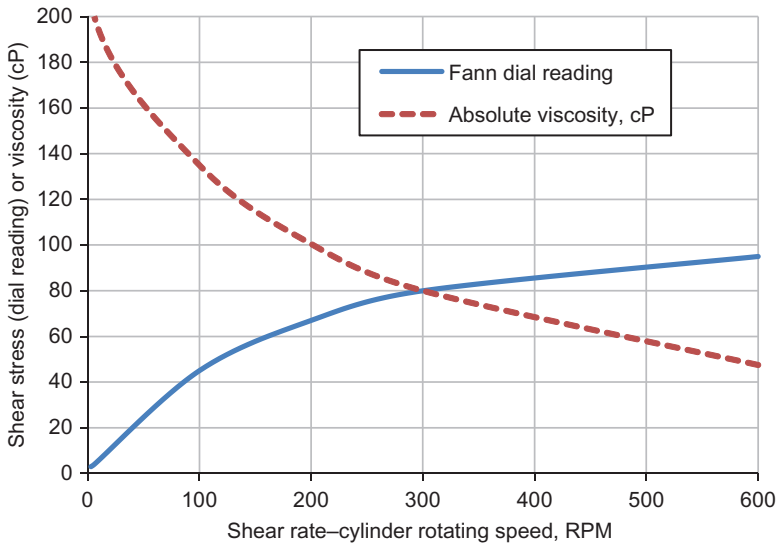
Figure 6.4 Representative Fann (or similar) viscometer dial readings and absolute viscosity. *Courtesy: Texas Drilling Associates.*

6.4 LAMINAR, TURBULENT, AND TRANSITIONAL FLOW

6.4.1 Laminar flow

In laminar flow, named from the Latin *lāmina*, meaning layered, lines of flow remain parallel, and mixing does not occur. Though difficult to achieve in practice, laminar flow is very efficient, with the pressure required to pump a fluid through a pipe (i.e., "pressure loss"), annulus or channel being linearly proportional to the flow rate.

$$P \propto Q \qquad\qquad (6.10)$$

The reader will note that this is a special case of the power law relationship (below) that collapses to this simpler form during laminar flow.

For pressure loss considerations, pressure increases linearly with flow rate (Q). Increasing flow rate 10% will increase pressure loss 10%. It is a very efficient flow regime, but in practice is very difficult to attain, especially with non-Newtonian fluids such as drilling muds.

Conceptually, laminar flow occurs when viscous forces are higher than inertial forces. Hence, in highly viscous fluids, laminar flow can be demonstrated with relative ease, while in fluids with very low viscosity (water, most gases, etc.), it may be difficult to establish fully laminar flow.

A dramatic example of laminar flow can be demonstrated with Karo syrup and food coloring and a suitable concentric cylinder arrangement. If the dye is injected carefully in various radially separated layers of an annulus, the inner cylinder can be rotated multiple turns, stopped, and reversed, and the dye will appear to smear and then "unsmear" or separate. This demonstrates how the layers do not mix.[14]

6.4.2 Turbulent flow

Fully developed turbulent flow, such as occurs through bit nozzles, is characterized by vigorous mixing across the entire cross-sectional area of the flow. One might think of examples such as the motion of high velocity smoke, jet plane exhaust, or the wake behind a high–speed water craft. In experiments where a dye is placed in a clear fluid, it is almost immediately dispersed throughout the fluid (whether liquid or gas) downstream of the injection point.

In turbulent flow, the pressure required to pump a fluid through a pipe, annulus or channel is proportional to the *square* of the flow rate.

$$P \propto Q^2 \qquad\qquad (6.11)$$

For pressure loss considerations, pressure changes as a square of the flow rate (Q) (instead of linear in the laminar case), raised to the second power if you will. Increasing flow rate 10% (or to 110% of the baseline) will increase pressure loss 21% compared to the baseline. Similarly, raising the flow rate

---

[14] Laminar flow demonstration courtesy of University of New Mexico Physics and Astronomy, online at https://youtu.be/_dbnH-BBSNo and accessed June 9, 2018.

by 50% would increase pressure by 2.25 times $(1.50^2 = 2.25)$, and doubling the flow rate would increase pressure by a factor of four.

High velocity flow through properly sized bit nozzles is believed to be fully turbulent, and hence the bit pressure drop realized instantaneously across those bit nozzles is proportional to the square of the flow rate.

Annular and drill pipe flow is most likely transitional in nature as discussed below.

6.4.3 Transitional flow

Transitional flow, as its name implies, is somewhere in-between fully laminar flow and fully developed turbulent flow. In transitional flow, the pressure is proportional to the flow rate raised to an exponential power between 1 and 2. For example, the exponent might be 1.42, 1.86, or any other value between 1 and 2 for a particular fluid and flow rate regime.

Unfortunately, for calculation purposes, the value of this exponent is not at present predictable for transitional flow encountered in drill string components and in annular spaces.

In addition, a rotating drill string and eccentric placement of the drill string within the hole or prior casing adds more unpredictability to the flow characteristic. Related vibration modes of both the drill string and the fluid can add yet more. Hence, relatively inaccurate assumptions are made during design phases of the well.

6.4.4 Reynolds number

For classic Newtonian *pipe* flow, the transition between laminar and turbulent flow is widely reported to be a function of the dimensionless Reynolds number (R_e). For Newtonian fluids flowing in a pipe, R_e itself is classically defined to be

$$R_e = \frac{\rho_{\text{cons}} \times \overline{V}_{\text{cons}} \times D_{\text{cons}}}{\mu_{\text{cons}}} \tag{6.12}$$

where ρ_{cons} is the fluid density (pounds mass per cubic foot); $\overline{V}_{\text{cons}}$ is the average fluid velocity (feet per second); D_{cons} is the diameter of the pipe (feet); and μ_{cons} is the absolute viscosity (pounds mass per feet-second). (The subscript "cons" refers to "consistent units," a term often used in other textbooks and academic works.)

In conventional US Oilfield units, using flow rate instead of the more general velocity, this equation becomes, with conversion factors,

$$R_e = \frac{MW \times Q}{\mu \times D} \times 378.92 \qquad (6.13)$$

(Derivation of the conversion constant is contained in this book's Chapter 9, Appendices, (section 9.1).

where MW is the fluid density (pounds per gallon); Q is the flow rate (gallons per minute); D is the diameter of the pipe or hole (in.); μ is the absolute/dynamic viscosity (centipoise) (or $Fann_{300}$ dial reading); and 378.92 is the conversion factor.

For annular flow, the oilfield version of Reynolds becomes

$$R_e = \frac{MW \times Q \times (d_h - d_p)}{\mu \times \left(d_h^2 - d_p^2\right)} \times 378.92 \qquad (6.14)$$

where d_h is the inside diameter of the hole or prior casing (in.) and d_p is the outside diameter of the inner pipe (in.).

For the annular case, the simple diameter in the case of the hole or pipe is replaced with the hydraulic diameter found by subtracting the OD of the pipe from the ID of the hole.

Addressing Reynolds number calculations for *annular* flow:

According to a publication of the American Petroleum Institute (API 13D), the annular flow Reynolds number should be calculated by substituting the difference between the hole diameter and the pipe diameter (i.e., the so-called hydraulic diameter) for the diameter of the pipe in the classic calculation.[15]

$$R_e = \frac{\rho \times \overline{V} \times (D_{hole} - D_{pipe})}{\mu} \qquad (6.15)$$

or in US Oilfield units as above,

$$R_e = \frac{\rho \times Q}{\mu \times (D_{hole} - D_{pipe})} \times 378.92 \, [\text{SIC in API13D}] \qquad (6.16)$$

$$R_e = \frac{\rho \times Q}{\mu \times (D_{hole} + D_{pipe})} \times 378.92 \, [\text{corrected from API13D}] \qquad (6.17)$$

(Further details of the derivation above are in this book's Chapter 9, Appendices, section 9.2.)

---

[15] API Recommended Practice 13D, revised 2006, p7 and p29, electronic PDF copy.

where, in both cases, D_{hole} refers to the inside diameter of the borehole and D_{pipe} refers to the outside diameter of the pipe in the hole, with either consistent units (feet) or US Oilfield units (inches). The derivation of the conversion factor to enable use of US Oilfield units is found in the Appendix of this book.

Note that in the first form, a cursory look at $R_e = (\rho \times \overline{V} \times (D_{hole} - D_{pipe}))/\mu$. Eq. (6.15) could lead one to conclude that there was a greater indication of laminar flow (smaller R_e) in the bottom hole assembly (BHA) –by–hole annulus than in the drill pipe–by–hole one, a counterintuitive result of the flow becoming more laminar as the cross-sectional area decreased. However, when one takes into account the reduction in cross-sectional flow area with increasing pipe diameter and the corresponding increase in velocity (assuming *flow rate* remains constant), this leads to a more sensible conclusion, visible when the flow rate version in US Oilfield units is examined [Eq. (6.17)].

Nonetheless, and especially when drill string rotation is present (not accounted for in this approach), using a conventional R_e to determine flow regime should be attempted only with much caution and is likely to give unsatisfactory results except in the cases of fresh water or seawater being pumped.

Most college texts report, based on work done by Reynolds and others over the past century, that the transition from laminar to turbulent flow begins at Reynolds number 2100 and is fully turbulent above 4000. However, this is in idealized conditions and is only valid and demonstrated with Newtonian fluids and fixed geometries, which of course we have neither in wellbores except for pumping fresh or seawater or perhaps a base oil. Solids-laden and emulsified drilling muds are not Newtonian. Importantly, we do not have fixed geometries, especially in the case of fully rotating drill strings.

This Reynolds number relationship's measure of laminar or turbulent flow, which is fundamentally a ratio of the inertial forces to the viscous forces, has serious problems with both nonuniform and rotational wellbore geometries and fluids used in wellbores, which are typically very non-Newtonian.

Since the drill string is usually rotating, fully laminar flow rare in practice with today's pump rates and corresponding annular velocities. Years of drilling engineering and field practice suggest that the flow in the annulus (and through the drill string) is at least partially turbulent. This is evidenced by the exponent on flow rate that is used in annular and drill

string friction pressure loss equations. The exponent is almost never 1.0 (fully laminar) nor 2.0 (fully turbulent) but, rather, is almost always in-between the two, typically midrange or slightly more toward the turbulent case. The author has *never* observed the exponent to be 1.0 as would be necessary for laminar flow, at normal operational pump rates.

Ideally, these inaccurate assumptions should be calibrated with wellbore pressure measurements of the actual well while actual drilling operations are being conducted, and calculations reflecting those calibrations made accordingly. Doing so can accurately determine the transitional flow exponent.

6.5 BINGHAM PLASTIC FLOW

Another category of fluid flow is referred to as Bingham Plastic behavior.[16] In Bingham flow, the fluid being investigated or characterized will require a threshold stress to initiate movement. Any SS below this level will *elastically* deform the fluid or surface of the fluid, but removal of the SS will result in the fluid "springing" back to its original position. Once movement or flow is initiated when the SS threshold is reached, then additional SS added will make the fluid flow faster in a linear fashion. Hence, the fluid behavior is that of a straight line, with a positive y–intercept (the threshold stress, formerly referred to as the Bingham stress), and usually a positive sloping line on the Cartesian plot of SS versus SR.

Once past the yield stress, the flow can be either laminar (as would be expected at first plastic movement) or transitional or turbulent in nature.

Modeling of a Bingham fluid is straightforward referring to Fig. 6.5. Bingham fluids are modeled with two parameters, the PV and the yield stress as discussed previously. These take the familiar straight line form of

$$y = mx + b \tag{6.18}$$

where x is the shear rate, m is the slope of the line, b is the y-intercept, and y is the shear stress. Substitution of PV, YP and SS, SR results in

$$SS = PV \times SR + YP \tag{6.19}$$

---

[16] Named after E.C. Bingham, an American chemist and rheologist (who also cocoined the term "rheology"), 1878−1945.
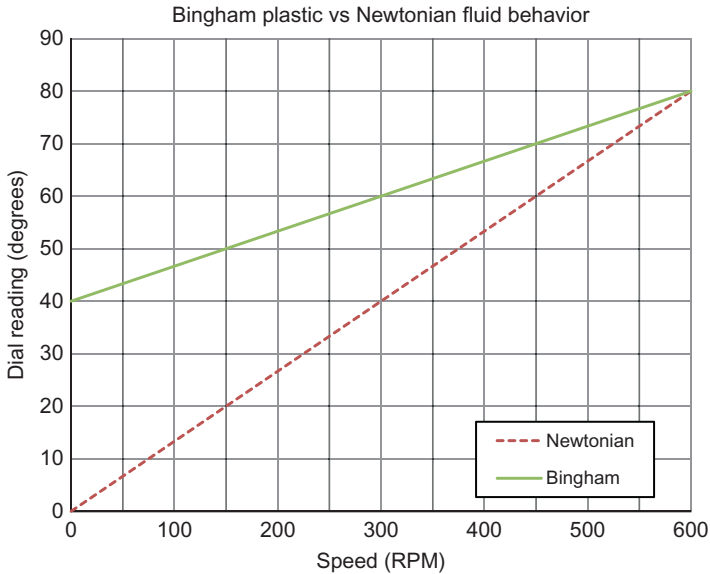
Figure 6.5 Bingham flow contrasted with Newtonian flow.

Importantly, note that Bingham fluids do not ordinarily exhibit a true y-intercept threshold stress (or yield stress) but are elastic before the linear plastic portion occurs.

As importantly, with modern mud systems, the Bingham model is not sufficient for estimating pressure losses downhole, largely due to inaccuracies in determining downhole values of PV and YP as it changes with temperature and pressure and is affected by various contaminants.

For a fully discussion of the equations involved for associated calculation, please see Chapter 3, Hole Cleaning, on pressure drops or other references such as Darley and Gray.[17]

In addition, at very LSRs, for example, 3−6 RPM viscometer readings or lower, the Bingham YP approximation for the LSR viscosity is not reliable, especially for polymer and newer generation mud formulations.

Nonetheless, the Bingham model is very helpful in field quality control checks of the mud system.

[17] H.C.H. Darley, G.R. Gray, Composition and Properties of Drilling and Completion Fluids, fifth ed., Gulf Publishing, 1988.

6.6 POWER LAW AND HERSCHEL−BULKLEY FLUIDS

While Bingham modeling serves as an excellent and time-honored way to conduct quality control testing on muds in a field lab environment, it is not sufficiently accurate to be used to predict downhole pressures, particularly in more critical wells. Those wells might be deemed critical due to their geographic location (near population centers, schools, or offshore for example). They also might be considered critical due to the difficulty of the well itself to successfully drill, perhaps requiring navigation through a narrow pore pressure/fracture pressure "window" or through high-pressure high-temperature subsurface zones.

In such cases, rheologists and other researchers have long noted that drilling muds do not rigorously conform to a Bingham model, so others have been applied.

6.6.1 Simple power law

Power law fluids are modeled with SS τ being proportional to the SR γ raised to some exponent n:

$$SS = k \times SR^n \tag{6.20}$$

The exponent n is commonly referred to as the "flow behavior index" and k is the "consistency index." Those values, in turn, may be computed as functions of PV and YP from the Bingham Plastic model as follows:

$$n = 3.322 \times \log\left(\frac{2 \times PV + YP}{PV + YP}\right) \tag{6.21}$$

and

$$k = 511^{(1-n)} \times (PV + YP) \tag{6.22}$$

Further, the *effective* viscosity (which at any given point on the SS−SR curve is still the slope of the line, or rather, the tangent to the power law curve) may be expressed as

$$\mu_{\text{effective}} = k \times SR^{n-1} \tag{6.23}$$

In the case of simple power law fluids, an extrapolation of high SR behavior back to the zero SR point would appear to give a yield stress. However, true power law fluids do not have a yield stress. Because of this

potential extrapolated *appearance* of a yield stress (a "pseudo" yield stress much like the extrapolation of a Bingham Plastic modeled fluid), these power law fluids are sometimes referred to as *pseudo-plastic* fluids.

6.6.2 Power law with yield stress (Herschel−Bulkley)

While the power law model with suitable parameters will reasonably model mid to high SR regions, it still suffers at the LSR region as it models the SS versus SR curve as going through the origin. Hence, a power law model with the addition of a YP will model lower SRs in a superior fashion. Such a model was developed and is called the Herschel−Bulkley model, given below.

$$SS = SS_0 + k \times SR^n \tag{6.24}$$

or in more customary nomenclature

$$\tau = \tau_0 + k \times \gamma^n \tag{6.25}$$

A further complication is that the yield stress used in the Herschel−Bulkley model may not match that in the Bingham model. According to API 13D, the best value to use is commonly referred to as the "LSR YP" calculated to be

$$\tau_Y = 2 \times \theta_3 - \theta_6 \tag{6.26}$$

This Herschel−Bulkley yield stress should be between zero and the Bingham YP.

Note that if a high polymer water based mud is being contemplated or evaluated, even this LSR YP may not suffice, and in that case, API 13D describes an iterative solution to finding a better value.

This is also discussed later, but the reader should be reminded that the weakness in all of these models, including Herschel−Bulkley, lies in the fact that the mud systems are time-dependent, temperature-dependent, and to some extent pressure-dependent. Hence, high accuracy at best will only be achieved for a limited combination of temperature, pressure, and flow characteristics. The well planner must use these models and his or her experience to temper the results during the planning stages of the well. However, the better solution to these inaccuracies once the well is being drilled is fully discussed in Chapter 5, Pressure Drop Calculations, and is based on calibrating the modeling to the wellbore performance itself.

Comparison of drilling fluid with common rheological models
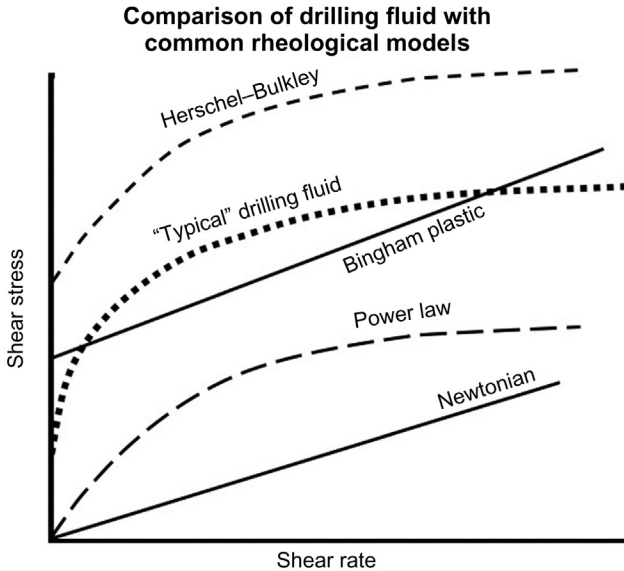
Figure 6.6 Summary illustration of primary oilfield rheology models. Models are intentionally separated for illustration purposes. *Courtesy: Texas Drilling Associates.*

To recap the primary models used for oilfield drilling fluids (Fig 6.6), we have

- Newtonian,
- Bingham plastic,
- Power law, and
- Herschel—Bulkley.

Fig. 6.6 shows compares them graphically. However, note that each model has been separated from the others for clarity. That is, the four models shown in the figure are not different results of modeling the same exact sample of drilling fluid. For example, the fluid modeled with the Herschel—Bulkley model is a more viscous fluid than the Bingham Plastic or Newtonian ones.

Use of these models is covered in more detail in Chapter 5, Pressure Losses, previously.

6.7 GEL STRENGTH

Gel strength measurements, while conceptually similar to a yield stress, are measured in a completely different fashion. Whereas the yield stress (or YP) of a Bingham fluid is the *y*-intercept based on the 300 and

600 RPM Fann (or similar Couette style) rotary viscometer readings extrapolated to the axis in a straight line, the gel strength is measured from a static fluid. Procedurally, the gel strength is measured after 10 seconds, 10 minutes (both required by API 13D), or 30 minutes or some other specified time of the viscometer being static, and then starting the viscometer at the slowest possible speed, either manually or on 3 RPM for most instruments. The SS (measured in degrees deflection of the dial indicator) will for most typical mud systems reach an elastic maximum and then fall back to some smaller value steady state. The maximum value is defined as the gel strength that is measured and reported by the mud engineer.

Importantly, the gel strength should rapidly rise to a value suitable to suspend drilled cuttings, and then be "flat," meaning that there is little or no additional gel strength development with time past perhaps 10 minutes. This helps ensure that when it is time to get the fluid moving again, that it does not require excessive pressure to generate the SS needed to get the fluid moving again.

Gel strength will be discussed later in greater detail.

6.8 TEMPERATURE AND PRESSURE EFFECTS

Modeling the rheology of suspensions such as drilling fluids is further complicated by the response of the fluids to changes in both temperature and pressure. This has been studied and reported extensively, yet only interpolative solutions based on real-well data seem to be able to predict these effects in a reasonable fashion. The specific effects are further detailed in Chapter 2, Bit Hydraulics on downhole properties.

There are several different mechanisms at work with the pressure and temperature-dependent properties. As the liquid phase of the suspension is heated, it generally becomes less viscous. As it is subjected to pressures, it generally becomes more viscous. Similar statements could be made regarding the density of most suspensions.

Chemistry also plays a role as temperature is changed especially with highly alkaline muds. Electrochemistry becomes important as well, as the ionic activity of any electrolyte.

Suffice to observe that while specific (and generally simple) mud formulations have been studied with respect to temperature and pressure effects, generalized accurate predictions of the real mud behavior remains elusive at this writing.

6.9 THIXOTROPIC FLUIDS

Most drilling fluid rheology properties are also time–dependent. That is, the viscosity and/or yield stress (or gel strength) changes with time. This is well known in the case of gel strengths where the mud engineer will commonly conduct gel strength tests with a static time of 10 seconds and then repeat the test at 10 minutes (satisfying the API test requirements) and often also repeat the test at 30 minutes. The result is that the gel strength is higher with longer time periods.

Not as well-known is that most of these fluids also change their SS response to SR over time. That is, measurements of SS could be made at a constant SR, and those measurements would change over time as the fluid sheared. A common method of evaluating whether a fluid is thixotropic or not is to conduct a so-called hysteresis loop test, where the SR is gradually increased from zero to a maximum over time and then gradually reduced back to zero over a similar time. A thixotropic fluid will show significantly different results on the "upsweep" versus the "downsweep" as shown in Fig. 6.7.[18]
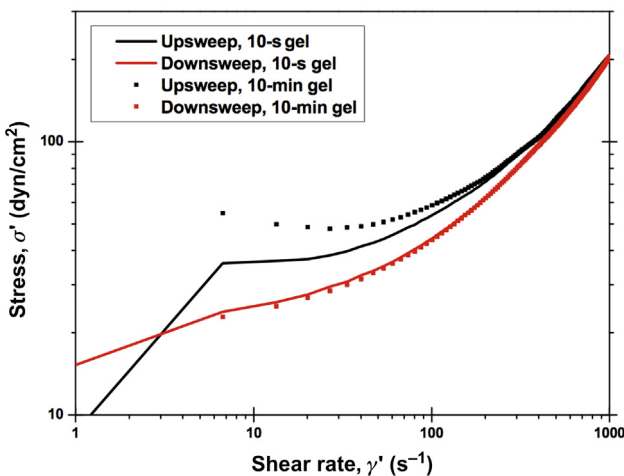
Figure 6.7 Example of thixotropic fluid behavior (Maxey).

[18] J. Maxey, Baker Hughes Drilling Fluids, Thixotropy and yield stress behavior in drilling fluids, AADE-07-NTCE-37, 2007, p. 5.

6.10 OTHER TOPICS

In a book about hydraulics, drilling fluids, rheologies, hole cleaning, and all of their effect on drilling efficiencies, it is sometimes a struggle to place a particular discussion in the best location. The author has chosen to put several items that are sometimes associated with rheology discussions in Chapter 3, Hole Cleaning, as that is where they seem to have the most importance to engineers, company men, and toolpushers. Some of these additional factors include

- velocity profiles,
- slip velocities,
- viscoelasticity,
- elastic modulus,
- viscous modulus, and
- barite sag.

Please refer to Chapter 3, Hole Cleaning, for discussion on these factors.

Downhole Properties

Contents

7.1 INTRODUCTION

A major issue confronting the well–planning engineer, and all personnel after the well is spudded, is that of identifying various parameters to be used in the model(s) of choice in computing wellbore hydraulics. The fundamental problem is that neither the annular geometries involved nor the fluid properties are accurately known downhole, even when high-quality surface measurements are available.

Only steel pipe measurements—internal and external diameters and connection dimensional details of drill string components or casing strings—can be accurately measured as inputs. In addition, system pressures or Δp can be measured, either via the standpipe only or with the enhancement of pressure while drilling (PWD) tools, to help back-calculate the

annular pressure component of the total friction pressure during circulation. Back-calculations can provide fluid rheology data for input into computer software that can model many different parameters to better understand limitations such as maximum and minimum equivalent circulating density (ECD) to fit the available pore pressure and fracture gradient window.

7.2 MEASUREMENT LOCATIONS

Surface fluid property measurements, while primarily useful for quality control purposes, if used uncritically beyond that, can lead to large errors in predicted or actual downhole pressures. Relationships and predictive equations that use surface properties (plastic viscosity—PV, yield point—YP, mud weight—MW, etc.) tend to understate annular pressure drops, overstate bit pressure drops, and the effect on drill string pressure losses is somewhat unpredictable, though internal drill string pressure losses may be marginally better typically than annular relationships.

Surface mud measurements on a rig site are typically conducted at atmospheric pressure and at either room temperature, 120°F, or a higher specified temperature, depending on the test protocol. Higher pressure and temperature experiments may be conducted, but typically these must be done in shore-based research laboratories and suffer from not being contemporaneous with the progress of the drilling well.

Downhole fluid property measurements are not typically available for direct measurement of fluid rheological, intrinsic, or extrinsic properties. Rather, environmental variables are measured, such as temperature and pressure, and the properties may sometimes be inferred from those direct downhole environment variables.

Similarly, most chemical properties downhole are not directly measured or inferred, though some electrical properties are measured when logging the well.

7.3 TEMPERATURE EFFECTS

In most drilling areas, temperature of the earth increases with depth, usually in the range of 0.8—3.0°F per 100 ft, most commonly around 1.5°F per 100 ft.

Drilling fluid liquid densities change with temperature.

For oils, the base density may change from type to type (and indeed even for the same type such as diesel if the product is from a different hydrocarbon source or refinery), but the density versus temperature relationships are similar as shown below (for constant pressure)[1].

For water, the relationship is similar, as shown below (Figs. 7.1 and 7.2).

Pressure also affects density of commonly used drilling fluids, increasing the density with increasing pressure.

For water-based muds as well as noncritical wells industry practice has been to more or less ignore this effect as it was fairly well offset by the decrease in density with temperature.

For oil-based and synthetic-based fluids, especially for critical wellbores, both the temperature effect and the pressure effect can be quite large, and in critical wells care must be taken to know the drilling fluid density under simultaneously high pressures and high temperatures.
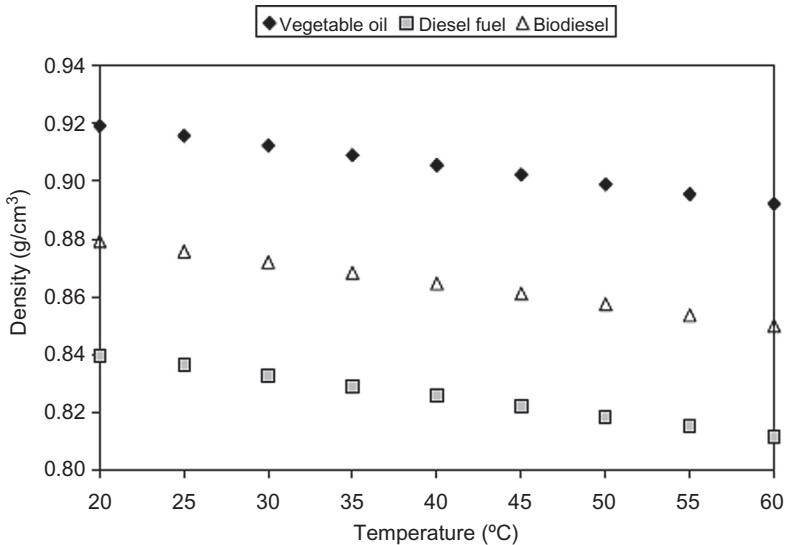
Figure 7.1 Density versus temperature for investigated oils. *After I. Nita, et al., Study of density and viscosity variation with temperature for fuels used for diesel engine, Ovidius Univ. Ann. Chem. 22 (1) (2011) 59.*

---

[1] I. Nita, et al., Study of density and viscosity variation with temperature for fuels used for diesel engine, Ovidius Univ. Ann. Chem. 22 (1) (2011) 59.

Water density vs temerature
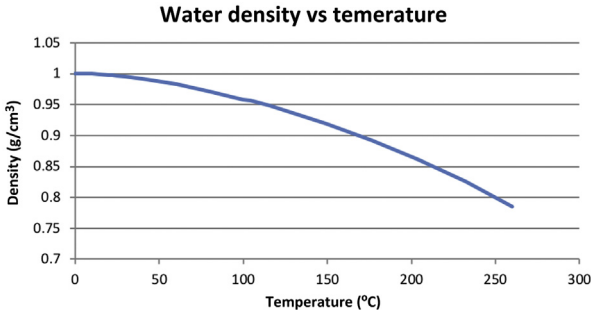
Figure 7.2 Water density versus temperature.

This can usually be obtained from the drilling fluid provider, or even better, with a direct measurement while drilling (MWD) or pressure while drilling (PWD) measurement that will usually be available for critical wells.

Note that density may also change over time, whether circulating or static. For the circulating case, changes in density may be from an influx of fluid from the formation. If the influx is slow and is salt water, this change may be difficult to accurately and quickly detect.

If the fluid is static, the liquid phase of the mud may leak into the formation, resulting in a higher density, at least across from the formations where the seepage losses are occurring.

Further, when the fluid is static, the temperatures will in most parts of the wellbore be changing—moving back toward the geothermal gradient compared to the altered gradient of the circulating wellbore. This change of temperature can either increase or decrease the localized density depending on the direction of the change while static. In very general terms, the hottest circulating part of the wellbore is usually around one-third of the well depth up from the bottom. Hence, if the well becomes static, the lower one-third tends to heat up and the upper two-thirds tend to cool down (see the associated discussion).

Note that two other issues can mask the effect of temperature and pressure or render those predictions inaccurate. The first problem is the surface density measurement itself. Most mud engineers (not generally degreed engineers) will use an unpressurized mud cup to weigh the mud. While simple to use, it is not very accurate depending on both the mud and the skill of the mud engineer. It must be calibrated at or around the

MW being measured as its calibration does not hold true from the low to the high end of its range.

Second, there are often entrained microbubbles of air or formation methane or other gases in the mud at the surface. The gas may eventually come out of the mud naturally, and mud "degassers" can assist, but even a small amount of gas can yield erroneous mud engineer surface density measurements.

One solution to the second problem above is to employ the use of pressurized mud balances, which work by compressing the gas bubbles to a size where their effect on mud density measurements may be effectively ignored.

Most liquids exhibit a reduction in shear stress versus shear rate (or more commonly "viscosity") as temperature increases. The degree of temperature "thinning" varies substantially with different base liquids (water, oils, synthetics) and with viscosity modifying additives used.

As can be seen, both (brine) water and assorted oils exhibit this reduction in viscosity with temperature, but to a varying degree[2].

As seen, temperature also affects the densities of various base liquids. The temperature effect is almost universally found to decrease the fluid bulk density as the temperature is increased. This effect is typically both predictable and repeatable for a given fluid.

Increasing temperature decreases viscosity. Increasing temperature decreases density.

As in the case of density described above, viscosity of common drilling fluids is also affected by Temperature and pressure. In general terms, higher temperatures will lower viscosity of a fluid, and higher pressures will raise the viscosity. These may be offsetting but more commonly in oil and synthetic fluids are not, depending on the pressure and thermal gradients with depth (Fig. 7.3).

This is illustrated in Fig. 7.4. The investigation was for a diesel at four different temperatures. The higher the temperature, the lower the effect of pressure on the viscosity.

Nor is this effect limited to the base fluids. Ibeh experimentally showed and reported that pressure and temperature affect viscosities, both PV and YP, which are commonly used for quality control purposes in drilling fluids, as well as used for modeling. Some of Ibeh's results

---

[2] B.S. Massey, Mechanics of Fluids, second ed., Van Nostrand Reinhold Company Ltd, London, 1970, p. 17.

Viscosity of common liquids variation with temperature
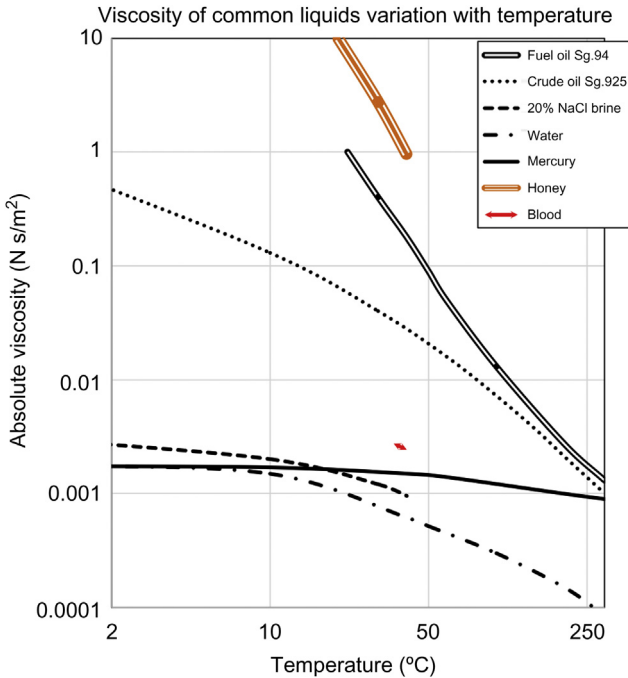
Figure 7.3 Absolute viscosity of common fluids.

showing the effects of temperature and pressure, on an 18 ppg representative oil–based mud, are shown in Fig. 7.5.

Without belaboring the point, it is clear from the above that both temperature and pressure have huge effects on at least this oil-based mud.

As with all drilling technology, new developments are certainly encouraging. Recently, two notable developments have been used.

The first is the use of micronized barite as a weighting material. This barite is typically about 20 times smaller particle size than conventional barite. Rheology of the micronized particle size barite muds is significantly lower than that of comparable MW mud using conventional barite, perhaps due to less viscosity required to suspend the smaller sized barite.

Further, synthetic-based muds have been developed whose viscosities are not nearly as affected by temperature. This can be especially important in either high temperature high pressure (HTHP) wells or deepwater
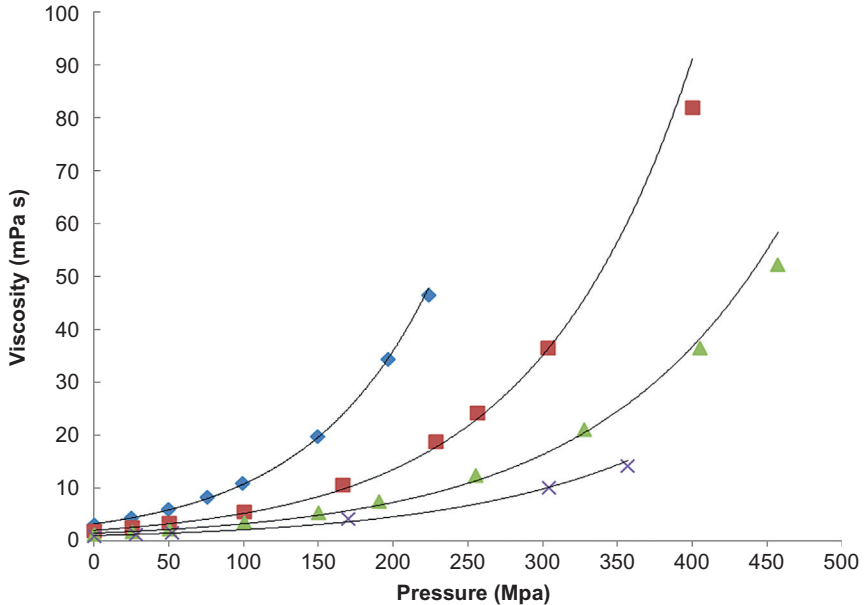
Figure 7.4 Variation of viscosity with pressure [diamonds = 298K (77°F), squares = 323K (122°F), triangles = 348K (167°F), X = 373K (212°F)][3].

wells. The improvement realized with these newer formulations is shown in Fig. 7.6.

Note additionally that this effect is difficult to predict and may not be repeatable. That is, a change in viscosity that occurs as the fluid is heating up may not "repeat" when cooling back down—a hysteresis effect of sorts, except not a repeatable hysteresis.

Even with the best data, predictions suitable for critical wells can be elusive. In a recent Gulf of Mexico deepwater well, a modern estimate of downhole ECD in the annulus bottom hole was found to be in error by 0.2−0.4 ppg when measured with a PWD tool. This might not be overly worrisome or troublesome in most wells, especially if the rig-site personnel were closely monitoring the well, but in critical ones where the window between pore pressure and fracture pressure is narrow, this error could be catastrophic.

[3] C. Schaschke, et al., Density and viscosity measurement of diesel fuels at combined high pressure and elevated temperature, Processes 1 (2013) 30−48. accessed 05.04.15.
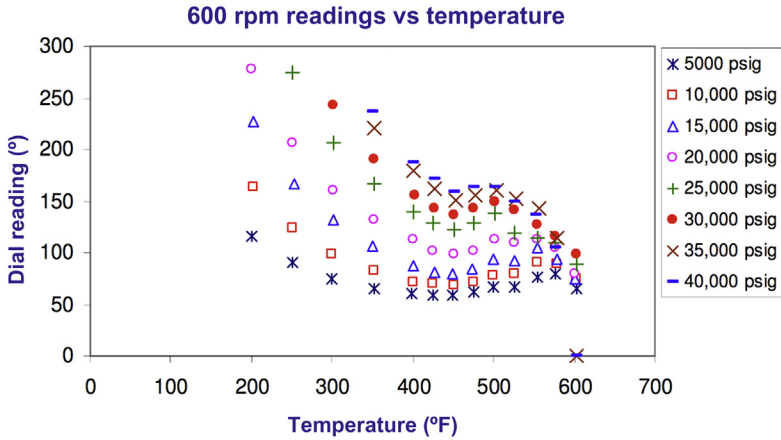
Figure 7.5 Viscosity of 18.0 ppg MO based mud affected by both temperature and pressure. *MO*, mineral oil. *After C.S. Ibeh, Investigation on the Effects of Ultra-high Pressure and Temperature on the Rheological Properties of Oil-based Drilling Fluids (Masters thesis), Texas A&M University, December 2007[25].*

With such uncertainty surrounding both the rheology and the density of non-aqueous drilling fluids (NADFs) (and even water based muds (WBMs)) downhole, for critical wells it is highly recommended to utilize downhole real-time or recording PWD tools. In the absence of PWD, careful monitoring and analysis of standpipe pressures may suffice.

Drilling and completion (D&C) fluids' temperature often do not match geothermal gradients in the well. As D&C fluids are circulated and are subject to erratic and varied duration static periods for tripping, logging, installing casing, waiting on cement, unscheduled events that cause flow to stop, equipment problems and other down times. Even with current computing horsepower available, the complexities of accurately predicting these effects may be too difficult for relatively simple spreadsheet methods (though "goal seeking" functions help enormously, especially if some calibrating data is available).

---

[25] C.S. Ibeh, Investigation on the Effects of Ultra-high Pressure and Temperature on the Rheological Properties of Oil-based Drilling Fluids (Masters thesis), Texas A&M University, December 2007
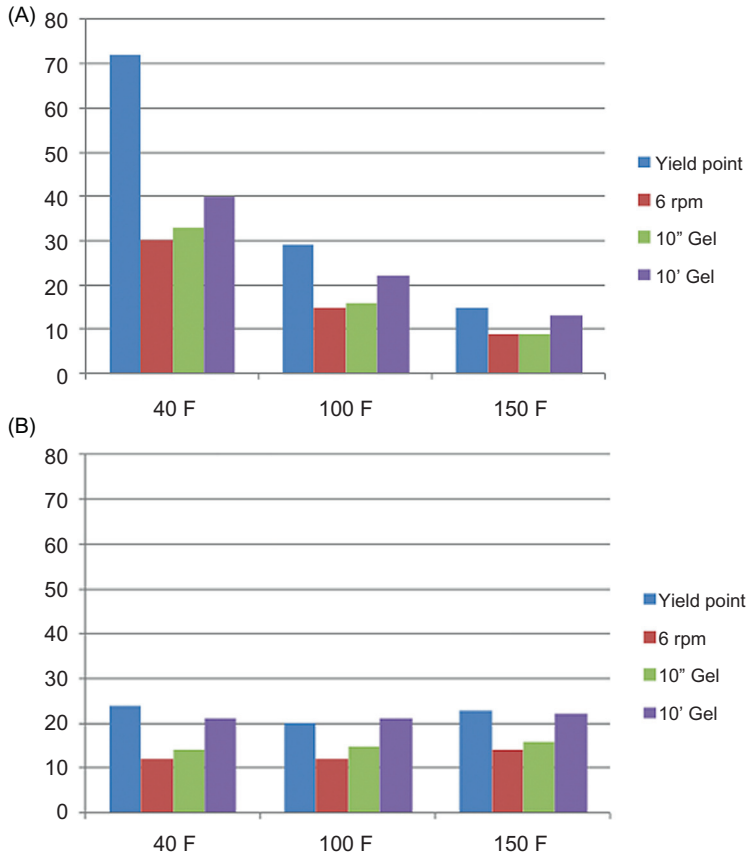
Figure 7.6 Typical NADF response to temperature and a relatively temperature-independent formulation. (A) Conventional synthetic-based NADF and (B) temperature-independent synthetic-based NADF. *Courtesy: F. Growcock, A. Patel, The revolution in non-aqueous drilling fluids, in: AADE-11-NTCE-33[4].*

More sophisticated computer models are designed to make these pre-dictions more accurately, usually with iterative numerical solutions and variable input data or ranges for specific conditions.

Recently, Sweatman, Mitchell, and Young[5] reported on many of these complexities recently, due to a growing need for accurate modeling in deepwater and in HTHP wells.

---

[4] F. Growcock, A. Patel, The revolution in non–aqueous drilling fluids, in: AADE-11–NTCE-33, 2011.

[5] R.F. Mitchell, R. Sweatman, G. Young, Modeling reveals hidden conditions that can impair wellbore stability and integrity, in: SPE/IADC 163476, SPE/IADC Drilling Conference, The Netherlands, March 5–7, 2013.
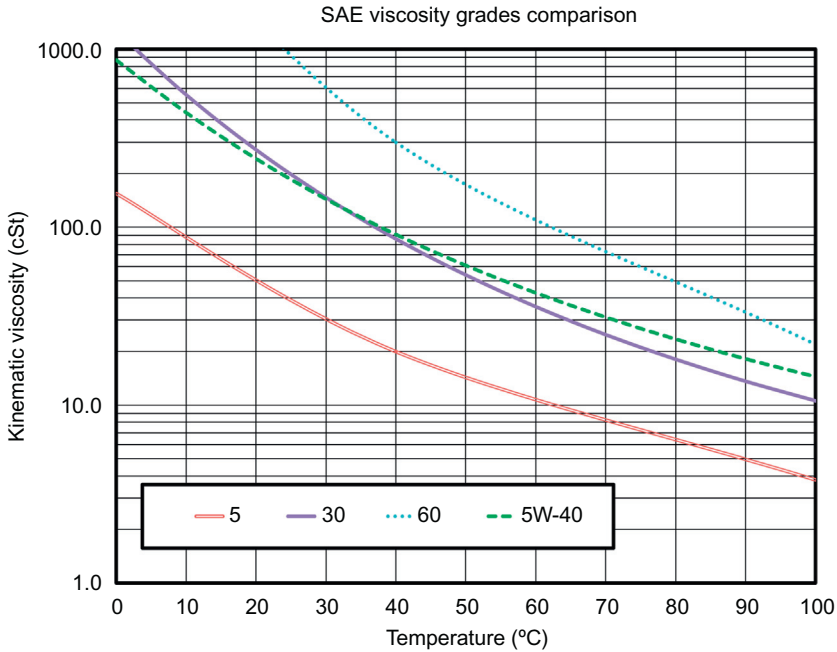
Figure 7.7 Single and multigrade viscosities.

Note: A common misconception exists regarding multigrade engine oils (SAE 0W-20, 5W-30. 10W-40, etc.) largely due to the way they are labeled. The misconception is that a multigrade oil will increase in viscosity with increasing temperature.

The reality is that the labeling reflects the equivalent viscosity grade at a low and high temperature. As an example, a 5W-40 grade oil would exhibit viscosity at low temperature similar to a 5 grade oil at that low (winter) temperature, and at high temperature, the same oil would exhibit a viscosity similar to a 40-weight oil at that high temperature. However, the viscosity of the 5W-40−weight oil at the high temperature would still be lower than at the low temperature as shown in Fig. 7.7 (after KEW[6] and Bennett[7]).

---

[6] M. Williamson, KEW Engineering, Ltd., U.K., 2018. Available from: <http://www.kewengineering.co.uk/Auto_oils/oil_viscosity_explained.htm> (accessed 27.08.18).

[7] Glenn Bennett Corp. Available from <https://www.glennbennettcorp.com/hubfs/PDF/Viscosity-Reference.pdf>, 2018 (accessed 27.08.18).

Since properties of fluids commonly used as drilling muds vary with temperature, it naturally becomes important to determine the temperature profile as the mud circulates from top to bottom and back to top again. The two classes of determination of temperature would be by computer modeling and by direct measurement of the temperature.

The American Petroleum Institute (API) Recommended Practice 13D (June 2006) addresses this (the temperature prediction) somewhat. It recommends two computer modeling techniques that can be "easily programmed in a spreadsheet program" and gives satisfactory results for non-critical well situations on temperature prediction over ranges that they have been calibrated[8,9].

Wells that may be thought of as critical, however (e.g., they carry a *higher risk* of well control or other issues and/or a *higher consequence* of a usually normal risk), will likely need more sophisticated thermal modeling in order to determine the temperature profiles to then calculate changes in hydrostatic pressures (both ECD and equivalent static density—ESD). These temperature profiles, coupled with significant changes in density and flow rheologies downhole, can lead to nonobvious results such as changing an apparent overbalanced condition into an underbalanced condition leading to flow if not dealt with appropriately.

From one of the two references in the RP13D publication, the important variables are the surface temperature, the bottom hole temperature, and the typical change in temperature as the well is deepened. This increase in temperature with depth is usually in the range of 1 or 2°F per 100 ft (of vertical depth), though some regions exhibit changes in temperature with depth that are slightly lower or higher than these values. This change in temperature per 100 ft of depth is referred to as the geothermal gradient. Having knowledge of any two of the three primary variables makes prediction of the third relatively straightforward.

There is a slight complication offshore, where in deeper water the temperature gradient of the water column is to get colder as the depth of the ocean is reached, sometimes being just above freezing on bottom (at the mud line). The relationship between surface temperature, the

[8] I. Kutasov, A. Targhi, Better deep-hole BHCT estimations possible, Oil & Gas J. (May, 1987), Vol. 85.
[9] I. Kutasov, Method corrects API borehole circulating-temperature correlations, Oil Gas J. (Vol. 100), (Jul. 2002). p. 47.

geothermal gradient, and the bottom hole temperature may be reasonably calculated.

As described in API RP13D, the temperatures may be modeled with the equations below for determining geothermal gradients, bottom hole circulating temperature, and bottom hole static temperature, respectively:

$$t_{gw} = \frac{(T_{bhs} - T_0)}{(D_{tvd} - D_w)} \tag{7.1}$$

$$T_{bhc} = -102.1 + \left[3354 \times t_{gw}\right] + \left[\left(1.342 - 22.28 \times t_{gw}\right) \times T_{bhs}\right] \tag{7.2}$$

$$T_{bhs} = T_0 + t_{gw} \times (D_{tvd} - D_w) \tag{7.3}$$

where

D_{tvd} is the true vertical depth;

T_s is the surface temperature;

T_{bhc} is the bottom hole circulating temperature;

T_{bhs} is the bottom hole static temperature;

D_w is the water depth (offshore), or 0 for land wells;

t_g is the geothermal gradient;

t_{gw} is the geothermal gradient offshore, adjusted for water depth; and

T is the surface temperature below weather affected zone (50 ft depth recommended by 13D).

These equations work reasonably well when two of the three primary variables are available by direct measurement. They work less well when the parameters must be assumed from a secondary source or estimate. However, for most production wells, which have the advantage of one or more exploration and productions wells nearby where the temperature data has already been obtained, they are quite satisfactory for estimating both bottom hole circulating temperature, and bottom hole static temperature.

These temperature estimates should also be compared to logging while drilling (LWD) and wireline logging temperatures where possible, in order to confirm (and ultimately refine) the results.

Importantly, note that predicting temperature, while a necessary part of improving downhole hydraulic modeling is not sufficient for doing so, due the cautions with respect to viscosity and density discussed previously and below.

7.4 MUD LINE TEMPERATURE OFFSHORE

Offshore, mud line temperature must be estimated until data is available from drilled wells. API 13D[10] provides a relatively convenient process to estimate mud line temperature. It takes the form of two empirical equations with water depth as the variable in each, one for use up to 3000 ft water depth and the second for use below that point.

For water depths up to 3000 ft:

$$T_{ML} = 154.43 - 12.214 \times \ln(D_W) \qquad (7.4)$$

and for water depths greater than 3000 ft:

$$T_{ML} = 41.714 - 0.0003714 \times D_W \qquad (7.5)$$

Considerable data is now available from various sources worldwide that can serve as a calibration to the API 13D method of estimating mud line temperature. That method assumes that the mud line is in equilibrium or near equilibrium with the ocean bottom. Research over the decades has shown that in deeper waters there is a relatively predictable temperature gradient with depth of the water column down to a depth of $3000-4000$ ft, and the water temperature is relatively constant at an annual average of "around 40°F (4.4°C) that prevails to abyssal depths" as one article phrased it[11] (Fig. 7.8).

API 13D also gives an equation of the following form for use in predicting the combined effects of pressure and temperature on common base oil or synthetic fluids or brines[12].

$$\rho_{dh} = \left[\left(a_1 + b_1 \times P + c_1 \times P^2\right) + \left(a_2 + b_2 \times P + c_2 \times P^2\right) \times T\right] \qquad (7.6)$$

where

ρ_{dh} is the density of the base oil, synthetic or brine;
P is the downhole pressure;
T is the downhole temperature; and
$a_1, b_1, c_1, a_2, b_2, c_2$ are the pressure and temperature coefficients.

[10] Rheology and hydraulics of oil-well drilling fluids, in: API Recommended Practice 13D, fifth ed., American Petroleum Institute (API), June 2006, p. 21.

[11] F. Joseph, et al., Geothermal Gradients and Subsurface Temperatures in the Northern Gulf of Mexico, in: Search and Discovery Article #30048. <http://www.searchanddiscovery.com/documents/2007/07013forrest/>, 2007 (accessed 27.08.15).

[12] Rheology and Hydraulics of Oil-Well Drilling Fluids, API Recommended Practice 13D, Fifth Edition, June 2006.
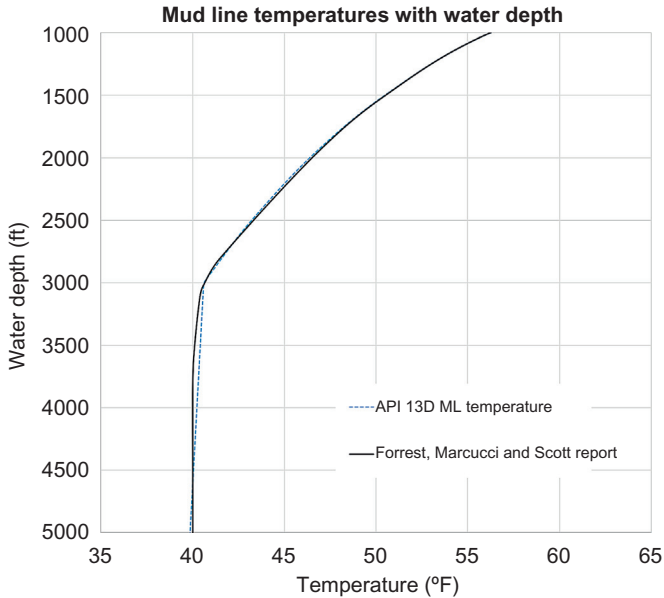
Figure 7.8 Mud line temperature versus water depth.

Table 7.1 Representative pressure and temperature coefficients for Eq. (7.6)

	Pressure coefficients			Temperature coefficients		
	a_1 (lbm/ gal)	b_1 (lbm/gal/ psi)	c_1 (lbm/gal/ psi^2)	a_2 (lbm/gal/ °F)	b_2 (lbm/gal/ psi/°F)	c_2 (lbm/gal/ psi^2/°F)
CaCl$_2$ (19.3 wt.%)	9.9952	1.77E − 05	6E − 11	− 2.75E − 03	3.49E − 08	− 9E − 13
Mineral oil	6.9912	2.25E − 05	− 1E − 10	− 3.28E − 03	1.17E − 07	− 3E − 12
Internal olefin	6.8358	2.23E − 05	− 2E − 10	− 3.39E − 03	1.12E − 07	− 2E − 12
Diesel	7.3183	5.27E − 05	− 8E − 10	− 3.15E − 03	7.46E − 08	− 1E − 12
Paraffin	6.9692	3.35E − 05	− 5E − 10	− 3.46E − 03	− 1.64E − 08	2E − 13

These pressure and temperature coefficients are given in Table 7.1, again after API[13]. Additional coefficients for this generalized equation may be found in other industry sources[14].

---

[13] ibid.

[14] M. Zamora, et al., Study on the volumetric behavior of base oils, brines, and drilling fluids under extreme temperatures and pressures, in: SPE 160029, SPE Drilling & Completion, September 2013.
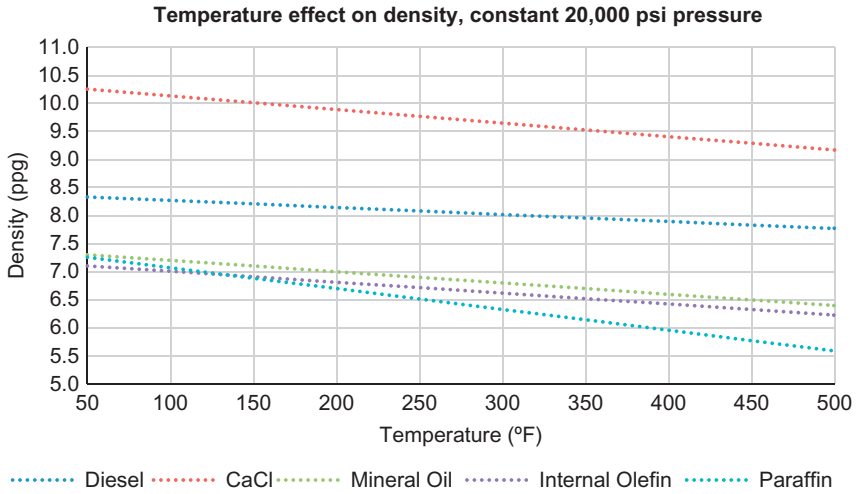
Figure 7.9 Temperature effect on density.
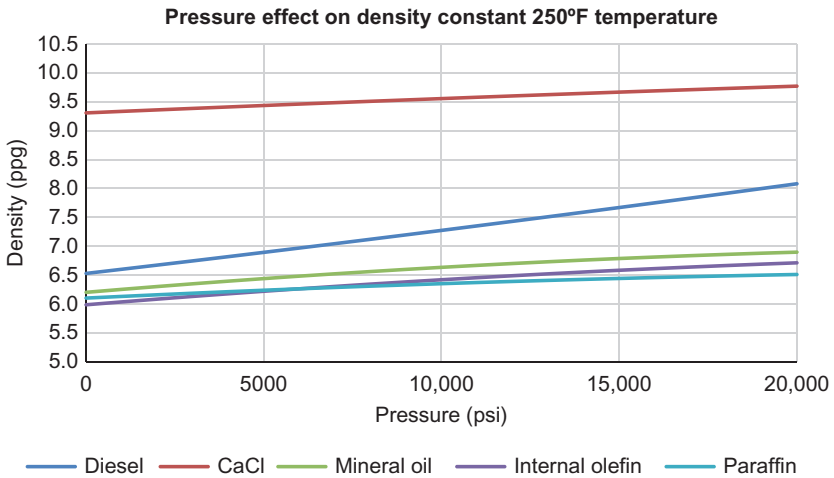
Figure 7.10 Pressure effect on density.

To illustrate, using the API technique, representative temperature effects and pressure effect are shown in Figs. 7.9−7.11.

Note that implicit in the above discussion is that a reasonably accurate model or measurements of temperature are needed for critical wellbores.

FIELD
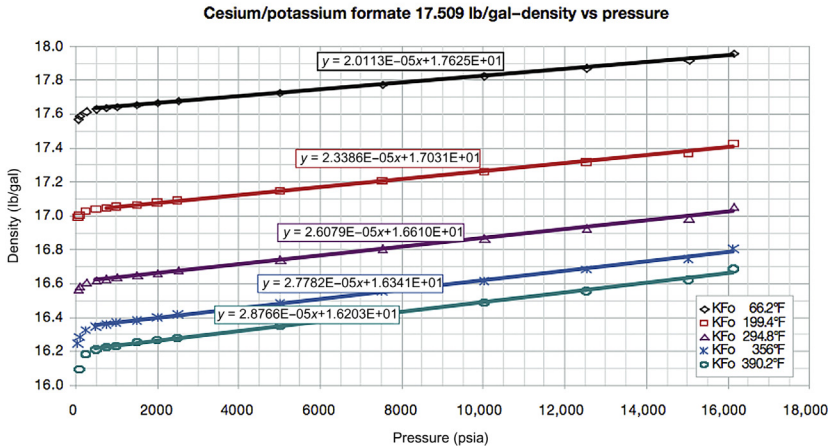
Figure 7.11 Density of cesium formate at different temperatures versus pressure. *Courtesy: Cabot Specialty Fluids, Formate technical manual, in: Chemical and Physical Properties, Version 9, 01/2013[15].*

Depending on the well type, the circulating system rates and geometries, and geothermal gradient one can have opposite effects on density downhole even with the same mud system. This was thoroughly analyzed, reported, and graphically depicted in a recent SPE paper by Zamora et al.[16]. The modeled temperature profiles and their effects on density for a deepwater well case are shown below from that paper[17] (Fig. 7.12).

In a somewhat different comparison graphic in that same study[18], the variation in ESD versus depth is shown for three drilling mud formulations for two different wells, one a land HTHP well and the second a deepwater well (Fig. 7.13).

Importantly, the combination of drilling rate and hole cleaning efficiency can also significantly affect downhole density. Aldea et al. report that the contribution of cuttings to density in the annulus can vary from around 1.0 ppg to over 2.5 ppg[19]—certainly of extreme concern for critical wells with limited fracture strength.

[15] Cabot Specialty Fluids, Formate technical manual, in: Chemical and Physical Properties, Version 9, 2013.

[16] M. Zamora et al., 2013, op. cit.

[17] ibid.

[18] ibid.

[19] C. Aldea, Hole cleaning: the Achilles' heel of drilling performance?, in: AADE-05-NECE-29, April 5–7, 2005.
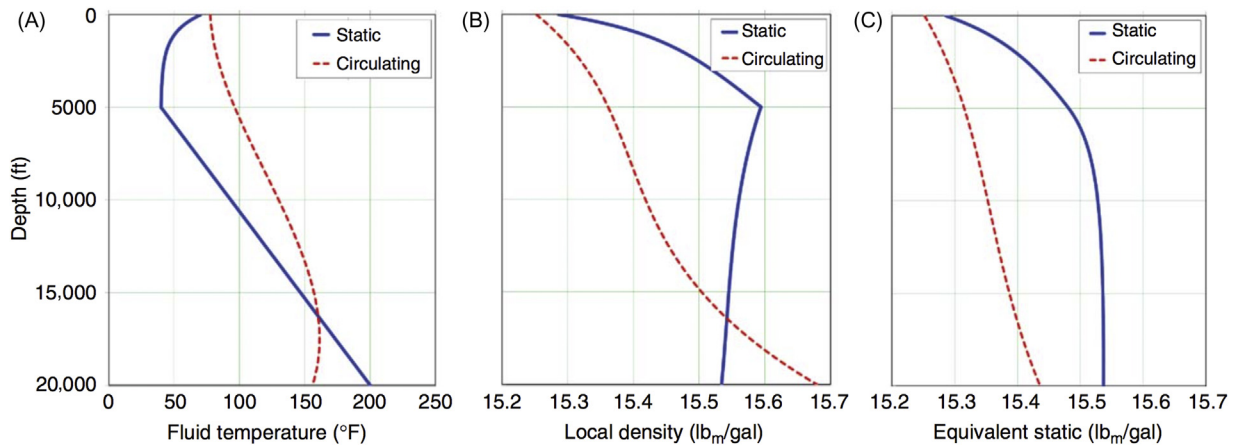
Figure 7.12 Variation in downhole (DH) temperature and pressure profiles for a deepwater case.
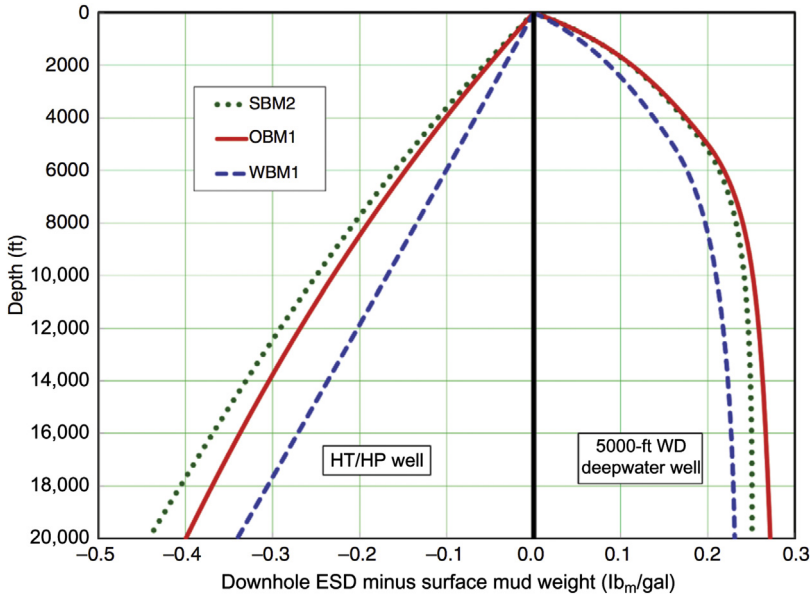
Figure 7.13 Downhole ESD profiles for three drilling fluid systems for an HP/HT and a 5000 ft deepwater well. *ESD*, equivalent static density.

7.5 DYNAMIC OR TRANSIENT EFFECTS

When the well is neither circulating nor has been static for a long time, transient effects can also be modeled. (This is especially true and commonly modeled for cementing operations, as shown in such a model demonstrated by Mitchell et al.[20] in Fig. 7.14.)

In deepwater drilling, the temperature variation with both depth and time transients is even more problematic, owing to the relatively cold–water column above the mud line. In Fig. 7.15 the temperature profiles measured in a deepwater well are shown after an 8–day circulation followed by shut-in for 9 days, with the undisturbed condition modeled.

Note that for wells deemed of critical importance or higher risk, thermal modeling software packages and services are available commercially to assist the well design team in performing those critical analyses.

---

[20] R.F. Mitchell, R. Sweatman, G. Young, Modeling reveals hidden continuous that can impair wellbore stability and integrity, in: SPE/IADC 163476, presented at the 2013 SPE/IADC Drilling Conference and Exhibition, Amsterdam, The Netherlands, 2013.
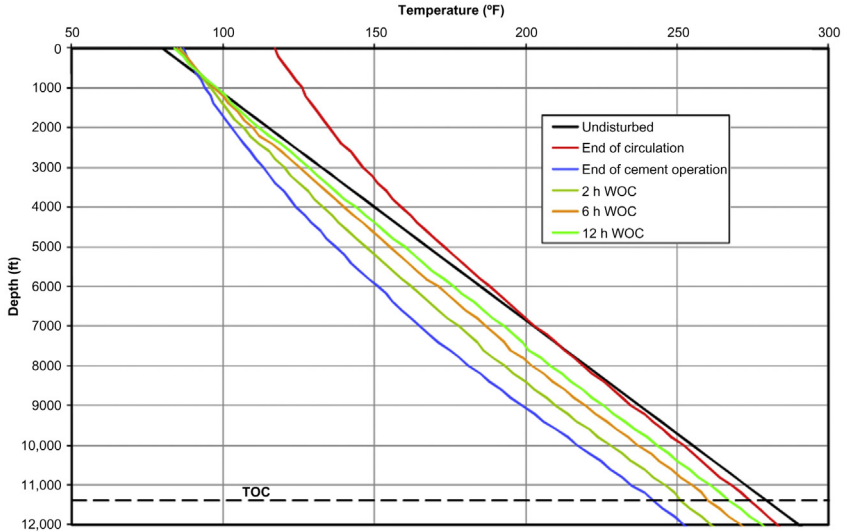
Figure 7.14 Transient, circulating, and transient temperatures. *WOC*, waiting on cement; *TOC*, top of cement.
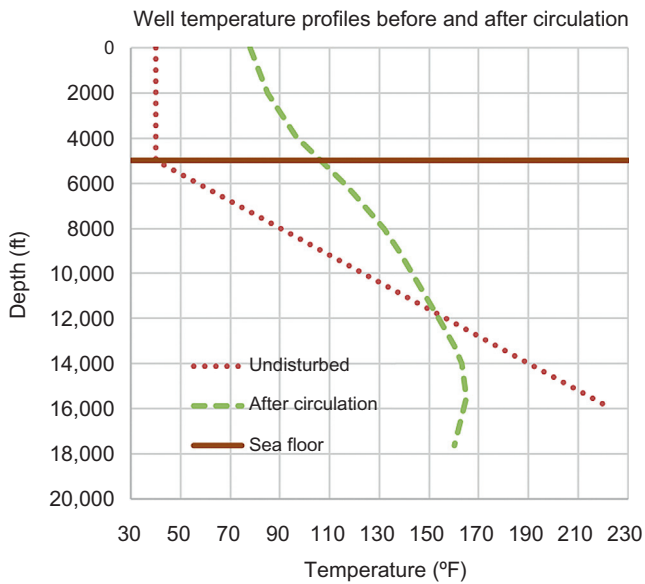
Figure 7.15 Deepwater well temperatures after an extended circulation time. *Courtesy: IADC.*

7.6 PRESSURE EFFECTS

Pressure also affects the viscosity and density of common drilling fluid base liquids, though oil–based products are typically more affected by this than are water-based muds. As pressure increases, viscosity increases. As pressure increases, density increases.

A University of Tulsa study found that for base oil they tested (n–paraffin based oil) the pressure effect on density was very predictable under isothermal conditions[21].

The combined effect of temperature and pressure on viscosity and density may be experimentally determined but may prove elusive to model in the absence of data. The Tulsa study found, for example, with the n–paraffin oil, that isothermal compressibility was not constant for all temperatures.

Tulsa further investigated the temperature and pressure effects on a drilling fluid, composed of the n–paraffin oil, water, and other mixing agents such as emulsifiers. They found a similar, yet not identical, relationship between pressures, temperatures, and densities. Ultimately, the study concluded that if suitable pressure volume temperature (PVT) lab data was available, that downhole density prediction was reasonable. In their particular study, the predictive or correction equation was reported as

$$\rho(P, T) = \left(A \times T^2 + B \times T + C\right) \exp[(D \times T^2 + E \times T + F) \times P] \quad (7.7)$$

where

$A = -5.357\text{E} - 06 \text{ ppg}/^\circ\text{F}^2$,
$B = -1.267\text{E} - 03 \text{ ppg}//^\circ\text{F}$,
$C = 8.717 \text{ ppg}$,
$D = 9.452\text{E} - 11 ^\circ\text{F}^2/\text{psig}$,
$E = -1.530\text{E} - 08 ^\circ\text{F}/\text{psig}$,
$F = 4.192\text{E} - 6 \text{ psig}^{-1}$.

While certainly cumbersome, this was reported to be accurate to within 0.25% for all pressures and temperatures tested, as shown in the nearby comparison graph (Fig. 7.16) from the same study. (The study did not comment on whether the modeling error was real or an artifact of the measurements.)

In addition, it was not clear from the Tulsa measurements whether one could *predict* the behavior of either the base liquid or whole drilling fluid in the absence of PVT data—for example, if a new mud were being

[21] Miska, et al., Advanced Cuttings Transport Study, 2004, pp. 117−123.
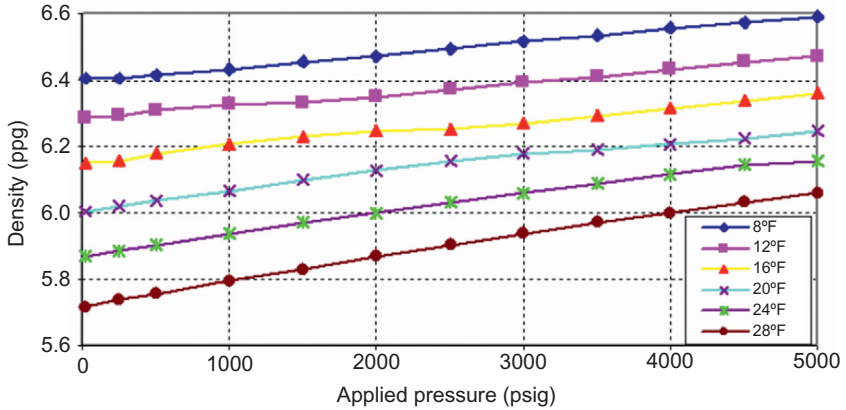
Figure 7.16 Effect of pressure on density of *n*-paraffin oil for different temperatures[22].
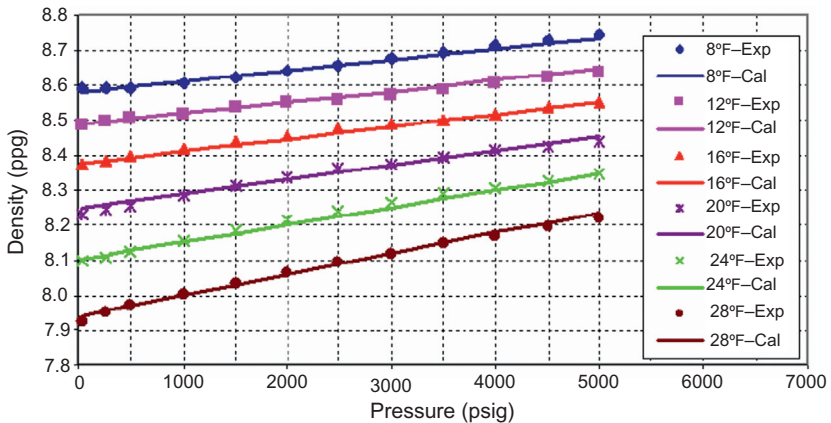
Figure 7.17 Experimental versus modeled density as a function of pressure for a *n*-paraffin drilling fluid emulsion at various temperatures. *After Miska, Advanced Cuttings Transport Study, p. 123* [23].

used or the composition of the drilling fluid varied somewhat from the drilling fluid that actually was tested (Fig. 7.17).

In a real wellbore as opposed to a laboratory, the density and the temperature will be changing with depth simultaneously. Various possibilities for a 30,000 ft well and a range of temperature gradients and MWs are shown in the nearby tables. For the onshore case unadjusted pressures as a function of depth and surface MW are given Table 7.2. Downhole

[22] Miska, et al., Advanced Cuttings Transport Study, 2004, p. 119.
[23] Miska, et al., Advanced Cuttings Transport Study, 2004, p. 123.

temperatures are given as a function of depth and geothermal gradient are tabulated in Table 7.3.

These geothermal gradients can vary sharply from one geographic location to another, as shown in the map of measured bottom hole temperatures in Texas at 12,000 ft depth below (Fig. 7.18).

Table 7.2 Pressure versus depth for various mud densities
Hydrostatic pressures with depth and mud weight

(units are feet and pounds per gallon, respectively)

Depth	Mud weight						
	8.3	8.6	9.6	12.0	15.0	18.0	19.2
1	0.4337	0.4472	0.5000	0.6240	0.7800	0.9360	1.0000
100	43	45	50	62	78	94	100
200	87	89	100	125	156	187	200
300	130	134	150	187	234	281	300
400	173	179	200	250	312	374	400
500	217	224	250	312	390	468	500
1000	434	447	500	624	780	936	1000
2000	867	894	1000	1248	1560	1872	2000
3000	1301	1342	1500	1872	2340	2808	3000
4000	1735	1789	2000	2496	3120	3744	4000
5000	2168	2236	2500	3120	3900	4680	5000
10,000	4337	4472	5000	6240	7800	9360	10,000
15,000	6505	6708	7500	9360	11,700	14,040	15,000
20,000	8674	8944	10,000	12,480	15,600	18,720	20,000
25,000	10,842	11,180	12,500	15,600	19,500	23,400	25,000
30,000	13,010	13,416	15,000	18,720	23,400	28,080	30,000

Table 7.3 Downhole static temperature versus depth and geothermal gradient (70°F surface temperature, typical of land locations)

Depth	Geothermal gradient (deg/100 ft)					
	0.8	1.0	1.5	2.0	2.5	3.0
0	70					
200	72	72	73	74	75	76
400	73	74	76	78	80	82
600	75	76	79	82	85	88
800	76	78	82	86	90	94
1000	78	80	85	90	95	100
2000	86	90	100	110	120	130
3000	94	100	115	130	145	160
4000	102	110	130	150	170	190
5000	110	120	145	170	195	220
6000	118	130	160	190	220	250

(*Continued*)

Table 7.3 (Continued)

Depth	Geothermal gradient (deg/100 ft)					
	0.8	1.0	1.5	2.0	2.5	3.0
7000	126	140	175	210	245	280
8000	134	150	190	230	270	310
9000	142	160	205	250	295	340
10,000	150	170	220	270	320	370
12,000	166	190	250	310	370	430
14,000	182	210	280	350	420	490
16,000	198	230	310	390	470	550
18,000	214	250	340	430	520	610
20,000	230	270	370	470	570	670
22,000	246	290	400	510	620	730
24,000	262	310	430	550	670	790
26,000	278	330	460	590	720	850
28,000	294	350	490	630	770	910
30,000	310	370	520	670	820	970
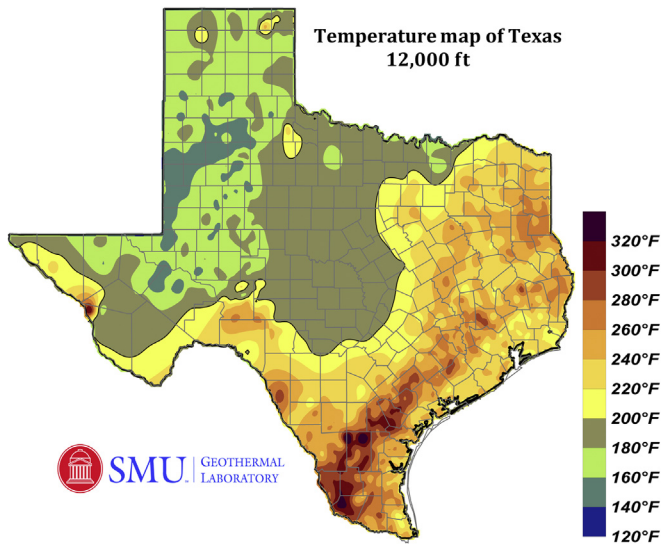
Figure 7.18 Texas downhole temperatures vary significantly with location. *Courtesy: SMU. Richards, Maria and David Blackwell, 2008. Map of Texas temperatures at 10,000 feet, in: Geothermal Energy Chapter of the Texas Renewable Energy Resource Assessment for the Texas Comptrollers Office, Virtus Energy, Austin, Texas[26].*

Similarly, if no additional data is available, the gradients may be estimated from isochronal gradient maps usually available from regional cementing companies and other sources.

---

[26] Maria Richards, David Blackwell, Map of Texas temperatures at 12,000 feet, in: Geothermal Energy Chapter of the Texas Renewable Energy Resource Assessment for the Texas Comptrollers Office, Virtus Energy, Austin, Texas, 2008.

7.7 ANNULAR CUTTINGS LOAD EFFECT ON DENSITY

Complicating the modeling problem further (although predictably so) is the added density of the drilling fluid in the annulus as a function of flow rate, drilling rate, and the cuttings transport ability of the mud. In addition, modeling of the pressure losses or friction effects is not ideal.

To illustrate, assume a mud will carry cuttings up and out of the wellbore with zero slippage. (See Chapter 3, Hole Cleaning for a full discussion of the carrying capacity of a mud.) If drilling is faster, then for a given flow rate, there will be less "dilution" of the cuttings in the annulus unless flow rate is increased. Increasing the flow rate will, of course, increase the ECD purely from fluid friction effects. The total pressure on the bottom of the hole will include the hydrostatic pressure plus the annulus friction losses plus the cuttings load in the annulus.

In the nearby graph, (Fig 7.19), the combined effect of flow rate-related friction loss and cuttings load in the annulus (and its effect on the bottom hole pressure or ECD). Note that for this illustration, hole cleaning is assumed to be adequate, but the upper left corner of the plot is most likely not achievable steady state in a real wellbore. The well would likely pack off before steady state was reached.

For example, at a depth of 20,000 ft and 16.0 ppg mud, the hydrostatic pressure would be 16,640 psi. Using a commonly available calculation of pressure loss in the annulus and assuming a flow rate of 500 gal per minute, the friction loss might be another 600 psi.

Note also that Fig. 7.19 assumes a perfect cuttings transport, where cuttings are made at the bit and then flow at the same rate as the mud up and out of the borehole. Any slippage or recirculation of the cuttings has the effect of increasing the number of cuttings in the wellbore at any given time, thus raising all of the family of curves shown upward (adding even more to bottom hole pressure).

Obvious in the figure but well worth emphasizing is that simply pumping faster may not improve overall efficiency of the drilling operation, especially at near-balance conditions (wellbore pressure near balanced with formation pore pressure) where the rate of penetration (ROP) is most sensitive to added ECD and where problems such as lost returns and/or kicks may be more likely (depending on the casing program and other factors). This ECD (resulting in a higher overbalance) has
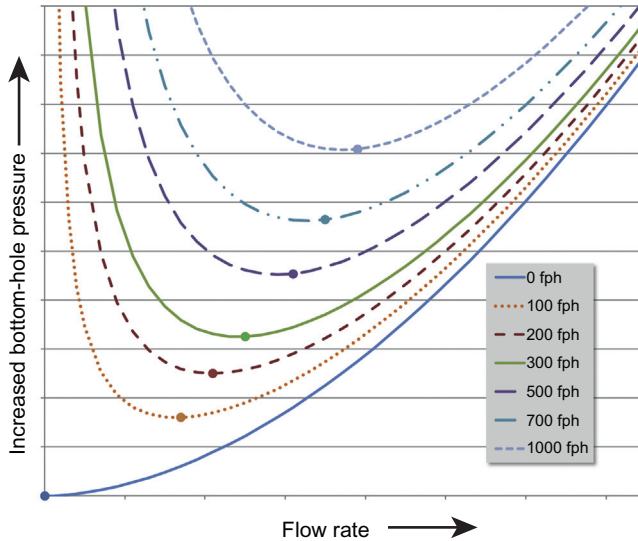
Figure 7.19 Combined effect of flow rate and drilling rate on bottom hole pressure due to cuttings loading and fluid friction loss.

a very deleterious effect on ROP, especially if the hydrostatic MW is nearly balanced to the pore pressure of the formation being drilled.

Rather, at any given ROP there is a clear minimum ECD that is reached due to the combined effects of flow rate and cuttings load. In general, this minimum increases with increased ROP due to the need to remove more cuttings as drilling is faster.

While temperature is usually thought to have a more pronounced effect than pressure, this is obviously a function of the MW, the depth, and the geothermal gradient for a particular wellbore. It has even been reported that for water-based fluids, the net effect of temperature and pressure can be close to offsetting in magnitude and in opposite direction. This cannot be said in all cases, especially with respect to oil–based fluids.

In Fig. 7.20, the change in density due to the combined effect of pressure and temperature are shown for four different base liquids. All of the muds show an increase in density down to around 6000 ft depth, presumably due to pressure.

After that point, the temperature effect becomes more pronounced, "balancing" the effect of pressure at between about 12,000 and 18,000 ft, depending on the mud, and beyond that point the density is lower down-hole than measured at the surface.

Combined effect of temperature and
pressure on base oils
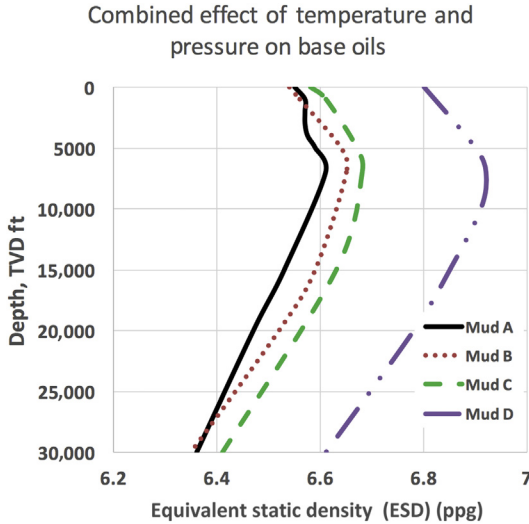
Figure 7.20 Combined effect of temperature and pressure with depth for several drilling fluids.

7.8 CONTAMINATION EFFECTS

Drilling fluids are highly treated, chemically, in order to provide the required fluid rheologies and shear thinning characteristics. As rock is drilled, contaminating materials can substantially alter the properties of the fluid downhole. The contamination could be from a fluid influx (oil, gas, or salt water from the formation flowing into the wellbore), or from the solids in the formation rock itself (clays, salts, coals, sulfur, carbonates, etc.).

Conversely, excessive base liquid loss to the formation (out of the drilling fluid) can also alter the properties of the fluid. This is especially true with water-based muds and is more pronounced when circulating bottoms up after a trip.

Whether chemically reactive or not, fine-to-coarse drill solids, having a substantial effect on the carrying capacity of the mud, are also classified as contaminants (even when chemically nearly inert) to be dealt with as the mud reports to the surface. (See the Chapter 3, Hole Cleaning section on carrying capacity index for more discussion of the effects of drill solids on carrying capacity.)

7.9 SALT EFFECTS ON OIL AND SYNTHETIC FLUID-BASED MUD SYSTEMS

With oil and synthetic-based muds, salt is of particular concern. Too little or too much salt can result in poor drilling fluid characteristics and a poor-quality wellbore. A freshwater or less saline water influx might cause the former, while drilling through a rock salt layer or dome might cause the latter.

This is due to the tendency of water to move by osmosis from lower to higher "activity" or put another way, the higher salinity regions. If salt content of the water phase of the oil or synthetic mud emulsion becomes too high, water will be pulled out of the formation into the mud. Conversely, insufficient salt will result in water migrating from the water phase of the mud into the saltier formation.

Some companies use a "balanced activity" mud in an attempt to overcome both of these problems. The water phase salinity is kept approximately the same as the formation water salinity, thus minimizing any water transfer in or out of the rock or mud.

Each of these is discussed in more details in the following.

7.9.1 Background

Though permeability varies by orders of magnitude in various sedimentary rocks, most exhibit some degree of porosity, typically in the range of 1%−30%, depending a number of factors, including specific rock type and depth.

That pore space is usually filled with formation water, usually with chloride content ranging from less than 1000 mg/L (fresh) to more than 350,000 mg/L, 10 times that of sea water.

Oil and synthetic-based muds will also usually have an internal water phase, which lowers costs and curiously, helps viscosify the mud. Through osmotic effects, the internal water phase of the nonaqueous drilling fluid can be pulled by the salinity in the formation water into that formation. If this formation is a water sensitive shale, wellbore problems such as sloughing shale, sticky shales, and excessive hole enlargement can result.

The industry solution to this is to add salt, usually in the form of calcium chloride ($CaCl_2$) to the water phase of the oil or synthetic-based mud, in order to balance or exceed the salinity of the formation water.

However, there are at least two distinct philosophies on which the level of chlorides in the water phase should be, or better, two technology solutions to deal with this issue. These are discussed briefly below. For a detailed examination of oil and synthetic-based muds, please see Growcock et al.[24] state of the art treatise, tentatively titled at this time "Oil-Based Muds—The Non-Aqueous Drilling Fluids Handbook."

7.9.2 Balanced activity oil-based muds

One philosophy is to balance the level of salinity (or "activity") in the mud with that in the formation. This technique requires careful monitoring of those salinities, both in the water phase of the drilling fluid as well as in the formation. The former is routinely done by mud engineers, but the latter is less frequently tested. The usual manner of determining the formation chloride level is to measure the relative humidity above a specially prepared sample of cuttings from the well. The relative humidity is highly correlated to the chloride level in the cuttings.

Once the formation activity is known, the chlorides in the drilling fluid can be adjusted up or down through the addition of $CaCl_2$ or freshwater, respectively.

When the fluid is properly balanced, it is extremely stable over long periods of time and may have very consistent properties with little added chemicals. This author's personal "best" well in this low maintenance regard was a well that went an entire week with zero additives—the only cost of the drilling fluid was the charge of the mud engineer who was monitoring it!

Note that formation activity varies within formations, so the mud system will typically only be perfectly balanced to a small section of the open hole. If the section of hole that was balanced is on the low end of the range of salinities in the exposed formations, this can result in some water transfer to the formations in other sections of the open hole.

Similarly, drilling into a formation that is of higher salinity can also result in water transferring via osmosis to the saltier shale, again with the possibility of wellbore enlargement, weakened or sloughing shale, and changed drilling fluid characteristics.

---

[24] F. Growcock, et al., Oil-Based Muds—The Non-Aqueous Drilling Fluids Handbook, Elsevier, 2020. (tentatively to be published in 2020)

7.9.3 Excess salt oil-based muds

Because of this chance of water transfer into the formation and the associated problems, most operators and mud companies prefer to maintain excess chloride levels in the water phase of the drilling fluid, high enough so that no section of the exposed formation will ever have higher salinity than the drilling fluid.

While this approach is somewhat easier for the mud engineer, it can result in large amounts of chemicals being used in the mud on a routine basis. This is due to the excess chloride in the water phase of the mud attracting water from the less saline formation water, effectively causing dilution of the wellbore mud with formation water.

As this dilution occurs, several related imbalances occur.

- The oil/water ratio (OWR) changes in the direction of more water and less oil.
- Additional base oil must be added to maintain some minimum or desired level of the OWR.
- Additional emulsifier and wetting agents must be added to maintain appropriate concentrations in the oil and water phases.
- Additional rheology modifying additives must be introduced.
- If the mud is weighted with barite or hematite, more weighting agent must be added.
- The salinity of the water phase of the mud drops, requiring the addition of more calcium chloride.
- The addition of calcium chloride results in more water being drawn from the formation into the drilling fluid (or go back to the top of this list and start again in what becomes a never-ending cycle of chemical additions to the drilling fluid! Some mud engineers simply refer to this cycle as "building mud"!)

As a result, this approach tends to be much costlier than the balanced activity approach as diagramed in Fig. 7.21.

The excess salt approach does, however, have the advantage of being somewhat easier on the mud engineer to run (there are not as many careful measurements of salt required and no measurements of the formation salinity at all are conducted). Importantly, some think that by causing the water transfer to go from the formation to the drilling fluid there is some benefit, perhaps including strengthening the formation slightly. This may or may not be accurate and remains a "target rich" area for further investigation and observation. Note that while the excess salt system is easier on
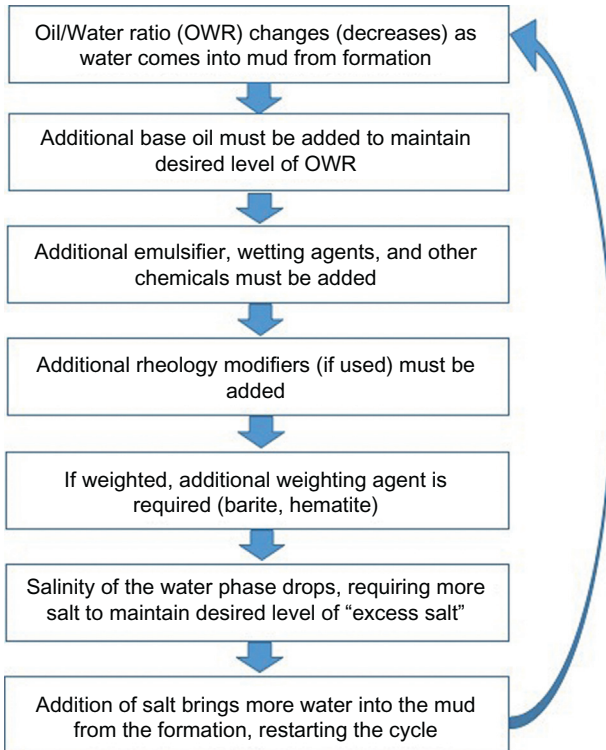
Figure 7.21 Excess salt "cycle."

the mud engineer to run, others on the rig site may find it to be more difficult to run. Those rig crew members physically tasked with performing the bulk chemical additions may work extra hard in order to "keep up" with the cycle of chemical additions and water influx this approach causes.

7.10 TIME EFFECTS

The time a fluid has been mixed or used, as well as the time the fluid is downhole [exposed to temperature, pressure, and effects of formations, formation fluids, drying (by losing water or base oil across the filter cake to the formation), and contamination], can also affect fluid properties. This is usually in an unpredictable manner.

The typical explanation is that reactive solids in the fluid are reacting more with time, as either more exposed sites on the relatively long-chained polymer chemicals react with drilling fluid components.

Conversely, some reactive sites may be effectively neutralized as their chemical reaction slows down over time.

As with other effects, these time-related effects are difficult to predict with any reasonable degree of accuracy.

7.11 OTHER EFFECTS ON DOWNHOLE PROPERTIES

Other effects are also known to change downhole drilling fluid properties. Perhaps the most important is shearing the fluid through the bit nozzles and other high shear rate regions of the circulation system. As the fluid, designed to be non-Newtonian in nature with respect to shear rates, undergoes change in shear rates, its properties change, often irreversibly.

7.12 SUMMARY

While much productive work has been done in modeling downhole properties of drilling fluids in laboratory (controlled) conditions, it remains a daunting task, likely never accomplished in the real world, to accurately and repeatedly model actual wellbores.

It must be noted that, generally speaking, oil and synthetic fluid-based systems *exhibit more stability* over their designed operating range than water-based systems.

Pumps

Contents

8.1 INTRODUCTION

Fundamentally, pumps compress fluids and hence store energy via that compression. There are different mechanical ways to accomplish this but in terms of energizing the fluid, they all have similar results. Each type has strengths and weaknesses, and parameters that can influence the selection include the following:
- type of fluid being pumped,
- pressures required,
- flow rates required,
- maintenance considerations,
- interchangeability of pumps and pump parts,
- operators' or workers' familiarity with the machines,
- duty cycles required,
- spare parts' availability and costs,
- costs
  - up front capital,
  - continuing maintenance, and
  - operating (power consumption, efficiency).

- infrastructure issues, piping, portability, etc.,
- space requirements (offshore, especially floating drilling), and
- weight.

> ## 8.2 CLASSIFICATION OF PUMPS

Just as there are many applications for pumps in the oilfield, there are many different ways of energizing or pressurizing fluids. They fall into two broad categories—kinetic and positive displacement. A brief description of several more common types is included below.

> ## 8.3 KINETIC

Kinetic pumps energize the fluid by accelerating it to higher velocities. This is typically done through the use of a rotating impeller (usually with liquids). The fluid is accelerated, and in so doing, energy is stored in the fluid as kinetic energy. Due to conservation of energy, this kinetic energy, when slowed, results in increased pressure.

8.3.1 Centrifugal pumps

Centrifugal pumps are based on a simple concept. Take a rock, put it in an old-style sling (like the one the Biblical David used to incapacitate Goliath), swing it around (developing the centrifugal force), and let it go and it will fly off with considerable velocity in the direction released—just ask Goliath. Centrifugal pumps work similarly, by accelerating the liquid to a high velocity and then letting it exit. The loose equivalent of the velocity of the rock at the instant it is released is the "head" of liquid the pump will produce. That head is the height of a vertical open top column of fluid that the pump will support—say 75 ft. The reason it is referred to in this way (instead of the more conventional "pressure") is that for a centrifugal pump, the *height (or "head") of the fluid column will be the same regardless of the fluid density*. A column of mercury will stand the same height as a column of water, though the pressure measured at the outlet of the pump would be 13.5 times higher from the former than the latter (due to

the hydrostatic fluid pressure having a density component, where the "head" does not). Similarly, the energy required to produce that head would increase with the higher density fluid.

Put another way, this means that the centrifugal pumps are actually constant head devices when run at the same RPM, regardless of the fluid density.

When the suction pressure or pressure near the blade of a rotating impeller is low enough (below the vapor pressure of the liquid), localized "boiling" (albeit at ambient mud temperature) can occur. The formation of the gaseous pockets is not by itself troubling but the collapse of the bubbles as pressure subsequently increases creates shock waves that can be extremely damaging to equipment or anything else. Cavitation is usually avoided by precharging the pump suction slightly with another pump.

Impellers are designed by pump manufacturers to minimize cavitation and maximize pump efficiency. As they are pumping abrasive solid–laden muds around the rig, they do erode and otherwise wear and must be replaced from time to time.

For even loading of drilling fluid into the centrifugal pump, a long straight section of pipe is preferred on the suction side of the pump as shown in Fig. 8.1. Practitioners recommend a minimum of five pipe diameters of straight pipe leading into the suction. Since this is often not practical, and 90-degree elbows are commonly used relatively close to the suction side, the resulting flow into the centrifugal pump inlet is uneven as in Fig. 8.2. This in turn can lead to cavitation, uneven pump loading,
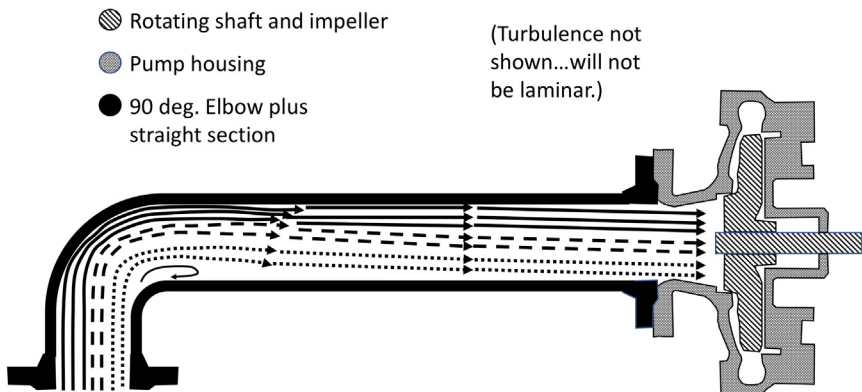
Figure 8.1 A length of straight pipe is preferred between any pipe elbows and the centrifugal pump suction inlet due to uneven flow at the exit of the elbow.

- ▨ Rotating shaft and impeller
- ⬤ Pump housing
- ⬤ 90 deg. elbow

(Turbulence not shown...will not be laminar.)
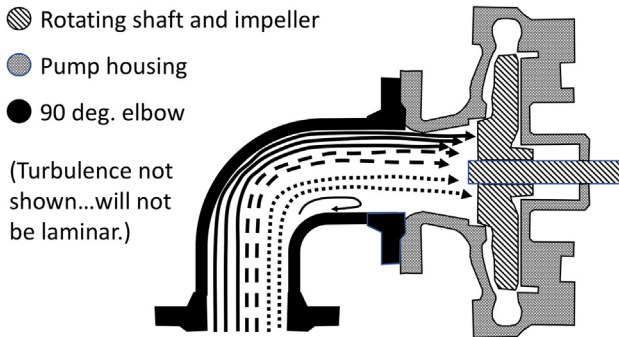
Figure 8.2 Uneven loading of centrifugal pump suction inlet due to uneven flow profile at the exit of a pipe elbow.

and premature pump failure. The use of inlet guide vanes (IGVs) and other flow straighteners, conditioners and diffusers have been shown to help, including the worst case condition of an elbow being close to the inlet of the pump. The IGVs and flow conditioners also improve overall pump efficiency.

The primary use for centrifugal pumps rig site is in moving mud around location, not in pumping mud downhole. This may be simply moving mud from one tank to another, or pumping the mud from a tank to another pump, or at the beginning and end of the well transferring the mud to/from trucks or boats or elsewhere. Centrifugal pumps are also used to feed most solids control equipment, and in the case of hydro–cyclone type solids control equipment, the output of the pump should match the requirements of that solids control device.

In order to minimize gyroscopic effects of the high speed spinning impeller in the centrifugal pump and corresponding premature wear of bearings caused by those gyroscopic effects triggered by vessel motion, the axis of the pump rotation should optimally be along the bow to stern line (with the plane of the impeller perpendicular to that line).

8.3.2 Turbine pumps

Turbine pumps are centrifugal in nature but have some characteristics of positive displacement. While that sounds oxymoronic, for different functions, they behave or operate differently.

First, the way they impart energy to the liquid is kinetic (and hence centrifugal) in nature. However, they typically have multiple "stages," with each stage generating a little incremental pressure. Since each stage is incremental, the risk of cavitation is lower.

Clearances are said to be very tight, and hence, the reference to them having some characteristics of positive displacement pumps.

Mostly due to their compact size and multiple stage capability, their typical application is with clean water (fresh or waste) with minimal solids content. (Their relatively close tolerances cannot long survive abrasive slurries such as drilling muds.)

They are often used in high head but relatively low-volume applications, such as pumping water a significant height.

Rarely do they find service in the drilling world at present.

8.4 POSITIVE DISPLACEMENT PUMPS

For higher pressure applications that centrifugal pumps cannot deliver, positive displacement pumps are used. They come in several different types, and within each type there is a variety of designs from different manufacturers.

8.4.1 Progressive cavity

In a progressing cavity pump, a molded rubber spiral internal profile stator is mated with a polished chrome spiral rotor, powered typically by an electric motor. A cavity, bounded by the contact from the rotor to the stator, moves from the inlet end of the pump to the outlet end as the rotor is rotated.

Standard water-treatment applications' design calls for about 90 psi per motor stage, with additional stages put in series to get higher (or additive) pressures.

Uses include transfer of mud and liquids, both on the surface and downhole as in pumping crude oil or water from the reservoir to the surface.

Interestingly, drillers discovered decades ago that if pressurized fluid (such as a drilling mud or water) is pumped into the pump, the progressive cavity pump will work in reverse as a motor, extracting energy from the pressurized fluid and producing significant torque through the rotor that can power downhole tools such as a drill bit. When used in such fashion, the assembly is referred to as a "mud motor."

8.4.2 Triplex

Triplex pumps are the most common configuration of high–pressure pumps found on today's drilling rigs, second only to lower pressure centrifugal pumps. Though they are manufactured by a variety of companies and have a wide range of pressure and flow rate capabilities, they all operate in a very similar fashion.

The pumps have a mechanical end, consisting of the input drive shaft usually driven by one or more electric motors. Older land rigs may be driven by belts or chain drives from diesel engines. The drive shaft is geared to a crankshaft, which serves to convert rotary motion into linear motion in the conventional fashion, similar to crankshafts on car engines, pedals on bicycles, etc.

The linear motion of the connecting rods transfers the power to the fluid ends of the pump, which are simply high-pressure cylinders fitted with pistons and seals (called swabs) on the pistons.

An important feature of triplex, duplex (discussed below), and other positive displacement piston or cylinder pumps is that the fluid end liner is changeable. Since it is changeable, equipment designers have made it adjustable in diameter and pressure rating. A smaller, thicker walled liner may be used for higher pressure applications, while a larger (but thinner wall thickness) liner may be used for higher volume applications. Some rigs have sufficient spare capacity on pumping systems that liner changes are infrequent, but others with more limited pumping equipment. These less-capable rigs will typically use a lower pressure/high-volume fluid end arrangement for the "top-hole" (larger diameter) sections, and at some point deeper in the well change to a smaller volume/higher pressure fluid end arrangement.

On the input stroke of a particular cylinder (there are three for a triplex pump), the check valve to the high-pressure side of the rig pumping is closed, and the companion check valve to the suction line for the pump is open, thus allowing filling the cylinder with mud, either from a gravity tank or, more commonly, a centrifugal pump pressurized precharge line.

On the power or output stroke, the check valves reverse—the outlet side to the high-pressure rig plumbing opens while the suction side is closed (see Fig. 8.3).

Since the pump pistons are only compressing the fluid in one direction, they are sometimes referred to as "single-acting" pumps.

Mud is compressed slightly, storing energy we measure as pressure in the compression of the fluid.
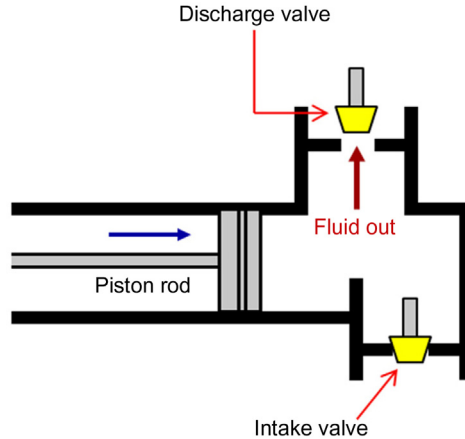
Figure 8.3 Single-acting cylinder schematic, typical of "triplex" pumps. *Courtesy: Texas Drilling Associates.*

To compute the pump output (triplex only):

$$\text{Pump output} = 0.0102 \times D_{\text{LINER}}^{2} \times L_{\text{STROKE}} \times \text{SPM} \times \eta \qquad (8.1)$$

where pump output is the flow rate out (GPM); D_{LINER} is the inside diameter of the pump cylinder "liners" (in.); L_{STROKE} is the length of travel of the pistons (in.); SPM is the pump speed in strokes per minute; and η is the pump volumetric efficiency, % (usually taken or measured to be 97%−99%).

Example: Determine the triplex pump output in GPM at 98% efficiency and 110 SPM.

Liner diameter	= 7 in.
Stroke length	= 12 in.
Pump output	= $0.0102 \times 7^2 \times 12 \times 110 \times 0.98$
	= 647 GPM

Importantly, note that one "stroke per minute" is in reality one revolution per minute, and not 1/3 RPM. The possible confusion is believed to be tied to the way stroke rates are measured, which is typically to measure *one* of the three cylinders with a contact or noncontact switch.

Hence, a stroke includes the action of all three cylinders, single-acting.[1]

---

[1] http://www.drillingformulas.com/basic-understanding-about-positive-displacement-in-drilling-industry/ accessed September 28, 2016.

8.4.3 Duplex/double-acting

Duplex pumps have two cylinders instead of three for the triplex but also differ in another important way that affects pump calculations. In a duplex pump, the fluid ends are arranged so that each cylinder pumps in both directions. That is, regardless of the direction of the piston movement, fluid is being simultaneously pressurized on one side of the piston and input/filled on the other side of the piston. Due to the piston rod itself, the volume of the two "halves" of the cylinder pumping cycle is not identical, but the variation is relatively small.

Such pumping in both directions is referred to as "double-acting" and is said to produce smoother pump pressure (without smoothing accumulators).

Since the pump pistons are pumping in both directions, the equation used for "double-acting" pumps must take into account the fact that the side of the pump with the piston rod has less net cross-sectional area pumping than the free end. Inspection of Eq. (7.2) readily shows that the liner volume displacement is counted twice (hence double-acting), and the rod volume displacement is deducted once (Figs. 8.4 and 8.5).where D_{LINER} is the liner diameter (in.); L_{STROKE} is the stroke length (in.); and D_{ROD} is the rod diameter (in.).

Example: Determine the duplex pump output in GPM at 95% efficiency and 110 SPM.
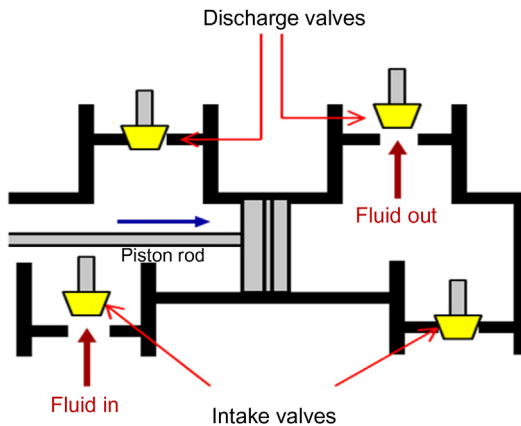
Figure 8.4 Double-acting cylinder schematic typical of "duplex" pumps—higher output piston motion shown—cf. with Fig. 8.5.

$$\text{Pump output} = 0.006804 \times \left(2 \times D_{LINER}^2 - D_{ROD}^2\right) \times L_{STROKE} \times SPM \times \eta \qquad (8.2)$$

Courtesy: Texas Drilling Associates.
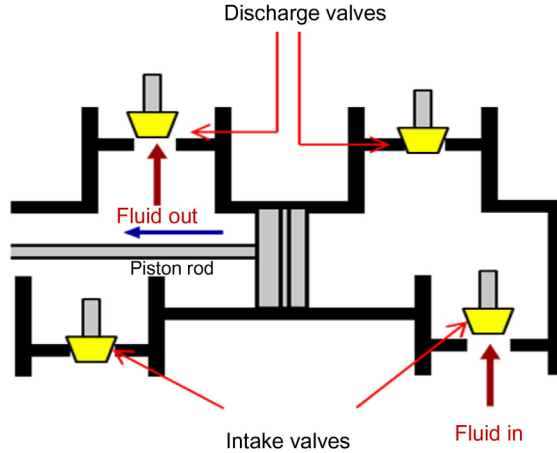
Figure 8.5 Double-acting cylinder schematic typical of "duplex" pumps—lower output piston motion shown—cf. with Fig. 8.4. *Courtesy: Texas Drilling Associates.*

Liner diameter	$= 7$ in.
Stroke length	$= 12$ in.
Rod diameter	$= 2.5$ in.
Pump output	$= 0.006804 \times [2 \times 7^2 - 2.5^2] \times 12 \times 110 \times 0.95$
	$= 783$ GPM

One stroke per minute is one revolution per minute. Hence, a stroke includes the action of both cylinders, double-acting.

8.4.4 Hex pumps (six vertical cylinders)

The hex pump, introduced by NOV, utilizes six vertical single-acting cylinders. The cylinders are sequentially compressed by the action of a ring-cam plate, in much the same fashion as smaller "swashplate" design hydraulic fluid pumps. There is no crankshaft per se as in the case of duplex and triplex designs. The pump is said to save space (footprint) while enjoying improved performance ranges.

When single-action pumps are involved (like triplex or hex), the more generic equation for calculating pump output becomes

$$\text{Pump output} = \text{Area}_{\text{LINER}} \times L_{\text{STROKE}} \times N_{\text{cylinders}} \times \text{SPM} \times \eta \qquad (8.3)$$

where $\text{Area}_{\text{LINER}}$ is the cross-sectional area of the compression cylinder; L_{STROKE} is the length of the compression cycle; $N_{\text{cylinders}}$ is the quantity of single-acting cylinders compressing, six in the case of hex pumps; SPM

is the rotational speed of the crankshaft or cam of the pump, revolutions per minute; and η is the volumetric efficiency, fraction.

In customary US Oilfield Units, this becomes

$$Q = \left(\frac{\pi}{4}\right) \frac{D_{\text{LINER}}^2 \times L_{\text{STROKE}} \times N_{\text{cylinders}} \times \text{SPM}}{231} \times \eta$$

where Q is the volumetric flow rate (GPM); D_{LINER} is the diameter of the liners and cylinders (in.); 231 is the unit conversion factor; and the rest of the terms are as described above.

For the particular case of hex pumps, this becomes

$$Q = \left(\frac{\pi}{4}\right) \times \frac{D_{\text{LINER}}^2 \times L_{\text{STROKE}} \times 6 \times \text{SPM}}{231} \times \eta$$

$$Q = 0.0203 \times D_{\text{LINER}}^2 \times L_{\text{STROKE}} \times \text{SPM} \times \eta$$

$$Q = \frac{D_{\text{LINER}}^2 \times L_{\text{STROKE}} \times \text{SPM}}{38.5} \times \eta$$

8.5 EFFICIENCIES

If one were trying to determine the available hydraulic power on a pump given a shaft input rating, that rating would suffer two inefficiencies before pressurized drilling fluid exited the fluid end.

The first would be a *mechanical inefficiency* that is normally estimated to be 85% for the mechanical end of a typical triplex pump.[2] The lost 15% is largely in the crankshaft and gearing, with a small amount lost to other mechanical friction points.

The second loss would be a *volumetric inefficiency* due to imperfect volumetric displacement of the pump pistons in their cylinders. The second loss varies somewhat depending on the manufacturer, model, and condition of a pump but is usually taken to be in the 95%–99% range. This range is typical of pumps that have a centrifugal precharge pump feeding the input. Without the centrifugal precharge, the triplex volumetric efficiency may be only 90%–93%.

---

[2] At this writing, no reports have been received on the "Hex" pumps' mechanical and volumetric efficiencies.

This second inefficiency (volumetric) is often measured on the rig site, with a "bucket and stopwatch" technique, albeit the "bucket" is usually a 50–100-barrel tank volume used to pump out of or into.

Hence, taking into account all inefficiencies, the possible pump output for a given shaft input limit can be written as

Generally, the hydraulic power can be obtained by assuming a mechanical efficiency of power transfer of about 85% and a volumetric efficiency of 93%–99%.

Back to computing pump output, the mathematical relationship would be

$$\text{Power}_{\text{out}} = \text{Power}_{\text{in}} \times \eta_{\text{mechanical}} \times \eta_{\text{volumetric}} \qquad (8.4)$$

where $\text{Power}_{\text{out}}$ is the actual hydraulic power produced at the exit of the high-pressure fluid ends of the pump, hp (or kW); Power_{in} is the shaft input horsepower to the mechanical end of the pump, hp (or kW); $\eta_{\text{mechanical}}$ is the mechanical efficiency of the pump, dimensionless or % (typically 85%); $\eta_{\text{volumetric}}$ is the volumetric efficiency of the fluid ends of the pump, dimensionless or % (typically 93%–99%).

As an example, a NOV P-1500 triplex pump has a rated input of 1500 hp, a mechanical efficiency of 85%, and a volumetric efficiency of 98%. The available output horsepower would be given as

$$\text{Power}_{\text{out}} = 1500 \times 0.85 \times 0.98$$

$$\text{Power}_{\text{out}} = 1500 \times 0.833$$

$$\text{Power}_{\text{out}} = 1249.5 \text{ hp}$$

Rearranging the hydraulic horsepower equation, we readily observe that maximum volume may be calculated at maximum pressure as follows:

$$Q_{\text{MAX}} = \frac{\text{HHP}_{\text{MAX}} \times 1714}{P_{\text{MAX}}} \qquad (8.5)$$

where Q_{MAX} is the maximum volumetric flow rate (GPM); HHP_{MAX} is the maximum hydraulic horsepower; and is the maximum system operating pressure rating (psi) (or kPa).

If this power were used for a 4000-psi maximum pressure system, the maximum volume flow rate that *could* be produced would be 535.4 GPM. If this volume of 12.3 ppg drilling fluid were flowing through a bit fitted with five 16/32″ diameter nozzles (with a combined total nozzle flow area

Table 8.1 Typical volumetric efficiencies with and without precharge
Positive displacement slush pump efficiency

Volumetric efficiency			
	SPM	Without precharge (%)	With precharge (%)
Duplex pumps	<40	95	~ 98
	>40	90	~ 93
Triplex pumps	All	93	~ 99

Best to measure efficiency with the "bucket and stopwatch" technique.

(TNFA) equal to 0.9817 square inches), the bit pressure drop would be calculated to be

$$\Delta P_{bit} = \frac{MW \times Q^2}{12,775 \times TNFA^2} \tag{8.6}$$

$$\Delta P_{bit} = \frac{12.3 \times 535.4^2}{12,775 \times 0.9817^2}$$

$$\Delta P_{bit} = 286.4 \text{ psi}$$

Note that the volumetric efficiencies are not entirely due to pump design (such as flexing in the crankshaft under load, clearances in bearings, leakage across piston seals, leakage across fluid end check valves, etc.). The output efficiency is also strongly influenced by aeration (or any other species of entrained gas) of the drilling or other purpose fluid being pumped. In essence, anything that reduces the theoretical geometrical volume output of the pump cylinders is included in the volumetric efficiency portion of the calculation.

On a drilling rig, the mud pumps are powered by motors with a finite amount of power. Generally, the hydraulic power can be obtained by assuming a mechanical efficiency of power transfer of about 85% and a volumetric efficiency of 93%−99% (Table 8.1).

Appendix

Contents

9.1 REYNOLDS NUMBER CONVERSION FACTOR FOR US OILFIELD UNITS

Given that for an annulus, the Reynolds number is given by

$$R_e = \frac{\rho \times \overline{V} \times (D_{\text{hole}} - D_{\text{pipe}})}{\mu} \tag{9.1}$$

in consistent units (yielding a dimensionless Reynolds number). To express in oilfield terms and units,

$$V = \frac{Q}{A} \tag{9.2}$$

And therefore,

$$R_e = \frac{\rho \times \left(\frac{Q}{A}\right) \times (D_{\text{hole}} - D_{\text{pipe}})}{\mu} \tag{9.3}$$

However, in order to use standard US Oilfield Units and have the R_e be dimensionless, some conversion is needed. In oilfield units, the expression above results in the units of

$$\frac{4 \times \left(\frac{\text{pounds}}{\text{gallon}}\right) \times \left(\frac{\left(\frac{\text{gallons}}{\text{min}}\right)}{\text{in.}^2}\right) \times \text{in.}}{\pi \times \text{centipoise}} \tag{9.4}$$

or

$$\frac{4 \times \text{pounds} \times \left(\frac{1}{(\text{min} \times \text{in.})}\right)}{\pi \times \text{centipoise}}$$

Since

$$1488\text{cP} = 1\frac{\text{pound}}{\text{ft} \times \text{second}} \tag{9.5}$$

substitution yields

$$\frac{4 \times 1488 \times \text{centipoise} \times \text{pounds} \times \left(\frac{1}{(\text{min} \times \text{in.})}\right)}{\pi \times \text{centipoise} \times \left(\frac{\text{pounds}}{(\text{ft} \times \text{s})}\right)} \tag{9.6}$$

simplifying to

$$\frac{4 \times 1488 \times \text{pounds} \times \left(\frac{1}{(\text{min} \times \text{in.})}\right)}{\pi \times \left(\frac{\text{pounds}}{(\text{ft} \times \text{s})}\right)} \tag{9.7}$$

$$\frac{4 \times 1488 \times \text{pounds} \times \left(\frac{(\text{ft} \times \text{s})}{(\text{min} \times \text{in.})}\right)}{\pi \times \text{pounds}} \tag{9.8}$$

$$\frac{4 \times 1488 \times \text{ft} \times \text{s}}{\pi \times \text{min} \times \text{in.}} \tag{9.9}$$

Further to

$$\frac{4 \times 1488 \times 12}{\pi \times 60} = 378.916 \tag{9.10}$$

9.2 REYNOLDS NUMBER FORM WITH US OILFIELD UNITS FOR ANNULUS

Hence, for pipe the classic Reynolds number given by

$$R_e = \frac{\rho \times \overline{V} \times D}{\mu} \tag{9.11}$$

For an annulus, given that the hydraulic diameter is $D_{\text{hole}} - D_{\text{pipe}}$, becomes

$$R_e = \frac{\rho \times \overline{V} \times (D_{\text{hole}} - D_{\text{pipe}})}{\mu} \tag{9.12}$$

From above, the $\overline{V}$ is Q/A or proportional to $Q/(D_{\text{hole}}^2 - D_{\text{pipe}}^2)$. Substituting yields

$$R_e = \frac{\text{MW} \times Q \times \left(d_{\text{hole}} - d_{\text{pipe}}\right)}{\mu \times \left(d_{\text{hole}}^2 - d_{\text{pipe}}^2\right)} \times 378.92 \tag{9.13}$$

which can be rewritten as

$$R_e = \frac{\text{MW} \times Q \times (d_{\text{hole}} - d_{\text{pipe}})}{\mu \times (d_{\text{hole}} - d_{\text{pipe}})(d_{\text{hole}} + d_{\text{pipe}})} \times 378.92 \qquad (9.14)$$

Simplifying

$$R_e = \frac{\text{MW} \times Q}{\mu \times (d_{\text{hole}} + d_{\text{pipe}})} \times 378.92 \qquad (9.15)$$

9.3 REYNOLDS NUMBER FORM WITH US OILFIELD UNITS FOR INSIDE PIPE

The classic Reynolds number for a circular pipe is given by

$$R_e = \frac{\rho \times \overline{V} \times D}{\mu} \qquad (9.16)$$

From above, the $\overline{V}$ is Q/A or proportional to $Q/(D_{\text{hole}}{}^2)$. Substituting yields

$$R_e = \frac{\text{MW} \times Q \times (d_{\text{hole}})}{\mu \times (d_{\text{hole}}^2)} \times 378.92 \qquad (9.17)$$

which can be rewritten as

$$R_e = \frac{\text{MW} \times Q \times (d_{\text{hole}})}{\mu \times (d_{\text{hole}})(d_{\text{hole}})} \times 378.92 \qquad (9.18)$$

Simplifying:

$$R_e = \frac{\text{MW} \times Q}{\mu \times (d_{\text{hole}})} \times 378.92 \qquad (9.19)$$

9.4 GALLONS PER MINUTE TO AVERAGE VELOCITY FOR A PIPE OR ANNULUS

Average flow velocity is given as volumetric flow divided by cross-sectional area, or

$$\bar{v} = \frac{Q}{A} \tag{9.20}$$

In conventional oilfield units, this would be

$$v = \frac{4}{\pi} \times \frac{\frac{\text{gallons}}{\text{min}}}{\text{in.}^2} \tag{9.21}$$

yielding a nonstandard unit. Hence to convert to an average feet/second

$$v = \frac{4}{\pi} \times \frac{\frac{\text{gallons}}{\text{min}}}{\text{in.}^2} \times \frac{144 \text{in.}^2}{\text{feet}^2} \times \frac{\text{feet}^3}{7.4805 \text{gallons}} \times \frac{\text{min}}{60 \text{s}} \tag{9.22}$$

$$v\frac{\text{feet}}{\text{s}} = \frac{\text{GPM}}{2.447988 \times \text{pipe diameter}^2} \cong \frac{\text{GPM}}{2.448 \times \text{pipe diameter}^2} \tag{9.23}$$

Or

$$\bar{v}\frac{\text{feet}}{\text{s}} = \frac{0.40850 \times \text{GPM}}{\text{pipe diameter}^2} \cong \frac{0.409 \times \text{GPM}}{\text{pipe diameter}^2} \tag{9.24}$$

where GPM is gallons per minute and pipe diameter is in inches.

Similarly, for the case of the annulus,

$$v\frac{\text{feet}}{\text{s}} = \frac{\text{GPM}}{2.448 \times (d_2{}^2 - d_1{}^2)} \tag{9.25}$$

Or

$$v\frac{\text{feet}}{\text{s}} = \frac{0.409 \times \text{GPM}}{(d_2{}^2 - d_1{}^2)} \tag{9.26}$$

where d_2 is the outer surface inside diameter and d_1 is the outside diameter of the inner surface.

9.5 TURBULENT FLOW PIPE PRESSURE LOSS FROM FANNING FRICTION FACTOR DEFINITION

Recall that the Fanning friction factor is defined by

$$f_F = \frac{d}{2 \times \rho \times v^2} \times \frac{\Delta p}{\Delta l} \qquad (9.27)$$

Rearranging for pipe pressure loss per unit length

$$\frac{\Delta p}{\Delta l} = f_F \times \frac{2 \times \rho \times v^2}{d} \qquad (9.28)$$

If oilfield units of psi pressure, ft length, ppg density, ft/s velocity, and in. diameter are desired, the conversion needed becomes

$$\frac{\Delta p}{\Delta l} = f_F \times \frac{2 \times \rho \# \times v^2 \text{ft}^2}{d \text{gal in.s}^2} \times \frac{7.4805 \text{gal}}{\text{ft}^3}$$
$$\times \frac{\text{ft}^2}{144 \text{in.}^2} \times \frac{12 \text{in.}}{\text{ft}} \times \frac{\text{s}^2}{32.2 \text{ft}} \qquad (9.29)$$

which reduces to

$$\frac{\Delta p}{\Delta l} = f_F \times \frac{2 \times \rho \times v^2}{d} \times \frac{7.4805 \times 12}{144 \times 32.2} \frac{\text{pounds}}{\text{in.}^2 \text{ft}} \qquad (9.30)$$

and

$$\frac{\Delta p}{\Delta l} = f_F \times \frac{2 \times \rho \times v^2}{d} \times \frac{1}{51.654} \frac{\text{pounds}}{\text{in.}^2 \text{ft}} \qquad (9.31)$$

then

$$\frac{\Delta p}{\Delta l} = f_F \times \frac{\rho \times v^2}{25.827 \times d} \frac{\text{psi}}{\text{ft}} \qquad (9.32)$$

9.5.1 Fanning diagram (Fig. 9.1)
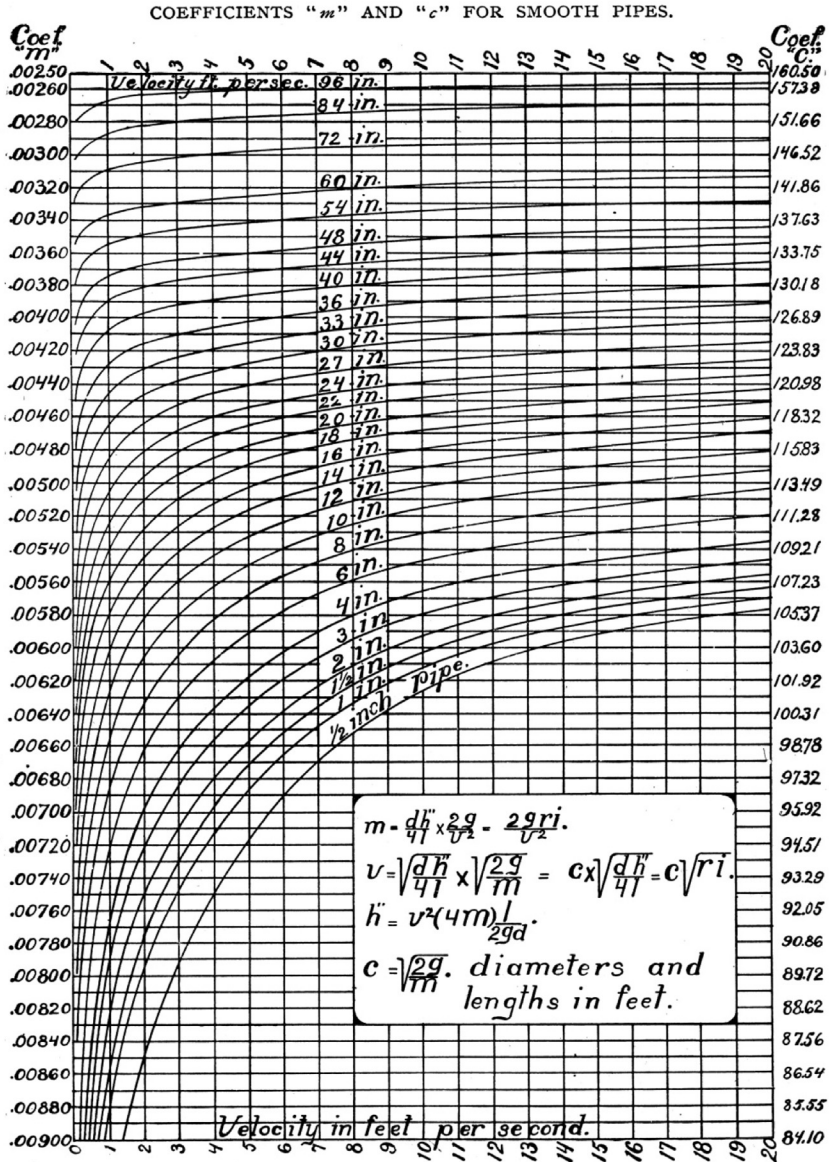
Figure 9.1 Fanning diagram. Note $4m$ in h'' equation, as m was Fanning's designation for his friction factor that was 1/4 the size of the Darcy−Weisbach one (i.e., Moody's). *From J.T. Fanning, 1906, prior to Moody.*

9.5.2 Moody diagram (Fig. 9.2)
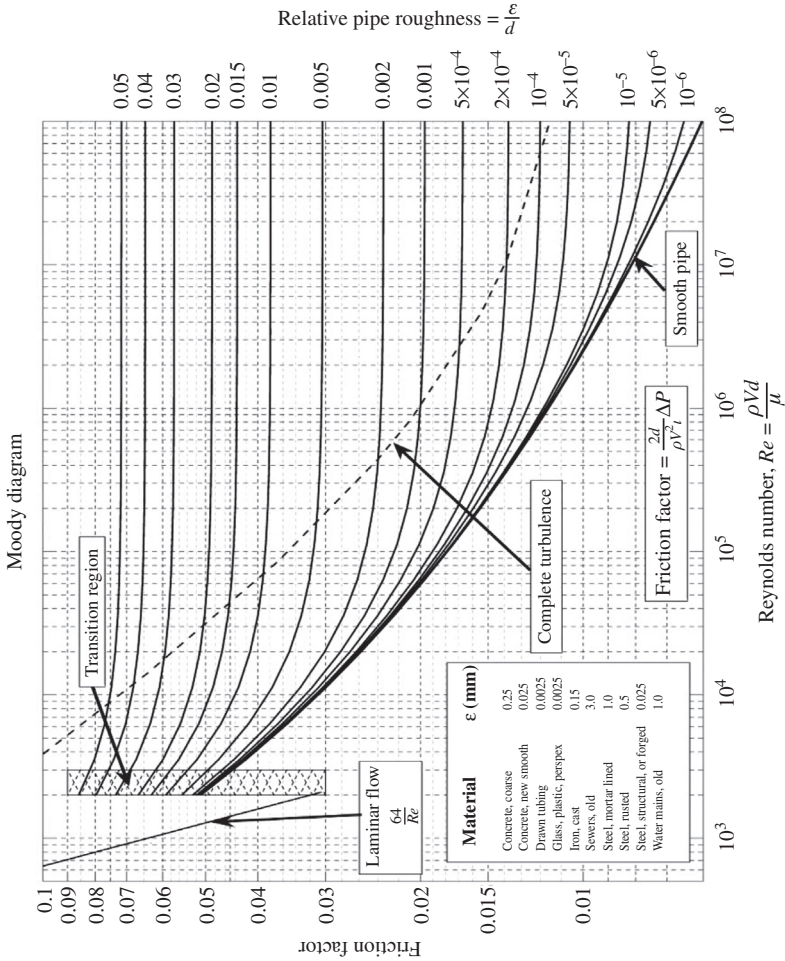
Figure 9.2 Moody friction factor diagram (cf. with Stanton Chart).

Note that the Moody (or Darcy−Weisbach) friction factor f_D is NOT the same as the Fanning friction factor, f_F. Rather,

$$f_D = 4 \times f_F$$
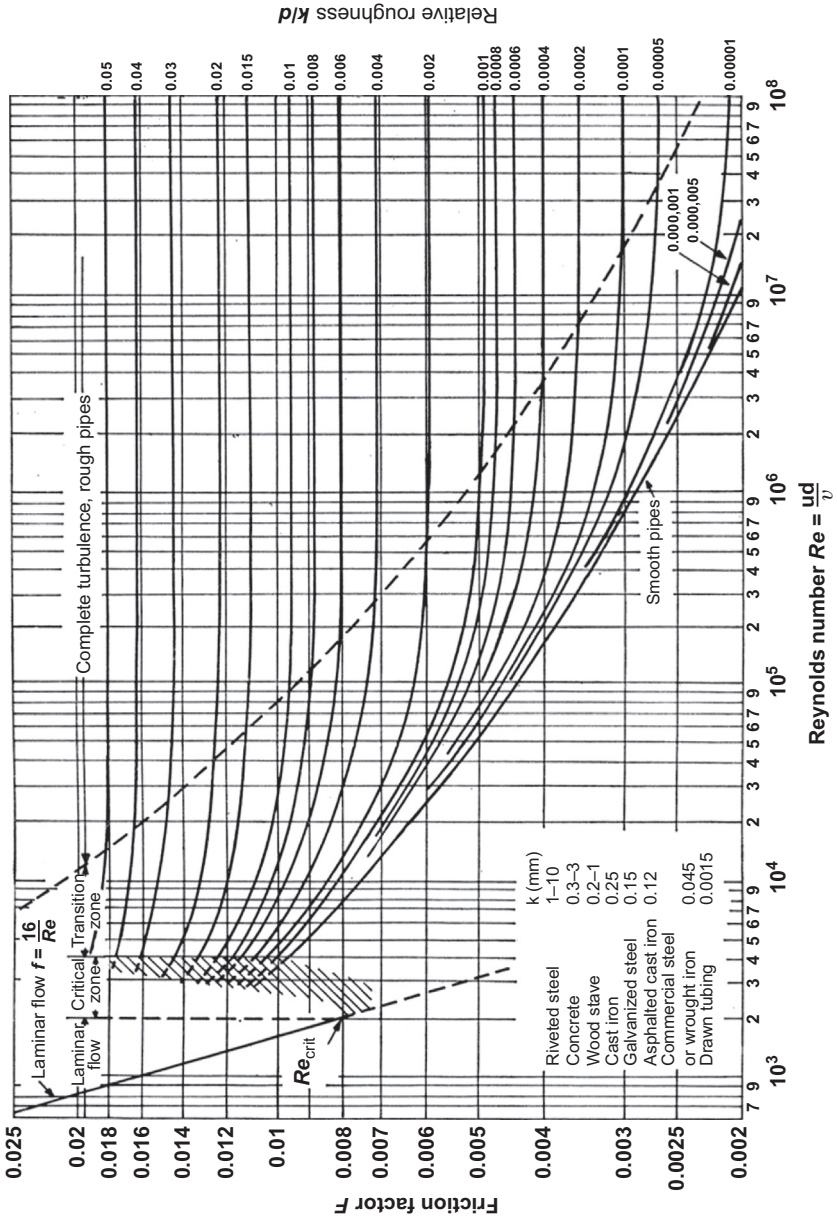
Figure 9.3 Fanning friction factor diagram (cf. with Moody diagram).

Unless noted, the Fanning friction factor (Fig. 9.3) is used throughout this text. With the availability of easier numeric computations, it is the hope of this author that eventually all will switch to the Moody/Darcy–Weisbach factors to avoid future confusion.

9.6 HYDRAULIC DIAMETER DERIVATION

The hydraulic diameter is defined as

$$d_{\text{hydraulic}} = \frac{4 \times \text{cross} - \text{sectional area}}{\text{wetted perimeter}} \qquad (9.33)$$

or

$$d_H = \frac{4 \times A_{\text{annulus}}}{P} \qquad (9.34)$$

Expanding:

$$d_H = \frac{4 \times \left[\left(\frac{\pi}{4} \right) \times \left(d_2^2 - d_1^2 \right) \right]}{\pi \times (d_1 + d_2)} \qquad (9.35)$$

Reducing

$$d_H = \frac{\left(d_2^2 - d_1^2 \right)}{(d_1 + d_2)} \qquad (9.36)$$

Simplifying:

$$d_H = d_2 - d_1 \qquad (9.37)$$

9.7 DERIVATION OF THE EFFECTIVE VISCOSITY TERM "K"[1]

Viscosity by definition is the shear stress divided by shear rate. If shear stress has the units of dynes/cm^2, and shear rate has the units of reciprocal seconds, the viscosity will have the units of poise. With the Fann viscometer, the dial reading may be converted into dynes/cm^2 by multiplying by 5.11, and the Fann RPM can be converted into reciprocal seconds by multiplying by 1.703. For the Power Law equation:

$$\tau = K(\gamma)^n \qquad (9.38)$$

A similar conversion would yield

[1] L. Robinson, Private correspondence, 2012.

$$K = \frac{R_{300} \times 5.11 \times 100 \left(\frac{cP}{poise}\right)}{300 \text{RPM} \times 1.703 \left(\frac{s^{-1}}{RPM}\right)} = 511^{(1-n)} \times R_{300} \qquad (9.39)$$

The *K*-value would therefore have units similar to viscosity except for the exponent on the shear rate term. The term "equivalent cP" described these units in the *Applied Drilling Engineering*[2] book.

The value of "*n*" can be found without unit conversion since it is a dimensionless number. For two cases, the 600 and the 300 RPM Fann readings:

$$R_{600} = K \times 600^n \text{ and } R_{300} = K \times 300^n \qquad (9.40)$$

These two equations could be solved for "*n*" by dividing the second equation into the first and taking the logarithm of both sides. This produces

$$n = 3.322 \times \log \frac{R_{600}}{R_{300}}, \text{ or in terms of PV and YP} \qquad (9.41)$$

$$n = 3.322 \times \log \frac{2 \times PV + YP}{PV + YP} \qquad (9.42)$$

9.8 BOYCOTT SETTLING

As an historical note, the text of Dr. Boycott's letter to the British Journal *Nature* in 1920 reads as follows:

Sedimentation of blood corpuscles (see Table 9.1).

I have noticed lately that if oxalated or defibrinated blood is put to stand in narrow tubes, the corpuscles sediment a good deal faster if the tube is inclined than when it is vertical. Thus with tubes bout 2.7 mm internal diameter there were, after 20 hours, 4, 23, 35, and 42 per cent. of clear serum with tubes inclined at 0, 22 ½°, 45°, and 67 ½°, respectively. In another rough experiment with tubes of different diameters, all filed to a height of 40 mm. with diluted blood, after 5 hours there were the following proportions of clear serum:

---

[2] A. T. Bourgoyne, K. K. Millheim, M. E. Chenevert, F. S. Young, in: Applied Drilling Engineering. SPE Textbook Series, vol., 2 p. 476. Society of Petroleum Engineers (SPE), (1986).

Table 9.1 Dr. Boycott's red blood cell sedimentation data.

mm diam.	Vertical Percent	11½° Percent	22½° Percent	33½° Percent
2.7	6	20	29	51
8	5	10	15	21
14	4	5	9	12

The phenomenon seems to depend on the vertical height of the columns of blood, and it occurs to me that the slight Brownian movement of the lower corpuscles may interfere with the sedimentation of those above. But I should be glad if someone would tell me the explanation: the phenomenon is perhaps well known in some other form. [Dr.] A. E. Boycott. Medical School, University College Hospital, W.C.[3]

9.9 DERIVATION OF OPTIMUM ΔP_{BIT} AND ΔP_{CIRC}

The pressure loss through the drilling fluid circulating (ΔP_{CIRC}) system can be expressed as $\Delta P_{\text{CIRC}} = K\,Q^u$, where K is a constant, Q is the flow rate, and n is the exponent on that flow. (If the flow is laminar, $u = 1$ and if turbulent, $u = 2$.)

The standpipe pressure (P_{SURF}) can be expressed as the sum of two pressure losses: ΔP_{CIRC} and ΔP_{BIT}.

9.9.1 Derivation of maximum hydraulic jet impact force at the bit

The derivation for maximum hydraulic impact depends upon the limiting conditions from the drilling rig. The obvious limiting hydraulic condition will be the amount of power available to drive the mud pumps. The second obvious limiting condition will be the maximum standpipe pressure. Each of these conditions will be discussed below and result in slightly different mathematical optimum operating points.

Importantly, at this writing, there is little evidence that one optimization is superior to the other.

---

[3] A.E. Boycott, Sedimentation of blood corpuscles, Nature 104 (1920) 532.

9.9.1.1 Derivation of the optimum jet impact force for the surface pressure limit condition (API's Region 1)

As wells get deeper, the limits on surface pressure prevents utilization of all available hydraulic power. The surface pressure becomes the limiting condition. The pressure drop through the bit nozzles would be the difference in pressure between the maximum standpipe pressure, P_{MAX}, and the circulating pressure drop, ΔP_{CIRC}.

$$\Delta P_{BIT} = P_{MAX} - \Delta P_{CIRC} \qquad (9.43)$$

The circulating pressure loss, ΔP_{CIRC}, is proportional to the flow rate, Q, raised to an exponent, u, or

$$\Delta P_{CIRC} = K \times Q^u \qquad (9.44)$$

The hydraulic impact force, F, derived earlier, is related to the pressure drop across the bit nozzles, or

$$JIF = K \times Q \times (\Delta P_{BIT})^{0.5} \qquad (9.45)$$

Again, to maximize the force with respect to flow rate, the force equation (expressed in terms of flow rate) must be differentiated and the differential set equal to zero.

Since

$$\Delta P_{BIT} = P_{MAX} - \Delta P_{CIRC} \qquad (9.46)$$

Substituting

$$JIF = K \times Q \times (P_{MAX} - \Delta P_{CIRC})^{0.5} \qquad (9.47)$$

Substituting again

$$JIF = K \times Q \times (P_{MAX} - K' \times Q^u)^{0.5} \qquad (9.48)$$

or

$$JIF = K \times \left(Q^2 P_{MAX} - K' \times Q^{u+2}\right)^{0.5} \qquad (9.49)$$

Differentiating

$$\frac{\partial JIF}{\partial Q} = \frac{K \times \left(2 \times Q \times P_{MAX} - K' \times (u+2) \times Q^{u+1}\right)}{(Q^2 \times P_{MAX} - K' \times Q^{u+2})^{0.5}} = 0 \qquad (9.50)$$

For this to be true, the numerator must be equal to zero; and since K is not, then (after rearranging)

$$2 \times Q \times P_{MAX} = K' \times (u + 2) \times Q^{u+1} \qquad (9.51)$$

rearranging

$$P_{MAX} = \frac{1}{2} \times (u + 2) \times K' \times Q^u \qquad (9.52)$$

rearranging more

$$P_{MAX} = \frac{(u + 2)}{2} \times K' \times Q^u \qquad (9.53)$$

substituting

$$P_{MAX} = \frac{(u + 2)}{2} \times \Delta P_{CIRC\ OPT} \qquad (9.54)$$

Recalling that

$$P_{MAX} = \Delta P_{BIT} + \Delta P_{CIRC} \qquad (9.55)$$

Or

$$\Delta P_{CIRC} = P_{MAX} - \Delta P_{BIT} \qquad (9.56)$$

And

$$\Delta P_{BIT} = P_{MAX} - \Delta P_{CIRC} \qquad (9.57)$$

$$P_{MAX} \times \left(\frac{2}{u + 2}\right) = P_{MAX} - \Delta P_{BIT\ OPT} \qquad (9.58)$$

$$\Delta P_{BIT\ OPT} = P_{MAX} - P_{MAX} \times \left(\frac{2}{u + 2}\right) \qquad (9.59)$$

$$\Delta P_{BIT\ OPT} = P_{MAX} \left(\frac{u + 2}{u + 2} - \frac{2}{u + 2}\right) \qquad (9.60)$$

$$\Delta P_{BIT\ OPT} = P_{MAX} \left(\frac{u}{u + 2}\right) \qquad (9.61)$$

QED

9.9.1.2 Derivation of the optimum jet impact force for the power limited condition (API's Region 3)

On a drilling rig, the mud pumps are powered by motors with a finite amount of power. Each conversion of energy will entail some loss of efficiency, dealt with in the chapter on pumps. For our purposes, we will confine the discussion to hydraulic horsepower actually output by the pumps at the surface.

This hydraulic horsepower is the product of the surface (or standpipe) pressure and the flow rate.

$$\text{HHP} = \frac{P_{\text{SURF}} \times Q}{1714} \tag{9.62}$$

where HHP is the hydraulic horsepower (hp); P_{SURF} is the surface (or standpipe) pressure (psi); and Q is the flow rate (GPM).

For the hydraulic case, where the limit condition is the available hydraulic power on the drilling rig, the limit condition could be expressed as

$$\text{HHP} = P_{\text{SURF}} \times Q = K \tag{9.63}$$

Since the standpipe (or surface) pressure consists of the sum of two components, P_{SURF} can be written as

$$P_{\text{SURF}} = \Delta P_{\text{CIRC}} + \Delta P_{\text{BIT}} \tag{9.64}$$

This can also be written

$$\frac{\text{HHP}}{Q} = \Delta P_{\text{CIRC}} + \Delta P_{\text{BIT}} \tag{9.65}$$

Solving this equation for ΔP_{BIT} and expressing ΔP_{CIRC} in terms of Q and u:

$$\Delta P_{\text{BIT}} = \frac{\text{HHP}}{Q} - KQ^u \tag{9.66}$$

The expression derived which related the hydraulic impact (force) to the pressure drop through the bit nozzles was

$$\text{JIF} = K \times Q \times (\Delta P_{\text{BIT}})^{0.5} \tag{9.67}$$

This force may now be calculated in terms of flow rate from the calculation for the pressure drop through the bit nozzles:

$$\text{JIF} = K \times Q \times \left(\frac{\text{HHP}}{Q} - KQ^u\right)^{0.5} \tag{9.68}$$

or rearranging terms:

$$\text{JIF} = K \times \left(Q \times \text{HHP} - K \times Q^{u+2}\right)^{0.5} \tag{9.69}$$

This is the expression for the force of the fluid striking the bottom of the hole. To find the maximum value, differentiate with respect to flow rate and set the differential equal to zero.

$$\frac{\partial \text{JIF}}{\partial Q} = \frac{K \times \left(\text{HHP} - K \times (u+2) \times Q^{u+1}\right)}{(Q \times \text{HHP} - K \times Q^{u+2})^{0.5}} = 0 \tag{9.70}$$

For this to be true, the numerator must be equal to zero or

$$K \times \left(\text{HHP} - K \times (u+2) \times Q^{u+1}\right) = 0 \tag{9.71}$$

or

$$K \times \text{HHP} = K^2 \times (u+2) \times Q^{u+1} = 0 \tag{9.72}$$

reducing

$$\text{HHP} = K \times (u+2) \times Q_{\text{OPT}}^{u+1} = 0 \tag{9.73}$$

Since HHP is the product of the standpipe pressure and the flow rate, this could be written as

$$P_{\text{SURF OPT}} \times Q_{\text{OPT}} = K \times (u+2) \times Q_{\text{OPT}}^{u+1} = 0 \tag{9.74}$$

Solving for the optimum surface (or standpipe) pressure, results in:

$$P_{\text{SURF OPT}} = K \times (u+2) \times Q_{\text{OPT}}^{u} \tag{9.75}$$

Recall that the pressure loss through the circulating system was

$$P_{\text{CIRC}} = K \times Q^u \tag{9.76}$$

Substituting, the optimum surface (or standpipe) pressure would therefore be

$$P_{\text{SURF OPT}} = (u + 2) \times P_{\text{CIRC OPT}} \qquad (9.77)$$

The optimum pressure drop through the bit nozzles would be the difference between the optimum surface pressure and the optimum circulating pressure, or

$$\Delta P_{\text{BIT OPT}} = P_{\text{SURF OPT}} - \Delta P_{\text{CIRC OPT}} \qquad (9.78)$$

Substituting

$$\Delta P_{\text{BIT OPT}} = P_{\text{SURF OPT}} - \frac{P_{\text{SURF OPT}}}{u + 2} \qquad (9.79)$$

Reducing

$$\Delta P_{\text{BITOPT}} = P_{\text{SURFOPT}} \times \left(1 - \frac{1}{u + 2} \right) \qquad (9.80a)$$

$$P_{\text{BITOPT}} = \left(1 - \frac{1}{u + 2} \right) P_{\text{CIRCOPT}} \qquad (9.80b)$$

Understanding that for optimum conditions the $P_{\text{SURF OPT}}$ is the maximum possible surface pressure $P_{\text{MAX OPT}}$, this may be simplified as

$$\Delta P_{\text{BITOPT}} = \frac{u + 1}{u + 2} \times P_{\text{SURFOPT}} \qquad (9.81a)$$

$$P_{\text{BIT OPT}} = \left(\frac{u + 1}{u + 2} \right) P_{\text{CIRC OPT}} \qquad (9.81b)$$

If the $(u + 1/u + 2)$ fraction of the standpipe pressure is applied across the jet nozzles, the hydraulic impact will be the maximum value possible for the hydraulic power limited case.

Note that there is a mathematical discontinuity between API Region 1 and Region 3.

9.9.2 Derivation of equation for maximum hydraulic horsepower at bit

To find the maximum hydraulic power available at a drill bit for any flow rate, the expression for hydraulic power must be differentiated with respect to flow rate and the derivative set equal to zero.

Hydraulic horsepower can be expressed by the equation:

$$\text{HHP} = K'' \times P \times Q \tag{9.82}$$

For the bit, this becomes

$$\text{HHP}_{\text{BIT}} = K'' \times \Delta P_{\text{BIT}} \times Q \tag{9.83}$$

or

$$\text{HHP}_{\text{BIT}} = K'' \times (P_{\text{MAX}} - \Delta P_{\text{CIRC}}) \times Q \tag{9.84}$$

The circulating pressure loss is proportional to the flow rate raised to the exponent u power. Substituting this into the HHP equation along with a constant of proportionality k results in

$$\text{HHP}_{\text{BIT}} = K'' \times (P_{\text{MAX}} - K \times Q^u) \times Q \tag{9.85}$$

or rewritten as

$$\text{HHP}_{\text{BIT}} = K'' \times (Q \times P_{\text{MAX}} - K \times Q^{u+1}) \tag{9.86}$$

Differentiating this equation with respect to the flow rate, Q,

$$\frac{\partial \text{HHP}}{\partial Q} = K'' \times [P_{\text{MAX}} - K \times (u+1) \times Q^u] = 0 \tag{9.87}$$

Since K'' is not zero, the term in the bracket must be zero, or, for optimum conditions,

$$P_{\text{MAX}} - K \times (u+1) \times Q^u = 0 \tag{9.88}$$

$$P_{\text{MAX}} = (u+1) \times K \times Q_{\text{OPT}}{}^u \tag{9.89}$$

$$P_{\text{MAX}} = (u+1) \times P_{\text{CIRC OPT}} \tag{9.90}$$

or

$$\Delta P_{\text{CIRC OPT}} = \frac{P_{\text{MAX}}}{u+1} \tag{9.91}$$

Recalling that

$$P_{\text{MAX}} = \Delta P_{\text{BIT}} + \Delta P_{\text{CIRC}} \tag{9.92}$$

or

$$\Delta P_{\text{CIRC}} = P_{\text{MAX}} - \Delta P_{\text{BIT}} \tag{9.93}$$

and

$$\Delta P_{\text{BIT}} = P_{\text{MAX}} - \Delta P_{\text{CIRC}} \tag{9.94}$$

The optimum pressure loss through the bit would be the difference between the maximum standpipe pressure (P_{MAX}) and the optimum circulating pressure loss (ΔP_{CIRC}).

$$\Delta P_{\text{BIT OPT}} = P_{\text{MAX}} - \Delta P_{\text{CIRC OPT}} \tag{9.95}$$

$$\Delta P_{\text{BIT OPT}} = P_{\text{MAX}} - \Delta P_{\text{CIRC OPT}} \tag{9.96}$$

$$\Delta P_{\text{BIT OPT}} = P_{\text{MAX}} - \frac{P_{\text{MAX}}}{u + 1} \tag{9.97}$$

$$\Delta P_{\text{BIT OPT}} = P_{\text{MAX}} \left(1 - \frac{1}{u + 1} \right) \tag{9.98}$$

$$\Delta P_{\text{BIT OPT}} = P_{\text{MAX}} \left(\frac{u}{u + 1} \right) \tag{9.99}$$

QED

This relationship, having been derived from differentiating HHP with respect to flow, applies to both the standpipe pressure limited case and the horsepower limited case. Both of these applications are discussed in the following sections.

9.9.2.1 Discussion of the optimum hydraulic horsepower for the maximum pressure limited condition (API's Region 1)

For what the API calls Region 1, which is characterized as being limited by the maximum allowable standpipe pressure (P_{MAXSP}), the previously derived equation for HHP optimization across the bit is straightforward substitution of P_{MAXSP} for the P_{MAX} in the equation. No further discussion is required.

$$\Delta P_{\text{BIT OPT}} = P_{\text{MAXSP}} \left(\frac{u}{u + 1} \right) \tag{9.100}$$

9.9.2.2 Discussion of the optimum hydraulic horsepower for the power limited condition (API's Region 3)

For API Region 3, the P_{MAX} from the derivation is a function of flow rate Q, $(P_{\text{MAXSP}(Q)})$ and is limited by the available power.

$$\Delta P_{\text{BIT OPT}} = P_{\text{MAXSP}(Q)} \left(\frac{u}{u+1} \right) \tag{9.101}$$

Knowing the rig equipment limits, the well designer can compute the maximum hydraulic horsepower (in customary units) available from the pumps as

$$\text{HHP}_{\text{MAX}} = \frac{P_{\text{MAX}} \times Q_{\text{MAX}}}{1714} \tag{9.102}$$

Once this HHP_{MAX} value is known, the $P_{\text{MAXSP}(Q)}$ becomes

$$P_{\text{MAXSP}(Q)} = \frac{\text{HHP}_{\text{MAX}} \times 1714}{Q} \tag{9.103}$$

and the HHP optimization for any flow rate becomes

$$\Delta P_{\text{BIT OPT}} = \frac{\text{HHP}_{\text{MAX}} \times 1714}{Q} \times \frac{u}{u+1} \tag{9.104}$$

As with other optimizations, the intersection of the green wasted energy line with the optimization line defines both the optimized flow rate and the maximum pressure achievable at that flow rate.

Note that for optimizing hydraulic horsepower across the bit, there is no discontinuity in API's Region 2 as there is for optimizing jet impact force in API Region 2.

9.10 NOZZLE TABLES AND CHARTS

First, note that a nozzle size calculator for up to eight jet nozzle sizes is located online at http://www.texasdrillingassociates.com/hydraulics/NozzleCalculator.htm.

The first presentation (Table 9.2) is the most conventional, where the number of nozzles (columns) are chosen based on the bit, the area desired is found under that column heading, and then the nozzle size is read from the nozzle size column on the far left in 1/32 of an inch diameter.

Table 9.2 Nozzle combinations and total nozzle flow areas

					Number of nozzles					
1/32 of in.	1	2	3	4	5	6	7	8	9	10
7	0.038	0.075	0.113	0.150	0.188	0.225	0.263	0.301	0.338	0.376
8	0.049	0.098	0.147	0.196	0.245	0.295	0.344	0.393	0.442	0.491
9	0.062	0.124	0.186	0.249	0.311	0.373	0.435	0.497	0.559	0.621
10	0.077	0.153	0.230	0.307	0.383	0.460	0.537	0.614	0.690	0.767
11	0.093	0.186	0.278	0.371	0.464	0.557	0.650	0.742	0.835	0.928
12	0.110	0.221	0.331	0.442	0.552	0.663	0.773	0.884	0.994	1.104
13	0.130	0.259	0.389	0.518	0.648	0.778	0.907	1.037	1.167	1.296
14	0.150	0.301	0.451	0.601	0.752	0.902	1.052	1.203	1.353	1.503
15	0.173	0.345	0.518	0.690	0.863	1.035	1.208	1.381	1.553	1.726
16	0.196	0.393	0.589	0.785	0.982	1.178	1.374	1.571	1.767	1.963
18	0.249	0.497	0.746	0.994	1.243	1.491	1.740	1.988	2.237	2.485
20	0.307	0.614	0.920	1.227	1.534	1.841	2.148	2.454	2.761	3.068
22	0.371	0.742	1.114	1.485	1.856	2.227	2.599	2.970	3.341	3.712
24	0.442	0.884	1.325	1.767	2.209	2.651	3.093	3.534	3.976	4.418
26	0.518	1.037	1.555	2.074	2.592	3.111	3.629	4.148	4.666	5.185
28	0.601	1.203	1.804	2.405	3.007	3.608	4.209	4.811	5.412	6.013
30	0.690	1.381	2.071	2.761	3.451	4.142	4.832	5.522	6.213	6.903
32	0.785	1.571	2.356	3.142	3.927	4.712	5.498	6.283	7.069	7.854

Table 9.3 Nozzle combinations to obtain a particular total nozzle flow area (TNFA)

TNFA	Number of nozzles												
in.^{2}	Two	Three	Four	Five	Six								
0.0982	8	8											
0.1112	8	9											
0.1243	9	9											
0.1388	9	10											
0.1473			8	8	8								
0.1534	10	10											
0.1603			8	8	9								
0.1695	10	11											
0.1733			8	9	9								
0.1856	11	11											
0.1864			9	9	9								
0.1963						8	8	8	8				
0.2010			9	9	10								
0.2033	11	12											
0.2094						8	8	8	9				
0.2155			9	10	10								
0.2209	12	12											
0.2224						8	8	9	9				
0.2301			10	10	10								
0.2355						8	9	9	9				
0.2401	12	13											
0.2454									8	8	8	8	8

0.2462			10	10	11															
0.2485						9	9	9	9											
0.2592	13	13																		
0.2623			10	11	11															
0.2631						9	9	9	10											
0.2777						9	9	10	10											
0.2784			11	11	11															
0.2800	13	14																		
0.2922						9	10	10	10											
0.2945															8	8	8	8	8	8
0.2961			11	11	12															
0.3007	14	14																		
0.3068						10	10	10	10											
0.3106										9	9	9	9	9						
0.3137			11	12	12															
0.3229	14	15																		
0.3229						10	10	10	11											
0.3313			12	12	12															
0.3390						10	10	11	11											
0.3451	15	15																		
0.3505			12	12	13															
0.3551						10	11	11	11											
0.3689	15	16																		
0.3697			12	13	13															
0.3712						11	11	11	11											

Table 9.3 (Continued)

TNFA — Number of nozzles

in.²	Two	Three	Four	Five	Six															
0.3728															9	9	9	9	9	9
0.3835										10	10	10	10	10						
0.3889			13	13	13															
0.3889						11	11	11	12											
0.3927	16	16																		
0.4065						11	11	12	12											
0.4096			13	13	14															
0.4241						11	12	12	12											
0.4303			13	14	14															
0.4418						12	12	12	12											
0.4510			14	14	14															
0.4602															10	10	10	10	10	10
0.4610						12	12	12	13											
0.4640										11	11	11	11	11						
0.4732			14	14	15															
0.4801						12	12	13	13											
0.4955			14	15	15															
0.4970	18	18																		
0.4993						12	13	13	13											
0.5177			15	15	15															
0.5185						13	13	13	13											
0.5392						13	13	13	14											

	1	2	3	4	5	6	7	8	9	10	11	12	13	14	15	16	17	18	19	20
0.5415			15	15	16															
0.5522										12	12	12	12	12						
0.5568															11	11	11	11	11	11
0.5599						13	13	14	14											
0.5653			15	16	16															
0.5806						13	14	14	14											
0.5890			16	16	16															
0.6013						14	14	14	14											
0.6136	20	20																		
0.6236						14	14	14	15											
0.6412			16	16	18															
0.6458						14	14	15	15											
0.6481										13	13	13	13	13						
0.6627															12	12	12	12	12	12
0.6680						14	15	15	15											
0.6780	20	22																		
0.6903						15	15	15	15											
0.6934			16	18	18															
0.7141						15	15	15	16											
0.7378						15	15	16	16											
0.7424	22	22																		
0.7455			18	18	18															
0.7517										14	14	14	14	14						
0.7616						15	16	16	16											
0.7777															13	13	13	13	13	13

(Continued)

Table 9.3 (Continued)

TNFA	Number of nozzles																			
in.^{2}	Two	Three	Four	Five	Six															
0.7854						16	16	16	16											
0.8038			18	18	20															
0.8130	22	24																		
0.8376						16	16	16	18											
0.8621			18	20	20															
0.8629										15	15	15	15	15						
0.8836	24	24																		
0.8897						16	16	18	18											
0.9020															14	14	14	14	14	14
0.9204			20	20	20															
0.9419						16	18	18	18											
0.9603	24	26																		
0.9817										16	16	16	16	16						
0.9848			20	20	22															
0.9940						18	18	18	18											
1.0354															15	15	15	15	15	15
1.0370	26	26																		
1.0492			20	22	22															
1.0523						18	18	18	20											
1.1106						18	18	20	20											
1.1137			22	22	22															
1.1198	26	28																		

1.1689						18	20	20	20						
1.1781										16	16	16	16	16	16
1.1842			22	22	24										
1.2026	28	28													
1.2272						20	20	20	20						
1.2548			22	24	24										
1.2916						20	20	20	22						
1.3254			24	24	24										
1.3560						20	20	22	22						
1.4021			24	24	26										
1.4205						20	22	22	22						
1.4788			24	26	26										
1.4849						22	22	22	22						
1.5555			26	26	26										
1.5555						22	22	22	24						
1.6260						22	22	24	24						
1.6383			26	26	28										
1.6966						22	24	24	24						
1.7211			26	28	28										
1.7671						24	24	24	24						
1.8040			28	28	28										
1.8438						24	24	24	26						
1.9205						24	24	26	26						
1.9972						24	26	26	26						
2.0739						26	26	26	26						
2.1568						26	26	26	28						
2.2396						26	26	28	28						
2.3224						26	28	28	28						
2.4053						28	28	28	28						

Figure 9.4 Total nozzle flow area chart.

This table is a copy of that in the text, copied here for convenience. (Note that earlier nozzles sizes suffered from a degree of nonuniformness in accuracy, but more modern ones are very close to their nominal size.)

Table 9.3 is somewhat different, though of course the underlying math is the same. In the below table, the columns represent whether there are 1, 2, 3, or more nozzles, and the leftmost column is the area desired. This format, though not as common, is easier to use when mixing nozzle sizes.

Lastly, Fig. 9.4 is presented that embeds total nozzle flow area for 1−10 nozzles.

INDEX

Note: Page numbers followed by "*f*" and "*t*" refer to figures and tables, respectively.

Engineering / Energy

PRACTICAL WELLBORE HYDRAULICS AND HOLE CLEANING

Unlock faster, more efficient, and trouble-free drilling operations

MARK S. RAMSEY, P. E.

Learn the most economically efficient ways of optimizing wellbore hydraulics to both improve ROP and ensure hole cleaning in today's challenging oil and gas wells.

Wellbore hydraulics and hole cleaning designs are critical parts of any efficient drilling operation, but drilling engineers, field personnel, and managers must search through multiple applications to gather all the solutions—many of which are now obsolete. *Practical Wellbore Hydraulics and Hole Cleaning* delivers one updated resource with the needed explanations, equations, examples, and descriptions important for wellbore hydraulics including hole cleaning.

Topics such as the impact of temperature and pressure on drilling fluid properties are covered. Hole cleaning is addressed for both vertical and deviated wells. The importance of bit hydraulics optimization and nozzle size selections, drilling fluid challenges, pressure drop calculations, downhole properties, and pumps rounds out the information contents. A single optimization of a bit run can easily save thousands of dollars in fuel costs alone.

Packed with example calculations, *Practical Wellbore Hydraulics and Hole Cleaning* gives the drilling engineer the tools necessary for effective operations-friendly bit hydraulics and hole cleaning design and execution.

Key Features

- Provides practical techniques to ensure hole cleaning in both vertical and deviated wells
- Addresses errors in predictive wellbore hydraulics modelling equations and provides remedies
- Teaches ways to improve economic efficiencies of drilling oil and gas wells through the use of calculations, case studies and guidelines

About the Author

Mark S. Ramsey, P. E. is the Principal and Owner of Texas Drilling Associates. His consulting engineering company provides well planning, rig team training, DWOPs/CWOPs, accident investigations, research, product development and launch services. He authors and teaches both introductory and advanced public and proprietary drilling courses on six continents, including a Master of Science level drilling course. He also teaches professional engineering ethics. Clients include majors, independents, drilling companies, and service companies (such as ExxonMobil, BP, Apache, Baker-Hughes, Schlumberger, Transocean, and others worldwide.) Mr. Ramsey previously worked for Exxon in both drilling research and drilling operations and was named a "Distinguished Instructor" for consistent high-quality instruction. He earned a Bachelor of Science in Mechanical Engineering from Texas Tech University, who honored him as "Distinguished Engineer" in 2016. He holds numerous patents and is a registered Professional Engineer in the state of Texas.